




1981

## Electron Spin Resonance Studies of Membrane Fluidity of Normal and Malignant Human Neural Tissues

Robert P. Wersto  
*Loyola University Chicago*

Follow this and additional works at: [https://ecommons.luc.edu/luc\\_diss](https://ecommons.luc.edu/luc_diss)

 Part of the [Biochemistry, Biophysics, and Structural Biology Commons](#)

---

### Recommended Citation

Wersto, Robert P., "Electron Spin Resonance Studies of Membrane Fluidity of Normal and Malignant Human Neural Tissues" (1981). *Dissertations*. 1979.

[https://ecommons.luc.edu/luc\\_diss/1979](https://ecommons.luc.edu/luc_diss/1979)

This Dissertation is brought to you for free and open access by the Theses and Dissertations at Loyola eCommons. It has been accepted for inclusion in Dissertations by an authorized administrator of Loyola eCommons. For more information, please contact [ecommons@luc.edu](mailto:ecommons@luc.edu).



This work is licensed under a [Creative Commons Attribution-NonCommercial-No Derivative Works 3.0 License](#).  
Copyright © 1981 Robert P. Wersto

ELECTRON SPIN RESONANCE STUDIES OF  
MEMBRANE FLUIDITY OF NORMAL  
AND MALIGNANT HUMAN NEURAL TISSUES

by

Robert P. Wersto

A Dissertation Submitted to the Faculty of the Graduate  
School of Loyola University of Chicago in Partial  
Fulfillment of the Requirements for the Degree of  
Doctor of Philosophy

June

1981

## ACKNOWLEDGMENTS

I would like to express my gratitude to the members of my committee and to the faculty members at Loyola University Medical Center who supported and assisted this effort.

I would like to thank Dr. James R. Norris, Dr. Michael Bowman and Dr. Marion Thurnauer of Argonne National Laboratory for their assistance and comments concerning electron spin resonance. Also, I would like to thank Drs. Reichman and Yarzagaray and the senior residents, both past and present, of the Department of Neurosurgery, Loyola University Medical Center for their enthusiasm and assistance in obtaining human brain biopsy specimens in the early stages of this study, and Dr. E. Ross, Department of Neuropathology, Loyola University Medical Center for pathological verification of the tumors grown in athymic "nude" mice.

I wish to thank my fellow graduate students in particular, Bruce Bianchi, for criticism, assistance, and friendship during my tenure as a graduate student.

I would like to thank my parents and brother for their patience, understanding and support while completing this dissertation. Finally, very few words can express my gratitude for the constant help and support of Nancy.

## VITA

Robert P. Wersto is the son of Peter and Anne Wersto. He was born on March 5, 1954, in Chicago.

He received his B.S. degree with an ACS Chemistry and Biology dual major from Valparaiso University, Valparaiso, Indiana in 1975. From July 1975 until July 1980, he entered graduate school in the Department of Biochemistry at Loyola University Medical Center under the direction of Dr. Joseph Bernsohn. From September 1980, until present, he is a post-doctoral fellow in the Division of Infectious Diseases and Immunology, Department of Pediatrics, University of Rochester Medical Center, Rochester, New York.



## TABLE OF CONTENTS

	Page
ACKNOWLEDGMENTS	ii
VITA	iii
LIST OF FIGURES	vii
LIST OF TABLES	xi
CONTENTS OF APPENDIX	xiii
LIST OF ABBREVIATIONS AND DEFINITIONS	xiv
INTRODUCTION	1
REVIEW OF THE LITERATURE	
I. Structure of the Plasma Membrane	
A. Bilayer Structure and Component Motions	11
B. Membrane Models	20
II. Concept of Fluidity	26
III. Membrane Hydrocarbon Flexibility Gradients	56
IV. Fluidity of Biomembranes	76
A. Plasma membrane preparations	76
B. Whole cell correlations	79
C. Fluidity of normal and transformed cells	85
1. Fluorescent polarization	87
2. Electron spin resonance	101
3. Additional physical methods	113
V. Lipid Alterations of Normal and Transformed Cells	114
A. General tumor models	116
B. Normal brain	122
C. Brain tumors	125
D. Lipid alterations <u>in vitro</u> in relation to other transformation systems	132

## TABLE OF CONTENTS

	Page
ELECTRON SPIN RESONANCE THEORY ORDER PARAMETERS	137
Spin Hamiltonians	141
ESR spectra of Paramagnetic Nitroxides	143
Anisotropic Motion and Order Parameters	145
Equivalence of Order Parameters and Experimental Spectra	156
MATERIALS AND METHODS	158
Description of Cell Lines	158
Tissue Culture - General Methods	161
Correlates of Malignancy	164
Cell Colony formation in soft agar	167
Tumor production in "Nude" Mice	168
Lipid Extraction and Fractionation	169
Thin-Layer Chromatography	172
Preparation of Fatty Acid Methyl Esters	174
Determination of Protein, Phosphorus, and Cholesterol	174
Gas-Liquid Chromatography	176
Electron Spin Resonance: Spin Labels	179
Electron Spin Resonance: Incorporation of Spin Labels into Cells	182
Electron Spin Resonance Measurements	183
RESULTS	185
DISCUSSION	270
A. Relevance of Lipid Alterations to Normal and Transformed Cells <u>in vitro</u>	293
B. Lipid Alterations in Relation to Normal and Malignant Neural Tissues <u>in vivo</u> and <u>in vitro</u>	296

## TABLE OF CONTENTS

	Page
C. Fidelity of Spin Label Studies	307
D. Summary and Conclusion	314
REFERENCES	319
APPENDIX	376

## LIST OF FIGURES

Figure	Page
1. Dynamic rotations of phospholipids, protein, and cholesterol within a lipid bilayer	29
2. Chain-chain isomerizations of lipid hydrocarbon chains	30
3. Structure of the common phospholipids and cholesterol	36
4. Transition temperature and phase aggregation in membranes	38
5. Molecular shapes and fluidity	43
6. Comparison of polarity and order gradients in membrane bilayers	57
7. Comparison of NMR and ESR bilayer order gradients	59
8. Orientation of the spin-label nitroxide group	144
9. Energy levels and allowed transitions for nitrogen	146
10. Fremy's salt spectral splittings	147
11. Anisotropic motion of lipid spin labels in membrane environments	151
12. Hyperfine splittings of the nitroxide spin labels	153
13. Transformation assays	166
14. Structure of the nitroxide spin labels	180
15. Orientations and penetration depth of the 5-NS, 12-NS, and 16-NS spin labels	181

## LIST OF FIGURES

Figure	Page
16. Tumor production in athymic "nude" mice	186
17. Composite spectra of the V5-NS spin label incorporated into the NFB line and the five tumor devised cell lines	221
18. Comparison of the 5-NS spectra of the E1202 and TE907 medulloblastoma cell lines and the NFB line	222
19. Comparison of the 5-NS spectra of the glioma derived SA4 and SA101 lines with the NFB cell line	227
20. Comparison of the 5-NS spectra of the glioma derived 251 MG 3C cells with the NFB cell line	232
21. Composite spectra of the 12-NS spin label incorporated into the NFB line and the five tumor derived cell lines	234
22. Comparison of the 12-NS spectra of the E1202 and TE907 medullablastoma derived cell lines with the NFB cells	235
23. Comparison of the 12-NS spectra of the glioma derived SA4 and SA101 lines with the NFB cell line	239
24. Comparison of the 12-NS spectra of the glioma derived 251 MG 3C cells with the NFB cell line	244
25. Composite spectra of the 16-NS spin label incorporated into the NFB line and the five tumor derived cell lines	246
26. Comparison of the 16-NS spectra of the E1202 and TE907 medullablastoma derived cell lines with the NFB cells	249

## LIST OF FIGURES

Figure	Page
27. Comparison of the 16-NS spectra of the glioma derived SA4 and SA101 lines with the NFB cell line	254
28. Comparison of the 16-NS spectra of the glioma derived 251 MG 3C cells with the NFB cell line	256
29. Comparison of the $T_{\parallel}$ splittings for the 5-NS, 12-NS, and 16-NS spin labels incorporated into the cell lines	258
30. Comparison of order parameters (SGAF) and malignancy between the five tumor derived cell lines and the NFB cells	260
31. Spin label flexibility gradient in the malignant E1202 cell line	262
32. Spin label flexibility gradient in the malignant SA4 cell line	263
33. Spin label flexibility gradient in the 251 MG 3C cell line	264
34. Spin label flexibility gradient in the non-tumorigenic TE907 cell line	265
35. Spin label flexibility gradient in the non-tumorigenic SA101 cell line	266
36. Spin label flexibility gradient in the NFB cell line	267
37. Comparison of the order parameter (SGAF) determined flexibility gradients between the five tumor derived cell lines and the NFB lines	269

## LIST OF FIGURES

Figure	Page
38. PC+SPH/(PE+PS+PI) molar ratios as a function of temorigenicity	274
39. Rapid reduction of spin labels in viable intact neural tumor cells	313
40. Fatty acid methyl ester chart from Varian 2100 Gas Chromatograph (EGSS-X as liquid phase)	384

## LIST OF TABLES

Table	Page
1. Cell culture dynamics of human brain tumors <u>in vivo</u> and <u>in vitro</u>	187-188
2. Comparison of lipid composition between human cell lines	191
3. Comparison of phospholipid classe between cell lines	194
4. Phosphatidyl Choline fatty acid percentage composition of cell lines	197-198
5. Phosphatidyl Serine and phosphatidyl Inositol fatty acid percentage composition of cell lines	202-203
6. Phosphatidylethanolamine fatty acids percentage composition of cell lines	208-209
7. Fatty acid chain length and saturation of phospholipid classes	214-215
8. Comparison of ESR order parameters for Probe (5, 12) Tensor values Txx=Tyy=6.1G Tzz=32.4G	223
9. Comparison of corrected ESR order parameters for Probe (5,12) Tensor values Txx=6.1G Tyy=5.8G Tzz=32.4G	225
10. Comparison of ESR order parameters for Probe (5,12) Tensor values Txx=6.3G Tyy=5.8G Tzz=33.6G	229
11. Comparison of corrected ESR order parameters for Probe (5, 12) Tensor values Txx=6.3G Tyy=5.8G Tzz=33.6G	230



## LIST OF TABLES

Table	Page
12. Comparison of ESR order parameters for Probe (5, 12) Tensor values $T_{xx}=T_{yy}=6.1G$ $T_{zz}=32.4G$	236
13. Comparison of corrected ESR order parameter for Probe (12, 5) Tensor values $T_{xx}=T_{yy}=61.6G$ $T_{zz}=32.4G$	237
14. Comparison of ESR order parameters for Probe (12,5) Tensor values $T_{xx}=6.3G$ $T_{yy}=5.8G$ $T_{zz}=33.6G$	241
15. Comparison of corrected ESR order parameter for Probe (12, 5) Tensor values $T_{xx}=6.3G$ $T_{yy}=5.8G$ $T_{zz}=33.6G$	242
16. Comparison of ESR order parameter for Probe (16, 1) Tensor values $T_{xx}=T_{yy}=6.1G$ $T_{zz}=32.4G$	247
17. Comparison of corrected ESR order parameters for probe (16,1) Tensor values $T_{xx}=T_{yy}=61.6G$ $T_{zz}=32.4G$	248
18. Comparison of ESR order parameter for Probe (16, 1) Tensor values $T_{xx}=6.3G$ $T_{yy}=5.8G$ $T_{zz}=33.6G$	252
19. Comparison of corrected ESR order parameter for Probe (16, 1) Tensor values $T_{xx}=6.3G$ $T_{yy}=5.8G$ $T_{zz}=33.6G$	253
20. 5-doxyl stearate probe trans-gauche fatty acid conformations	381
21. 12-doxyl stearate probe trans-gauche fatty acid conformations	382
22. 16-doxyl stearate probe trans-gauche fatty acid conformations	383



## LIST OF ABBREVIATIONS AND DEFINITIONS

5-NS	5-doxy1 stearate spin label (2-(3-Carboxypropyl) -4, 4-dimethyl- tridecyl-3-oxazolidinyloxy1)
12-NS	12-doxy1 stearate spin label (2-(10-carboxyldecyl) -2-hexyl-4-4- dimethyl-3-oxazolidinyloxy1)
16-NS	16-doxy1 stearate spin label (2-(14-carboxytetradecyl-2-ethyl- 4, 4-dimethyl-3-oxazolidinyloxy1)
E1202	Human medulloblastoma cell line
NFB	Normal human brain cell line
SA4	Human glioblastoma cell line
SA101	Human astrocytoma cell line
TE907	Human medulloblastoma cell line
251 MG 3C	Human astrocytoma cell line
3T3	3T3 mouse fibroblast cell line
Py-3T3	Polyoma virus transformed 3T3 mouse fibroblast cell line
SV40-3T3	Simian virus 40 transformed 3T3 mouse fibroblast cell line
SV101-3T3	Simian Virus 40 transformed 3T3 mouse fibroblast cell line
An	Anistropic splitting factor
BHK	Baby hamster kidney
BSA	Bovine serum albumin
CEF	Chick embryo fibroblasts
CHL	Cholesterol

## LIST OF ABBREVIATIONS AND DEFINITIONS

DDMPC	Diperdeuteromyristoylphosphatidylcholine
DMEM	Dulbecco's modified Eagle's Medium
DMPC	Dimyristoylphosphatidylcholine
DMPE	Dimyristoylphosphatidylethanolamine
DNMR	Deuterium nuclear magnetic resonance
DOPC	Dioleoylphosphatidylcholine
DPH	1, 6-diphenyl-1, 3, 5-hexatriene
DPMA	Dipalmitoylphosphatic acid
DPPC	Dipalmitoylphosphatidylcholine
DPPE	Dipalmitoylphosphatidylethanolamine
DPPG	Dipalmitoylphosphatidylglycerol
DPPS	Dipalmitoylphosphatidylserine
DSC	Differential scanning calorimetry
DSPC	Distearylphosphatidylcholine
EDTA	Ethylenedinitriolotetraacetic acid
EPR	Electron paramagnetic resonance
ESR	Electro spin resonance
FCS	Fetal calf serum
FLGPM	Fluid lipid globular protein mosaic model

## LIST OF ABBREVIATIONS AND DEFINITIONS

FLUIDITY	As used in this dissertation, fluidity refers to the increase or decrease in spin label motion sensed by electron spin resonance techniques. Intuitively, fluidity refers to the relative motional freedom of membrane lipid components. This term here, is used interchangeably with order, however, the reader should be cognisant that the terms are not equal: a membrane can be fluid with respect to lipid acyl chain isomerations, and ordered with respect to the placement of these chains to hydrophilic/hydrophobic interfaces.
LGPM	Lipid globular protein mosaic model
NMR	Nuclear magnetic resonance
PBS	Phosphate buffered saline
PC	Phosphatidylcholine
PE	Phosphatidylethanolamine
PI	Phosphatidylinositol
PL	Phospholipid
POPC	Palmitoyl-oleoyl-phosphatidylcholine
PPLO	Pleuropneumonia-like organisms
PS	Phosphatidylserine
PYL	Perylene
S	Polarity corrected order parameter
S'	Flexibility order parameter
S''	Order parameter of a nitroxide rotating in a cone of semi-variable angle

## LIST OF ABBREVIATIONS AND DEFINITIONS

SCD	Deuterium order parameter
SGAF	Tensor corrected polarity corrected order parameter
SMOL	Segmental order parameter
TEMPO	2, 2, 6, 6-tetramethylpiperidnyl-1-oxyl

## INTRODUCTION

The mammalian plasma membrane represents both an asymmetric static and dynamic specialized barrier that maintains the structural and functional integrity of numerous cellular processes. Induction of neoplasia could be manifested by abnormalities in the supramolecular organization of the membrane matrix itself as well as abnormalities in the diverse reactions of cell surface molecules.

Uncontrolled proliferation of malignant tissues comprises activities such as cell growth, division, communication, movement, differentiation, immune recognition, and metastasis. The proposal that neoplasia is essentially a "membrane disease," initially considered by Wallach (1975), is supported by significant evidence that reproducible alterations in membrane biochemistry accompany the transition from the non-transformed to the transformed state. Tumor and transformed cell surfaces often possess simplified membrane components rather than structurally complex, tumor-specific molecules. Generally, the basis for many changes in neoplasia center around the physical organization of membrane components. Although numerous cell surface

properties are modified in tumor and transformed cells, few are universal for the neoplastic state (Weiss, 1967; Capalidi and Green, 1972; Oseyoff et al., 1973; Nicolson, 1975; Robbins and Nicolson, 1975).

Differences in plasma membrane fluidity between normal and neoplastic cells have been sought to explain gross changes in lectin agglutination, altered lateral mobility of membrane components, and other differences such as changes in surface charge or ion density, modified adhesion and contact inhibition of growth, altered permeability and transport through the membrane, impaired intracellular communication, and an abnormal presence of tumor-specific transplantation antigens and cryptic embryonic antigens (Robbins and Nicolson, 1975). The concept of membrane fluidity refers to the overall relative motional freedom which membrane lipid and protein components may undergo and is contrasted to mobility which describes the rotational, lateral, and transverse motions of single membrane components. In fluid membranes, components undergo great diversity of dynamic movement. For example, lipids may possess: a) very rapid motion about C-C bonds in the phospholipid hydrocarbon chains; b) rapid angular motion of rigid steroids; c) rapid lateral diffusion of



phospholipids in the plane of the membrane bilayer; d) rotational motion of lipids bound tightly to embedded protein; and e) a variable flip-flop of phospholipids from one monolayer to the other (Marsh, 1975).

Because membrane lipids (i.e. phospholipids) exist in a constrained environment within the bilayer proper, fluidity can more correctly be defined as a liquid crystalline state (Phillips, 1972). In this state, the lipids are not rigidly packed into an ordered conformation, but rather the thermodynamic state of the lipid phase resembles that of liquid hydrocarbons. The strongest attractions are between adjacent polar headgroups rather than their adjoining hydrocarbon chains (Luzzati, 1968). The distinction between an ordered gel phase and a liquid crystalline state is characterized by a transition temperature. Mobility of membrane components is hindered in an ordered array below the transition temperature and increased above the transition temperature. Overall, membrane fluidity is determined by the concentration of membrane-associated protein, cholesterol, and phospholipids, and by the degree of the fatty acid

acyl side chains. Fluidity and microviscosity of a membrane environment do not refer to identical membrane properties. Fluidity can be defined as the reciprocal of viscosity as it is for isotropic liquids. The majority of membrane environments, however, are not isotropic since they do not possess equal dynamic mobilities in all directions. Therefore, there may not be any correlation between the degree of order in a system and the rate of individual molecular motions (Neal et al., 1976). Fluidity within a biomembrane may be asymmetric as in the case of opposing monolayers with identical fatty acid composition that have different headgroup orientations (Chapman, 1975).

Numerous investigators using cloned tissue culture cell lines have sought to explain membrane compositional differences between normal and transformed cells. The systems employed in most cases were cell lines which had been transformed by chemical carcinogens, oncogenic viruses, or ionizing radiation, as opposed to spontaneous transformants arising from "normal" cell populations. Unfortunately, because of the diversity of the test systems, a remaining unanswered critical question is what are the changes endemic to neoplastic cells, versus the changes in a particular

transformed system. For example, virally-transformed cells usually possess unique immunologic individuality with transplantation antigens located on the cell surface specific for a given virus which are independent of the host. On the other hand, tumors induced by chemical agents, ionizing radiation, or the implantation of biologically "inert" plastic films, along with spontaneous tumors, exhibit membrane associated transplantation antigens that are specific for a given tumor rather than its carcinogenic agent (Wallach, 1975).

Cells in vitro offer an experimental advantage over neoplastic cells in vivo. Under in vitro conditions, normal and tumor cell populations may be studied under identical, reproducible culture conditions. This removes the hormonal, enzymatic, osmotic, immunal and stress effects that would otherwise play a role in host (in vivo) conditions. Excluding tissues in primary cultures, cell lines in vitro may not represent a homogenous cell population. These cells may undergo changes in cellular properties, both on the macro- and micro-molecular levels after long periods of subcultivation with the net consequence of selective overgrowth of a transformant in a normal cell population or vice versa. This selection process may be even more dramatic in the case of primary

cultures. Often mesenchymal elements will proliferate to a greater extent than normal or tumor cells, forming a line of contaminating fibroblasts. Cells in culture represent a unique example in which the normal constraints on growth and division are absent. Cell types which may not normally proliferate are afforded the opportunity for unlimited growth in contrast to tumors in vitro. Since cells in vitro are dependent upon media and sera for growth and maintenance, metabolic characteristics may be modified substantially by the addition or removal of nutritional supplements. Tissue culture affords the greatest potential for the autonomy of malignant cells outside their host. It must be remembered that cells in a culture compose a special type of cell population which, because it may be biochemically manipulated after a period of time in culture, may not be closely related to its counterpart in vivo. A striking example of the cellular variability under culture conditions can be observed with mouse 3T3 fibroblasts. This cell line is rarely tumorigenic when injected at high concentrations ( $10^8$  cells) in mice and is classified as "normal" (Aaronson and Todaro, 1968). "Normal" 3T3 cells attached to small glass beads and implanted into BALB/c mice, however, form hemangioendothel-

omas (Boone, 1975).

Semantic problems have arisen in the nomenclature defining the types of abnormal cells used for tumor membrane model systems. A distinction may be made between "tumor" cells, those which are transformed in vivo and generally grown in vivo and cells which may be transformed either in vivo or in vitro but are grown exclusively in vitro. Transformation is generally not considered synonymous with neoplastic alteration since a transformed or oncogenic cell must be induced by a specific agent and may not be tumorigenic (i.e., capable of producing a tumor when placed in a suitable environment such as an animal host). In contrast, a neoplasm refers to an abnormal proliferation of cells, usually characteristic of a cancerous growth, that is capable of tumorigenic activity. The common markers used for the verification of transformation include a change in morphology (cell type and colony type), a loss of contact inhibition, a loss of cell orientation, an increase in number of nucleoli, a change in the nuclear to cytoplasmic ratio (Porter et al., 1973; Colvard and Temnick, 1975), an increase in the saturation density (Stoker and Macpherson, 1961; Todaro and Green, 1963; Stoker, 1967, Dulbecco, 1970), a change in serum

requirements (Stoker, 1967; Dulbecco, 1970; Holley and Kiernan, 1971; Smith, 1971; Temin et al., 1972), chromosomal aberrations, a loss of anchorage dependence (Macpherson and Montagnier, 1964; Dulbecco, 1970; Shin et al., 1975), an ability to produce tumors in animals and semi-solid medium, and loss of senescence (finite life span). The presence or absence of any single marker does not prove or disprove the transformation of cells.

Tumorigenicity is the strongest marker; however, certain cultures of normal cells possess the capability of growing as transplantable tumors in animals with defective immune responses. These defective responses are often caused by irradiation, drugs, or anti-thymocyte serum (Freeman and Hueber, 1973). Because of cultures with this capability, studies that have been performed on the fluidity differences between normal and virally transformed cells such as SV40 transformed fibroblasts, may not represent the veritable situation for spontaneous neoplasms, and therefore, may not be suitable as a general model of the fluidity characteristics for neoplastic tumorigenic cells.

Cell surface alterations between tumor and normal cell surface systems must be closely scrutinized as a consequence of the above considerations. A logical alternative would be the study of a neoplastic cell

system that comprises a transformed pair representing both the benign and malignant tumorigenic states. The cell lines used for this dissertation arose from spontaneous tumors in vivo, induced presumably from unknown viral or chemical agents, and the cells from these cultures can be characterized by their potential for tumorigenicity in both in vivo (athymic "nude" mice) and in vitro (semi-solid medium) assays. Direct comparisons between normal and neoplastic tissues are complicated by the fact that tumor cells arise in vivo from unknown precursor cells and may not be of the same histological or embryological origin as normal tissues. Malignant and benign gliomas and medulloblastomas represent idealized pairs from which cells of the same undifferentiated stem cell origin can be compared and contrasted with respect to membrane features. Furthermore, human brain tumors also possess a vertical increase of tumorigenic potential with the pathological grading of the tumor [i.e. from benign (I) to malignant (IV)], as well as a horizontal increase of the malignant potential with the invasiveness of the tumor (i.e. from fibroblastic meningiomas to glioblastomas).

The scope of this dissertation is an examination of the possible phospholipid structural and motional

plasma membrane fluidity changes that occur in spontaneous malignant and benign human neoplasms. Cells of the same embryological origin that possess striking contrasts in growth properties and tumorigenicity have been examined. The lipid (cholesterol, phospholipid and fatty acid acyl side chains) composition of these cells and membrane fluidity measured by magnetic resonance spin label probes have been investigated. The experimental approach was not designed to substantiate unequivocally similarities or differences between normal and transformed tissues by spin label techniques, but to examine the possible role of phospholipid headgroup profiles rather than fatty acid composition upon the modulation of membrane fluidity in a well defined malignant and benign cell system in vitro.



## REVIEW OF THE LITERATURE

## I. Structure of the Plasma Membrane

## A. Bilayer Structure and Component Motions

Presently, there is no remarkable model that accurately encompasses molecular experimental data and hypotheses into a generalized system truly representative of all types of membrane structure and function in neoplasia. Rather than review all the previously proposed membrane models, it is more appropriate to consider the basic mosaic models with regard to lipid and protein organization. A single model, therefore, cannot be exclusively applied to all membranes, to all membrane components, or to all given states of a particular membrane system, even though some degrees of similarity may exist among different membranes.

The fundamental structure of the mosaic models is based on the pauci-molecular model of Danielli-Davson (1935). This model was proposed as a consequence of the characteristics of lipid films (Gorter and Grendal, 1925; Danielli and Harvey, 1935). Biological membranes were considered to consist of bilayered phosphatides positioned with the polar lipid headgroup of the phospholipids oriented at the membrane surface and

the hydrocarbon chains forming an internal apolar region. Membrane proteins located at the polar surface interacted with the lipid components through ionic or hydrogen bonding. Further refinement of membrane ultrastructure observed in electron micrographs advanced the "unit membrane" model (Robertson, 1959). The design implied that the non-lipid components may be asymmetrically distributed across the membrane with the hydrophilic proteins on the external surface forming extended  $\beta$  pleated sheets. For a number of reasons, most particularly the inconsistencies of assuming the basic structure of myelin for more complex membrane systems, the Danielli-Davson model or "unit membrane" hypothesis was considered an oversimplification of biomembrane structure. Lipids in this model are arranged as a closely packed phospholipid bilayer possessing rigid, fully extended hydrocarbon chains. The fatty acid acyl side chains, however, are more likely to be disordered, due to entropy, and probably approach the same type of state as observed for liquid hydrocarbons. Phospholipids are not necessarily densely packed filling every available space, but rather, their surface area per lipid molecule in a biomembrane is less than that of a closely packed array. Since the phospholipids are not tightly packed, it is possible for apolar

regions of proteins to penetrate the bilayer. The proteins associated with lipid components that require ionic bonding as suggested in the "unit membrane" model have led to numerous proposals regarding the structure of lipid biomembranes (Sjostrand, 1963; Benson, 1966; Green et al., 1967). Based upon the hydrophilic and hydrophobic regions of the lipid and protein components as well as the asymmetric distribution of phospholipids, membrane proteins, glycolipids, and glycoproteins, the bilayer itself is asymmetric. The bilayer form of the basic biomembrane structure has been confirmed by X-ray diffraction studies (Blasie and Worthington, 1969, Engelman, 1970; Blaurock, 1971; Wilkins et al., 1971), nuclear magnetic (Glaser et al., 1970; Chan et al., 1971; Lee et al., 1972), electron spin resonance (Hubbell and McConnell, 1968; Keith et al., 1968; McConnell and McFarland, 1970; Tourtelotte et al., 1970; Hubbell and McConnell, 1971; Jost et al., 1971; Kornberg and McConnell, 1971a, 1971b; Scandella et al., 1972), and differential scanning calorimetry studies (Steim et al., 1969; Reinert and Steim, 1970; Papahadjopoulos and Kimelberg, 1973; Chapman et al., 1974). Although an asymmetric bilayer configuration is applicable to myelin membranes, mycoplasma plasma membranes, and erythrocyte ghosts,

there is evidence that the bilayer can be discontinuous, and in some cases (erythrocytes), it can be penetrated by membrane proteins which extend through the bilayer structure. In some cases it has been shown that bilayers are stabilized by the presence of cholesterol.

In order to compensate for the inadequacies present in the Danielli-Davson pauci-molecular model, several modified mosaic models were proposed (Singer, 1971; Vanderkooi and Green, 1970; Wallach, 1975). Lipid-protein interactions neglected in the pauci-molecular membrane model have been incorporated into a generalized mosaic structure by Nathanson (Nathanson, 1904). Parpart and Ballentine (1952) attempted to integrate erythrocyte proteins into the bilayer membrane by proposing a protein continuum with 50 Å cylindrical lipid plugs. These channels span the width of the bilayer with the headgroups of the amphipathic lipids oriented towards the hydrated walls so as to form apolar channels. This model unfortunately does not account for lipid-protein interactions, phospholipid behavior, and two-dimensional spatial encoding of information. The mosaic models are an attempt to integrate membrane structure with function by accounting for stable cell surface patterns in which the disposition of membrane components is ordered to allow for

array encoding of molecular recognition sites. Structural variety seen in many of the mosaic models is based upon the following considerations. 1) The mosaic models should possess a lower free energy or greater thermodynamic stability than the Danielli-Davson structure, and this is based solely on the thermodynamics of reactions between hydrophobic and hydrophilic areas of soluble membrane proteins (Singer, 1971). 2) The majority of membrane protein is in an  $\alpha$ -helical conformation in contrast to a  $\beta$ -pleated sheet. 3) Phospholipids are partially accessible to enzymatic degradation in intact preparations. 4) There is a paucity of protein binding on the lipid polar headgroups (Glasser et al., 1970). Because of the large variability in the proportions of membrane protein and lipid as well as the complexities in lipid and protein interactions, membrane models have attempted to address membrane structure rather than function.

Biomembranes constitute a barrier that separates two metabolically and physio-chemically dissimilar domains. They are a plastic, condensed, noncovalently bonded array of diverse proteins and lipids that possess an unlimited number of two dimensional aggregates. Functionally, biomembranes should possess an asymmetrical arrangement

since opposing sides face different environments. In vivo and in vitro genetic influences may result in different membrane contents (Wallach and Winzler, 1974), and fatty acid acyl side chain composition changes corresponding to variations in cell cycle, age, and serum concentration.

Many of the problems that plague some mosaic models involve protein-lipid interactions and lateral and transverse diffusion of proteins in the plane of the bilayer. Apolar protein-lipid interactions thermodynamically require that portions of membrane proteins, rather than the apolar side chains alone, penetrate through or are in association with the hydrophobic membrane core (Wallach and Winzler, 1974). The peptide bond itself is hydrophilic (Nozaki and Tanford, 1971; Tanford, 1972), and it would be thermodynamically improbable that peptide bonds could exist in an hydrophobic environment without the expenditure of a large amount of energy. Because there are restrictions on protein conformation within an apolar environment, the majority of membrane protein tends toward a helical conformation. The fatty acid side chains, as a consequence, must be arranged to maximally interact in the plane of the bilayer with the hydrophobic amino acids which protrude from the protein core. This

arrangement would allow special interactions between protein and lipid adjacent to one another as in the case of synaptic discs where extensive penetration of the bilayer by the protein occurs (Zampighi and Robertson, 1973).

Physical studies upon the disposition of proteins in biomembranes have led to further difficulties in formation generalized model of membrane structure. Membrane protein has been estimated to occupy at least one-half of the bilayer volumes (Vanderkooi and Green, 1970; Singer, 1971). Surface pressure measurements on erythrocyte lipids in spread monolayers (Bar et al., 1966), however, indicate that when no protein is present, a bilayer would fill the space available for fatty acid side chain interactions with only a relatively small amount of compressibility. The addition of protein in the range of 30 - 40 volume % would pack the acyl side chains to such a degree that there would be maximal compression and minimum freedom of motion. This is in opposition to ESR studies (Hubbell and McConnell, 1969) indicating considerable fluidity for the fatty acid side chains in lipid-proteins dispersions.

The problem of physical orientation of proteins within biomembranes is compounded by oversimplification of

diagramming membrane structures. From X-ray diffraction data the cross-sectional area of a single phospholipid side chain is estimated to be  $20.4 \text{ \AA}^2$  (Luzzati, 1968);  $20 - 23 \text{ \AA}^2$  from the calculation of bond angles, interatomic distances, and van der Waals atomic radii (Pauling, 1942); and  $20.5 - 24 \text{ \AA}^2$  for spread monolayers (Bar et al., 1966). For a phospholipid with two acyl chains at maximal compression, the cross-sectional hydrocarbon area is  $40 - 48 \text{ \AA}^2$ , and in hydrated bilayers, lecithin has a measured interfacial area in the range of  $70 - 87.5 \text{ \AA}^2$  (Bar et al., 1966; Small et al., 1966; Luzzati, 1968; Engelman, 1969). This is in contrast to  $37 \text{ \AA}^2$  necessary for the choline headgroup of lecithin. Since there is insufficient polar headgroup cross-sectional area to cover the hydrocarbon side chains, uncovered water-hydrocarbon interfaces could possibly exist. X-ray diffraction studies (Blaurock, 1972) indicate there may be considerable penetration of protein into lipid bilayers with a calculated lipid bilayer thickness of  $40 \text{ \AA}$  (Blaurock, 1973a, 1973b). A statistical thermodynamic approach by Parsegian (1967) further substantiates that large uncovered nonpolar areas are probable for egg phosphatidylcholine as compared to long chain saturated aliphatic acids (Parsegian, 1968) or



liquid paraffin mixtures. Only by forming a ninety degree angle between the plane of the glycerol polar headgroup with the acyl side chain could phosphatides cover the entire surface of a bilayer hydrophilically. This arrangement would be most energetically unfavorable due to the juxtaposition of polar and apolar regions (Finean, 1961). The degree of protein association and penetration has been further substantiated by phospholipase C digestion on model and natural membranes (Glaser et al., 1970). Protein configuration is independent to some degree of the structural integrity of the phospholipids as has been determined by proton magnetic resonance measurements of membrane phospholipid acyl side chains after enzymatic digestion of membrane protein. To some degree, aliphatic side chains are independent of the surrounding protein, although some membrane bound proteins such as cytochrome oxidase are immobilized by a surrounding single layer of phospholipid (Jost et al., 1973).

Enzymatic digestion of the phospholipids of plasma membranes reveal that the polar headgroups are readily accessible to cleavage (Glaser et al., 1970) with approximately 30% being hydrolysis resistant and presumably tightly bound to biomembrane protein. Sub-mitochondrial membranes, however, are totally attacked

by phospholipase C (Zwaal et al., 1971; Lenax et al., 1972) Erythrocyte ghosts treated with phospholipase C (Finean et al., 1971) showed a 50% decrease in surface area due to the hydrolysis of 70% of the phospholipids that occupy the surface area of the membrane.

#### B. Recent Membrane Models

The lipid globular protein mosaic model (LGPM) proposed by Wallach (1968; Wallach and Zahler, 1966; Wallach and Winzler, 1974) considers domains composed of protein and lipid which are assembled as tangentially mobile patchworks penetrating the bilayer core to varying degrees. In contrast to the simple bilayer, contact occurs between protein and lipid components in both polar and non-polar regions of the biomembrane. Bilayer lipids adjacent to membrane proteins possess a compositional and orientational organization that is influenced by the surrounding protein. The ordering influence of the protein is localized not only on the outer surface where it may be irregularly coiled, but also on the cytoplasmic face of the bilayer and within the apolar core. Penetrating proteins occur mainly in  $\alpha$ -helical rods, each containing a hydrophobic face. Occurring as single rods or closely packed forms, the  $\alpha$ -helical proteins are grouped

into subunits and penetrate the discontinuous bilayer from the inner to the outer surfaces.  $\beta$ -structures, with properly oriented hydrophobic amino acid residues, also could provide regions necessary for lipid-protein interactions. A low protein-to-lipid ratio would allow a small proportion of lipid to exist in association with the apolar residues of the  $\alpha$ -chains. The hydrophobic interactions would be decreased due to the increasing distance of the remaining lipid-protein clusters. Because of the distribution of the polar amino acid residues of the penetrating protein, fatty acid side chains would be forced to lie at the membrane surface forming apolar channels. Membrane cholesterol, proposed to exist in clusters (Wallach et al., 1975), and membrane phospholipids can undergo cooperative transitions of state within microdomains. These phospholipid microdomains are constrained and are stabilized by the protein across the framework of the membrane. Experimental evidence has verified many of the tenets proposed in the LGPM model. Proteins in several types of membranes are surrounded by shells of lipids, and cooperative phase transitions occur in erythrocyte and thymocyte plasma membranes (Jost et al., 1973; Trauble and Overath, 1973; Wallach et al., 1974).

In contrast to the tenets of the LGPM model, the fluid lipid globular protein mosaic model (FLGPM) hypothesized by Singer (1971; Singer and Nicolson, 1972) states that the conformation of membrane proteins is independent of the lipid components. Membrane lipids form a dynamic mosaic fluid at physiological temperature as a result of the fluidity of phosphatidyl hydrocarbons. The distribution of proteins is considered to be random except for short-range protein-protein interactions. Experimental evidence supports the random characteristics of membrane protein movement and the lateral mobility of other membrane components. Rhodopsin protein molecules exist in a random, liquid-like state in frog retinal receptor disc membranes (Blaise and Worthington, 1969). Membrane components disperse within minutes after cell fusion or hybridization (Frye and Edidin, 1970). Membrane phospholipids are known to undergo rapid lateral motion as has been determined by electron spin resonance measurements (Kornberg and McConnell, 1971; Barnett and Grisham, 1972; Devaux and McConnell, 1972; Scandella et al., 1972; Trauble and Sackmann, 1972; Shimshik and McConnell, 1973; Lee et al., 1974), fluorescence polarization studies (Waggoner and Stryer, 1970; Rudy and Gilter, 1972;

Cogan et al., 1973; Vanderkooi and Callis, 1974) fluorescent eximer formation (Galla and Sackmann, 1974), and partitioning of hydrophobic radioisotope labels (Rigaud et al., 1972). Consequentially, individual membrane components appear to undergo translational and rotational diffusion within the plane of the bilayer although the diffusion rates are dependent upon the lipid composition, temperature, and additional physical environmental factors. The rates of motion are governed by the effective viscosity of the lipid matrix which approaches that of light machine oil (Edidin, 1974). Structural constraints may be present for different types of antigen and lectin receptors.

The organization of some surface receptors may be non-random (Nicolson and Yanagimachi, 1974) but membrane phospholipids can also exist in domains due to specific lipid-lipid interactions or the presence of divalent cations (Shimshik et al., 1973; Jacobson and Papahadjopoulos, 1975). The FLGPM model attempts to integrate experimental evidence of pure phospholipid bilayer systems with the protein transpositions occurring in biomembranes. This model, however, does not allow for stable cell surface patterns required for specific recognition, and does not implicate the role of

cholesterol in the regulation of membrane fluidity. The FLGPM model may be a valid prototype of membrane structure for nuclear membranes and the plasma membranes of some prokaryotic organisms, but like the LGPM model, it is not applicable to all membranes in general.

A subtle modification of the mosaic models emphasizes the hydrophobic packing of protein within bilayers to form a time-averaged continuum with long-range stable sequences of protein patterns. The protein crystal model (Vanderkooi and Green, 1970) propounds that both proteins and lipids, rather than either one component exclusively (LGPM and FLGPM models) form the bilayer. This is envisioned as protein molecules floating half-submerged in a lipid field. Based upon the limited points of contact between crystallized protein molecules, the model portways that membranes are assembled as a lattice of proteins. The spacing between protein molecules is filled with phosphatides oriented so that their fatty acid acyl side chains fit into depressions and their polar head-groups remain on the surface.

Changes in hydrophobic interactions could affect the geometrical arrangement of the membrane components by allowing a "break" in the structural integrity of the

bilayer which would increase the apolar surface area exposed to water. Thermodynamic considerations favor a decrease in energy forcing lipid-protein structural interactions, and at the same time large electrostatic forces exist between polar lipid headgroups, headgroups and polar residues of proteins, and proteins themselves. The protein crystal structural model was originally supported by the solubilities of cytochrome c-phospholipid complexes in organic solvents (Das and Crane, 1964), salt extraction of cytochrome c and lipid depleted mitochondria with phospholipids (Kimelberg and Lee, 1969; Lenaz et al., 1969), and hydrogen ion titrations of halophilic bacteria (Brown, 1965). Based upon chemical (Vanderkooi and Green, 1970b), x-ray diffraction (Blaise et al., 1965, 1969; Blaurock and Wilkins, 1969), and electron microscopic data (Fernandez-Moran, 1962; Blaise and Worthington, 1969; Gras and Worthington, 1969), the model has been applied to retinal rod outer segments (Vanderkooi and Sundaralingam, 1970) and mitochondria devoid of cytochrome oxidase (Vanderkooi et al., 1972). The protein crystal model may only be applicable for two-dimensional arrangements such as that in the outer segments of retinal rods.

## II. The Concept of Fluidity

The concept of membrane fluidity is based on the thermodynamic and dynamic properties of model membranes composed of phospholipids, glycolipids and dispersions. Liposomes have been studied in relation to their fluid and non fluid properties: The roles of divalent ions, the importance of cholesterol interactions, and the orientation of polar headgroups. Membrane fluidity has been simplistically defined as the degree of saturation/unsaturation of the acyl side chains present in the phospholipids (Chapman and Wallach, 1968; Oldfield and Chapman, 1972). Membrane fluidity is influenced by both intrinsic and extrinsic controls. It may be extrinsically controlled by the level of dietary fatty acids (Linden, 1973 a, b) in the case of E. coli auxotrophs, or the precursors of phosphatidyl polar headgroups (Schroeder et al., 1976 a, b). In contrast, fluidity can be intrinsically modified by the unknown mechanisms controlling trans headgroup phospholipid exchange and biosynthesis or by the defluidizing effect of cholesterol. The focus of the present role of membrane fluidity in the literature has not primarily concerned itself with the molecular movement of bilayer components themselves, but rather the suggestion that many membrane-bound enzymes of



plasma membrane and intracellular organelles are under the influence of membrane fluidity for enzymatic orientation and catalysis.

A functional definition of membrane fluidity depends on the conformational orientation of hydrocarbon chains of one lipid molecule influencing the cooperative arrangements in neighboring chains. Biomembranes, in contrast to pure bilayers or liposomes, possess a microheterogeneous environment in which differing constituents of membranes affect the importance of stabilizing hydrophobic interactions. For the simple case of lipid-water phase interactions at constant temperatures, the degree of fluidity is a direct reflection of the phase transition temperature of the phosphatides. Fluidity is influenced not only on an orientational basis but also by the melting temperature of the fatty acyl group.

X-ray diffraction studies (Shipley et al., 1972) have verified that the fatty acyl side chains of phospholipids undergoing a phase transition can exist in two states: a gel phase below the transition temperature in which the hydrocarbon chains are rigidly packed into a crystalline array and a liquid crystalline phase in which the hydrocarbon chains are flexible, possessing movement

comparable to liquid paraffins. Biological membranes possess the same qualitative characteristics as those exhibited by synthetic phospholipid dispersions above their fluid phase transition (Melichor et al., 1970; Seelig and Seelig, 1974; March, 1975; Davis, 1979). Biomembranes, however, have lipid domains partially in an ordered (gel) phase (Oldfield et al., 1972; Smith et al., 1979). Lipids may be immobilized with proteins into complexes although this immobilization is not synonymous with order (Blaurock and Stoeckenius, 1971; Stier and Sackmann, 1973).

Membrane phospholipid acyl side chains show the greatest motion above the gel-liquid crystalline phase transition. This intrinsic fluidity results from rotational isomerizations about C-C bonds of the acyl hydrocarbon chains (Hubbell and McConnell, 1971; Trauble, 1971; Seelig and Niederberger, 1974) (Figure 2). Below the transition temperature, saturated fatty acid acyl chains are all extended in a trans position. The chains are tightly and regularly packed perpendicular to the plane of the membrane with the hydrocarbon axes nearly parallel in a hexagonal lattice (McAlister et al., 1973). For paraffin crystals, the hydrocarbon chains become more widely spaced (Muller, 1932) because of chain rotations

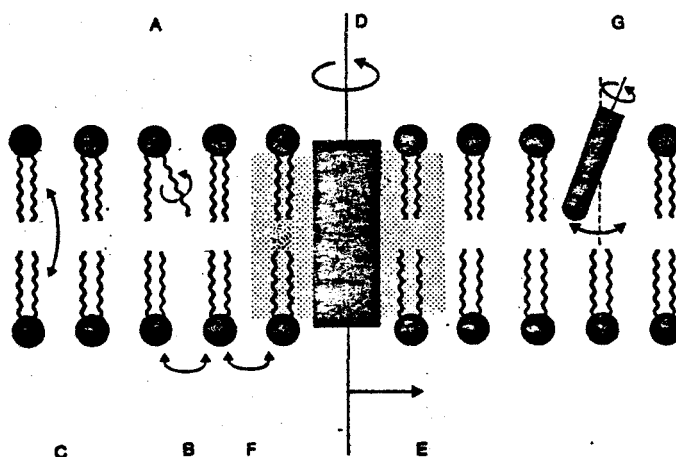


FIG 1: Dynamic rotations of phospholipids, proteins, and cholesterol within a lipid bilayer. A. Very fast rotations about C-C bands of phospholipid hydrocarbon chains. B. Rapid lateral diffusion of phospholipids in the plane of the bilayer. C. Transverse flip-flip of phospholipids from one monolayer of the membrane to the opposing monolayer. D. Rotational diffusion of proteins. E. Lateral diffusion of proteins (slow with respect to phospholipid lateral diffusion). F. Rotation of boundary lipid of proteins. The lipid composition may not be asymmetric. G. Angular motion of steroids, such as cholesterol. (Adapted from Marsh, 1975.)

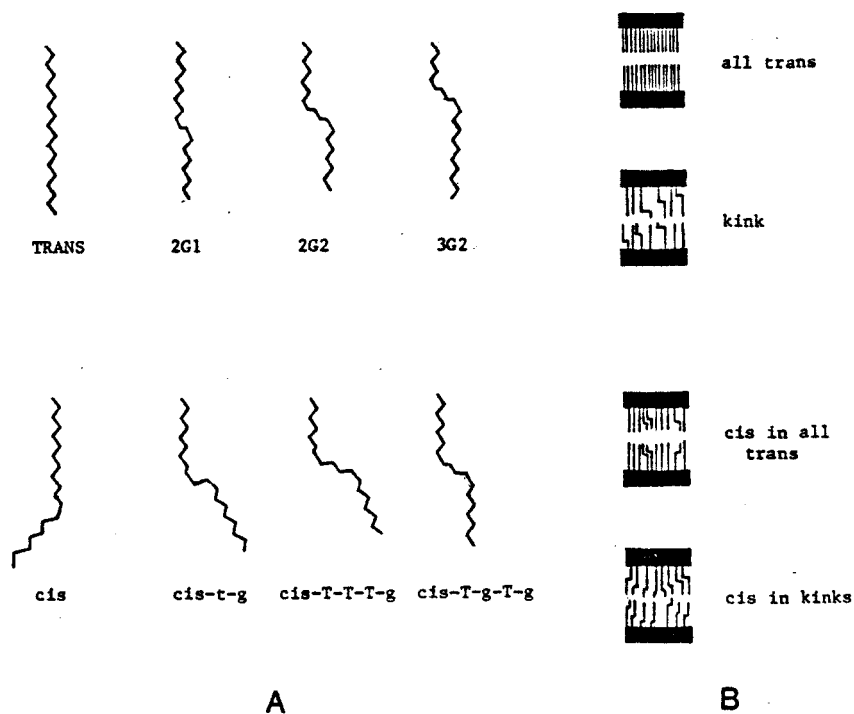


FIG 2: A. Carbon-carbon chain isomerization of lipid hydrocarbon chains. B. Effects of chain isomerizations in lipid bilayer blocks. The hydrocarbon angle in saturated changes  $\alpha$  is  $111^\circ$ , and that of cis and trans double bands  $\beta$  and  $\gamma$  respectively are  $123^\circ$ . (Redrawn with adaptation from Lagaly *et al.* (1977) and Jain and Wagner (1980).)

about their axes so that the effective rotational radius is increased without changing electrostatic force interactions. Cooperative chain motions, such as bending or flexing, are a result of trans conformations rotating about a C-C bond  $120^\circ$  to form a gauche configuration. These highly mobile C-C rotational isomers, with a lifetime on the order of  $10^{-6}$  sec (Seelig and Niederberger, 1974) create lateral motions along the hydrocarbon axis (Trauble, 1972; Trauble and Eibl, 1974; McConnell, 1975). The change of a single trans to a gauche configuration forces the acyl chain into a widened L-shaped structure. The effect of two gauche rotations in opposite directions separated by an unaltered trans bond (denoted as  $g^+ t g^-$  or  $g^- t g^+$ ) results in a kink perpendicularly shifting the part of the molecule distal to the kink. Although the chain remains parallel to the segment before the kink, it is shortened by one methylene group and is laterally displaced about  $1.5 \text{ \AA}$  (Trauble and Haynes, 1971; Seelig and Niederberger, 1974; Seelig and Seelig, 1974) (Figure 3). The overall image of a  $\beta$ -coupled gauche kink is that of closely packed spoons with interchain interactions caused by van der Waal's attractions (Jackson, 1976). A kink creates a vacancy for a neighboring chain to kink into, and only energy from interchain repulsion

would be able to force the kinking of a chain into the area of a non-kinked neighbor. Macroscopically,  $\beta$ -coupled gauche kinks result in a reduction of the bilayer thickness, an increase in the area occupied by each molecule, and an increase in total bilayer volume (Philips and Chapman, 1968; White, 1970; Trauble and Haynes, 1971; Demel et al., 1972; Sheetz and Chan, 1972; Nagle, 1973).

Liposomes composed of phosphatides with identical fatty acid acyl groups at the 1' and 2' position on the glycerol backbone exhibit highly cooperative changes between gel and liquid crystalline states. In an aqueous media, this phase change represents the transition from a solid all trans state of hydrocarbon chains to an isomerization with gauche-trans rotations. Thermodynamically, the enthalpy of this transition, which occurs over a characteristic temperature range, is the energy required for forcing all the hydrocarbon chains into gauche positions, disrupting van der Waal's forces between neighboring parallel chains, and breaking the organization of ordered solvent around polar lipid headgroups (Kimelberg, 1977).

The transition temperature of pure lipid phospholipid bilayers is usually characterized by a large endothermic change with a sharp melting point (Stein

et al., 1969; Blazyk and Steim, 1972). Endothermic melting points can be detected by a variety of physical techniques. Often, the limits of the transitions are detected by differential scanning calorimetry (DSC) which detects the transition midpoint temperature ( $T_m$ ) and the upper ( $T_2$ ) and lower ( $T_1$ ) limits of the melting phase (Chapman et al., 1967, Chapman and Wallach, 1968; Papahadjopoulos, 1968; Steim et al., 1969; Phillipis et al., 1970; Hinz and Sturtevant, 1972). For dipalmitoylphosphatidylcholine (DPPC), the midpoint transition occurs at  $41^\circ\text{C}$  (Phillips et al., 1970; Shimshik and McConnell, 1973a). Above this temperature the bilayer thickness is decreased by  $6-7 \text{ \AA}$  and the area occupied per molecule is increased from  $48 \text{ \AA}^2$  to  $65-70 \text{ \AA}^2$  (Phillips and Chapman, 1968). Depending upon the degree of hydration, however, the midpoint ( $T_m$ ) may occur in the range of  $41^\circ\text{C}$  to  $45^\circ\text{C}$  (Ladbrooke and Chapman, 1969; Hinz and Sturtevant, 1972; Chapman et al., 1974; Jacobson and Paphadjopoulos, 1975). By forming small unilamellar vesicles from multilamellar vesicles (MLV liposomes), the transition temperature is broadened, and the  $T_m$  is lowered by approximately  $3-5^\circ\text{C}$  (Jacobson and Papahadjopoulos, 1975). Above the transition temperature for DPPC lateral compressibility increases (Linden et al., 1973) along with a large

enthalpy change ( $\Delta H = 8.66 \text{ kcal mole}^{-1}$ ) and entropy change ( $\Delta S = 27.6 \text{ cal deg}^{-1} \text{ mole}^{-1}$ ) (Phillips et al., 1969).

In the fully hydrated state, the transition melting temperature of a pure phospholipid bilayer depends upon the length of the lipid hydrocarbon chains, the degree of unsaturation, the chemical structure of the polar head-group, the presence of divalent ions, and the placement of cis or trans double bonds (Chapman et al., 1967; Gaffney and McConnell, 1974; Jacobson and Papahadjopoulos, 1975; Papahadjopoulos et al., 1976a). Saturation of the fatty acid side chain increased the  $T_m$  with increasing chain length while unsaturated chains correspondingly lower the  $T_m$ . Cis C-C bonds are common in isomerizations of unsaturated chains, and these lower the  $T_m$  by placing a permanent kink in the chain which interferes with regular trans or gauche isomerizations. The difference in the  $T_m$  between dioleoylphosphatidylcholine (DOPC; 18:2) and distearylphosphatidylcholine (DSPC; 18:0) illustrates a decrease in  $T_m$  with desaturation ( $-22^\circ\text{C}$  for DOPC contrasted to  $58^\circ\text{C}$  for DSPC) (Phillips et al., 1972). Because trans-unsaturated hydrocarbon chains [vaccenic acid (18:1 n-7), for example] (Lehninger, 1970) are rare, naturally occurring phospholipids are expected to possess a decreased  $T_m$ . In the case of naturally occurring



phospholipids, however, an unsaturated hydrocarbon chain predominantly occupies the 2' position; whereas, the 1' position is usually occupied by a fully saturated acyl chain.

Headgroups play a major role in influencing the melting temperature of a particular lipid (Figure 4). For example, replacement of choline in dimyristolyphosphatidylcholine (DMPC) with ethanolamine (forming dimyristolyphosphatidylethanolamine (DMPE) increases the  $T_m$  from 23°C to 48°C (Oldfield and Chapman, 1972; Chapman et al., 1974; Van Dijck et al., 1976). Removal of the choline moiety from DMPC resulting in dimyristolyphosphatidylglycerol has little effect upon the transition temperature (Kimelberg and Papahadjopoulos, 1974; Jacobson and Papahadjopoulos, 1975). Generally, distances between headgroups increase with increasing acyl desaturation, resulting in weaker intra-molecular headgroup interactions and diminished melting temperature effects (Yeagle, 1978). Accordingly, headgroup conformation may change during a phase transition. Above the melting temperature, egg phosphatidylcholine (egg PC) (with an average of 1-2 double bonds per hydrocarbon molecule) and DMPC have the same conformation (Yeagle et al., 1977). This is observed with X-ray diffraction techniques (Lesslaur et al., 1972),

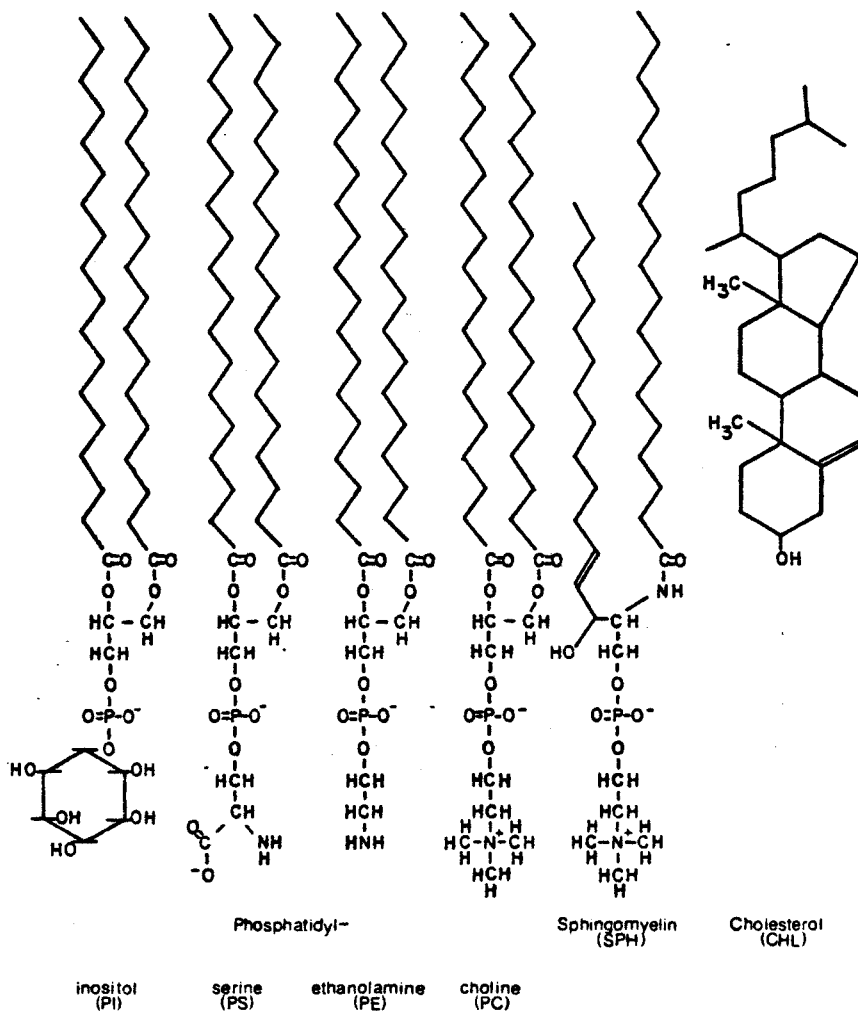


FIG 3: Structural orientations of common phospholipids and cholesterol.

and one is able to conclude that the phosphate group of PC and the N-methyl group of DPPC exist in the same plane above and below the phase transition temperature.

Naturally occurring phosphatides, as contrasted to nonideal mixtures of fatty acids from synthetic sources, exhibit lower melting temperatures with a broad endothermic melting range, possibly due to the microheterogeneity of the lipids (Wallach, 1975). Egg PC consisting of 34% 16:0, 20% 18:1, and 11.2% 18:2 hydrocarbon chains (Papahadjopoulos and Miller, 1967) shows a  $T_m$  of  $-5^{\circ}\text{C}$ ; whereas, beef brain phosphatidylserine (PS) consisting of 49% 18:0, 37% 18:1, and 4% each of 20:1, 20:4, and 22:6 acyl groups (Papahadjopoulos and Miller, 1967) melts from  $5-20^{\circ}\text{C}$  (Kimelberg and Papahadjopoulos, 1974) or from  $0-12^{\circ}\text{C}$  (Jacobson and Papahadjopoulos, 1975).

The behavior of natural membranes composed of various proportions of lipid components in aqueous environments exemplifies a more complicated phase organization. Binary mixtures yield either two endothermic or two exothermic deflections at temperatures shifted from the melting temperatures of either of the pure components. This decrease in the transition temperature and the broadening of its range, is a consequence of the coexistence of fluid and solid (liquid crystalline and gel) phases

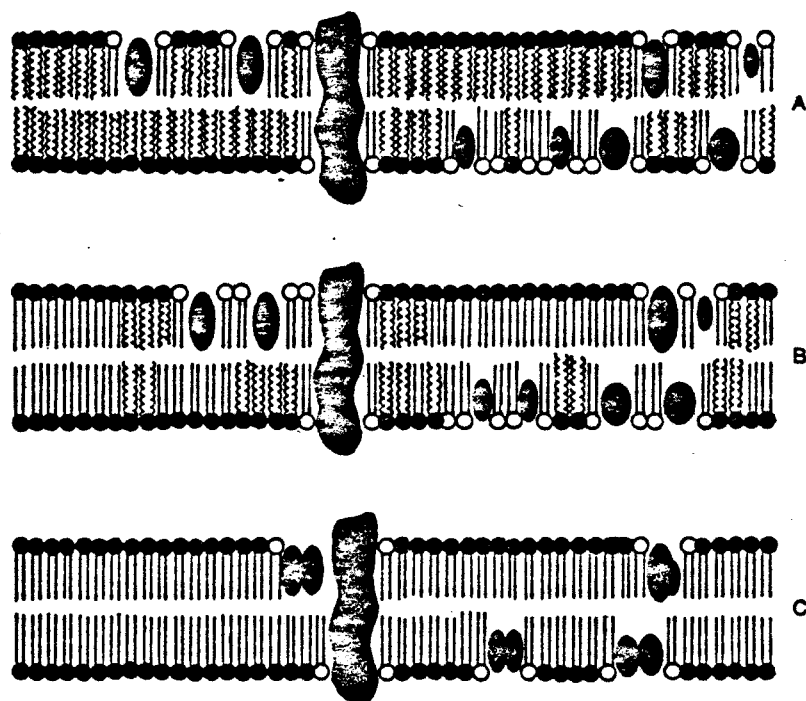


FIG 4: Effect of transition temperature and phase aggregation. A. Above the transition temperature all the lipids exist in a fluid state, and proteins are free to diffuse laterally in the membrane plane. B. The membrane is depicted at a temperature between the fluid and gel phases. Several lipids have begun the phase transition to a rigid gel state (straight tails) whereas others exist in the fluid liquid crystalline state (wavy tails). Proteins are excluded from regions of rigid lipids into aggregates. C. The membranes in the gel state where all lipid is rigid and proteins are maximally aggregated. (Adapted from Linden and Fox, 1975.)

(Phillips et al., 1972) (Figure 5). Domains with different phase separations result in either complete solid and fluid miscibility in lipids of similar structures (Shimshik and McConnell, 1973a, b; Grant et al., 1974, Wu and McConnel, 1974; McConnell, 1975b) or complete fluid phase miscibility with solid phase immiscibility (McConnell, 1975b). A phase diagram of this type of mixture shows a lower transition temperature ( $T_1$ ) at the start of unequal melting and a lateral phase separation (solidus curve characteristics). This is compared to the liquidus or fluidus portion of a phase curve which represents the terminal melting of both fluid and solid phases. Broad intermediate phase transitions may be the result of differing headgroups as is the case for DMPC and DMPE complexes (Phillips et al., 1970, 1972; Chapman et al., 1974). Intermediate fluidity is also observed in binary mixtures of phospholipids with identical headgroups, where the saturated acyl side chains differ by two methylene groups (Phillips et al., 1972). Homogeneous saturated acyl side chains situated on headgroups possessing a net negative charge and heterogeneous fatty acid acyl side chains with charged or neutral headgroups additionally exhibit broad, discrete, intermediate phase transitions (Ladbroke and Chapman, 1969; Chapman et al., 1974; Kimelberg and Papahadjopoulos, 1974;

Papahadjopoulos et al., 1974; Jacobson and Papahadjopoulos, 1975).

Macroscopic evidence for the organization of solid, fluid, and intermediate lateral phase domains exists for a large variety of pure lipid binary mixtures as well as for heterogeneous biomembranes. This data has been obtained from freeze-fracture electron micrographs and X-ray diffraction studies. "Banded" linear repeating ridges that indicate the presence of solid phases (Vervegaert et al., 1972; 1973; Shimshik et al., 1973) are observed in freeze-cleaved phospholipid bilayers. The banded spacings are characteristic of the phosphatidyl fatty acid components (Verkleij et al., 1972) and indicate the large intramolecular cohesive forces which enable the phospholipids to migrate rapidly within the bilayer plane. Fluid regions, on the other hand, are visualized by smooth appearing surfaces (Pinto daSilva and Branton, 1972; Vervegaert et al., 1973; Chen and Hubbell, 1973; Shimshik et al., 1973; Grant et al., 1974; Kleemann et al., 1974; Verkleij et al., 1974). X-ray diffraction studies (Engleman, 1970, 1971; Esfahani et al., 1971; Levine and Wilkins, 1971; Wilkins et al., 1972) have shown that the frozen and fluid hydrocarbon chains possess diffraction bands

at 4.2 Å and 4.6 Å, respectively. Similar properties of binary lipid mixtures are seen by examining molecular details of the thermotropic phase transitions.

The spin label TEMPO (2,2,6,6-tetramethylpiperidiny-1-oxyl) is slightly soluble in fluid hydrocarbon and relatively insoluble in crystalline phases (Hubbell and McConnell, 1968). Due to the probe's enhanced partitioning into fluid lipids, an analysis of the spectral parameters (splitting of the high field hyperfine line) indicates the proportion of TEMPO in the hydrocarbon phase to the total probe present in both the apolar and aqueous phases. Changes in the spectral heights reflect changes in the partition coefficient of TEMPO and can be used to quantitate the amounts of lipid in solid and fluid domains. Construction of phase diagrams with the TEMPO partitioning function plotted against temperature indicate the occurrence of any discontinuities over a 1-2°C range. Characteristic phase transitions agree with the  $T_m$ 's determined by DSC (Phillips et al., 1968, 1970). The rate of exchange frequency of the lateral phase separations measured by TEMPO partitioning is greater than  $10^7 \text{ sec}^{-1}$  at 30°C, accounting for the rapid kinetics of melting and freezing (Dupont et al., 1972; McConnell et al., 1972).

Transition temperatures and endothermic gel+liquid crystal transition are influenced by the degree of hydration (Chapman et al., 1967). Approximately 10 moles of water are bound per mole of phosphatidylcholine which is unable to crystallize at 0°C (Williams and Chapman, 1970). Overall, the hydration of the polar headgroups results in a lowering of the transition temperature by highly cooperative phase changes (Lippert and Peticolas, 1971; Chapman et al., 1967; Vekslı et al., 1969).

Associated with the thermodynamics of the gel-liquid crystalline transition temperature and its molecular basis in the orientations and isomerizations of the C-C bonds of the phosphatidyl hydrocarbon chains, is the presence or absence of cholesterol within the bilayer (Figure 6). The role of cholesterol in biomembranes is one of a modulator since cholesterol is able to directly influence chain-chain interactions and thereby affect the enthalpy of transition. In the phospholipid bilayer the steroid is oriented so the 3'- $\beta$ -hydroxy group is placed in the region of the polar headgroups and the remaining hydrophobic portion of the molecule is parallel to the phospholipid chains



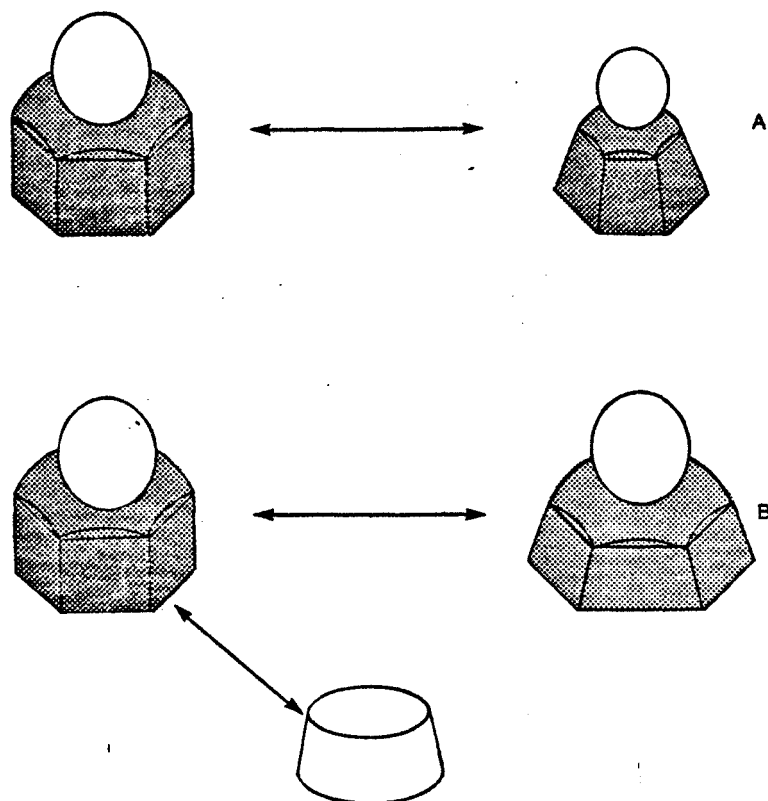


FIG 5: Molecular shapes and fluidity. A. Phospholipids with identical fatty acid composition, but with phosphatides possessing large and small headgroups, left and right respectively. B. Phospholipids with identical headgroup composition, but varying acyl side chain composition. Cholesterol, center, preserves the copacking as lipids with differing geometrics in stable bilayers. (Adapted from Wieslander et al., 1980.)

(Chapman, 1968; Rand and Luzzati, 1968). In the gel state, hydrocarbon chains in the presence of cholesterol tend to favor a fluid state in contrast to the transition temperature in which the sterol molecules defluidize the acyl chains (Oldfield et al., 1972; Demel and DeKruyff, 1976). If the concentration of cholesterol is increased up to 30 mole %, the phosphatidyl acyl chains assume a more disordered state than that below the transition temperature. Cholesterol, therefore, condenses the average area per molecule causing an ordering of the hydrocarbon C-C-rotations of fluid bilayers. Cholesterol induces a degree of "intermediate" fluidity so that at all temperatures the cooperativity of the acyl side chains are either increased or reduced depending upon the physical structure (Chapman, 1968; Ladbroke et al., 1968; Oldfield and Chapman, 1972).

Under freeze fracture electron microscopy, the regular banded regions thought to be solid lipid domains in binary pure lipid mixtures are not apparent (Verkleij et al., 1974; Kleemann and McConnell, 1976). DMPC-cholesterol vesicles below the phase transition at 10 mole % sterol (15°C) indicate the existence of two particle phases: a particle-rich and a particle-poor phase.

String-like arrays are induced below the  $T_m$  when the cholesterol concentration is doubled (20 mole %). This is contrasted with the lack of mobility for particles in pure DMPC vesicles (Kleemann and McConnell, 1976). Within liposomes composed of a single species of phospholipid, the distribution of cholesterol is random. This is apparent below the phase transition temperature through disappearance of the string-like arrays or bands (increase in smooth fracture faces) (Verkley *et al.*, 1972).

X-ray diffraction data indicate that cholesterol, up to 7.5 mole %, increases the thickness of the water layer of hydration in DPCC from 9 Å to 27.5 Å. This modification as seen by freeze-cleavage techniques is also supported by X-ray scattering experiments (Shechten *et al.*, 1972; Tradieu *et al.*, 1973; Haest *et al.*, 1974). Sharp angle spacings (4.2 Å, characteristic of crystalline paraffin chains) increase with the addition of cholesterol to 4.45 Å diffuse spacings. Fluidization of the acyl chains by cholesterol occurs with 7.5 to 50 mole % of cholesterol (Ladbroke *et al.*, 1968). Lateral motions of the chains are also increased, with a constant thickness of the hydration layer. Additionally, the water binding capacity of egg PC is only

slightly affected by the addition of cholesterol to dispersions (Lundberg, 1974). Bilayer thickness in fluid systems may be increased at low sterol concentrations (Johnson, 1973; Newman and Huang, 1975) from 39 Å to 42 Å (Levine and Wilkens, 1971). At intermediate cholesterol concentrations, the cooperativity of the gel→liquid crystalline phase transition is reduced (Trauble, 1977) as has been determined by laser Raman studies of phosphatidylcholine-sterol bilayers (Lippert and Peticolas, 1971).

Differential scanning calorimetry (DSC) studies have established the basis for the effects of cholesterol within bilayers. Increasing amounts of cholesterol above 20 mole % cause a lowering of the transition temperature and a decrease in the heat of transition (Ladbroke et al., 1968). Increasing the sterol concentration above 20 mole % decreases the  $T_1$  melting temperature along with the increasing the final melting temperature  $T_2$ , thereby broadening the overall phase diagram. At high cholesterol concentrations (in the range of 50 mole %), the endothermic transition temperature appears to be completely abolished although laser Raman vibrational spectra indicate that the gel→liquid crystalline transition does exist.

In summary, cholesterol has a buffering effect upon the endothermic phase transition where the chains are more mobile below the transition temperature in the presence of a sterol. The inverse is also true: in the presence of sterol, the acyl chains are less mobile above the  $T_m$ . Due to the size and irregular surface of the steroid ring, hydrocarbon chains with their small cross-sectional area are prevented from flexing above the  $T_m$  (Phillips and Finer, 1974). Hydrocarbon chains also exhibit all trans-perpendicular packings in the gel phase. The effects of cholesterol, observable by DSC methods, are not only limited to choline phosphatides but have also been demonstrated for sphingomyelin and cerebrosides (Oldfield and Chapman, 1972).

Cholesterol's influence on molecular motions, isomerizations, and rotations can additionally be determined by magnetic resonance of naturally occurring isotopes ( $^1\text{H}$ ,  $^2\text{H}$ ,  $^{31}\text{P}$ ,  $^{13}\text{C}$ ,  $^{15}\text{N}$ ,  $^{15}\text{NMR}$ ), specifically labeled deuterium NMR (DNMR) biomembranes, or pure phospholipid bilayers. For example,  $^1\text{H}$  NMR and  $^{13}\text{C}$  NMR provide evidence of reductions in chain mobilities for egg PC dispersions by cholesterol (Keough et al., 1973; Darke et al., 1972; Lee et al., 1971). Spectral

signals are broadened in equimolar mixtures of cholesterol and sphingomyelin cholesterol and phosphatidylcholine in high resolution proton NMR at 220 MHz (Oldfield and Chapman, 1972). Above transition temperature the hydrocarbon chains in the presence of cholesterol are inflexible and is consistent with results obtained for equimolar cerebroside and cholesterol dispersions (Oldfield and Chapman, 1972). Intermediate order-disorder phases are relatively temperature insensitive from 20°C to 60°C to DPPC-cholesterol dispersions (Drake et al., 1971). Deuterium NMR, which gives rise to well-defined splittings for specifically deuterated phosphatides, shows that with the addition of cholesterol (1:1 molar ratio) to pure bilayers of diperdeuteromyristoylphosphatidylcholine (DDMPC), the rotations of the acyl side chains are restricted (Oldfield et al., 1971). As expected, the irregular steroid ring does not penetrate to the apolar ends of the hydrocarbon chains where it could affect the motion of the hydrocarbon chains to a great extent (Drake et al., 1971; Hubbell and McConnell, 1971). Both intact chains (Ladbrooke and Chapman, 1969; Dekruyff

et al., 1972 and  $\beta$ -hydroxyl groups are required for steroid interactions with lipid hydrocarbon chains and this has been confirmed by ESR studies (Hsia et al., 1972; Hsia and Boggs, 1972). Viscous sites exist for phospholipid-cholesterol complexes above the transition temperature of the phospholipids (Chapman, 1975). The binding of cholesterol to a phospholipid molecule with the lowest transition temperature in a binary mixture implies that cholesterol may selectively bind to protein localized in only fluid regions (Dekruiff et al., 1974). X-ray diffraction and DSC measurements support the existence of nonrandom domains where cholesterol has selectively been bound to proteins (Engelman and Rothman, 1972; Hinz and Sturtevant, 1972; Verkley et al., 1974). Cooling of DDMPC-cholesterol complexes below the  $T_m$  results in a slight decrease in the mobility of deuterium-labeled hydrocarbon chains along with an increase of the average time distributions of rotations. The hydrocarbon chain of cholesterol itself exhibits considerable rotational movement detectable in DDMPC mixtures by  $^2\text{H}$  NMR (Kroon et al., 1975).

Cholesterol's effect on the fluidity profile determined by electron spin resonance (ESR) techniques on phospholipids (egg PC-cholesterol, 2:1 molar ratio) and other lipid classes (Oldfield and Chapman, 1971) indicates that the first eight carbon atoms adjacent to the bilayer surface are held rather rigidly (Hubbell and McConnell, 1971). Hydrocarbon motions increase with an increased probability of gauche transitions for the remaining methylene atoms moving towards the end of the chain and the center of the bilayer (Chan et al., 1972; Tiddy, 1972). The orientation of the bulky steroid ring restricts the motion of the first eight methylene groups of the phosphatidyl acyl side chain, possibly due to the creation of molecular "cavities." There is little effect by the flexible hydrocarbon chain on cholesterol to immobilize the remaining phosphatide methylene carbons (Rothman and Engelman, 1972; Schrier-Mucillo et al., 1973). In summary, the condensing effect of cholesterol is restricted to a specific hydrocarbon section of a phosphatide molecule. The motion of the third and eleventh carbons of oleic acid in stearyl-oleoylphosphatidylcholine detected by NMR is marginally decreased or unaffected by the addition of cholesterol although the rotational mobility of the



fourteenth carbon of stearylinooleoylphosphatidyl choline is increased (Stoffel et al., 1974).

In both the gel and liquid crystalline states the mobility of fatty acid side chains near polar headgroups are similar. Neither  $^{31}\text{P}$ -NMR nor  $^2\text{H}$ -NMR detect any significant effect of cholesterol on headgroup orientations (Stockton et al., 1974; Cullis et al., 1975).

Both steroid molecules as well as phospholipid molecules tumble about their axes at very fast rates (McConnell and Gaffney, 1970). Using the spin label 4-[2'-(N-oxy-4',4'-dimethyl oxazolidine)] - stearate where the nitroxide group is positioned 4 methylene groups from the polar end, the mobility at the distal end of the hydrocarbon chains is different in DPCC cholesterol dispersions in the gel and liquid crystalline states (Oldfield and Chapman, 1971). Qualitatively, line shape differences are observed for DMPC-cholesterol dispersions and egg PC-cholesterol mixtures using a paramagnetic spin label located twelve methylene groups from the polar carboxyl end. The egg PC-cholesterol dispersion exhibits an isothermal increase in fluidity as compared to DMPC-cholesterol mixtures. Increasing the concentration of cholesterol causes an

observable fluidization of the DMPC-based mixture and a corresponding ordering of the egg phosphatidylcholine system. With the incorporation of a spin labeled cholestane molecule in egg PC vesicles, increasing amounts of added cholesterol increased the order (Hsia et al., 1971). It has been shown that a more parallel (Hemminga, 1975) and perpendicular packing of the fluid fatty acid side chains is produced with the addition of cholesterol (Butler, 1970; Hsia et al., 1970).

Exogenous factors, such as the rapid reversible binding of divalent cations (especially  $\text{Ca}^{2+}$  or  $\text{Mg}^{2+}$ ), are able to modulate membrane fluidity by affecting the surface charge of the bilayer. This modification is generally localized to the polar headgroup region of the bilayer or superficially exposed hydrocarbons that are separated by steroid spacers in cholesterol-lipid dispersions (Abrahamsson et al., 1977). The effect of metallic cations are generally observed with phospholipid headgroups having a net negative charge in contrast to zwitterionic phosphatides such as phosphatidylcholine.  $\text{Ca}^{2+}$  ions destabilize spherical phosphatidylglycerol-phosphatidylcholine liposomal bilayers and induce a highly organized cylindrical lamellae

structure (van Dijck et al., 1978). In concentrations greater than 1 mM, they abolish the characteristic transition temperature of phosphatidylserine (PS) and phosphatidylglycerol (PG) dispersions (Jacobson and Papahadjopoulos, 1975). Concentrations of  $\text{Ca}^{2+}$  in the 2 mM-10 mM range cause the phase transition of PS-PC bilayers to separate into two phases: a solid PS domain, with chelating  $\text{Ca}^{2+}$  bridges, and a more fluid PC phase (Ohnishi and Ito, 1973, 1974; Galla and Sackmann, 1975). Physical methods have further substantiated the evidence of solid fatty acid domains induced by divalent salts (Papahadjopoulos et al., 1974; Jacobson and Papahadjopoulos, 1975; Papahadjopoulos and Poste, 1975). This same effect is observed in eggphosphatidylcholine-phosphatidic acid dispersions (Ito and Ohnishi, 1974) but not when charged phospholipids such as dipalmitoylphosphatidylglycerol (DPPG) or phosphatidylethanolamine (PE) are substituted for PC. Discrepancies caused by differences in the headgroup structure, incongruities in the miscibility properties of the phosphatide hydrocarbon chains, or dissimilarities in the headgroup ionization pH could explain the disappearance of phase separations with an increase in the transition temperature (e.g., DLPG:DLPC or DMPG:DMPC

dispersions) (Verkleij et al., 1974; Van Dijck et al., 1975). It is estimated that one  $\text{Ca}^{2+}$  molecule for every two charged phospholipid molecules is able to force the lipid into a highly packed configuration (Verkleij et al., 1974; Van Dijck et al., 1975).  $\text{Mg}^{2+}$  ions are one tenth as effective as  $\text{Ca}^{2+}$  cations and appear to form less stable bridges. Binding is accompanied by an increase in the transition temperature (by 10-20° C) of beef brain phosphatidylserine and DMPG vesicles (Kimmelberg and Papahadjopoulos, 1974; Trauble and Eibl, 1974; Verkleij et al., 1974; Jacobson and Papahadjopoulos, 1975; Papahadjopoulos, 1976b). Heavy metal ions, for example  $\text{UO}_2^{2+}$ , significantly increases the transition temperature of anionic phosphatides (Chapman et al., 1974).

The effects of  $\text{Ca}^{2+}$  and  $\text{Mg}^{2+}$  on fluidity are variable. Doubling the concentration of  $\text{Ca}^{2+}$  from 2 mM to 4 mM causes a decrease in the ESR order parameter (Saurebauer et al., 1977). The increased charge on the polar headgroup is strongly dependent upon the geometry of the polar region (Van Dijck et al., 1978), and the repulsion between neighboring headgroups has been suggested to account for the increase in hydrocarbon chain mobilities (Trauble and Eibl, 1974).  $\text{Ca}^{2+}$ -induced complexing

has been implicated in nerve conduction and most prominently in cell surface adhesion where  $\text{Ca}^{2+}$  ions chelate to surfaces (Ohnishi and Ito, 1974). Monovalent ions in the suspending buffer of phospholipid dispersions and in biomembrane systems can interfere with modulation of membrane fluidity. Phase transitions can be induced isothermally by altering the pH (Trauble and Eibl, 1974; Jacobson and Papahadjopoulos, 1975): for DPMA (dipalmitoylphosphatidic acid) the  $T_m$  is decreased from  $67^\circ\text{C}$  to  $58^\circ\text{C}$  when the pH is increased from 6.5 to 9.1, respectively. This effect has been postulated to be the result of a change from negative charge to complete ionization at a basic pH of the phospholipid headgroup (Jacobson and Papahadjopoulos, 1975; Van Dijck, 1978). Deprotonation of phosphatidylethanolamine results in a decreased transition temperature (Eibl, 1977; Eibl and Wooley, 1979). Pretransitions occur in phosphatidylcholine (Chapman et al., 1967), phosphatidic acid (Harlos et al., 1979), and phosphatidylglycerol dispersions (Watts et al., 1978). These pretransitions, as is the case for 1,2 dihexyl-decylphosphatidylethanolamine, are dependent upon the ionic charge of the headgroup. This structural analogue to dipalmitoylphosphatidylethanolamine (DPPE) is used to circumvent the ester hydrolysis of

diacylphosphatidylethanolamines at high pH and has been applied in the study of ionic strength endothermic phase transitions of phosphatides (Eibl and Blume, 1979; Harlos et al., 1979; Jahnig et al., 1979; Blume and Eibl, 1980). With NaCl concentrations of 0.75 M to 1.5 M at pH>13, the polar headgroup is deprotonated and possesses one net negative charge per molecule. Under these conditions, a pre-transition always occurs before the main transition temperature indicated by DSC analysis (Stumpel et al., 1980).

### III. Membrane Hydrocarbon Flexibility Gradients

Theoretical models have been proposed (Marcelja, 1974; Scott, 1974; Jacobs et al., 1975; Jackson, 1976; Cotterill, 1976; Kimura and Nakano, 1979) to account for the apparent freedom of fatty acid acyl side chains towards the methyl end of the chain and the contrasting restriction in the polar headgroup region. Collectively, this temperature-dependent flexibility gradient exists not only on the basis of chain thermodynamics and statistics but also on the basis of data from electron spin resonance, deuterium magnetic resonance, and fluorescence polarization techniques (Figure 8). The state of bilayer hydrocarbon chains monitored by either ESR or DNMR measurements is presently contradictory.

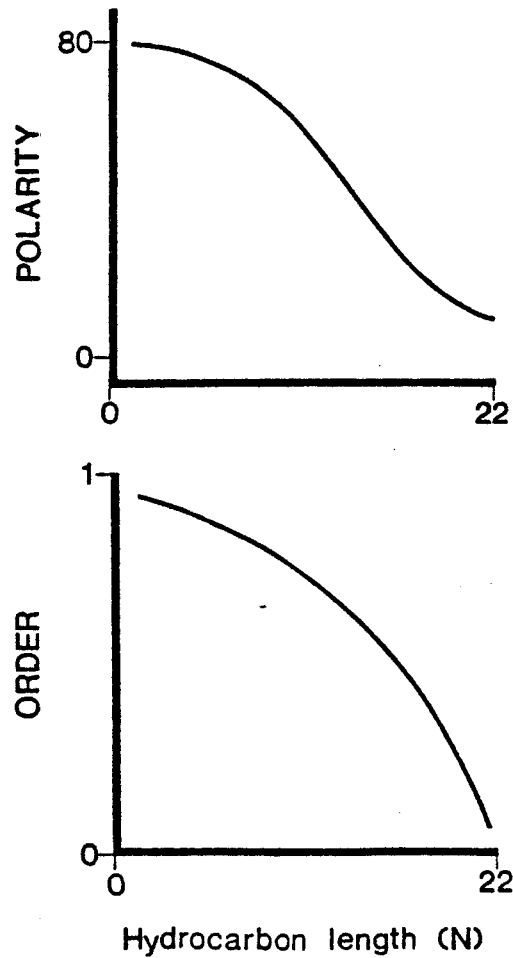


FIG 6: Comparison of the polavity and order gradients in membrane bilayers progressing from the water: hydrocarbon interface to the hydrophobic bilayer interior approximately at a 22 methylene group penetration depth. (From Jain and Wagner, 1980.)

NMR techniques detect a plateau of constrained order up to eight methylene groups from the glycerol backbone; whereas, ESR order parameters perceive the rotations as a biphasic increasing disorder gradient (Figure 9).

Parameters of  $^2\text{H}$  NMR (deuterium magnetic resonance, DMR) spectra can be quantitatively analyzed for the deuterium order parameter,  $S_{\text{CD}}$ , and the segmental order parameter,  $S_{\text{mol}}$  (Seelig and Seelig, 1977). The segmental order parameter,  $S_{\text{CD}}$ , is defined by the order of a carbon-deuterium (C-D) methylene bond normal to the plane of the bilayer. The orientation of individual C-C segments will coincide with the axis of the hydrocarbon chain when it is frozen in an all-trans configuration. This allows the two parameters to be related by the equation  $S_{\text{mol}} = -2 S_{\text{CD}}$  (Appendix I). The order parameter  $S_{\text{mol}}$  provides information on the ordering of the chain axis and is compatible with the order parameter determined by electron spin resonance.  $S_{\text{mol}}$  relates to the average momentary angle of the chain with respect to the bilayer normal ( $\beta$ ). The geometric configuration of the chain structure can be correlated with chain geometry obviating the need for statistical analysis.



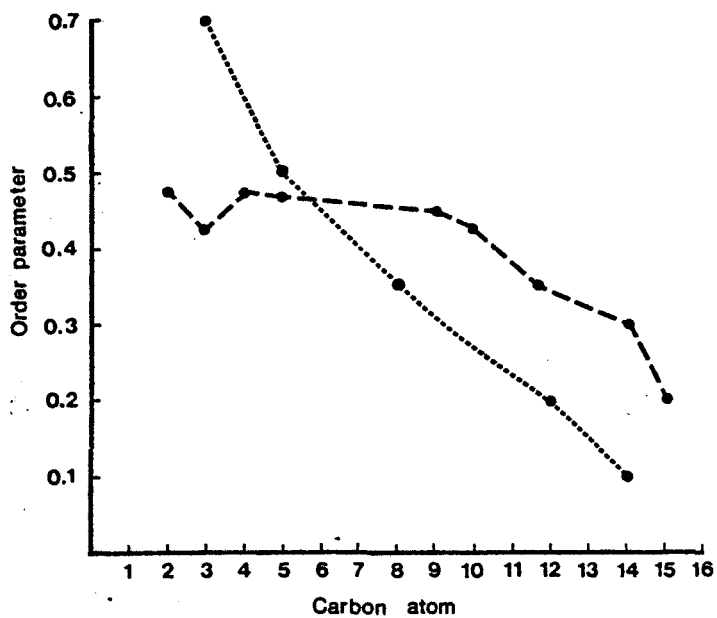


FIG 7: Comparison of the NMR (---) and ESR (.....) order parameters as a function of lipid hydrocarbon penetration length. (Redrawn from Seelig and Seelig, 1977.)

Deuterium magnetic resonance is able to differentiate between order and fluidity within a bilayer.  $^2\text{H}$  NMR of dipalmitoyl-3-sn-phosphatidylcholine (DPPC) where the second carbon atom of the palmitic acid chain is labeled with deuterium nuclei displays three separate signals. These arise for the observed magnetic resonance at approximately 30 kHz with the hydrocarbon chain at the 1' position on the glycerol backbone and at 14 kHz and 23 kHz with the acyl chain at the 2' position (Seelig and Seelig, 1974, 1975). The differences in conformation between the 1' and 2' chains are supported by X-ray diffraction studies on crystalline bilayers of dilauroylphosphatidylethanolamine (Hitchcock et al., 1974) and DPPC-water dispersions (Buldt et al., 1978). Compared to the corresponding hydrocarbon chain at the 1' position, the 2' chain is bent at the first segment and penetrates less deeply into the bilayer core. The first segment of the 2' chain is oriented essentially parallel to the bilayer surface (Seelig and Seelig, 1975; Schindler and Seelig, 1975) in contrast to the chain located at the 1' position which is extended perpendicular to the bilayer surface. Restraint or twisting of one chain segment in the headgroup region affects the motion of other portions of the hydrocarbon

chains. For example, two small quadrupole splittings (2-3 kHz) are observed for the C-3 segment and for the C-10 through C-15 segments (Seelig and Seelig, 1974b). Fatty acid acyl side chains are, therefore, not totally equivalent since identical segments of two chains can be positioned at slightly different distances from the polar headgroup-water interface and have different rotational movements. In all cases a zig-zag in the order parameter is present between carbons two and four (Seelig and Browning, 1978).

Bilayers of DPPC (Seelig and Seelig, 1975), dimyristoyl-3-phosphatidylcholine (DMPC) (Oldfield et al., 1971), dipalmitoyl-sn-phosphatidylethanolamine (DPPE) (Seelig and Browning, 1978), dipalmitoyl phosphatidyl serine (DPPS) 1-palmitoyl-2-oleoyl-phosphatidylcholine (POPC) (Seelig and Seelig, 1977; Seelig and Waespe-Sarcevic, 1978), and  $\omega$ -d<sub>3</sub>-stearic acid in multilamellar dispersions of egg phosphatidylcholine (Stockton et al., 1976) indicate that with the exception of the terminal 6 or 7 segments only a slight variation is observed in the deuterium order parameter,  $S_{mol}$ . A constant rate of motion exists for segment conformations in the hydrocarbon chain towards the tenth methylene group (i.e.  $n = 10$ ) after which there is a large increase in molecular rotations.

The decrease in order approaching the terminal end of the fatty acid acyl side chain can be correlated with the rotational freedom exhibited by a hydrocarbon tail in a less densely restricted area. Plateaus not observable on an ESR timescale may be due to a higher probability of kinks ( $g^+ \leftrightarrow g^-$  or  $g^- \leftrightarrow g^+$ ) in the polar headgroup region (Smith et al., 1978). The exact effect of a kink appears to return the axis of the acyl chain to a position approximately normal to the bilayer plane (or previous conformation) before the first disruption of configuration by a single gauche isomerization. Specifically for POPC, the divergence in order profile between the fifth and ninth carbon atoms is a result of the cis double bond stiffening (Seelig and Seelig, 1977). Qualitatively, the greatest perturbations of the flexibility profile are caused by hydrocarbon isomerizations rather than negatively charged headgroups [e.g., DPPS (Seelig and Browning, 1978)] or protein in the bilayer (Dahlquist et al., 1977).

Cholesterol qualitatively conserves the flexibility gradient detected by deuterium magnetic resonance. In the region of two to ten methylene carbons from the polar headgroups, order is constant and rapidly decreases toward the terminal methyl

group (Stockton and Smith, 1976). Cholesterol stabilizes unusual conformations of steroid-hydrocarbon chain interactions when it is intercalated into egg phosphatidylcholine bilayers. Due to the length of the extended sterol acyl side chain ( $70 \text{ \AA}$ ) which is greater than the effective half-thickness of a phosphatidylcholine bilayer, the sterol hydrocarbon chain is either inserted into the phosphatide acyl side chains of the opposing monolayer or is compacted into unusual configurations. Nine configurations for the sterol hydrocarbon chain are possible. Three, however, are highly improbable due to the small surface area of the cholesterol molecule ( $70 \text{ \AA}^2$  for cholesterol linolenate) and the placement of the hydrophobic cholesterol acyl moiety within the polar headgroup region (Valic et al., 1979). The remaining configurations cannot affect the plateau region (determined by DMR order parameters) to any extent because of the constant packing of inflexible steroid rings between hydrocarbon chains. Since the diameter of the sterol hydrocarbon chain is approximately one-half of the diameter of the ring nucleus, it may be able to produce slight constraints upon the fatty acid acyl carbons in the region from the tenth to eighteenth methylene group (Smith et al., 1978).  $^2\text{H}$  NMR of

non-selectively perdeuterated cholesterol esters (Valic et al., 1979) exhibits considerably smaller (less than one-half) order parameters than that of corresponding phosphatide hydrocarbon chains. Favored conformations are possible in which the sterol hydrocarbon side chains assume a "horseshoe" configuration. The arc that is formed is partially similar to the geometrical calculation for a potential helical arc that could be formed by palmitic acid chains (Stockton et al., 1976).

Deuterium magnetic resonance is able to differentiate between order and fluidity of a particular system. For a lipid bilayer, the terms are not synonymous, and there exists no well-defined relationship equating the two parameters.  $^2\text{H}$  NMR deflects the coexistence of disordered hydrocarbon chains within ordered bilayers. A ternary dispersion composed of sodium decanoate:decanol:water has an order parameter  $S_{\text{mol}} \approx -0.6$  in the constant plateau region (Seelig and Niederberger, 1974b; Neiderberger and Seelig, 1974) while the microviscosity is estimated as 0.05 poise (Schindler and Seelig, 1973, 1974). DPPC bilayers, however, are a less ordered system ( $S_{\text{mol}} = 0.4-0.5$ ), but the microviscosity determined by ESR diffusion studies is increased tenfold (Devaux and McConnell, 1972; Trauble

and Sackmann, 1973). The lyotropic liquid crystal (soap) bilayer of decanol is ordered yet highly fluid in contrast to a DPCC bilayer which is less ordered and less fluid. Fluidity is therefore independent of the deuterium order parameter (Seelig, 1977). Other soap-like bilayers possess constant order only for the first nine to ten methylene groups (Charvolin et al., 1973; Seelig and Niederberger, 1974b), becoming disordered thereafter. Deuterium magnetic resonance indicates that constant order up to the tenth methylene group is a general characteristic of equal length saturated fatty acyl phosphatidyl side chains in bilayer arrangements.

Electron spin resonance techniques using nitroxide-labeled derivatives of fatty acids, phospholipids, and sterol molecules have provided evidence that the rotation of hydrocarbon chain increases as the probe is moved from the headgroup region toward the center of the lipid bilayer. Derived from the hyperfine splittings of experimental spectra, the ESR order parameter, denoted  $S$ , is a numerical value corresponding to the fluidity of a specific region. Unlike the NMR order parameters ( $S_{CD}$  or  $S_{mol}$ ) which measure segmental motion, the ESR order parameter is a measure of the average orientation of a spin label with respect to the bilayer

plane. A value of  $S=1$  means that within a time frame of  $10^{-8}$  sec molecular motion does not significantly change the orientation of the  $\pi$ -orbital for the unpaired spin. Various motions of the label have been assigned to numerical values of the order parameter less than unity ( $S < 1.0$ ). Spin labels undergoing isotropic motion can be used to measure rotational correlation times in the range of  $10^{-7}$  to  $10^{-9}$  seconds (McCally et al., 1972; Shimshick and McConnell, 1972). Anisotropic motion, exemplified by rotating spin labels in biomembranes, produces a time-averaged spectra which is the ESR order parameter (Seelig, 1970; Hubbell and McConnell, 1971). ESR and NMR are sensitive to molecular motions on a time scale of  $10^{-8}$  seconds and  $10^{-5}$  seconds, respectively. The ESR spectra arising from spin labels are a composite of complex dipole-dipole, spin-exchange, and polarity interactions. Qualitative and quantitative hyperfine splittings observed in the spectra are motion dependent (Hamilton and McConnell, 1968; McConnell and McFarland, 1970; Hubbell and McConnell, 1971; Shimshick and McConnell, 1972; McCalley et al., 1972), and concentration dependent (DeVaux and McConnell, 1972; Kornberg and McConnell, 1971).

Model bilayers probed with spin labels at varying positions on the acyl chains (Waggoner



et al., 1969; Hubbell and McConnell, 1971) can accurately sense the average mobilities of phosphatide hydrocarbon side chains. The freedom of motion for phospholipid or fatty acid spin labels increases with increasing distance from the polar carboxyl group and corresponds to variations within the interior of the bilayer. Incorporated into smectic liquid crystals (Seelig, 1970) or phosphatide dispersions (Hubbell and McConnell, 1971), the doxyl derivatives of fatty acid hydrocarbon chains with the spin label at a specific position on the backbone contain an unpaired electron in a  $\pi$  orbital situated on the oxazolidine ring R which is parallel to the backbone of the hydrocarbon chain. The rotation of the nitroxide group then mirrors the rotation and flexibility of the surrounding hydrocarbon chains. As the distance between the label and the polar carboxyl group increases, the amplitude of motions of spin labeled fatty acids increases, and this may be expressed as a linear decrease in  $\log S$  with increasing number ( $n$ ) of methylene groups separating the label and the polar group. The profile of increasing motion with increasing  $n$  has been termed the "flexibility gradient" and is present in both DPPC bilayers and liquid crystals (Hubbell and McConnell, 1971). This relationship is presumed to be the result

of an increasing probability of gauche isomerizations (Seelig, 1970). The center of the bilayer is generally more fluid and more hydrophobic than the headgroup region as determined by a decrease in the isotropic splitting constant, and this appears to be a general property of spin labels in bilayers. Hubbell and McConnell (1971) and Seelig (1970) have interpreted this flexibility gradient as being consistent with a bilayer model which assumes rapid trans-gauche isomerizations, occurring with equal probability at each methylene position on the hydrocarbon chain. This model, however, does not account for the increasing motion in an array of parallel packed hydrocarbon chains (McFarland and McConnell, 1971).

Fatty acid spin labels can be esterified on the glycerol backbone of lysophosphatidylcholine forming a spin-labeled phosphatidylcholine molecule. When intercalated into egg phosphatidylcholine bilayers, the spin label shows a greater than logarithmic decrease in the order parameter (Seelig, 1970; Hubbell and McConnell, 1971). The model of spin-labeled phosphatide motion has been modified to include increasing probability of gauche isomers near the terminal methyl group. In this case, the majority of the hydrocarbon axis may be perpendicular to the

bilayer plane but bent in another region. Chain orientation is gradual throughout the bilayer (Levine and Wilkins, 1971). ESR studies of oriented bilayers have determined that the rate of cooperative interactions of trans-gauche bendings are rapid on the order of  $10^{-8}$  seconds.

Spectra of spin-labeled phospholipids in oriented lecithin bilayers with an increasing spin-label separation (n) (5, 8, 12, and 16 methylene groups) exhibit a flexibility gradient. The time-averaged orientation of chains near the terminal methylene group is perpendicular to the bilayer normal; whereas, the plane of the oxazolidine ring is tilted when the nitroxide is positioned in the polar headgroup region.\* Gaussian analysis of the spectral shape shows that the degree of tilt is dependent upon the positioning of the nitroxide group in the bilayer. The most probable angles of tilt were found to be approximately 5°, 20°, 30°, and 31° corresponding to insertion depths of 16, 12, 8, and 5 methylene groups, respectively (McFarland and McConnell, 1971).

---

\*N is the separation between the carboxyl group and oxazolidinoyl ring containing the nitroxide. The actual depth of insertion is given as (n+2) and is reported here as this value.

Hydrocarbon chains closest to the polar headgroup region of a bilayer are collectively tilted with respect to the bilayer plane. Trans-gauche<sup>+</sup>-gauche<sup>-</sup> isomerizations of the hydrocarbon chain near the terminal methylene carbon are more probable than in the polar headgroup region. As a result of these rotations, the degree of packing allows larger amplitude high frequency motion towards the bilayer center. A tilt of 30° near the headgroup region produces an approximately 12% increase in the hydrocarbon chain density around the terminal methyl groups. The hydrocarbon chains are normal to the bilayer although the carbon atom density of a bilayer in the hydrocarbon chain region is nearly constant (Wilkins et al., 1971; McConnell and McFarland, 1971).

Tilt of hydrocarbon chains is biophysically significant. It has been suggested that phosphatide polar headgroups create amphiphilic or hydrophobic pockets in the bilayer by rotation of a group of tilted phosphatides 180° about an axis perpendicular to the bilayer plane. Long range lipid or lipid-protein interactions may be due to a "domino effect" of multiple groups of tilted phosphatides (McFarland and McConnell, 1971). Recalculation of the degree of tilt in ensemble

averaged order parameters\* (Gaffney and McConnell, 1974a) for hydrated bilayers of egg phosphatidylcholine and egg phosphatidylcholine-cholesterol dispersions (2:1 molar ratio), indicates that the flexibility gradient measured by intercalated spin labels involves both a frequency and amplitude gradient. The amplitude of hydrocarbon rotations and isomerizations (i.e. motions) produces a flexibility gradient; moreover, since  $S_c$  is not equivalent to  $S$ , a frequency gradient can coexist which is similar to the frequency-amplitude deuterium order parameter.

$^2\text{H}$  NMR studies of oriented bilayers of C-5 deuterated DPPC inclined at a magic angle with respect to the magnetic field exhibit a collapse of the quadrupole splittings (Seelig and Seelig, 1974a). Rotations about the lipid hydrocarbon axis or isomerizations about the individual C-C bonds are axially symmetric around the bilayer plane, and no collective tilt is present with a lifetime longer than  $10^{-6}$  seconds. Additional  $^2\text{H}$  NMR studies of ternary soap-like bilayers (Charvolin et al., 1973; Seelig and

---

\*It must be remembered that the  $\pi$ -orbital of the nitroxide group in the oxazolidine ring is fixed in geometry with respect to the long axis of the corresponding fatty acid, and therefore, rotations of the hydrocarbon chain are mimicked by rotations of the nitroxide  $\pi$ -orbital.

Niederberger, 1974a) imply that no tilt or bending on an NMR timescale exists for the hydrocarbon chains in a bilayer.

There are qualitative and quantitative differences between the frequency-amplitude deuterium order parameter and those rotation derived ESR order parameters. These differences have been attributed to perturbations of the spin label in the surrounding hydrocarbon environment and to artifacts produced by spin-labelled phospholipids. Tilt has only been observed with spin-labelled phospholipids and not with spin-labelled fatty acids in egg phosphatidylcholine dispersions. NMR and ESR operate on different timescales. The lifetime of a tilted chain region is short on an  $^2\text{H}$  NMR timescale ( $10^{-5}$  to  $10^{-6}$  seconds) but long on an ESR scale ( $10^{-7}$  to  $10^{-9}$  seconds). This results in a slighter smaller deuterium order parameter value than the one calculated using ESR assumptions. (Gaffney and McConnell, 1974; Seelig and Seelig, 1974). Egg phosphatidylcholine bilayers appear to be an example of a system possessing a time-averaged tilting of hydrocarbon chains since ESR order parameter measurements indicate greater order than those made with deuterium magnetic resonance (Gaffney and McConnell, 1974; McConnell, 1976; Seelig and Seelig, 1977). The

ensemble-averaged order parameter\* (ESR) is equivalent to the frequency-amplitude  $^2\text{H}$  NMR order parameter and may be rationalized if the lifetime of tilt near the polar headgroup is from  $10^{-7}$  to  $10^{-5}$  seconds. In summary, the average motion of hydrocarbon chains has a rate approximating that of the nuclear quadrupole interactions but is in effect actually slower than the rate of hyperfine interactions.

The discrepancy between order parameters may also be attributed to perturbations of the microenvironment by spin labels. A penetrating nitroxide ring increases the hydrocarbon chain diameter approximately twofold. When the parallel packing of the chain is disrupted and additional space is created by the oxazolidine ring, disordered molecular motion is increased. Statistical-mechanical calculations indicate that spin label order parameters can only fit experimental data if chain-chain interactions are increased (Belle et al., 1974; Belle and Bothorel, 1974). A spin-labelled bilayer and a nonperturbed hydrocarbon bilayer, therefore, are geometrically non-equivalent (Seelig and Seelig, 1974). The large volume

---

\*The ensemble-averaged order parameter,  $S_C$  (McConnell, 1976) is defined by  $S_C = \frac{1}{2} \langle 3 \cos^2 \nu - 1 \rangle$  where  $\nu$  is the angle between the principal hyperfine axis  $z$ , and some axis fixed relative to the sample. The average is over all molecules in the sample at a given instant of time.

occupied by oxazolidine rings has been proposed (Mason and Polnaszek, 1979) to increase the slow motion effects rather than to lower the ESR order parameter. Slow motions in liquid crystals (with a frequency from  $10^{-7}$  to  $10^{-8}$  seconds) affect the widths and separations of spin label hyperfine spectra\* (Polnaszek and Freed, 1975). Two types of motion may lower the observed order parameter below its true value. The first motion which is fast on a ESR timescale (Hubbell and McConnell, 1969; McConnell and McFarland, 1970) can be described by a rotational correlation time about a symmetry axis,  $\tau_{R\parallel}$ . Motions with a frequency greater than  $2 \times 10^{-10}$  seconds (Mason et al., 1974) in the absence of any tilt angle occur with an axis normal to the bilayer plane. The axis, however, may diverge from the nitroxide orbital axis. Slow motion on the ESR timescale (Mason et al., 1974) can be defined by a rotational correlation time about a perpendicular symmetry axis  $\tau_{R\perp}$ . The value of  $\tau_{R\perp}$  for deuterated bilayers by  $^2\text{H}$  NMR measurements is longer than  $10^{-4}$  seconds. In contrast, spin-labelled lipids produce shorter  $\tau_{R\perp}$ 's, resulting in the distortion of surrounding hydrocarbon chains by

---

\*Correlation times as short as  $10^{-8}$  seconds affecting the degree of the ESR hyperfine widths are consistent with anisotropic motion described by the effective Hamiltonian in that time frame.



oxazolidine rings (Stockton et al., 1976). Variations in  $\tau_R$  produce significant effects on spectral hyperfine splittings and consequently on the calculated value of the ESR order parameter (Mason and Polnaszck, 1978). Values of  $\tau_R$  less than  $3 \times 10^{-7}$  seconds preferentially broaden the outer hyperfine maxima (Mason et al., 1974, 1977). ESR order parameters ( $S^S$ ) may be smaller than their corresponding true S value as a result of  $\tau_R$  being shorter than  $3 \times 10^{-7}$  seconds. Rigid limit orientations (Hwang et al., 1975; Mason et al., 1977) and pseudo-axial rigid limits (McFarland and McConnell, 1971; Schindler and Seelig, 1973; Gaffney and McConnell, 1974) produce similar effects with finite slow values of  $\tau_R$ . The slow motion time frame ( $10^{-6}$  to  $10^{-7}$  seconds) corresponds to a time-averaged tilting of the hydrocarbon chains, accounting for an increase in ESR order parameters for polar headgroup regions (Gaffney and McConnell, 1974).

Another model which attempts to account for the discrepancy in the degree of tilt on magnetic resonance timescales (Peterson and Chan, 1977) separates the order parameter into two components: one component is attributed to the trans-gauche isomerization  $s(S_\rho)$ , and the second is due to reorientation (tilt) motions of entire chains ( $S_\gamma$ ).

With this model, the overall order parameter is redefined as  $S = S_{\beta} S_{\gamma}$  with  $0.3 < S_{\gamma} < 0.58$ .

#### IV. Fluidity of Biomembranes

The physical properties of naturally occurring biomembranes can be studied utilizing the same methodologies that have been applied to the study of lipid dynamics in synthetic lipid dispersions. The heterogeneity of biological membranes, lipid-protein complexes and bulk lipid regions contribute to the apparent fluidity observed by exogenous probes. Experimental evidence indicates that lipid dispersions from extracted membrane lipids possess similar lipid orientations and motions to those observed in native biomembranes (except in the case of proteins that are lipid dependent, i.e., rhodopsin or ATPase).

##### A. Plasma Membrane Preparations

Fluorescence polarization studies have been used to obtain microviscosity values for a large variety of isolated plasma membranes (Feinstein et al., 1975). The apparent microviscosity ranges from one to ten poise (P). Microviscosity, defined in poise units, is an average weighted value of lipid dynamics due to the equal partitioning of DPH (1,6-diphenyl-1,3,5-hexatriene) and other fluorescent dyes into various lipid phases (Lentz et al., 1976; Stubbs et al., 1976). Protein, usually absent in model dispersions, produces the same qualitative effect as

cholesterol (Shinitzky and Inbar, 1976; Jonas, 1977; Jonas et al., 1977) by decreasing the overall microviscosity. This effect diminishes at cholesterol:phospholipid ratios above (1:2) (Shinitzky and Inbar, 1976). Low values of microviscosity (1-3 poise) were found for plasma membranes of human erythrocytes (Rudy and Gilter, 1972; Aloni et al., 1974; Vanderkooi et al., 1974; Feinstein et al., 1975; Kehry et al., 1977) using perylene, DPH, and DL-12-(9-anthroyl)stearic acid(12-AS). The same range of microviscosity is observed for other membranes. Bovine brain myelin (Feinstein et al., 1975) possesses an apparent microviscosity of 2.7 poise. Rabbit polymorphonuclear lymphocytes and human peripheral lymphocytes possess values of 3.35 P and 1.1 poise, respectively (Rudy and Gilter, 1972). Furthermore, DPH fluorescence polarization studies have been applied to determine the microviscosity of chick embryo myoblasts (Prives and Shinitzky, 1977), chick embryo heart (Kutchai et al., 1976), bovine heart mitochondria and bovine chromaffin granules (Shinitzky and Inbar, 1976), mouse microsomes (Tubsamen et al., 1976), mycoplasma membranes (Rottem et al., 1973), E. coli membranes (Overath and Trauble, 1973; Cheng et al., 1974; Overath et al., 1975), protoplast plasmalemma (Borochoy et al., 1976), and bacterial envelopes (Helgerson et al., 1974; Lanyi et al., 1974; Nieva-Gomez and Gennis, 1977).

The microviscosity of these systems is closely related to the microviscosity of white whale oil (1.15 poise), phosphatidylserine dispersions (1.73 poise), and phosphatidylserine:cholesterol mixtures (1:1 molar ratio).

Electron spin resonance of lobster walking nerve, (Ladbroke et al., 1968) using TEMPO partitioning, indicated a poise value between 0.25 and 25. Hubbell and McConnell (1969) showed that the ESR order parameter varied with the position of the nitroxide along the hydrocarbon chain as it is situated in biological membranes. Typical S values were 0.63 and 0.45 for nitroxide separation values of 5 and 12 respectively. Sarcoplasmic reticulum vesicles (McConnell et al., 1972) have nearly identical order parameter values of 0.63 (n=5) and 0.35 (n=12). These values are in disagreement with the order parameter of vesicles from Halobacterium cutribrium. For a separation value of n=12, the order parameter equaled 0.73; whereas, a value of S=0.35 was obtained for a nitroxide at the fifth position (Esser and Lanyi, 1973). Overall, isolated plasma membranes possess qualitatively restricted fluidity in the headgroup region and motional freedom at the terminal end of the hydrocarbon chains comparable to that of synthetic lipid dispersions. The discrepancy between the values obtained for eukaryotic plasma membrane preparations and Halobacterium cutirubium data could be a

result of the toleration of different salt concentrations which are necessary for growth and division systems.

#### B. Whole Cell Correlations

Direct evidence associating model membrane studies to complex in vivo membranes has been inferred from physical studies on several Mycoplasma species and the bacterium E. coli to a lesser extent. Mycoplasmas, unlike other prokaryotic organisms, have no cell wall or intracellular structures and resemble bacterial protoplasts. Studies of the plasma membrane show no extraneous intracellular membranous contamination, a feature that is also found in erythrocytes. Mycoplasmas, however, are capable of reproduction and growth. Perhaps the greatest advantage of mycoplasmas for membrane studies lies in their inability to synthesize long chain fatty acids (either saturated or unsaturated chains depending on the particular species) and their total dependency on media-derived cholesterol for growth. The membrane lipid composition of mycoplasmas can be controlled by the exogenous levels of growth medium lipids, thereby allowing the manipulation of the membrane organization. (For extensive reviews of mycoplasma membranes including both physical studies and control mechanisms for the regulation of membrane fluidity, the reader is referred to Razin, 1975; Baile et al., 1979; Rottem, 1980).

The numerous relationships between membrane biomolecules exhibited in more simple model systems are also expressed in Mycoplasma membranes, although the interrelationships between adjacent and transposed membrane components becomes more complex. Mycoplasma cells studied by differential scanning calorimetry (DSC) also possess an endothermic gel-liquid crystalline phase transition similarly observed with aqueous dispersions of lipids. The phase transition temperature is consistently dependent on the chain length and the degree of membrane lipid unsaturation (Steim et al., 1969; Reinert and Steim, 1970; Rottem et al., 1973; DeKruyff et al., 1972). It decreases with increased levels of fatty acid unsaturation. Mycoplasma phase transition temperatures range from a 20°C to a 25°C spread, and sometimes up to a 30°C span (McElhaney, 1974). In contrast to the well-defined phase transition of specific pure phospholipid dispersions, the broad phase transition of mycoplasma membranes possess low cooperativity (Oldfield and Chapman, 1972; McElhaney et al., 1973) as a result of the heterogeneity of mycoplasma lipid components and their differing transition temperatures (Chapman and Urbina, 1971; Saito and McElhaney, 1977). X-ray diffraction studies of A. laidlawii (Engleman, 1971) support the broadening effect for phase transitions in heterogenous bilayers.

Mycoplasmas can also be adapted to grow at varying concentrations of exogenous cholesterol (Rottem et al., 1973). A Mycoplasma mycoides subcapri clone has been adapted to grow with decreased cholesterol levels present in the culture medium. The cholesterol content of the adapted strain is less than 3% of the total membrane lipids and is in contrast to levels of 22-26% in the native strain. The cholesterol-depleted variant possesses a gel-liquid crystalline phase transition at 25°C which is not observed in the cholesterol-rich strain. The phase behavior, furthermore, is accompanied by changes in fatty acid composition, ultrastructure, and growth properties of the two cell types (Rottem et al., 1973a, 1973b; LeGrimellac and Leblance, 1978). The native sterol-rich strain was able to grow normally at temperatures lower than 25°C; whereas, growth was halted for the cholesterol-poor cells. Rottem et al. (1973a) proposed that cholesterol maintains the "intermediate" fluidity state which was absent in the sterol-poor strains, thereby allowing the continued function of membrane bound enzymes, such as ATPase. Furthermore, freeze fracture of the sterol-poor cells at 4°C indicates smooth-faced areas of lipid rich domains. The cholesterol-rich strain, on the other hand, does not possess thermotropic phase aggregates of membranous particles.

Electron spin resonance of spin-labelled fatty acids in A. laidlawii shows that flexibility gradients also exist within complicated heterogeneous membranes (Rottem et al., 1970). The fluidities of bilayers decrease slightly with increasing protein:lipid ratios as a result of the cooperative ordering of proteins. Protein:lipid ratios increase on aging in M. hominis, thereby decreasing nitroxide fluidity and affecting membrane-associated enzymes (Rottem and Greenberg, 1975). Enzymatic digestion of membranes with pronase (Rottem and Samuni, 1973) increases the fluidity. Heat denaturation and glutaraldehyde fixation (Rottem et al., 1970; Tourtellotte et al., 1970) do not affect the mobility of the spin labels, indicating the important role of lipid-lipid interactions in the determination of membrane fluidity. Enrichment of the cells with oleic acid increases the spin label fluidity; whereas, supplementation with palmitate, stearate, and elaidic acids decrease the freedom of motion for the nitroxide label. TEMPO partitioning studies, moreover, corroborate DSC and X-ray diffraction bilayer evidence for broad thermal phase transitions (Metcalfe et al., 1972).

Deuterium magnetic resonance spectroscopy of A. laidlawii grown at 37°C with perdeuterated lauric or palmitic acids (Oldfield et al., 1972) indicates that the mycoplasma bilayer exists in a constrained gel



configuration similar to dimyristoyl phosphatidylcholine. Oldfield et al. (1972) postulated that organisms with low levels of cholesterol or those lacking it completely possess separate gel and liquid crystalline domains within their membranes. Data from perdeuteration of the terminal methyl group of palmitic acid and biosynthetic incorporation into the plasma membrane bilayer lipids of A. laidlawii support the dual existence of gel and liquid crystalline regions below the growth and transition temperatures (Stockton et al., 1975). Above the growth temperature, the bilayer may exist in a liquid crystalline state. A plot of the deuterium order parameter versus deuteration position resembles the shape of the plots for egg phosphatidylcholine and dipalmitoyl phosphatidylcholine. The addition of cholesterol to A. laidlawii (Stockton et al., 1977) with deuterated phospholipid palmitate chains increases the spreading of the order parameter. Therefore, the ordering effect of cholesterol upon the deuterium order parameter flexibility gradient plateau region which exists for liquid crystal models, also affects the lipid organization in native biological membranes.

Calorimetric techniques have been applied to additional prokaryotes, in particular E. coli (Blazyck and Steim, 1972; Jackson and Sturtevant, 1977; Jackson and

Cronan, 1978) plasma, mitochondria, and microsomal membranes. The phase transitions of non- and low-cholesterol containing membranes are qualitatively identical to those observed for mycoplasma. E. coli plasma membranes, isolated from cells cultured with unsaturated fatty acid analogue growth supplements show a broad (15-25°C) DSC-determined gel to liquid crystalline phase transition. X-ray diffraction data substantiates this effect (Schechter et al., 1974; Overath et al., 1975; Linden et al., 1977; Harder and Banaszak, 1979). The  $T_m$  of whole cells, plasma membranes, and isolated phospholipid dispersions is dependent upon the fatty acid composition of that particular membrane (Baldassare et al., 1976). Saturated fatty acid levels shift the  $T_m$  to a sharp peak centered around 1°C. Substitution with monene unsaturates (16:1 and 18:1) shifts the phase transition below 0°C, indicative of an unusual intermediate phase.

ESR partitioning parameters (Linden et al., 1973; Sackmann et al., 1973; Rottem and Leive, 1977) determined using TEMPO and 5-doxylstearate indicate lateral phase separations of lipid clusters (Wunderlich et al., 1975) that were not resolved by DSC. It is possible to replace 50-85% of the natural fatty acids with deuterium analogues (Pluschke et al., 1978; Galley et al., 1979). Deuterium magnetic resonance using a superconducting magnet for

maximal sensitivity (61.4 MHz) yielded unique spectra if the label was attached at the C-2 position on the hydrocarbon backbone or at the cis-double bond of the 2' fatty acid. The sn-1 chain extends perpendicularly to the bilayer plane along its entire length while the sn-2 chain is bent perpendicularly only after the C-2 segment. The cis-double bond between C-9 and C-10 does not lie exactly parallel to the bilayer normal since the quadruple splittings for the C-9 and C-10 deuterons are different. These results are analogous to the tilt observed in POPC (1-palmitoyl-2-oleoyl-sn-glycero-3-phosphocholine) bilayers at 7-8°C (Seelig and Waespe-Sarcevic, 1978). Deuterium order parameters for cells supplemented with palmitic acid are similar to the  $S_{CD}$  of POPC dispersions at the sn-1 position, while the order parameter of cells enriched in oleate is similar to the sn-2 of POPC. Moreover, the plateau region, present in synthetic phospholipid dispersions, was also observed for both types of lipid enrichments. The deuterium order parameter, therefore, is independent of the composition of the fatty acid chains in biological membranes but is dependent on the distance of the deuterated segment from the polar headgroup.

#### C. Fluidity of Normal and Transformed Cells

Fluorescent and spin-labelled probe techniques have been extrapolated from model membrane studies to

examine the similarities and differences of normal and "transformed" cell systems in vitro. These techniques have been applied to study the effects of differentiation, phase of the cell cycle, growth factors, growth potential, and nutrition on plasma membrane functions. Comparison of these techniques on identical cell systems results in differing estimations of membrane fluidity. Overall, the dissimilarities in the mobility of membrane lipid components described by fluorescent or ESR methods may be partially based on a perturbation of the local micro-environment by a particular probe.

Fluorescent probes in general are bulky, hydrophobic molecules, dissimilar in structure to membrane components. They may not only produce structural aberrations upon intercalation into bilayers (comparable to the insertion of steroid spacers between fatty acid chains but also variations in bilayer free energy and entropy. The latter are presumably due to restrictions on adjacent hydrocarbon motional ordering induced by the probe itself. Spin label probes, on the other hand, are smaller in size and molecular shape and possess both hydrophobic and hydrophilic regions similar to native fatty acids and phospholipids. Both fluorescent probe and ESR studies are sensitive to changes in membrane polarity and may be influenced by heterogeneous domains of

lipid components. The methods, however, are sensitive to different average timescales of protein and lipid motion. Comparisons of microviscosity with magnetic resonance ordering must take into account the intuitive discrepancy that exists between these methods. The overall dilemma, therefore, of identifying variations in normal and transformed membrane systems is comprised not only of the physical limitations of the methodology employed but also the similarities and/or differences of the appropriate cellular models.

#### Fluorescent Polarization

Fluorescent polarization offers a sensitive and reproducible method for estimating membrane fluidity. As with other biophysical techniques, however, interpretation of data from probes localized in heterogenous lipid domains is difficult. A number of fluorescent dyes have been employed to estimate membrane fluidity (Azzi, 1975). The most frequently employed polarization probes, 1,6-diphenyl-1,3,4-hexatriene (DPH) and perylene (PYL), differ in their technique of incorporation into membranes. Hydrophobic DPH may be spontaneously intercalated into membranes by partitioning through the aqueous medium or by direct contact to the bilayer surface (Stubbs et al., 1976; Thompson et al., 1977). This probe, in contrast to perylene which must be coupled to a membrane component, dissolves in the plasma

membrane after a short exposure to intact cells. An equilibrium, however, is attained with time as the probe partitions into subcellular membranes. The rate of partitioning is specific for each cell type and must be taken into account for the correct interpretation of fluorescent data.

Using the degree of plasma membrane polarization to indicate relative probe partitioning, the movement of probe from plasma membrane to a cholesterol-poor, more fluid subcellular membrane would be reflected by a relative decrease in the plasma membrane polarization (Shinitzky and Inbar, 1974; DeLaat et al., 1978). Ambiguous results may be caused by changes in refractive index and filtering effects of the cell interior. These effects generally increase the degree of observable fluorescence for plasma membrane, although for these reasons, correct interpretation of membrane fluidity using fluorescent probes must be correlated with isolated membranes (Shinitzky and Barenholz, 1978).

The majority of fluorescence polarization studies have been carried out using normal and transformed fibroblasts in vitro and lymphocytes from patients of varying pathological states.

SV-40 transformed BALB/c 3T3 A-31 fibroblasts show an approximately 50% decrease in polarization upon

transformation compared to normal BALB/c 3T3 A-31 fibroblasts (Fuchs et al., 1975; Parola et al., 1976). Probed with DPH, the results were interpreted as indicating a decrease in membrane fluidity for the transformed variant. Normal hamster fibroblasts also possess a higher lipid microviscosity upon transformation (Shinitzky and Inbar, 1976) as well as fibroblasts derived from rat and hamster embryos (Inbar et al., 1977). In both transformed and normal cells the degree of microviscosity is controlled by the degree of cell-cell contact and can be modulated by changing cell culture densities. Membrane microviscosity decreases in subconfluent cultures (high lipid fluidity) but increases in confluent monolayers (low lipid fluidity or a more rigid membrane). The change in membrane microviscosity, however, is most pronounced for transformed cells in confluent conditions as compared with confluent cultures. Ordering of the lipids can be reversed by varying the cell culture density from confluency to subconfluency and vice versa.

The lower fluidity estimated by DPH is not a characteristic of cells transformed by SV-40. Rosenthal et al. (1978) studied the steady-state and nanosecond fluorescence of two variants of malignant Syrian hamster melanoma lines (Davidson and Bick, 1973). This cell system consists of two cell lines: a pigmented clone of

of the RPMI 3460 Syrian hamster cell line (W1) and a BUdr (Bromo-deoxyuridine)-dependent cell line (B4). The B4 cells represent a unique case in which the biological malignancy can be expressed by the presence of BUdr in the medium (at 0.1 mM concentration). Both nanosecond and steady-state fluorescent polarization studies confirm that the transformed cell membranes, B4 cells grown in the presence of BUdr, possess a higher microviscosity (therefore more rigid) than those of the corresponding normal untransformed cells (B4 cells grown without BUdr in the growth media). The opposite effect was exhibited by the melanoma cell line W1 (grown in both BUdr free and containing medium) from which the B4 variant was derived. These cell lines exhibit opposite responses to transformation: the B4 cells in media without BUdr resemble W1 cells grown in BUdr medium.

Comparisons between normal and RSV (Rous sarcoma virus) transformed quail embryo fibroblasts and their methylcholanthrene transformed counterparts (Nicolau et al., 1978) also exhibit similar decreases in fluidity (longer rotational correlation times) with transformation. The fluidity change is not dependent on the addition of serum to dividing cultures except to stimulate the growth of resting (non-dividing quiescent) contact-inhibited



cells. These fluorescence polarization differences are consistent with both intact cells probed with DPH and isolated membranes. The fatty acid compositions, however, of the normal and transformed cells do not differ (Perdue et al., 1971, 1972; Perdue and Miller, 1973) and neither do the cholesterol:phospholipid molar ratios. Nicolau et al. (1978) concluded that the fluidity of membrane lipids is dependent upon cell density for cell lines that are contact-inhibited (density dependent growth control); whereas, fluidity is independent of cell density in transformed cells that are not contact-inhibited.

Cell cycling produces significant increases in the DPH reported membrane fluidity of regenerating liver and Morris hepatoma 7777 cells (Cheng and Levy, 1979). Rapidly growing tumor membranes compared to isolated plasma membranes of quiescent rat hepatocytes shows a significant temperature dependent decrease in the microviscosity, quantitatively identical to that of fibroblastic cells (Fuchs et al., 1975; Shinitzky and Inbar, 1976; Nicolau et al., 1978; Rosenthal et al., 1978). The microviscosity measured from regenerating cells paralleled the value observed for the resting quiescent liver cells. This was accompanied by an increase in the cholesterol:phospholipid molar ratio (from 0.44 to 0.76) which is identical to that for normal hepatocytes and

Morris hepatoma 7777 cells, respectively. It appears, therefore, that for liver in vivo, cholesterol regulates the levels of membrane fluidity.

DPH has also been used to determine the effect of phospholipid headgroups and acyl side chain composition on membrane fluidity. Gilmore et al. (1979a) studied the DPH fluidity of LM cell variants under varying conditions of lipid supplementation. These cells have specifically been modified in vitro with substitutions in the phospholipid polar headgroup composition (Glasser et al., 1974; Blank et al., 1975; Schroeder et al., 1976b) or in the fatty acid composition (Wisnieski et al., 1973; Williams et al., 1974; Ferguson et al., 1974; Doi et al., 1978) or in both lipid components (Glaser et al., 1974). The rotational correlation time, a measure of microviscosity, increased and decreased, respectively, upon the substitution of ethanolamine for choline and with the supplementation of linoleate in the growth medium. This effect was observed for mitochondrial, microsomal, and plasma membranes; however, specific differences between the fractions were generally dependent upon the headgroup composition, although some less pronounced changes were caused by variations in the phospholipid fatty acid acyl side chain composition. DPH rotational correlation times of isolated phospholipids from individual membrane subfractions indicates that the

headgroup composition produces the major effect on membrane fluidity (Gilmore et al., 1979b). Membranes from cells supplemented with ethanolamine possess greater viscosities (less fluidity) than membranes isolated from choline-supplemented cells (Esko et al., 1977). Whole cells, on the other hand, exhibit the opposite trend with regard to membrane viscosity. This effect is attributed to the partitioning of DPH into the greater concentration of non-membranous neutral lipids rather than being localized in the surface bilayer of ethanolamine supplemented cells.

Taking into account the interference of triacylglycerols and alkyldiacylglycerols on DPH fluorescence polarization measurements, Pessin et al. (1978) studied the plasma membrane properties of normal and RSV (rouv sarcoma virus) transformed chick embryo fibroblasts. At 37°C, the rotational correlation time for transformed cell membranes intercalated with DPH was increased approximately 8% over membranes of normal dividing cells. This change was even larger for membranes of transformed confluent cells. Total lipid extracts from membranes of transformed cells also possess a higher fluorescence polarization, possibly caused by increases in phosphatidylethanolamine headgroup levels, 18:1 fatty acids, and decreases in polyunsaturated fatty acids. Whole cell

measurements are inversely proportional to the concentration of triacylglycerols and alkyldiacylglycerols stored as neutral fat droplets within the cytoplasm. The accumulation of fat droplets, moreover, correlates with the concentration of serum, the degree of cell growth, and the cell density. DPH fluorescence polarization studies indicate that there is a selective decrease in the fluidity of transformed cells (in particular, RSV-transformed fibroblasts). The effect, however, is only observed in isolated membranes or lipid preparations. The same effect observed in whole cell studies must be considered possibly artifactual.

LM cells in suspension cultures have been studied using a naturally occurring fluorescent compound,  $\beta$ -parinaric acid (Schroeder et al., 1976). A compensatory mechanism exists that corrects for differences in lipid composition of cells in monolayer and suspension cultures (Raison et al., 1971; Skler et al., 1975).\* LM cells modified with structural analogues of native phospholipids maintain their characteristic phase transition temperatures measured by DPH and ANS (8-anilino-1-naphthalene sulfonic acid) fluorescence probes (Schroeder et al., 1976a). In

---

\*This same type of effect is observed for the neuroblastoma N-2a clone (Charalampous, 1977, 1979). Differentiated cells grown as monolayers contained higher concentrations of PS and PC and lower concentrations of PE than the undifferentiated cells maintained in suspension culture.

contrast to previous studies (Skler et al., 1975; Williams and Chapman, 1968), the characteristic phase transition temperatures for plasma, mitochondrial and microsomal membranes are unaffected with as much as 50% of the headgroups substituted by analogues. The effect was also observed after resuspension of the respective isolated lipids.

"Homeoviscous adaptation" occurs not only in LM cells (Schroeder, 1978), but also in E. coli and Tetrahymena (Martin and Thompson, 1978). The adaptive changes of membrane fluidity are first observed in endoplasmic reticuli (Martin and Thompson, 1978) followed by dissemination to the other cellular membranes. Phospholipid headgroup metabolism, therefore, is implicated in the modulation of phospholipid headgroup composition and more importantly, phospholipid acyl side chain composition (Schroeder, 1978). Supplementation of choline directly affects the unsaturated to saturated fatty acid ratio, the degree of unsaturation (decreased in the plasma membrane fraction), and the chain length ratio (increased in the plasma membrane fraction) of the choline-containing phosphatides. The anionic phospholipids (PE, PG, PI, and PS) exhibit the same trends as phosphatidylcholine. Specific methylation of choline headgroups producing structural analogues decreases the unsaturated to

saturated fatty acid ratios and increases the average chain length ratio.

Membrane fluidity measured by different fluorescent probes report the microviscosity for specifically differing environments within the bilayer. Membranes of normal baby hamster kidney (BHK) cells and those persistently infected with lymphocytic choriomeningitis virus (LCV) along with BHK trypsinized RSV-transformed BHK cells show increased membrane fluidity when probed with pyrene and N-phenyl-1-naphthylamine fluorescent probes (Burleson et al., 1978). The latter probe indicates a less polar environment within membranes of the RSV-transformed cells.

A previous study by Edwards et al (1976) examined the membrane fluidity of normal and two Rous sarcoma transformed variants of baby hamster kidney cells (BHK). The transformed cell lines, BHK-t-1 and BHK-T-2, possess tumorigenic potential in vivo and in vitro as evidenced by the formation of tumore in weanling hamsters and by colony formation in soft agar. The non-transformed strain BHK-21 does not exhibit these malignant characteristics. Dissimilar fluorescent probes indicate there may be intrinsic differences not only between normal and transformed cells but also between the two tumorigenic strains themselves. Following transformation, N-phenyl-1-naphthylamine fluorescent probes reside in more polar environments

compared to the parental BHK-21 cells. The membrane of the BHK-T-1 variant is more fluid than that of its normal counterpart while the BHK-T-2 cells possess even less order than the BHK-T-1 cells. Small fluorescent probes such as pyrene possess long-range mobility (i.e., high diffusibility in both lateral and transverse planes of the membrane bilayer). Pyrene, therefore, describes lipid dynamics in large areas of the membrane since the probe readily diffuses within the bilayer; whereas, N-phenyl-1-naphthylamine monitors its immediate environment with little or no diffusion. Incorporated into BHK-T-1 cells, pyrene fluorescent excitation indicates that the plasma membranes of these cells are more restricted than either the BHK-T-2 or the BHK-21 cells. Since the excited lifetimes of fluorescence differ for all three cell types, Edwards et al. (1976) suggested that there may be differences in the membrane organization between not only normal and transformed cells but also between transformed cell types from one parental phenotype.

Transformation of baby hamster kidney (BHK) cells and mouse 3T3 fibroblasts by encephalomyocarditis (EMC), west nile (WN), and polyoma (Py) viruses is accompanied by an increase in fluorescence-determined membrane fluidity (Levanon et al., 1977). Fluidity increases were independent of the nucleic acid composition of the adsorbed

viruses (RNA naked, RNA enveloped, and DNA naked strands) or their structure and function. The increase in fluidity was virus-dependent due to dose dependency and inhibition of membrane alterations by the blockage of viral receptors.

These two studies contradict the DPH fluorescent polarization studies utilizing chick fibroblasts, L cells, and LM cells. The trends in fluorescence microviscosity for normal and transformed cells and membrane composition may be partially due to a previously uncontrolled intrinsic characteristic of each cell line. For example, DPH measured microviscosity of synchronized C1300 mouse neuroblastoma cells (DeLaat et al., 1977) indicates that the cell membrane of mitotic cells is more rigid than that of interphase cells. The microviscosity increases (less fluid) by a factor of two during mitosis, decreases during the S phase, and decreases and increases during the G1 and G2 phases, respectively. Cell cycle dependence of membrane fluidity has been supported by other studies (Furcht and Scott, 1974; Garrido, 1975). Additionally, the lipid composition of the cell membrane has been shown to be altered during the G1 phase (Shinitzky and Inbar, 1976).

Animal and human lymphocytes derived from various pathological conditions also exhibit decreases in fluorescent microviscosity when compared to cells derived from normal donors (Cooper, 1977, 1978). Due to the minimal



level of lipid metabolism, the lipid composition of erythrocytes and platelets reflects changes in the host serum lipids (Stubbs et al., 1976; Cooper et al., 1977, 1978). Probed with DPH, mouse malignant lymphocytes possess a more fluid membrane than normal lymphocytes, possibly due to a decreased cholesterol:phospholipid ratio (Inbar and Shinitzky, 1974; Shinitzky and Inbar, 1974; Inbar, 1976). SPH probe motion also indicates greater mobility (fluidity) for mouse GRSL ascites leukemia cells cultured in vitro and in vivo, Reuber H35 rat hepatoma in vitro and in vivo, and Novikoff solid and ascites hepatoma cells maintained intraperitoneally in rats when compared to mouse thymocytes and rat liver cells in vitro (RLC), respectively. Van Hoesen et al. (1979) attempted to correlate the apparent fluorescent microviscosity of these systems with the lipid composition of isolated plasma membranes. The phospholipid and polar lipid acyl side chain composition did not reflect variations in fluorescent sensed fluidity nor were the changes consistent with the method of growth (in vivo or in vitro). Rather, they were cell phenotype specific. Human lymphocytes and mononuclear cells from patients with malignant lymphomas and leukemias possess more fluid lipid bilayers compared to lymphocytes from normal patients or patients with non-malignant disorders (Inbar and Ben-Bassat, 1976; Ben-Bassat et al.,

1977). The microviscosity of human red blood cells, furthermore, has been reported to be altered by the cholesterol:phospholipid ratio (Cooper, 1978). As the cholesterol content decreases or the phospholipid content increases, the rotational diffusion of DPH indicates a decrease in membrane fluidity. Johnson and Robinson (1979) attribute the increased fluidity of leukemic and lymphomatous lymphocyte plasma membranes to the increased levels of free fatty acids and glycerides rather than cholesterol. No differences were observed between normal and malignant lymphocyte fluidities, cholesterol:phospholipid ratios, or phospholipid composition. Increased DPH fluidity, however, was manifested between mouse Gardner lymphoma cells and normal mouse splenic lymphocytes. This can be attributed to the previously mentioned evidence of alterations only within specific cell phenotypes.

The respiratory distress syndrome of newborns, possibly related to lipid irregularities of pulmonary surfactants (Gluck et al., 1972), has been studied using a fluorescent polarization assay (Shinitzky et al., 1976). Fluorescent polarization values above 0.320 have been shown to be positively correlated with the probable occurrence of respiratory distress syndrome (Blumenfeld et al., 1978) compared to values in the range of 0.2-0.3 found for normal mature fetal lungs.

## Electron Spin Resonance

ESR, NMR, and fluorescence polarization methods yield information concerning membrane dynamics, though only fluorescence probe techniques have been extensively applied to the study of membrane fluidity in neoplasia. In contrast to the diversity of normal and neoplastic cell types that have been utilized for fluorescence studies, ESR spin labelled membrane analogues have been used to probe lipid and protein motions in only three major cell systems. These include mouse 3T3 fibroblasts and their SV-40 transformed variant SV101-3T3 fibroblasts, normal chick embryo cells (CEF) and CEF cells transformed by Rous sarcoma virus, and Ehrlich ascites tumor cells.

Magnetic resonance offers some distinct advantages over fluorescence polarization probes. Polarization of fluorescent probes is an extrapolation of classical hydrodynamics from macroscopic systems used to describe the microviscosity of microscopic molecular domains. The application of equations for microviscosity that are based on a theoretical homogeneous system such as lipid dispersions to heterogeneous biological membranes may result in an oversimplified description of membrane component interactions which affect fluidity. Magnetic resonance techniques, on the other hand, describe the real time average motions of membrane biomolecules. Because a lipid

component may be isotopically enriched or replaced by a spin-label analogue, chain rotations, flexing, headgroup interactions, and effects of cholesterol, specific regions of phospholipid hydrocarbon chains observed during magnetic resonance studies may closely resemble actual lipid dynamics. The fluidity parameters described by ESR and NMR are specific in nature and therefore do not refer to the overall fluidity as does fluorescence polarization. ESR analyzed orientations should more accurately reflect lipid dynamics than fluorescent probe analysis although the spin label itself may perturb the local lipid microenvironment. This local perturbation is thought to account for the discrepancies between magnetic resonant and fluorescent derived fluidity parameters.

Early ESR data attempted to correlate the differences between contact-inhibited (i.e., normal) 3T3 fibroblasts and neoplastic 3T3 fibroblasts which were chemically or virally transformed. Barnett et al. (1974) probed simian virus 40 (SV40), polynoma virus (PV), murine sarcoma virus (MSV), and methylcholanthrene transformed 3T3 fibroblasts with the spin label 6-(4'-4'-dimethyloxazolidinyl-N-oxyl)-heptadecanate (10,3,

according to the terminology of Gaffney) and attributed the decrease in order parameter for transformed cells to greater fluidity of phospholipids. A later study (Gaffney, 1975) done on the identical cell system with increasing chain separation of the probe molecules exhibited no differences between normal and transformed cells. Thus, earlier ESR data on changes in membrane fluidity using the (10,3) probe are at best inconclusive since inconsistent data were observed for the (7,6) and (5,10) probes.

The 5, 10, and 14 doxyl stearate spin labels used to probe whole cells and isolated plasma membranes of 3T3 fibroblasts and SV101 3T3 fibroblasts (Hatten, 1975; Hatten et al., 1978) indicate no difference between normal and transformed variants. Cells grown in lipid-depleted serum that has been enriched with oleate or elaidate were controlled by some mechanism of fluidity regulation elucidated by a constant order parameter. The membrane fluidity appears independent of cell density, trypsinization, and mitotic stage of the cell cycle. Although the value of T was temperature-dependent and influenced by the membrane fatty acid composition, the phase transition temperatures for normal and transformed cells did not vary. The 5-doxyl stearate T splitting showed characteristic inflections at 14° and 18°C for

cells grown in regular serum, with a shift towards 25°C and 30°C for cells enriched with elaidate. Oleate enrichment resulted in a nearly linear temperature dependence with only one inflection point at 5°C.

Tempo partitioning studies (Hatten et al., 1978) indicate greater membrane complexity although they show no differences between critical temperatures for the 3T3 and SV101 transformed fibroblasts. Cells grown in regular serum possess critical temperatures at 12°C, 18°C, and 32°C in contrast to those supplemented with oleate (18:1 trans) that had phase transition temperatures of 4°C, 8°C, 22°C, and 32°C. Elaidate supplementation (18:2 trans) allows a greater number of phase separations to be sensed by tempo (17°C, 20°C, 26°C, 32°C, and 37°C). Partitioning studies with 5-doxy1 stearate in LM cells (Wisnieski et al., 1974) show characteristic temperatures of 9°C, 16°C, 22°C, 32°C, and 38°C (Wisnieski et al., 1974b) and phase behavior temperatures of 16°C and 35°C for isolated membrane lipid dispersions. In summary, temperature inflections are sensitive to phospholipid fatty acid acyl chain modifications which are supported by data from fluorescent polarization studies.

Yau et al. (1976) examined the correlation between phospholipid composition and membrane fluidity in normal, exponentially growing chick embryo fibroblasts and CEF

cells transformed by Rous sarcoma virus. Nitroxide spin labels located at 5, 12, and 16 methylene groups from the nitroxide moiety and the polar carboxyl end of the hydrocarbon chain on stearic acid were incubated with the cells in vitro for six to eight hours. The transformed cells showed increased rotational correlation times ( $\tau_c$ ) for the stearate probe labelled at positions 12 and 16. Compared to non-transformed normal cells, virally transformed cells demonstrated a decrease in the rotation of the nitroxide inferred as an increase in the order of the bilayer. Rotational correlation times were statistically significant for the probe with a nitroxide at the 16th position (16,1 probe) on the stearate chain. The decrease in the mobility of the label should correlate to decreased levels of unsaturated fatty acid membrane phospholipids of transformed cells which would allow tighter packing of the hydrocarbon chains. The implication of stearic restriction has been substantiated by a decrease in unsaturation level for all phospholipid classes of transformed cells, whether whole cell or isolated plasma membrane. Phospholipid saturation changes appear to be an intrinsic property of cellular transformation since they are not dependent on variations in the growth rate or viral infection for either of the transformed or normal cell types. Furthermore, since the phospholipid headgroup

composition and cholesterol content did not significantly change after transformation, it would be expected that the fluidity measured by the (5,12) probe (stearate labelled at the fifth position along the chain) should be identical for both phenotypes. The order parameters of this probe (5,12) indicate no difference between normal and transformed cell pairs near the polar headgroup region of the membrane bilayer. Rotational freedom of the (16, 1) probe varies with the percentage of arachidonic acid (20:4) as a result of less restricted motion of long chain polyunsaturated fatty acids.

The effects monitored by spin label probes (Yau et al., 1976) probably include those of the plasma membrane as well as those from membranes enveloping subcellular organelles. Considering the exceptionally long labelling time as compared to other studies (Barnett et al., 1974; Gaffney, 1975; Hatten et al., 1976), diffusion of the spin label over the eight-hour incubation period monitors the average motions of all cellular membranes. Yau et al. (1976) argue that the nitroxides preferentially reflect changes in plasma membrane structure based on comparisons of spectra for intact cells and isolated plasma membrane preparations. The solvent polarity of the probe, moreover, indicates that the isotropic hyperfine splitting constant was increased for the label



nearest the headgroup region and decreased in the region of the apolar hydrocarbon chains. These values were lower than the value of the solvent polarity for the free label dissolved in growth medium. ESR spectra of both normal and transformed variants indicates that the more restricted rigid headgroup region increase in rotation exists as the spin label moves towards an unrestricted environment (i.e., near the hydrocarbon tails or bilayer interior). A flexibility gradient or increase in rotational freedom, therefore appears to be a property of bilayer structure, irrespective of specific intrinsic membrane alterations.

SV101 transformed 3T3 fibroblasts have been reported to contain 50%-100% more cholesterol per cell than normal 3T3 fibroblasts (Scandella et al., 1979). The phospholipid content of transformed cells increases accordingly so that the cholesterol:phospholipid ratios for normal and transformed cells are identical. A value of 0.27 for the cholesterol:phospholipid ratio is consistent with other values reported for cells in vitro (Adam et al., 1975; Hatten and Burger, 1979). Intact transformed cells probed with a 5-doxyl stearate spin label coupled to the  $\beta$  position on phosphatidylcholine (spin-labelled phosphatidylcholine, SLPC) exhibit a temperature dependent increase in nitroxide probe motion as compared to the normal cells. These results are

inconsistent with previous studies utilizing the same cell system (Hatten et al., 1976; Gaffney, 1975). The latter studies utilized fatty acid spin labels which diffuse rapidly (i.e., 30 minutes to a few hours) into the lipid phase of a majority of cellular membranes indicating bulk membrane fluidity. After intercalation into the outer monolayer of the plasma membrane bilayer, the spin-labelled phosphatidylcholine should not diffuse as rapidly (requiring a transverse flip-flop motion from the outer to the inner monolayer) as the free stearate nitroxides. The length of the incubation time with the spin labels as well as the diffusion properties of the probes themselves (determined by molecular size) can possibly influence the interpretation of membrane fluidity characteristics for normal and transformed phenotypes.

The degree of lipid unsaturation modified in Ehrlich ascites tumor cells in vivo can be detected using the 5-doxy1 stearate probe (King et al., 1977). Isolated membranes from cells grown in animals that are fed fat deficient chow show a decrease in fluidity compared to cells derived from animals fed regular rodent chow. The two cell types showed similar phospholipid composition, phospholipid:cholesterol ratios, and distributions of fatty acid chain lengths. Cells from fat deficient animals were less unsaturated than cells from animals fed regular

diets; however, the unsaturation was concentrated in the middle of the fatty acid chains (positions 9, 10, 12, and 13). Temperature dependent phase diagrams of intercalated spin labels indicate discontinuities at 19°C and 31°C for animal cells grown on the regular diet compared to discontinuities of 24.5°C and 31.5°C for the cells from fat deficient animals. It was concluded by King et al. (1977) that the broader distribution of unsaturated fatty acids correlates to a lower order parameter and a shift to a lower phase transition for cells derived from animals which were fed regular diet chow.

The lipid composition of Ehrlich ascites cells can be modified in vitro as well (King et al., 1978). Modification of the unsaturated:saturated ration of membrane phospholipids, monitored by the labelling of cells in vivo for four hours with radioactive lipids, was manifested by selective changes in the rotation of the 5-doxyl stearate probe. The mobility of the probe decreased when membranes were enriched with saturated fatty acids and increased upon enrichment at the 12' position (12'-methyl myristate), increased the mobility of the intercalated spin label as expected with the removal of its steric restriction. The

fatty acid changes were observed only in the choline and ethanolamine phospholipid pools which possess rapid turnovers. Spin-label temperature phase diagrams indicate two temperature discontinuities. The phase transition occurring at 31°C is not influenced by variations in fatty acid composition; whereas, the transition between 20°C and 26°C is dependent upon the specific fatty acid enrichment. These temperatures are approximately identical to the phase transition of cells grown in vivo (King et al., 1977); however, they differ from the characteristic temperatures of LM cells probed with fluorescent labels.

Bales and Leon (1978) examined the spin label fluidity of XC sarcoma cells in vitro as well as their isolated membranes. Utilizing the commonly employed nitroxide spin labels, 5-doxy1 stearate, 12-doxy1 stearate, and 16-doxy1 stearate, correlations between the fluidity of whole cells and plasma membranes were only consistently observed for the 5-doxy1 stearate probe. Motion of the 5-doxy1 stearate and 16-doxy1 stearate probes were temperature dependent and inversely proportional to the temperature. No indications of phase transitions were observed for either probe in intact cells or in purified membranes. In contrast to previous investigations where the cell samples are placed in round capillary pipettes

within the microwave cavity, Bales and Leon (1978) utilized a flat quartz ESR cell to orient the samples. The order parameter of the 5-doxyl stearate probe did not vary for spectra recorded when the plane of the cell surface was oriented parallel or perpendicular to the external applied magnetic field. Detachment of the cells from the growth surface using EDTA did not alter the 5-doxyl stearate order parameter. Rotational correlation times of the TEMPO spin label, furthermore, did not vary with attachment of the cells or orientation of the applied magnetic field. A decreasing flexibility gradient is also observed as the probe is moved from the flexible hydrocarbon regions of the membrane towards the phospholipid headgroups. The headgroup region of intact cells, however, appears to be slightly more ordered than the same region in purified membrane preparations.

The correlation between the physical properties of transformed cell membranes during differentiation and their fatty acyl side chain composition has been examined using the 5-doxyl stearate probe (Simon, 1979). No difference was observed for the 5-nitroxide order parameter in either normal myoblasts or  $\text{MGl}^+ \text{D}^+$  cells. The  $\text{MGl}^+ \text{D}^+$  cells, a clone from a mouse myeloid leukemia cell, are able to differentiate into mature cells with the aid of a macrophage and granulocyte protein inducer (MGI).

Another clone,  $MGl^{+}D^{-}$ , cannot be induced to differentiate into mature cells by MGI. The  $MGl^{+}D^{-}$  cells, furthermore, possess a significantly greater degree of fluidity than the  $MGl^{+}D^{+}$  cells or their normal counterparts. This decrease in order correlates with the greater quantity of unsaturated fatty acids present in the plasma membrane. The  $MGl^{+}D^{-}$  clone contains approximately a two-fold increase in polar lipid acyl unsaturation as compared to the  $MGl^{+}D^{+}$  cells. Oleic acid (18:1) is predominantly increased in the  $MGl^{+}D^{-}$  polar lipids; whereas, the  $MGl^{+}D^{+}$  differentiating cells possess a higher level of phospholipid palmitic acid (16:0). The fatty acid unsaturation levels are, furthermore, temperature dependent. Decreasing the growth temperature from 37°C to 32°C increases the level of oleic acid (61% of the total acyl side chain composition) in  $MGl^{+}D^{-}$  cells. With a decrease in temperature to 28°C, only the non-differentiating clone  $MGl^{+}D^{-}$  was able to divide and grow. Growth at this temperature is accompanied by a substantial amount of 5,8,11,15,17-eicosapentenoate (20:5) and a large percentage of the unsaturated phospholipid acyl side chains (approximately 75%). Simon (1979) proposed that the ability of the myeloid leukemic cells to undergo differentiation in vitro results from the increased plasma membrane fluidity predicated upon phospholipid side chain composition. In this

respect, membrane fluidity and differentiation competence may be implicated in a cause and effect relationship. The similarity between fluidity and cell growth from undifferentiated cells to maturity, moreover, is supportive of Bergelson's "membrane differentiation" hypothesis for liver-hepatoma systems.

#### Additional Physical Methods

Differences in lipid composition of rat hepatocytes and rat hepatoma cells (Selkirk et al., 1971; VanHoeven and Emmelot, 1972) may be related to variations in the transition temperatures measured by electron diffraction under physiological conditions (Hui and Parsons, 1976): The transition temperature curves for both cell types reach a plateau at  $17.5^{\circ}\text{C}$ ; however, the origins of the increasing transition rates may be extrapolated to two different values. Hepatoma cells had a lower transition temperature ( $4-5^{\circ}\text{C}$  compared to normal liver at  $11.5^{\circ}\text{C}$ ), frequently indicating lower membrane microviscosity (Hubbell and McConnell, 1971) and increased fluidity.

Nicolau et al. (1975) using  $^2\text{H}$  and  $^{13}\text{C}$  NMR measured the "fluidity" of normal and SV-40 transformed hamster embryo fibroblasts. Insoluble low-speed centrifugation cell pellets, washed in  $\text{D}_2\text{O}$ , produced well-resolved NMR spectra. Resolution of the  $^{13}\text{C}-\text{T}_2$  splittings implied that the transformed cells possess increased

intermolecular membrane motions. However, it is difficult to interpret the data due to the heterogeneity of the particulate "membrane" preparation.

v. Lipid Alterations of Normal and Transformed Cells

Studies on phospholipid abnormalities in diverse normal and tumor cell systems have analyzed whole cells as well as subcellular fractions. The most comprehensive data have been obtained from phospholipid compositional investigations of mitochondria, nuclei, microsomes, whole cell homogenates, and plasma membrane fractions of mouse and rat liver, solid and ascites hepatomas, and sarcomas (for review, see Bergelson, 1972). Fewer studies have examined the phospholipid compositions of brain and its associated neoplasms. Normal and neoplastic liver, however, has been used as a model tissue for a variety of reasons. The availability of material for both in vivo and in vitro transformation model systems has lent itself not only to extensive studies of gross composition but also discrete changes such as positional specificity of acyl side chains upon the phospholipid glycerol backbone. Generalizations of the phospholipid membrane structure of normal and neoplastic liver are considered relevant to membrane abnormalities of normal and neoplastic brain. Although there are implicit and explicit differences in the metabolic and physiological functions of liver and



brain, it could be expected that the plasma membrane for both possesses a similar micro- and macro-molecular structure. From this point of view, the overall inter-relationship of membrane components is not only limited to the plasma membranes of liver and brain, but also includes the overall architecture of erythrocyte membranes. These generalizations are by no means mutually exclusive; each type of plasma membrane arising from different origins possesses distinct functions or discontinuous elements that are cell specific as in the case of energy metabolism and receptor-recognition sites.

The concept of "membrane dedifferentiation" has been hypothesized as a result of liver tissue studies to explain the alterations between phospholipid compositions of normal and tumor cell membranes (Bergelson et al., 1970, 1974). Lipid patterns (phosphatide, cholesterol, and glycolipid) characteristic of normal cellular plasma membranes are lost upon neoplastic transformation. With transformation, the lipid composition of tumors is qualitatively closest to that of fetal tissue, and both may be contrasted to the lipid organization of normal tissues. The overall variability in lipid composition can be considered a sequential progression: undifferentiated cells (fetal) > dedifferentiated cells (tumor) > differentiated cells (normal, possessing functional

individuality). Consistent trends in phospholipid plasma membrane patterns, however, are not observed. This is presumably a result of the difficulty in isolating homogeneous populations of plasma membranes. The "dedifferentiation hypothesis" also has a basis in the growth characteristics of tissues. For example, the growth of cells in vitro mirrors the sequence of dedifferentiation among cells. Undifferentiated cells or cells from fetal origins readily adapt to growth in culture and possess a finite lifespan. Tumor tissues, on the other hand, are variable in their response to the initiation of growth in vitro. Depending on the degree of differentiation, tumor cells may possess either a finite or infinite lifespan. Cells derived from differentiated "normal" tissues, however, possess a finite lifespan and are the most difficult to propagate in culture. The order of growth potential in vitro may be defined as fetal (undifferentiated)  $\geq$  tumor (dedifferentiated)  $>$  normal (differentiated).

#### A. General Tumor Models

Phospholipid variations are present in plasma membranes, subcellular organelle fractions, and gross homogenates of normal murine liver and chemically induced hepatic neoplastic cells. In general, hepatomas possess a significantly smaller amount

of all phospholipids (Weber and Cantero, 1975; Veerkamp et al., 1961; Figard and Greenberg, 1962; Dyatlovitskaya et al., 1969; Synder et al., 1969). Overall levels of the choline phosphatides are generally lower in neoplastic tissues than in corresponding normal liver (Giray, 1963; Synder et al., 1969; Bergelson et al., 1970, 1974). However, primary and transplanted hepatomas possess choline phosphatides in comparable quantities to normal tissues (Veerkamp et al., 1961; Bergelson et al., 1970; Synder et al., 1970). Individually, the quantities of sphingomyelin and phosphatidylserine are both increased in hepatomas (Weber and Cantero, 1957; Figard and Greenberg, 1962; Veerkamp et al., 1961; Dyatlovitskaya et al., 1969; Synder et al., 1969). the increase in sphingomyelin, moreover, appears to be a general characteristic of neoplastic liver (Wallach, 1975). Other phosphatides such as phosphatidylethanolamine and phosphatidylinositol show little variation in normal and tumor tissue.

The patterns of specific phospholipid disturbances in gross homogenates are not similar to enriched membrane fractions. Extensive analysis of hepatoma and Jensen rat sarcoma plasma membranes (Feo et al., 1970; Bergelson et al., 1970) indicates an increase in the tumor phosphatidylserine concentration. Sphingomyelin, however, is decreased in hepatoma and sarcoma tissue along with phosphatidyl-

choline. These changes, not surprisingly, are juxtaposed with other subcellular membrane fractions, particularly mitochondrial and microsomal membranes. Hepatomas contain a high concentration of diphosphatidylglycerol in microsomal subfractions; whereas, this component is completely absent in normal liver. The converse situation is present in hepatoma mitochondria where diphosphatidylglycerol concentrations are approximately one-half that of normal liver. Hepatoma derived mitochondria also contain increased levels of sphingomyelin and lyso-phosphatidylcholine.

Typically, the phospholipid patterns of hepatoma subcellular fractions resemble the phospholipid variation of whole tumor cells and are different from the distribution of lipids in normal liver. Rat and mouse normal liver mitochondria possess a greater concentration of phosphatidylethanolamine and a lesser concentration of serine and inositol phosphatides. Sphingomyelin is virtually non-existent in normal liver mitochondria (Bergelson et al., 1970; Kogl et al., 1960; Mitchell, 1969; Ruggieri and Fallani, 1968; Thiese and Bielka, 1968). Hepatoma mitochondria, on the other hand, contain significant amounts of sphingomyelin and lyso-phosphatidylcholine. The levels of phosphatidylinositol and phosphatidylserine are increased in hepatomas; whereas, the level of phosphatidylethanolamine may be equal to or lower than

that of normal tissues (Bergelson et al., 1970; Kogl et al., 1960; Mitchell, 1969; Ruggiere and Fallani, 1968; Thiese and Bielka, 1968).

Tumor organelles do not reflect the same lipid trends as observed in gross homogenates. Sphingomyelin and phosphatidylinositol levels for example, in normal liver microsomes are increased while the phosphatidylethanolamine to phosphatidylcholine ratio is decreased (Collins and Shotlander, 1961; Dallner et al., 1966; Getz et al., 1962, 1968; MacFarlane et al., 1960; Spiro and McKibbin, 1956; Strickland and Benson, 1960; Bergelson et al., 1970, 1974). Phosphatidylserine, lyso-phosphatidylcholine, and sphingomyelin concentrations are increased in hepatomas while the levels of both phosphatidylcholine and phosphatidylethanolamine are variable and generally comparable to the levels present in normal tissues. Only the levels of phosphatidylinositol are consistently less in hepatomas.

Enriched plasma membrane subtractions of rat hepatomas possess lower total phospholipid content compared to plasma membranes isolated from normal adult resting liver (Veerkamp et al., 1961; VanHoeven and Emmelot, 1972). The sphingomyelin and ethanolamine phospholipid concentrations are increased; whereas, the phosphatidylcholine, phosphatidylserine and phosphatidylinositol levels are decreased in plasma membranes of solid

hepatomas (Koizumi et al., 1980). Rat ascites hepatoma plasma membranes possess qualitatively identical phospholipid patterns (Koizumi et al., 1977). These trends are absent in plasma membrane preparations from non-hepatomal regions of hepatoma-bearing livers and pre-neoplastic liver. In general, the phospholipid patterns of neoplastic liver are partially copied in immature, postnatal liver tissue and provide supporting evidence for the embryonic characteristics of hepatomas (Koizumi et al., 1980). Utilizing the implied phospholipid bilayer asymmetry from erythrocyte studies (Bretscher, 1972; Gordesky and Marinetti, 1973; Verkleij et al., 1973) and applying this assumption to hepatoma membranes, Koizumi et al. (1980) proposed that the choline phosphatides in the outer leaflet of the plasma membrane are replaced by ethanolamine phosphoglycerides in multiplying hepatocytes, irrespective of whether the tissue is of normal or neoplastic origin. Plasma membranes from non-tumorigenic regions of hepatomas and regenerate livers, as expected, possess this proposed asymmetric characteristic to the same extent.

In summary, primary and chemically induced rat hepatomas (Veerkamp et al., 1962) possess: (1) a decrease in polyunsaturated fatty acids of all the phospholipid classes, (2) increases in the mono- and di-

unsaturated fatty acid species, (3) an appearance of 18:1 and 16:1 species, (4) a decrease in the main chain length with the appearance of 14:0 fatty acids, and (5) an increase in the cholesterol content. The general decrease in unsaturation was not present in mouse hepatomas. Thereby, variations in a specific phospholipid disturbance may be evident only with certain phenotypes of cells (VanHoeve et al., 1975) or may be the result of differences in the maintenance and production of hepatomas (i.e., solid transplantations versus i.p. transplantation and growth in ascites fluid (Koizumi et al., 1980).

Disturbances in the positional specificity of the phospholipid acyl side chains are more pronounced in hepatomas. In normal tissues, the 1'-position of the glycerol backbone is usually occupied by saturated fatty acids; whereas, the 2'-position generally has a high concentration of unsaturated fatty acids with the exception of 18:1 (Dyatlsvitshaya et al., 1974). In summary: (1) the fatty acid position on the glycerol moiety of the phospholipid molecule is less specific in hepatomas compared to normal liver, (2) neoplastic tissue has a higher concentration of mono-unsaturated and di-unsaturated species than does normal liver, and (3) the phosphatidylcholine glycerol backbone in hepatomas can be characterized by the high content of

1'-unsaturated, 2'-saturated species and a lower concentration of 1'-saturated and 2'-unsaturated species as compared to non-neoplastic liver (Bergelson and Dyatlsvitshya, 1973).

#### B. Normal Brain

Brain and nervous tissue, especially white matter, has been known to contain high concentrations of lipids since the beginning of the eighteenth century (Vauquelin, 1811). Differences in the phosphorus containing lipids (Couerbe, 1934) were predicted to be a pathological consequence of mental disease. Although this hypothesis was disproved, there are numerous pathological states in animals and humans that are a consequence of deviations from normal lipid and phosphatide metabolism (Siegel et al., 1976). More than half of the dry weight of normal human brain is lipid, and the lipid component, as a part of the membrane structure, can be divided into two major groupings: polar lipids (phospholipids and glycolipids) and neutral lipids (essentially cholesterol). Normally, triglycerides, free fatty acids, and sterol esters are present in only very small amounts.

The earliest investigations on brain lipids (Brante, 1949; Folch, 1955; Johnson et al., 1948a, 1948b, 1949) established the approximate composition of the major



phosphoglycerides for different areas of the brain and for normal brain of various age categories (Cumings et al., 1958; Balakrishnan et al., 1961). Unfortunately, the methodology employed did not allow for complete fractionation and resolution of the cephalins. With the advent of the chromatographic techniques of Rouser et al. (1961), more complete separation of the major lipid classes of cerebral gray and white matter in infants and adults was possible (O'Brien and Sampson, 1965a, 1965b). Gray matter contained 36-40% lipid; white matter contained 49-66%; and 78-81% of the dry weight of myelin was lipid. Gray matter possesses a higher molar percentage of phosphatidylethanolamine, phosphatidylcholine, and ceramides than myelin, the overall lipid composition of white matter is close to that of the myelin subfraction. White matter has a greater percentage of cholesterol and cerebroside; whereas, the molar percentages of phosphatidylserine and sphingomyelin are approximately equal for gray and white matter. A more complete study of fetal brain (Svennerholm, 1968) determined that the choline-containing phospholipids constitute 50 mole% of the total lipid with the ethanolamine phosphoglycerides amounting to nearly 30 mole%, and the remaining phosphatides (phosphatidylserine, phosphatidylinositol, and sphingomyelin) constitute slightly greater than 20 mole%. As

children grow older, the choline phosphoglycerides decrease to 35-40 mole% with a concomitant 5-10 mole% increase of phosphatidylethanolamine. Although white matter contains 25% less choline phosphoglycerides, it contains greater concentrations of serine phosphoglycerides and sphingomyelin than gray matter. The ethanolamine phosphoglyceride quantities are about the same in white and gray matter. Furthermore, 18:0 fatty acids constitute the majority of the fatty acids contained in ethanolamine phosphoglycerides of gray matter at all ages. In fetal brains, the polyunsaturated fatty acids of the linoleate series predominate along with 20:4(n-6) and 22:4(n-6) fatty acids. Also, these unsaturated fatty acids of the linoleic series decrease with age. The serine and inositol phosphoglycerides show higher concentrations of 18:0 fatty acids than that of the ethanolamine phosphoglyceride acyl side chains. However, at the same time, 16:0, 18:1, and 20:4(n-6) fatty acids enrich the inositol phosphoglycerides. Although the choline phosphoglycerides have a very low content of polyunsaturated fatty acids from the linolenic series, the major fatty acids are 16:0 and 18:1 whereby the concentration of 16:0 is greater in gray matter, and 18:1 increases in adult white matter. The increased concentration of monoene 18:1 is also increased in white matter phosphatidylcholine, while most of the 20:4(n-6)

and 22:6(n-3) fatty acids are present in gray matter phosphatidylcholine (White, 1974). No differences are seen in the levels of 18:2(n-6) and 22:4(n-6) phosphatidylcholine acyl side chains. Trends appear while examining the unsaturation index (UI) in the mean fatty acid unsaturation of normal brain. An inverse relationship is found to exist between the ethanolamine phosphoglycerides of gray and white matter. The unsaturation index increases with age in gray matter; whereas, the converse effect was found in white matter phosphatidylethanolamine. On the other hand, the unsaturation index value for the choline phosphoglyceride fraction is similar for infant and adult white and gray matters. Phospholipid and fatty acid compositions of resolved phosphoglyceride classes from microsomal subfractions of normal, adult human brain (Sun and Leung, 1974) agreed with the previous data showing an increase in 20:4(n-6) ethanolamine phosphoglycerides accompanied by an increase of 22:4(n-6) fatty acid, the elongation product of 20:4(n-6).

#### C. Brain Tumors

There appears to be a great variation in the phospholipid content of human brain tumors. The earliest investigation done on 38 intracranial neoplasms (Cumings, 1943) revealed substantially lower levels of phosphoglycerides in the tumor tissue with measurably higher

higher levels in their cystic fluids. Bronte (1949) concluded that a relatively low phospholipid content and a high esterified cholesterol content were characteristic of brain tumors. This tenet was substantiated by other studies (Randall, 1940; Cohen, 1955; Selversone and Moulton, 1957; Cumings et al., 1958) that reported tumors contain one-third to one-half of the phospholipid content of normal brain and relative changes occur in the amounts of individual phospholipid subfractions. For some brain tumors, the amount of phosphatidylcholine is decreased to a lesser extent than the phosphatidylethanolamine; while for other specimens, it has been shown that the phosphatidylcholine content is higher than that of corresponding normal brain with the highest concentration found towards the center of the neoplasm. Nayyar (1963), measured individual phospholipid components, and reported a decrease in phosphatidylethanolamine and sphingomyelin levels. Polar lipids from the CNS (Christen-lou et al., 1965) demonstrated a higher phosphatidylcholine:phosphatidylethanolamine ratio compared to normal tissue, and it was postulated that such a high ratio which usually decreases during intrauterine life is indicative of a low degree of cellular differentiation and organization. Whole cell studies on glioblastomas show increased levels of sphingomyelin and phosphatidylcholine and decreased levels of

phosphatidylserine and phosphatidylethanolamine with the most prominent changes in the center of the tumor. Astrocytomas, on the other hand only contain decreases in the phosphatidylethanolamine levels. Microsomal subfractions of glioblastomas possess the same changes observed in whole cell analyses. It was concluded that the increase in phosphatidylcholine and sphingomyelin were at the expense of phosphatidylethanolamine. Meningiomas show an increase in phosphatidylcholine and sphingomyelin [Gopal et al., 1963] that is similar to gliomas, along with an increase in phosphatidylcholine and a decrease in phosphatidylethanolamine. Other studies have reported greater levels of polar lipids except for cholesterol esters in glioblastomas [Slagel et al., 1967]. Phosphoinositides, important in nerve excitation, are concentrated in the tissue of several brain tumors [Kerr et al., 1964] and have been shown to have a high rate of turnover by radio-labelling [Ansell and Dohmen, 1957; Larrabee et al., 1963].

These attempts to examine the phospholipid content of brain neoplasms have produced variable results which may be due to small numbers of samples analyzed and the cellular complexities of the unfractionated tumor tissues. Fatty acid acyl profiles of the phospholipids

from microsomal subfractions more closely resemble those of fetal brain than those of normal human adult brain (Sun and Leung, 1974; White, 1973). Microsomal subfractions of human astrocytomas and glioblastomas contain approximately 80% unsaturation of the phosphatidylethanolamine acyl side chains. This is compared to 75.8% found in fetal brain and 70% found in normal adult brain. For the phosphatidylcholine group, the microsomal subfractions contain 10% less unsaturated fatty acids as compared to normal brain (from 60.6% to 50.6% in tumor tissue to 48.8% in fetal brain). There is also a general increase in 18:2 and 20:4(n-6) levels which suggests that neoplastic brain tissue lacks the enzymes for elongation and desaturation necessary for fatty acid metabolism. The unsaturation levels of phosphatidylethanolamine display a greater variety of acyl group changes compared to the phosphatidylcholine. Trends in different types and grades of brain tumors (White, 1973) show the same fatty acid shifts from their normal counterparts with the exception of oligodendrogliomas and an ependymoma which possess a high content of phosphatidylethanolamine 22:4(n-6) acyl side chains. The overall unsaturation index in the phosphatidylcholine fraction exceeds that of normal brain (UI of 62) when compared to meningiomas (UI of 90), metastatic carcinomas (103), and gliomas (92). Comparison of the phosphatidyl-

ethanolamine/phosphatidylcholine unsaturation index shows a selective increase in the choline phosphoglycerides with the largest increase being for gliomas (2.47) as compared to the four-fold selective increase in the phosphatidylethanolamine subclass of gliomas. The index appears to decrease from four to three during fetal to adult brain maturation. An interdependence exists between two of the essential fatty acid groups (n-6 and n-3 families) in the ratio of 22:5(n-6)/22:5(n-3) fatty acids. The ratio has been found to be altered in tumors, although it is at a functioning control level for the choline and ethanolamine phosphoglycerides.

Yates et al. (1979) examined the phospholipid patterns of brain biopsy specimens as well as the lipid composition of biopsy specimens grown in vitro. The lipid concentrations of in vivo tumors contain less cholesterol, sphingomyelin, and phosphatidylserine than the corresponding white matter. Phosphatidylcholine composition, however, was significantly increased beyond the level present in gray or white matter. Little variation from these trends was observed between well-differentiated and anaplastic astrocytomas or glioblastomas, and between a cerebellar medulloblastoma and peripheral neuroblastomas. Glioma cells in vitro, on the other hand, contained less cholesterol, sphingomyelin, and total ganglioside than

the parent in vivo specimens. Phosphatidylcholine concentrations were 25-30% greater than the level present in biopsy specimens. Neoplastic astrocytes in vitro contain a greater proportion of structurally simpler gangliosides than their corresponding parent tissues. Small concentrations of complex gangliosides, however, were present, indicative of a partial shift in ganglioside metabolism as a result of tissue culture. Malignant or rapidly growing tumors possess the greatest shift towards simplification of the ganglioside patterns. Furthermore, trace amounts of choline plasmalogen are usually present in normal brain. Both brain tumor specimens and their daughter cells in vitro contain similarly increased levels of ethanolamine and choline plasmalogen molecules above normal tissue levels. Therefore, it was inferred by Yates et al. (1979) that the in vivo phospholipid metabolism closely resembles the in vitro biosynthesis and degradation of phosphatides.

Generally, the percentage of ethanolamine phosphoglycerides is usually lowered in brain neoplasms; whereas, both choline phosphoglycerides and sphingomyelin are increased in biopsy specimens. This relationship appears to be most evident in the center of malignant tumors. Neoplastic brain cells may have lost the specificity for 18:2 fatty acid uptake, and its concentration is



extremely low in tumor tissue although not for fetal nor human adult brain. Sun and Leung (1974) proposed that overall 20:4(n-6) levels might be indicative of rapid cell growth while increases in 22:6(n-3) during development could be a measure of neuronal membrane maturity.

Considering the variability of pathological specimens (White, 1974), no striking correlations have been noted between the 20:4(n-6) and 22:6(n-3) phosphoglycerides for normal, benign, and malignant tissues. On the other hand, the 20:4(n-6) choline phosphoglyceride levels are directly proportional to cellular growth. For example, this level is increased two-fold for astrocytomas, gliomas, and metastatic carcinomas above normal brain levels. These tumors all grow rapidly in vivo and in vitro. The 20:4(n-6) choline phosphoglyceride level is also increased in meningiomas and other benign cell tumors which often represent an in vivo threat due to brain compression. Cells from these tumors proliferate rapidly in vitro but senesce after several passages. Microsomal subfractions (Sun and Leung, 1974) demonstrate that not only do the levels of phosphatidylcholine 20:4(n-6) fatty acids appear to be correct for the previous assumption, but also these molecules may account for a certain degree of rapid growth seen in malignancy. For example, grade I astrocytomas have 20:4(n-6) levels comparable to normal brain levels

which is indicative of some cellular differentiation (poor growth in vitro). Grade III astrocytoma levels increase approximately two-fold (depending upon the location of the tumor), corresponding to a greater degree of malignancy.

D. Lipid Alterations in vitro in Relation to Other Cell Transformation Systems

This section will specifically discuss the question whether the lipid changes observed for glioma and medulloblastoma derived cell lines are: a) general changes similar to those found for other normal non-neural neoplastic systems in vitro, and/or b) similar alterations to those observed for human brain in vivo and non-human neural systems in vitro.

One of the most widely used systems for examining the membrane alterations of normal and transformed cells are the 3T3 mouse fibroblasts and their respective transformed counterparts: SV40 or SV101 transformed 3T3 fibroblasts and polyoma transformed fibroblasts (Py3T3). Generally, the transformed variants of 3T3 fibroblasts, Py3T3 and SV101-3T3, contain lower total quantities of lipids per cell (based on dry weight) (Adam et al., 1975). The phospholipid content is specific for transforming virus and the cell type. Polyoma transformed cells

(Py3T3) and SV40 transformed cells have a higher lipid content compared to normal 3T3 cells (Adam et al., 1975; Perkins and Scott, 1978) while SV101 transformed cells have a lower lipid content. Cholesterol concentrations are statistically equivalent for normal and transformed phenotypes (Adam et al., 1974; Perkins and Scott, 1978) except for Scandella et al., (1979) who observed that the SV101-3T3 fibroblasts contain 50-100% more cholesterol than their normal counterparts. Considering the cholesterol concentration per surface area, it has been observed that malignant cells contain 50% more cholesterol than normal cells (Adam et al., 1975). SV40 transformed 3T3 fibroblasts (Perkins and Scott, 1978) contain greater amounts of phosphatidylcholine and phosphatidylinositol although the amounts of phosphatidylethanolamine and phosphatidylserine are similar for both normal and transformed cells. Sphingomyelin levels, on the other hand, are lower in transformed 3T3 cells. Regarding fatty acid alterations, several observations may be made:

a) nearly two-thirds of the phosphatidylcholine molecules contain the fatty acids 16:0 and 18:1 for both normal and transformed cells, b) there are greater quantities of 18:1 and 18:2 fatty acids in the SV40-3T3 phosphatidylethanolamine class although the 20:4, 22:4 and 20:3 levels

decrease, c) transformed cells contain smaller amounts of 18:0 and 18:1 in the phosphatidylserine and phosphatidylinositol subclasses and a greater amount of 20:4 in the phosphatidylinositol subclass, and d) there are no significant differences between the sphingomyelin acyl side chain compositions of normal 3T3 and transformed 3T3 cells. However, polyoma transformation of BHK cells indicates that there are no significant differences for all the phospholipid classes between the normal and virus transformed BHK cells (Micklem et al., 1976).

The lipid alterations observed in various experiments are specific for cell type. Detailed analysis of SV40 transformed WI-38 cells (forming the WI-38VA13A cell, a human diploid line) (Girardi et al., 1965) shows that the transformed cells contain less lipid and phospholipid compared to the normal WI-38 cells (Howard et al., 1973); However, both cell lines contain identical amounts of free cholesterol and cholesterol esters. Oncogenic transformation of WI-38 cells induces lower phosphatidylserine and phosphatidylinositol levels and higher sphingomyelin levels while the phosphatidylcholine and phosphatidylethanolamine levels are equivalent for both cell lines. The specific phospholipid fatty acid concentrations assayed in malignant WI-38VA13A cells do not correspond to the levels observed for SV-40 transformed 3T3 fibroblasts.

Transformed WI-38VA13A cells possess essentially the same fatty acid profiles with only a decrease in the 20:4 levels which is somewhat compensated by an increase in the 18:1 level. RSV transformation of chick embryo fibroblasts (Maldonado and Blough, 1980) produces lipid changes that are dissimilar to those for the SV40 transformation of 3T3 fibroblasts and WI-38 cells. Considering individual phospholipid concentrations, phosphatidylethanolamine and phosphatidylinositol levels are increased in RSV transformed cells; whereas, the phosphatidylcholine level is decreased although, phosphatidylserine and sphingomyelin levels are identical for both cell types. The transformed cells have increased amounts of 16:0 and 18:1 fatty acids among the phosphatidylethanolamine, phosphatidylcholine, phosphatidylserine, and phosphatidylinositol subclasses. Mazierre et al. (1980) examined normal and SV40-transformed hamster fibroblasts and observed that the tumorigenic cells possessed a lower degree of unsaturated fatty acids. Transformation was always accompanied by a decrease in palmitoleic (16:1) and oleic (18:1) fatty acid levels. Comparison of the fatty acid profiles for RSV-transformed chick embryo fibroblasts from the data of Maldonado and Blough (1981) and Yau et al. (1976) illustrates the variability that may

exist when comparing the same cell system under different growth conditions. Although the general changes are the same among these investigators, there are large variations for specific fatty acids which in one study are decreased in the RSV-transformed cells and are increased in the other study. This inconsistency exemplifies the fact that when considering neoplastic membrane changes, the trends in lipid profiles are not absolute but are cell type and transformation specific.

ELECTRON SPIN RESONANCE THEORY  
AND ORDER PARAMETERS

Magnetic resonance, in particular ESR and NMR, involves the absorption of radiation by a molecule and its transition from a stable ground state to an excited state of higher energy. Although the spectroscopic techniques differ in their analysis of the excitation obtained from various frequencies in the electromagnetic spectrum, all spectroscopic transitions are based on Planck's law.

$$\Delta E = h\nu \quad (1)$$

where  $\nu$  denotes the frequency of radiation,  $h$  is Planck's constant, and  $\Delta E$  is the energy difference between the ground and the excited states.  $\Delta E$  also is the basis of comparison for various spectroscopic transitions.

Magnetic resonance measures the interaction of a nuclear magnetic moment or an electron magnetic moment with a magnetic field. The resonance position is specific for molecular bonds and their orientations.

Effects of magnetic resonance absorption may be only observed in species which possess a magnetic moment. Nuclei such as  $^1\text{H}$ ,  $^{13}\text{C}$ ,  $^{31}\text{P}$ ,  $^{19}\text{F}$ ,  $^2\text{H}$ ,  $^{15}\text{N}$ , and  $^{33}\text{S}$ , with

an odd mass number and therefore a magnetic moment, are candidates for NMR measurements. Transition-metal ions, stable free-radicals, and transient free-radicals are the only molecular species possessing electron magnetic moments since there is no effective cancellation of spins by electron pairing. ESR, then, examines the energy transitions of a paramagnetic species (magnetic moment) induced by external static magnetic fields.

Electron and nuclear spins are quantized. Since according to quantum mechanical theory, only specific orientations are allowed relative to the magnetic field. For an unpaired electron with a nuclear spin of one-half there are only two allowable orientations,  $m_s = \pm \frac{1}{2}$ . In the absence of an applied magnetic field, the allowed state of an unpaired electron can be in one of two spin orientations since each orientation has coincident equal energy levels as described by quantum theory. Transitions induced by electromagnetic radiation, however, divide the electron quantum into two separate and distinct energy levels which are unequally populated. These orientations parallel or anti-parallel to the applied magnetic field (spin-up and spin-down, respectively), correspond to spin



states of  $m_s = -\frac{1}{2}$  and  $m_s = +\frac{1}{2}$ , respectively. The parallel orientation ( $m_s = -\frac{1}{2}$ ) is more densely populated than the anti-parallel orientation, and this preferred orientation possesses a lower energy. Furthermore, a population of spins exists rather than a single spin. Net absorption of radiation results in an energy transition only if there are fewer spin states in the upper anti-parallel orientation compared to the lower state. Thermal equilibrium can excite some of the lower state spins into the higher energy level. The ratio of the number of spins in the two levels can be described by the Boltzmann distribution:

$$N_{+\frac{1}{2}}/N_{-\frac{1}{2}} = \exp(-\Delta E/kT). \quad (2)$$

This distribution depends on the average thermal energy where  $k$  is Boltzmann's constant,  $T$  is the absolute temperature, and  $\Delta E$  is the energy difference between the two spin states levels. The process by which excited spin states lose energy and drop into the lower state maintaining the thermal equilibrium of the Boltzmann distribution is defined as the spin lattice relation and is characterized by the spin-lattice relaxation time,  $T_1$ .

Magnetic resonance energy levels for an electron within a magnetic field are defined by

$$E = \mu \cdot H \quad (3)$$

where  $\mu$  is the magnetic moment and  $H$  is the applied

The quantum mechanical description of an electron spin is related to the magnetic moment:

$$\mu = -g\beta S \quad (4)$$

where  $S$  denotes the electron spin,  $\beta$  is the Bohr magnetron, and  $g$  is the effective spectroscopic splitting factor (i.e., the  $g$ -factor which is species specific). Therefore, the energy levels in a magnetic field can be rewritten as

$$\Delta E = +g\beta HS = \pm \frac{1}{2}g\beta H. \quad (5)$$

The quantity  $\pm g\beta H$  is defined as the Zeeman interaction, and this term is related to Planck's law by simple substitution:

$$h\nu = \pm g\beta H \quad (6)$$

since the induced transitions are specific for a given frequency,  $\nu$ . For microwave energy absorption, the value of the ratio  $\nu/H$  determines the necessary resonance conditions. When  $h = 6.625 \times 10^{-27}$  erg-sec,  $\beta = 0.9273 \times 10^{-20}$  erg/Gauss (G), and the  $g$  value is approximately 2.00 for a variety of free-radicals, the  $\nu/H$  ratio equals 2.80 H. The intensity of the applied magnetic field for an ESR spectrometer operating at 9.5 GHz (X-band microwave region) is therefore  $9.5/2.8$  or 3.4 kG. For practical applications, ESR spectra scanning involves a fixed frequency which is matched to a continuously varying magnetic field energy level.

### Spin Hamiltonians

Spin Hamiltonian operators can be used to describe magnetic resonance transitions. The simplest example is a single electron with no hyperfine interactions and an isotropic  $g$  value of the form  $E = -\mu H$ :

$$H = g\beta H_z S_z \quad (8)$$

where  $S_z$ , the spin operator, may be replaced by the spin quantum numbers  $m_s = \pm \frac{1}{2}$ . Differing spin orientations complicate the format of the Hamiltonian such as the case for axial symmetry:

$$H = g_{\parallel} \beta H_z S_z + g_{\perp} \beta H_x S_x \quad (9)$$

where  $H_z$  denotes the magnetic field parallel to the  $z$  direction of the molecular axis and  $H_x$  is the magnetic field component along the perpendicular,  $x$  direction.

For spin probes which possess an unpaired electron in their nitroxide group, the spin operator for an axially symmetric system with hyperfine structure may be written

$$H = g\beta_e HS + g_N \beta_N HI + STI. \quad (10)$$

The magnetic field vector is defined by  $H$ ,  $\beta_e$  and  $\beta_N$  are the electron and nuclear magnetrons, respectively,  $g_N$  is the nuclear Zeeman splitting factor,  $g$  is the electron tensor,  $S$  is the electron spin operator,  $I$  is the nuclear spin operator, and  $T$  denotes the hyperfine coupling tensor. Under ESR experimental conditions, the second term which represents the nuclear Zeeman term or the interaction

between the nuclear spin and the magnetic field is usually negligible. This off-axis effect, however, is important in the analysis of spin-spin splittings in NMR. Spin Hamiltonian operators which are of significance for the slow motion of spin labels (as in the case of probes immobilized in membranes) can be represented by electronic Zeeman interactions and hyperfine (electron spin-nuclear spin) interactions in the form

$$H = \bar{g}_e \beta_e HS + S \bar{T} I. \quad (11)$$

The second rank tensors,  $\bar{g}$  and  $\bar{T}$  are angular dependent and can be diagonalized for the orientation of the principle axis of a nitroxide. Conventionally, the coordinate system places the N-O paramagnetic moiety with the x-axis along the N-O bond. The y-axis lies in the plane of the oxazolidine ring perpendicular to the x-axis, and the z-axis which is along the nitrogen  $2p_{\pi}$  orbital usually coincides with the direction of the g and T tensor elements.

In general, the g and T tensors can be represented by a second rank element because the positions and splitting of the lines depend on the magnitude and direction of the applied magnetic field relative to the nitroxide axes. This unique feature of ESR spectra, spectral anisotropy, is not observed in isotropic transition free radicals due to the delocalization of the free electron and the rapid motional averaging of small anisotropic shifts. Spectral

anisotropy is completely specified by the three  $g$  values and hyperfine constants parallel to the principal axes. For the majority of nitroxides, the values of the  $g$  and  $T$  tensors are:  $g_{xx} \approx 2.009$ ,  $g_{yy} \approx 2.006$ ,  $g_{zz} \approx 2.002$ ,  $T_{xx} \approx T_{yy} \approx 6$  Gauss, and  $T_{zz} \approx 32$  Gauss. These static values are determined by the incorporation of nitroxide derivatives into host crystals as substitutional impurities, and they depend on the polarity of the environment but differ from one crystal substitution to another. The tensor values, therefore, may differ or be in error when applying values from a static crystal to a particular noncrystalline system such as a biological membrane. In cases where the system is axially symmetric, the principal values may be designated as  $A_{\parallel} = T_{\parallel} = A_{zz} = T_{zz}$ ,  $A_{\perp} = T_{\perp} = A_{xx} = T_{xx}$ , and  $A_{yy} = T_{yy}$  \* and similarly for the  $g$ -factors:  $g_{\perp} = g_{xx} = g_{yy}$  and  $g_{\parallel} = g_{zz}$ .

### ESR Spectra of Paramagnetic Nitroxides

As previously stated, the lines of an ESR spectrum can be split by the interaction of the unpaired electron with the magnetic moments of neighboring nuclei. Since the unpaired electron is localized on the  $2p\pi$  orbital, the hyperfine splitting is principally due to its interaction

---

\*The principal tensor values are designated as either  $A$  or  $T$  and are used interchangeably as in this dissertation.

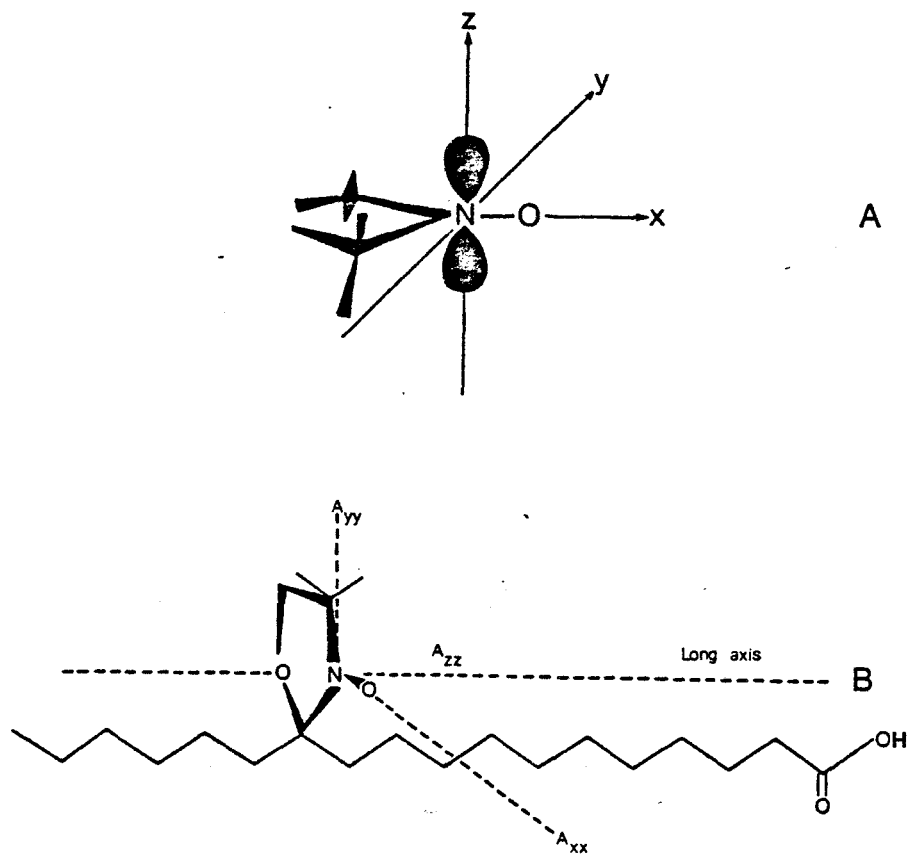


FIG 8 : Orientation of the spin-label nitroxide group.  
 A. Principal axes of the nitroxide group.  
 B. Orientation of the nitroxide axes in a stearic acid spin label. The  $A_{zz}$  vector of the nitroxide is parallel to the long axis of the fatty acid.  
 (Redrawn from Knowles et al., 1976.)

with the  $^{14}\text{N}$  nucleus.  $^{14}\text{Nitrogen}$ , with a nuclear spin  $I = 1$ , yields three hyperfine lines described by  $(2I+1)$ . Each nuclear spin is quantized, and three orientations are probable according to the allowable selection rules:  $I_z = -1, 0, +1$  for each spin state  $m_s = \pm\frac{1}{2}$ . A typical ESR spectrum, shown in Figure 11, possesses three main lines arising from the nitrogen hyperfine structure as well as small satellite lines from  $^{13}\text{C}$  hyperfine interactions (Figure 11). The energy level splittings can be described by the hyperfine splitting constant,  $A^*$  (in gauss). Three spectral lines are observed at:

$$H = H_0 - m_I A \quad (12)$$

where  $H_0$  defines the magnetic field intensity at the center spectral line.

### Anisotropic Motion and Order Parameters

The ESR spectrum of Fremy's salt (Figure 12) consists of three sharply peaked lines with approximately equal intensity where the splittings from the central line to the left and right hyperfine extrema are 11.0012 and 11.013 G, respectively (Faber and Fraenkel, 1967). Uniform splitting and distinctive intensity patterns are typical of isotropic motion associated with rapid tumbling of a nitroxide spin label in a low viscosity solvent. The

---


$$*h\nu = g\beta H \pm \frac{1}{2} A \mu_I$$

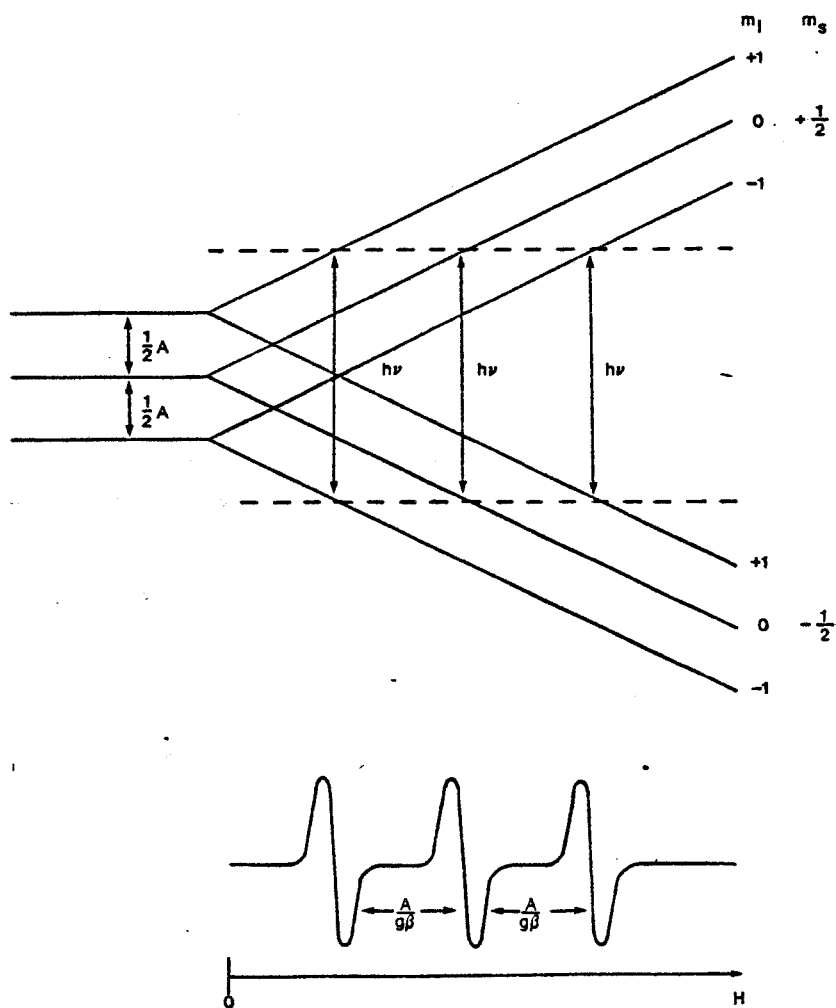


FIG 9: Hyperfine energy-level splittings and allowed transitions for nitrogen (nuclear spin  $I=1$ ). The number of energy-level splittings is mirrored in the number of splittings in the ESR spectrum (lower figure). (Adapted and not drawn to scale from Knowles et al., 1975.)



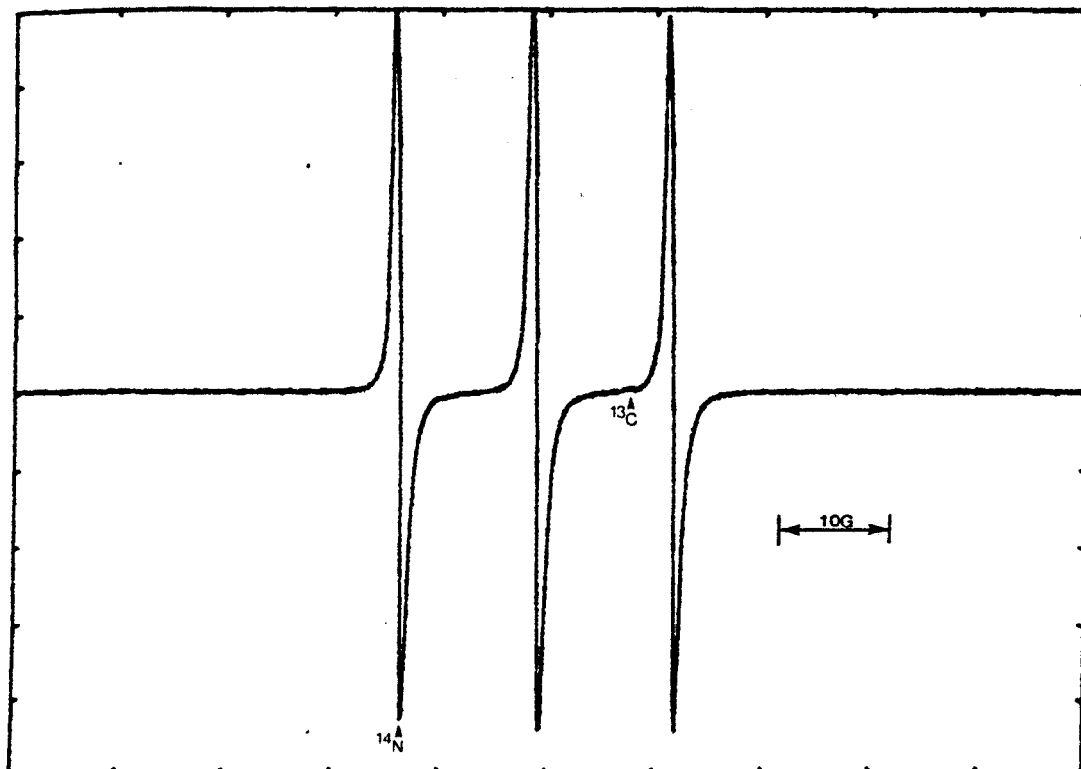


FIG 10: Typical ESR spectrum of Fremy's salt. The  $^{13}\text{C}$  components are negligible in contrast to the  $^{14}\text{N}$  splittings. The spectrum is characteristic of rapid isotropic motion.

spin Hamiltonian can be rewritten for isotropic motion:

$$H = g_0 \beta H S + T_0 S I \quad (13)$$

where the isotropic g-factor,  $g_0$ , and the isotropic hyperfine coupling constant,  $T_0$ , are defined by:

$$g_0 = \frac{1}{3}g = \frac{1}{3}(g_{zz} + g_{xx} + g_{yy}) \quad (14)$$

and

$$T_0^* = \frac{1}{3}T = \frac{1}{3}(T_{xx} + T_{yy} + T_{zz}), \quad (15)$$

respectively. With axial symmetry, these expressions can be simplified.

$$a_0 = \frac{1}{3}(A_{\parallel} + 2A_{\perp}) \quad (16)$$

$$g_0 = \frac{1}{3}(g_{\parallel} + 2g_{\perp}). \quad (17)$$

The isotropic tumbling of small molecules exhibits dependence on solvent polarity (Seelig, 1970; Seelig and Hasselbach, 1971), whereby isotropic splitting constants are increased as solvent polarity increases. The converse is also true: as the polarity decreases with hydrophobic solvents or environments, so does the splitting constant. The isotropic g factor, in contrast, decreases with increasing solvent polarity. The average decrease of  $a_0$  (from 15.1 gauss) at the C-4 position to 14.6 gauss at the tenth position (Seelig and Hasselbach, 1971) corresponds to an increase in hydrophobicity within the interior of the phospholipid bilayer.

---

\*The splitting constants T and A are identical and are used interchangeably.

In contrast to the rapid tumbling motion characteristic in isotropic systems, spin-labelled motion in membranes is restricted and must be described by immobilized anisotropic motion. A variety of models can be used to calculate lineshapes that approximate experimental spectra and these can reduce complicated lineshapes into a collection of parameters which allows comparisons between model and natural membranes. These models include: (1) anisotropic motion in the intermediate field, (2) rapid rotation about a molecular axis, (3) oscillation, and (4) wobbling of the long molecular axis (Griffith and Jost, 1976).

The description of nitroxide motion as a wobbling of a long molecular axis, used by H. M. McConnell for nitroxide orientations in biomembranes, has been supported by a number of investigators (Jost, 1971; Isacralachivilli et al., 1974; Van et al., 1974; Griffith, 1964; Birell et al., 1973a, 1973b). Motion of a nitroxide can be described as a restricted random walk of the R axis on the surface of a sphere, rapid motion within a conical section, and rapid oscillation about the angle  $\theta$  between the axis R and the sample axis z. The R axis is usually normal to the membrane plane although McFarland and McConnell (1974) have suggested that the ordering axis may be tilted by the angle  $\theta$ . A probability function can be described:

$$P(\beta) = \frac{\exp(-U(\beta)/kT)}{\int \exp(-U(\beta)/kT) \sin\beta d\beta} \quad (18)$$

for the probability ( $P(\beta)$ ) of molecular orientation of angle  $\beta$  (the angle between the  $2p\pi$  orbital of the nitroxide and the axis R of the hydrocarbon chain) with respect to the reference axis. An order parameter S is defined as a relative measure of the distribution of molecular orientations in relation to a reference axis (frequency-amplitude order parameter). The order parameter can be written as a time ensemble average of the squares of the direction cosines of the principal axis (Hubbell and McConnell, 1969a, 1969b; Seelig, 1970):

$$S = \frac{1}{2} \langle 3 \cos^2 \beta - 1 \rangle = \left( \frac{3 \int \cos^2 \beta P(\beta) \sin\beta d\beta}{2} \right) - \frac{1}{2}. \quad (19)$$

Order parameters are strongly dependent on the reciprocal of the anisotropy of the Zeeman and hyperfine interactions. The interpretation and measurement of order parameters depends on a time range of  $10^{-7}$  to  $10^{-9}$  seconds.

Derivation of order parameters, therefore, does not involve a specific rate of motion, but rather the monitoring of restricted and unrestricted motions of nitroxide probes that are fast on an ESR timescale (Hubbell and McConnell, 1971). If the frequency of the collective motions is greater than  $10^{-9}$  seconds and approach an NMR timescale ( $10^{-5}$  to  $10^{-7}$  seconds) (Polnaszek and Freed, 1975; Polnaszek, 1977; Rao et al., 1977), the calculated order parameter will be greater than the true value

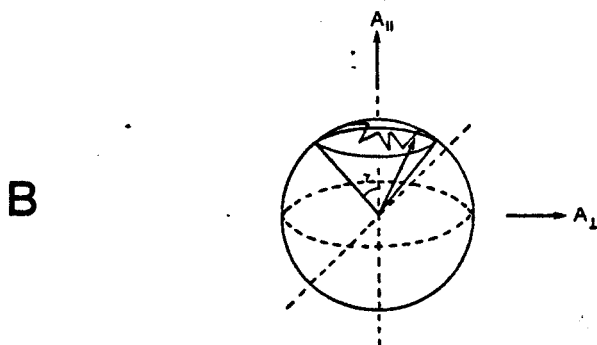
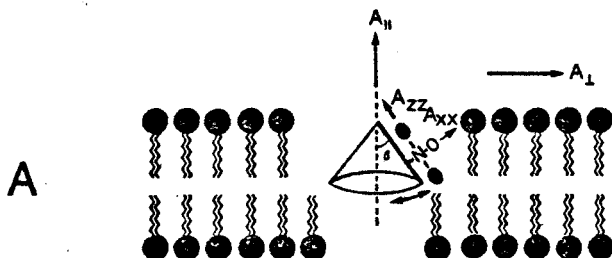


FIG 11: Anisotropic motion-lipid spin labels in membrane environments. A. Anisotropic motion of a lipid spin label within the outer monolayer of a lipid bilayer. The nitroxide principal z-axis ( $A_{ZZ}$ ) is parallel to the plane of the hydrocarbon chain. Motional averaging to the normal of the membrane surface ( $\beta$ ) and results in the  $A_{II}$  and  $A_I$  splittings. B. Restricted random walk of a lipid spin label normal to the membrane surface within a cone of the angle  $\gamma$ . (Redrawn from Knowles et al., 1976.)

indicating slower motion, necessitating computer fitting of calculated values to experimental data (Polnaszek and Freed, 1975).

A number of equations can be used to quantitatively analyze ESR spectra. The isotropic hyperfine constant  $a_0$  can be defined as:

$$a_0 = \frac{1}{3}(T_{zz} + 2T_{xx}) \quad (20)$$

for the nitroxide crystal state as compared to  $a'_0$  for a probe intercalated in a biomembrane:

$$a'_0 = \frac{1}{3}(T + 2T) \quad (21)$$

Assuming that the polarity of the environment around the probe is identical to that of the host crystal and spin-spin interactions are nominal (i.e., magnetically dilute solutions), the flexibility of lipid chains can be assessed using the order parameter  $S'$  (Seelig, 1970):

$$S' = \frac{(T_{zz} - T_{xx})}{(T_{zz} + 2T_{xx})} \quad (22)$$

Nitroxides rotating in a cone of a semi-variable angle (Israchaleachvilli et al., 1974) can be assumed to possess an isotropic hyperfine constant equal to

$\frac{1}{3}(T_{zz} + 2T_{xx})$ . Therefore,

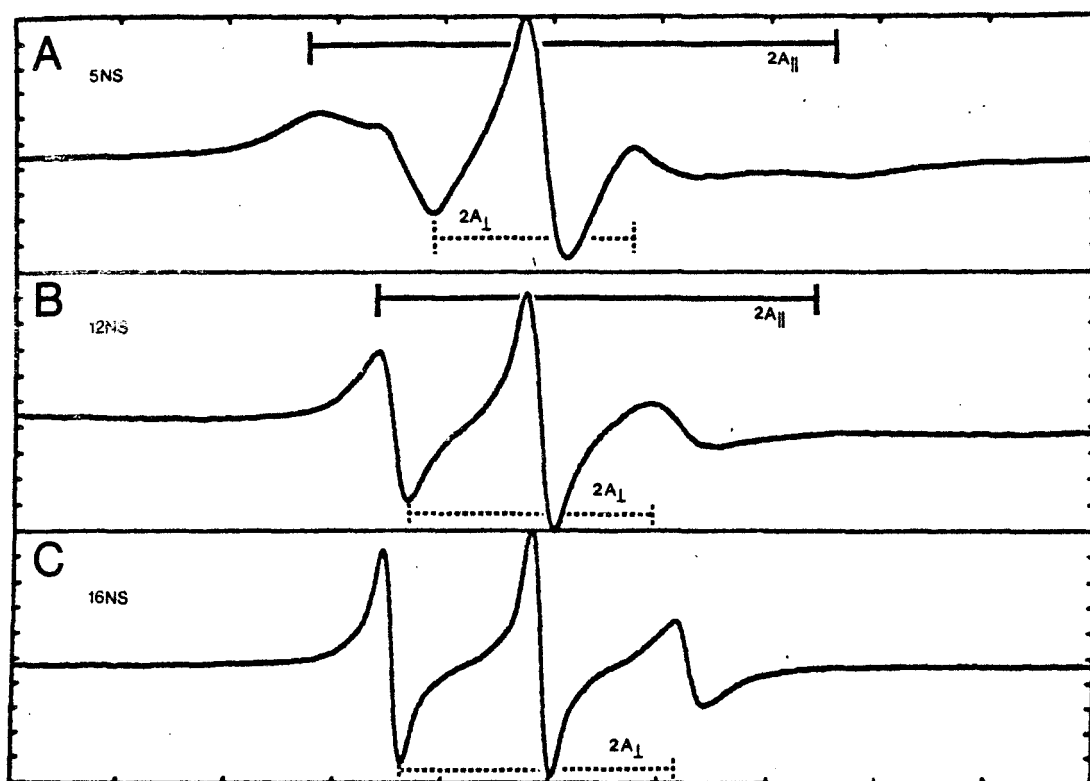


FIG 12: Hyperfine splittings of the nitroxide spin labels.  
A. Probe (5,12). B. Probe (12,5). C. Probe (16,1)  
doxyl stearate spin labels.

$$T = \frac{1}{3}(T_{zz} + 2T_{xx}) + -(T_{zz} - T_{xx}) S' \quad (23)$$

and

$$S'' = \left(\frac{1}{2}\right) \left[ \frac{(3T_{\parallel} - T_{xx})}{(T_{zz} - T_{xx})} - 1 \right]. \quad (24)$$

Sauerbeher et al. (1978) have pointed out that  $S'$  should equal  $S''$  if probe-probe interactions are negligible and if the polarity of the membrane is identical to that of the substituted host crystal. This may not be the case since isotropic splitting constants are sensitive to the polarity of the environment.

A polarity corrected order parameter (Hubbell and McConnell, 1971) can be derived through the division of the previous tensor elements by their respective isotropic splitting constants:

$$S = \frac{T_{\parallel} - T_1}{T_{zz} - T_{xx}} \frac{a_{\Omega}}{a_0}. \quad (25)$$

The values of  $T_{\parallel}$  can be calculated from resolved spectra with order parameters greater than 0.2 (Gaffney, 1976).  $T_1$  diverges linearly from its true value with decreasing order parameter; therefore, a correction factor must be used to calculate  $T_1$  from experimental separation of the inner extrema now defined as  $T_1'$ . The correction term is:

$$C = (4.06 \text{ MHz}) \left( 1 - \left( \frac{T_{\parallel} - T_1'}{T_{zz} - \frac{1}{2}(T_{xx} + T_{yy})} \right) \right) \quad (26)$$

where

$$T_1' = T_1 + C. \quad (27)$$



substitution of the polarity corrected order parameter using tensor elements derived for spin-labels on BSA (bovine serum albumin) (Hubbell and McConnell, 1971; Gaffney, 1976) yields the following order parameter:

$$S = \left( \frac{T_{\parallel} - T_{\perp} + C}{T_{\parallel} + 2T_{\perp} + 2C} \cdot 1.66 \right) \quad (28)$$

where

$$C = 4.06 - 0.053(T_{\parallel} - T_{\perp}'). \quad (29)$$

Probe-probe interactions may be measured by the value  $m$ ,

$$m = S'/S'' = (-) \left[ \frac{T_{\parallel} - T_{\perp}}{T_{\parallel} - a_n} \right] \quad (30)$$

or

$$m = \frac{T_{\parallel} - a_o'}{T_{\parallel} - a_o} \quad (31)$$

such that  $m$  values of 1 indicate no interactions; whereas,  $m$  values less than unity are indicative of probe-probe interactions. The above equations assume that membrane polarity sensed by nitroxide is identical with the polarity of the host crystal. As noted before, this may not be the case for biomembranes. Therefore:

$$m = m^o - \frac{2(\Delta T_{\perp})}{3(T_{\parallel} - a_o)} \quad (32)$$

where

$$m^o = S'/S'' \quad (33)$$

and is measured in magnetically dilute solutions.

### Equivalence of Order Parameters and Experimental Spectra

The simplest and most direct method of calculating order parameters (Griffith and Jost, 1976) utilizes the following assumptions:

- 1)  $A_{\parallel} = A_{\max}$  (the splitting between the outermost hyperfine extrema),
- 2)  $A_{\perp} \approx A_{\min}$  (the separation of the innermost extrema), and
- 3) the polarity of the biomembrane is not significantly different from that of the host crystal. These assumptions are made for equations 22 and 24 (Method I).

A more accurate approximation of equating experimental splittings with the theoretical hyperfine maxima and minima can be made if:

- 1)  $A_{\parallel} = A_{\max}$ , and
- 2) the  $A_{\perp}$  value can be calculated according to Gaffney (1976), or for values of  $S^{\text{app}}$  less than 0.8. Then:

$$A_{\perp} = A_{\min} + 1.32 + 1.86 \log (1 - S^{\text{app}}), \quad (34)$$

and polarity may be corrected by  $k$ :

$$k = \frac{A_{\perp}'}{A_{\perp}} = \frac{\left(\frac{1}{3}\right) (A_{\parallel} + 2A_{\perp})}{\left(\frac{1}{3}\right) (a_{O_{xx}} + a_{O_{yy}} + a_{O_{zz}})}. \quad (35)$$

The order parameter is then calculated using equation 22 (Method II).

This alternate method yields a better approximation of the true order parameter from experimental spectra. The value of  $T_{\perp}$ , however, can be calculated from powder spectra (i.e., spectra recorded at  $-196^{\circ}\text{C}$  where the structural integrity of the membrane is assumed to be unaltered but the motion of the intercalated nitroxide is inhibited). In this case,  $A_{\text{max}}^{-196}$  equals the  $A_{zz}$  value and the order parameter can be rewritten as:

$$S = \frac{3}{2} \left( \left( \frac{(A_{\parallel}/k) - \frac{1}{2}(a_{O_{xx}} + a_{O_{yy}})}{(a_{O_{zz}} - \frac{1}{2}(a_{O_{yy}} + a_{O_{xx}}))} \right) - \frac{1}{2} \right) \quad (36)$$

Otherwise, the  $T_{\perp}$  ( $A_{\perp}$ ) may be calculated from equation 16 and substituted into equation 21 (Method III).

Griffith and Jost (1976) calculated order parameter values using the three previous assumptions for spin labels located at methylene groups 5, 7, 12, and 16 from the polar hydrocarbon carboxyl chain. Methods II and III yielded good approximations (within 5-6% error); therefore, polarity correction negated the necessity of obtaining a powder spectra. The maximum variation between assumptions I and II and III varies with nitroxide position; for example, 26% variability at  $n=16$ , in contrast to 3% at  $n=5$ .

## MATERIALS AND METHODS

Description of Cell LinesNormal Human Fetal Brain, Line designation NFB.

Normal human fetal brain (Flow 3000, Flow Laboratories, Rockville, Maryland, USA) was derived from a normal 14-week male Negro fetus. This cell line was initiated through mechanical disaggregation and explantation into MEM containing 10% fetal bovine serum. Morphology in vitro appears as shortened fibroblast-like cells. Mitotic division is inhibited as the cell monolayer reaches confluency (i.e. cells exhibit contact inhibition). The human fetal brain used in this dissertation was passaged at confluency by the thin-film trypsin technique (0.25% trypsin)\* and was normally split at a 1:2 ratio. The line was at its tenth passage when received from Flow Laboratories, and consequently, as the passage level increased (up to senescence or cell death at passage 14), the split ratio was lowered to 1:1.5 or 1:1 to maintain the density of the cell population.

Human Glioblastoma, Line designation SA 4. The SA 4 line (R. Maunoury, St. Anne's Hospital, Paris, FRANCE) was initiated from a frontal glioblastoma of a

---

\*All cell lines, with the exception of NFB, were split at a confluency into a 1:2 ratio by the thin-film trypsin technique (Westermarck et al., 1973).

59-year-old male (Maunoury, 1977). Microscopically, the cells are spindle-shaped and arranged into parallel bundles, several layers thick. The chromosome range is bimodal (38-82), and the cells in vitro exhibit low contact inhibition. Population doubling time is approximately twenty-four hours, and the cells are capable of producing tumors in athymic "nude" mice.

Human Astrocytoma, Line designation SA 101. The SA 101 line (R. Maunoury, St. Anne's Hospital, Paris, FRANCE) was explanted from a frontal-temporal malignant astrocytoma in a 46-year-old female (Maunoury, 1977). SA 101 possesses an abnormal number of chromosomes with a single modal of 71. In vitro, the cells are flat with large nuclei that have an extensive amount of cytoplasm. Occasionally, the cells display multiple processes. The cells, in spite of the fact that they were isolated from a malignant tumor, do not grow to a confluent density greater than that of normal brain ( $8 \times 10^4$  cells/cm<sup>2</sup>) and do not possess the capability for tumor production in athymic "nude" mice. This line shows two specific glial properties: (1) the presence of glial fibrillary acid protein (GFA) by immunofluorescence and (2) a morphological stellar response to dibutryl cyclic AMP. Maunoury (1977) has pointed out that the GFA protein of the cell line, moreover, shows delicate, condensed fibrillary

patterns similar to normal fetal brain in vitro (Maunoury, 1976).

Human Medulloblastoma, Line designation E1202.

This cell line E1202 consisting of polygonal and fusiform cells was initiated from a left cerebellar astrocytoma in a six-year-old Caucasian female (R. McAllister, Children's Hospital of Los Angeles, Los Angeles, California, USA). E1202 is an abbreviation of the line's other designations: NIH E1202 #2 29B Smith or TE-671. These undifferentiated cells exhibit little or no contact inhibition (terminal density,  $2 \times 10^6$  cells/cm<sup>2</sup>) and are malignant in vitro and in vivo as ascertained by their freedom from anchorage-dependent growth and tumor production in either "nude" mice or antithymocyte-serum-treated hamsters (McAllister et al., 1977). Electron microscopy shows the absence of viral particles. A majority of cells are diploid while in vitro and have a chromosome number of 47.

Human Medulloblastoma, Line designation TE 907.

The TE 907 line (R. McAllister, Children's Hospital of Los Angeles, Los Angeles, California, USA) was received in the 13th passage and was initiated from a pediatric medulloblastoma. No additional information is available. Experimentally, the cells do not possess any tumorigenic potential either in vivo or in vitro as suggested by growth characteristics.

Human Astrocytoma, Line designation 251 MG 3C.

The 251 MG 3C line is a cloned variant of the 251 MG astrocytoma (A. Lindgren and J. Ponten, Wallenberg Laboratory, University of Uppsala, Uppsala, SWEDEN).

Initiated from a temporal lobe grade IV astrocytoma in a 58-year-old male, the cells exhibit astrocytic morphology in vitro. The 251 MG cell line has been well characterized regarding cell culture migration, terminal cell density (Westermarck et al., 1973; Ponten, 1975), mitotic figures, growth in soft agar (Westermarck, 1973; Carlsson and Brunk, 1977), serum dependence (Westermarck, 1973; Lindgren et al., 1975), and cell cycle kinetics (Lundgren et al., 1975; Lundgren, 1976). Experimentally, the cells are unique since they form colonies in soft agar but lack the ability to produce tumors in "athymic" mice.

Tissue Culture-General Methods

Dulbecco's modified Eagle's Medium (DMEM; high glucose formulation containing 4.5 grams liter<sup>-1</sup> D-glucose) was used for the growth and maintenance of all cell lines. The complete medium consisted of DMEM (pH 7.2) supplemented with 10% heat-inactivated fetal calf serum (FCS), 100 µg ml<sup>-1</sup> streptomycin, and 100 units ml<sup>-1</sup> penicillin G. Powdered media (Gibco, Grand Island, New York) was hydrated using freshly deionized double-

distilled water and sterilized through 0.22  $\mu\text{m}$  extractable-free membrane filters (type GSMF, Millipore Corporation, Bedford, Mass.). Medical grade implantable silicone tubing was used for all still and filter connections (Cole-Parmer Instrument Company, Chicago, Illinois). Cells did not attach or grew poorly when media was prepared with laboratory grade polyvinyl tubing (Tygon<sup>®</sup>, Norton Company). Sterility of the prepared media was ascertained using a 21-day quality control procedure. This involved inoculating suitable aliquots of sterile media into tryptic soy broth (BBL, Cockeysville, Maryland), blood agar (BBL), and Sabouraud broth (BBL) along with incubation in triplicate at both 25°C. and 37°C.

The same lots of medium (DMEM, Lot #R697251), serum (M.A. Bioproducts, Walkersville, Maryland, Lot #95919), trypsin, and EDTA were used for all experiments. Cells were routinely grown in 75  $\text{cm}^2$  plastic T-flasks (T-75, Corning Glass, Corning, New York), except for some experiments (such as line E1202) where 25  $\text{cm}^2$  T-flasks were used (T-25, Corning Glass, Corning, New York). They were maintained at all times in a 37°C. humidified 10%  $\text{CO}_2$ -air environment. All cell lines were passaged after a 10 minute incubation of 0.02% EDTA in divalent ion-free phosphate buffered saline (PBS) at 37°C. followed by total disaggregation using a thin film of 0.25% trypsin



(Westermarck et al., 1973). After centrifugation (200 xg x 10') in complete medium (DMEM with 10% FCS), the cells were counted in a hemocytometer (AO Brightline, 0.1 mm depth), and the viable cell population appropriately subcultured. Cell viability was determined by trypan blue dye exclusion (Kruse, 1973).

Plating efficiency of a particular cell line was assessed by seeding an appropriate number of cells in either 30 mm diameter (8 cm<sup>2</sup>) tissue culture dishes (Corning Glass, Corning, New York) or 10 mm diameter (2 cm<sup>2</sup>) multi-well plates (Linbro, Flow Laboratories, McLean, Virginia). Attached cells were trypsinized, dispersed, and counted 24 hours after the initial seeding. The relative plating efficiency (RPE) in this case is defined as the attachment percentage of cells, not the percentage of colonies formed. Plating efficiencies were always dependent on the concentration of serum. For some cell lines, the relative plating efficiency was increased if a thin film of serum was used for the initial attachment; whereas, this had no effect for the malignant cell lines. Cell densities are expressed as the number of cells per growth area (i.e. cells per cm<sup>2</sup>). Confluent densities were initially determined as above, except that seeding densities were adjusted so cell confluency would be attained in a three to four day period. The terminal

cell density (TCD) was ascertained by seeding slightly above the confluent density of each specific cell line and removing triplicate aliquots at appropriate intervals (72-96 hours) for trypsinization and subsequent counting. Terminal cell densities reflect the point at which there is no change in the maximum cell density for three 48 hour intervals. For all cell lines, media was replaced at 48 hour intervals, allowing growth to approach steady-state conditions. Cultures were routinely checked for PPL0 infection by the large volume infusion technique (Hayflick, 1973) and were found to be free of contamination. Experiments involving individual cell lines were completed with cells from no more than three passage levels.

#### Correlates of Malignancy

Cell colony formation in soft agar is a selective technique which allows the division and growth of cells possessing some degree of tumorigenic potential. Normal cells require adhesion onto a solid substrate in order to undergo cell division; whereas, division in neoplastic cells is not necessarily anchorage-dependent. The selectivity of this method is thought to be caused by the inhibitory effect of sulfated and acidic polysaccharides in the agar medium on normal cell multiplication (Montagnier, 1970, 1971). Soft agar has been utilized for

cell transformation by oncogenic viruses (Macpherson and Montagnier, 1964; Macpherson, 1965, 1966; Black, 1966; Montagnier et al., 1966; McAllister and Macpherson, 1969; Rubin, 1966; Williams, 1965) and by chemicals (Montesano et al., 1977; Colburn et al., 1978).

The production of colonies in soft agar and the development of tumors in immune deficient animals (i.e. athymic "nude" mice)\* are not mutually exclusive tests for tumorigenicity (malignancy). Therefore, if a cell line produces tumors in "nude" mice, it is suggestive of malignancy; however, non-production (i.e. rejection of the implant) is not supportive evidence for non-malignancy (Rygaard and Poulsen, 1969).

"Nude" mice are characterized by a suppression of T-cell mediated immunity although humoral and lymphoid cell responses to foreign cells remain functional (Kiessling et al., 1976). The degree of differentiation of tumors grown in "nude" mice corresponds to the initial degree of differentiation observed in vivo even after extensive periods of in vitro subculturing (Fogh and Hajdu, 1975).

---

\*Other systems include ALS (antilymphocyte serum) treated mice (Philips and Gazet, 1968; Stanbridge and Perkins, 1969), ATS (antithymocyte serum) treated hamsters (Wallace et al., 1971), cortisone treated hamsters (Foley et al., 1962). Regarding tumorigenicity, these three in vivo assays have been known to give inconsistent results (Petrieciani et al., 1974).

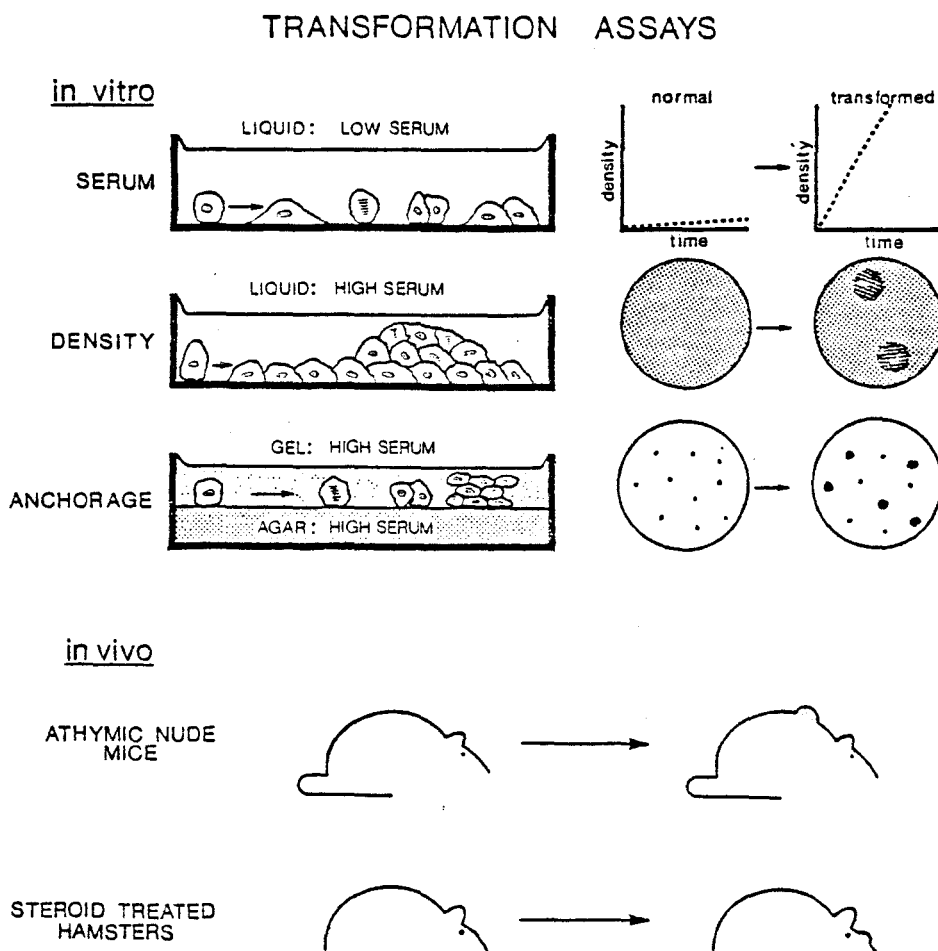


FIG 13: Transformation assays. The in vitro selective assays include serum, density, and anchorage independence. The loss of regulation is depicted on the left, with the accompanying observation on the right. The in vivo assays include athymic "nude" mice and steroid-treated hamsters. (Re-drawn with adaptation from Pollack et al., 1975.)

This generalization concerning differentiation is also applicable to colony formation in soft agar. The degree of tumorigenicity for chemically transformed mouse epidermal cells, for example, is influenced by the serum concentration and initial cell density and is not correlated with the colony forming efficiency in soft agar (Colburn et al., 1978). Production of colonies and tumors in vitro and in vivo, however, does strongly suggest that cells in culture maintain and possess some degree of their malignant potential.

Cell Colony Formation in Soft Agar. Colony formation in soft agar was performed as described by Macpherson and Montagnier (1964) with the volumes modified for 60 mm gridded tissue culture dishes (CoStar, Cambridge, Mass.). The agar medium consisted of 18.33 ml of 1.25% Difco Bacto Agar (Difco Laboratories, Detroit, Michigan) in tissue culture grade water, 14 ml of 2X Eagle's modified Essential Medium (MEM) (Gibco, Grand Island, New York), and 3.33 ml each of heat-inactivated fetal calf serum and tryptose phosphate broth (Difco Laboratories, Detroit, Michigan). Maintained at 45°C. to prevent solidification, 8.4 ml of the combined media was pipetted into dishes. The base layer was stored at 37°C. for no longer than one hour in a 10% CO<sub>2</sub>-air humidified environment after gelatinizing at room temperature. Cell suspensions from trypsinized

monolayers were mixed in the ratio of one volume of cells with two volumes of agar medium (0.5% agar concentration) to produce a 0.33% agar top layer. The top layer (1.8 ml) was gently pipetted onto the base layer, and the dishes were incubated at 37°C. in a 10%-90%-air humidified atmosphere. Cell concentrations were adjusted so there were either 100 or 1000 cells per dish. After a ten day incubation, colonies with a diameter of 0.1 mm to 0.2 mm were counted under a 25-50X stereomicroscope.

Tumor Production in "Nude" Mice. Animals, nu/nu mice of Swiss origin were obtained from the colony at Northwestern University School of Medicine. Female athymic mice, 4-6 weeks of age, were used for the implantation studies. These animals were maintained under pathogen-free conditions. Standard polypropylene mouse cages were filled with an appropriate amount of autoclavable mouse chow and bedding, fitted with polyester filter tops, and autoclaved. Sterile water, pH 2.8, was available ad libitum. Approximately three mice were housed per cage in a plexiglass glove box specially fitted with filtered air vents and maintained separately from other animals in a temperature regulated area free from traffic. Cages were changed twice weekly. Under these conditions, the animals had a life span of 10-12 months.

Trypsinized cell suspensions were injected subcutaneously at a concentration of  $1 \times 10^7$  viable cells in 0.1 cc between the shoulder blades. All injections were performed in triplicate on three separate animals. Prior to injection, gloves were rinsed with sterile water to remove any traces of talc which could possibly cause a cutaneous granulomatous reaction. The mice were observed three times a week and sacrificed before the tumor became necrotic. Portions of the excised tumor were placed in phosphate buffered formalin (pH 7.4) for histological examination.

#### Lipid Extraction and Fractionation

Cell cultures seeded in 25 cm<sup>2</sup> or 75 cm<sup>2</sup> tissue culture flasks at confluent density were incubated for 48 hours after passaging. The flasks were removed from the incubator and placed on ice. The medium was aspirated and replaced by a minimal amount of cold Ca<sup>2+</sup>-Mg<sup>2+</sup> free phosphate buffered saline (PBS, pH 7.2). Cells were scraped from the treated plastic surface with the aid of a rubber policeman, or for the malignant lines, E1202 and SA4, monocellular dispersions were produced by repeated washing in divalent cation-free PBS. The cells were washed at least five times, and the combined harvests were centrifuged at 1000 x g for 15 minutes. The supernatant was

aspirated, and the cell pellet washed with cold PBS. After being transferred to a one milliliter Duall tissue grinder (size 20, Kontes-Martin, Evanston, Illinois), suitable aliquots of the pellet were taken for protein determination. The cell suspension was again centrifuged and the supernatant aspirated. The pellet was homogenized according to Folch et al. (1975). Twenty volumes of cold  $\text{CHCl}_3:\text{CH}_3\text{OH}$  (2:1 v/v) were added to the pellet which was then homogenized two minutes by hand, vortexed for one minute, and rehomogenized; this procedure was performed continuously for a minimum of twenty minutes. After centrifugation at  $1000 \times g \times 10$  minutes, the homogenate was sequentially re-extracted with 20 volumes  $\text{CHCl}_3:\text{CH}_3\text{OH}$  (1:1 v/v) and 20 volumes  $\text{CHCl}_3:\text{CH}_3\text{OH}$  (1:2 v/v). The debris pellet was washed twice with 2 ml of  $\text{CHCl}_3:\text{CH}_3\text{OH}$  (2:1 v/v) to ensure maximal recovery of the lipids. The supernatants from each fraction were combined, and the total volume was determined. Chloroform was added to increase the final  $\text{CHCl}_3:\text{CH}_3\text{OH}$  ratio to 2:1. The solvent to sample ratio at this step was greater than 50:1, ensuring a high extraction efficiency (Nelson, 1975). With the addition of 0.9% NaCl (w/v) the aqueous volume was brought to 20%, and after a phase separation (centrifugation at  $1000 \times g \times 10$  minutes), the upper phase was removed by aspiration while the lower phase



was washed three times with Folch's theoretical upper phase to remove any remaining water soluble contaminants. The interface between phases was not removed in any of the washing steps, and the washed lower phase was brought to dryness under a stream of  $N_2$  at  $30^{\circ}C$ . Lipid residues were dissolved in a small volume of  $CHCl_3$  (less than one milliliter) and suitable aliquots taken for lipid phosphorus determinations and silic acid chromatography.

Silic acid chromatography was performed as described by Rouser et al. (1967; Dyer, 1978) with the modification to a micro-scale by Ferguson et al. (1975). Silic acid (Bio-Rad Sil A, 200-100 mesh, Bio-Rad Laboratories, Richmond, California) was activated before use at  $100^{\circ}C$ . for twelve hours. Approximately 0.3 grams were suspended in approximately 5 ml of methanol, vortexed, and the slurry poured into a 2 mm I.D. glass wool column (Chromaflex Column, Kontes-Martin, Evanston, Illinois). Until use, the packed columns were stored in methanol. The silic acid columns were sequentially washed with 5 ml of chloroform, 4 ml of methanol, and again with 5 ml of chloroform. Lipid samples were applied to the top of the column in a minimal amount of chloroform. The neutral lipid and cholesterol fractions were eluted by the addition of 6 ml of chloroform. Phosphatides were eluted from the column with 5 ml of methanol. The methanol

fraction containing phospholipids was then evaporated under  $N_2$  and redissolved in chloroform to determine lipid phosphorus. Neutral lipid-cholesterol fractions were dried under nitrogen, and appropriate aliquots were removed after the samples were redissolved in one milliliter of absolute ethanol. All organic reagents were either of ACS or AR quality.

### Thin Layer Chromatography

The method described by Skipski et al. (1964) was used for the thin layer chromatographic separation of individual phosphatide fractions. Forty grams of Silica Gel H (without  $CaSO_4$  binder) (Brinkman Instruments, DesPlaines, Illinois) were slurried with 80 ml of 1 mM  $Na_2CO_3$  for the preparation of four 200 mm x 200 mm plates. Phospholipid samples extracted with chloroform which had been evaporated under an  $N_2$  atmosphere and redissolved in  $CHCl_3:CH_3OH$  (2:1 v/v), were spotted onto the activated plate ( $100^\circ C.$ , 2 hours) with a 25  $\mu l$  Hamilton syringe. The developing system, modified from the original procedure (Skipski et al., 1964) to provide for a greater separation between the PE and PS+PI subclasses (Dyer, 1978), consisted of  $CHCl_3:CH_3OH:CH_3COOH:H_2O$  in the proportions of 25:15:5:3 (v/v). The resolved subclasses, lysophosphatidylcholine, phosphatidylcholine, phosphatidylethanolamine, and phosphatidylserine plus

phosphatidylinositol were identified by comparisons with known standards. Iodine vapor was used to detect the lipid subclasses that were quantitated by lipid phosphorus. When preparative separations were done for methanolysis of the individual lipid classes, rodamine G (0.25% w/v in butanol) was lightly sprayed onto the developed chromatograms and left in a nitrogen atmosphere for one-half to one hour. Iodine vapor was allowed to evaporate overnight under  $N_2$  before lipid elution for the phosphorus determinations was carried out. Lipids were scraped from the plates (X-acto knife, #12 blade) into 15 ml conical glass centrifuge tubes. Elution of the lipids from the silica gel was accomplished by sequentially adding 2 ml of  $CHCl_3:CH_3OH$  (2:1 v/v), 2 ml  $CHCl_3:CH_3OH$  (1:1 v/v), and two elutions of 2 ml each of methanol. The solvent fraction was evaporated under a stream of  $N_2$  at  $30^\circ C.$ , and aliquots of the samples, redissolved in  $CHCl_3:CH_3OH$  (2:1 v/v), were removed for the determination of phosphorus after methanolysis. Adsorption blanks in both cases (iodine and rodamine G visualization) consisted of 2 cm diameter regions of developed plates which had been scraped and eluted in the same manner as the phosphatide-containing areas.

### Preparation of Fatty Acid Methyl Esters

Methanolysis of the phospholipid fractions was performed by the method of Morrison and Smith (1964) using  $\text{BF}_3\text{-CH}_3\text{OH}$  (14% w/v) (Applied Science Laboratories, State College, Penn.). Briefly, three milliliters of esterifying agent was added to the appropriate phospholipid fraction in a glass culture tube fitted with a teflon insert in the screw cap which had been evaporated under a stream of nitrogen at  $30^\circ\text{C}$ . The tubes were placed in boiling water for ten minutes, cooled, and reboiled for an additional five minutes after 5 ml of hexane were added to each tube. The tubes were cooled again, and 5 ml of deionized water were added to affect phase separation. Saturated NaCl solution offered no advantage over deionized water for separation as in the modification of Dyer (1978). The upper hexane phase was removed, and the lower aqueous phase re-extracted twice with 5 ml of hexane. This solution containing the fatty acid methyl esters was adjusted to 100  $\mu\text{l}$  and stored under nitrogen at  $-20^\circ\text{C}$ . with anhydrous  $\text{Na}_2\text{SO}_4$  added as a drying agent.

### Determination of Protein, Phosphorus, and Cholesterol

Protein was determined by a micro-modification of the method of Lowry et al. (1951). Bovine serum albumin

(BSA, Cohn Fraction V, Sigma Chemical Company, St. Louis, Missouri) was used as the protein reference standard. Protein was determined at 750 nm in a 1 cm microcuvette containing the 1.2 ml reaction mixture.

Phosphorus was determined by a micro-modification of the method of Bartlett (1959). Samples in nitric acid washed concial centrifuge tubes (15 ml) were evaporated under a stream of nitrogen and digested with the addition of 300  $\mu$ l of 10 N  $H_2SO_4$  for a minimum of three hours at 160°C. The tubes were cooled, and upon the addition of two drops of 30%  $H_2O_2$  to each tube, the tubes were reheated for an additional one and one-half hours. After digestion, the samples were cooled to room temperature, and the following reagents were added sequentially with vortexing: 20  $\mu$ l of 5% ammonium molybdate, 50  $\mu$ l amino-naphthol sulfonic acid reagent,\* and 650  $\mu$ l of deionized water. Acid washed glass marbles were placed on the tops of the tubes and the samples were heated at 100°C. in a boiling water bath for seven minutes. After color development of the molybdate-inorganic phosphorus complex at 100°C., the absorbance at 795 nm was measured. Anhydrous  $KH_2PO_4$  was used as the inorganic phosphorus standard.

---

\*The 1-amino-2-naphthol-4-sulfonic acid (ANSA) was prepurified according to Fieser and Fieser (1935).

The micro-method was linear between 50 and 800 nanograms of inorganic phosphorus (as defined by a least squares fitting of the standard curve).

Cholesterol content of the samples was analyzed using the method of Rudel and Morris (1973). Total cholesterol was determined after silic acid chromatographic fractions were evaporated under a stream of nitrogen. Two milliliters of phthaldehyde reagent (consisting of 50 mg 0-phthaldehyde per 100 ml glacial acetic acid) was added per sample. After vortexing and incubating in the dark for 10 minutes, color was developed by adding one milliliter of concentrated sulfuric acid. Samples remained in the dark between 10 and 90 minutes after the addition of sulfuric acid until measurement of absorbance at 550 nm. Cholesterol ( $\Sigma$  grade, Sigma Chemical Company, St. Louis, Missouri) was used as the reference standard.

Cholesterol esters, dissolved in 3 ml of 95% ethanol were hydrolysed by the addition of 300  $\mu$ l of 33% (w/v) KOH and incubated at 60°C. for 15 minutes. Aliquots were removed and analyzed for free cholesterol as described above after cooling to room temperature.

#### Gas-Liquid Chromatography

Gas-liquid chromatography (GLC) of fatty acid methyl esters was performed on a Varian Aerograph model

2100 gas chromatograph equipped with a hydrogen flame ionization detector. The isolated peak areas were quantitated by digital integration (Varian Aerograph model 475 digital integrator coupled to a Varian Aerograph model A-6 recorder). Six foot glass columns, 2 mm internal diameter, were treated before use with dimethyldichlorosilane (Sylon-CT, Supelco Inc., Bellefonte, Penn.). The column packing consisted of 10% EGSS-X (ethylene glycol succinate methyl silicone)\* by weight on 100/200 mesh Gas-Chrom Q (Applied Science, State College, Penn.). Columns were preconditioned before use by heating at a rate of 0.5°C. per minute until reaching the column operating temperature. The column was maintained at 175°C., with the injector and detector temperatures maintained at 250°C. Nitrogen (high purity, 99.995%) was employed as the carrier gas. Air (methane-free) and

---

\*EGSS-X was chosen as the liquid phase because of its thermal stability over DEGS (diethylene glycol succinate). DEGS columns heated isothermally at 190°C. (Trapp, 1977) result in large amount of column bleed due to the volatilization of the upper phase at maximum operating temperature. EGSS-X, however, was heated isothermally at 175°C. well below the maximum operating temperature of 225°C., thereby minimizing baseline drift and noise due to the boiling off of the liquid phase. The McReynolds constants of DEGS and EGSS-X are 4581 and 4366, respectively (McReynolds, 1970). This indicates a slightly lower degree of polarity for the EGSS-X liquid phase. The Rohrschneider polarity indices (Mitruka, 1975) for DEGS and EGSS-X are 701 and 678, respectively. For any significant improvement in polarity, however, the difference between the polarity of the two liquid phases should be greater than 30.

hydrogen were used to achieve maximal sensitivity of the flame ionization detector. The flow rates of the gases were kept constant at 300 cc/min air, 30 cc/min hydrogen, and 30 cc/min nitrogen. Peaks were identified by comparison of the retention times versus carbon number with those of known standards (Fat and Oil Mixtures #3 and #6, purified unsaturated fatty acid mixtures (PUFA, #'s 1 and 3; Supelco, Inc., Bellefonte, Penn.). Methyl heptadecanoate (C17:0) (Supelco, Inc., Bellefonte, Penn.) was occasionally added to the sample mixture as both a retention-time and an integration internal standard. Additional identification of the fatty acid methyl esters was performed on a 3% OV-17 column (phenyl silicone) at 200°C. This non-polar liquid phase is unable to separate unsaturated and saturated fatty acid methyl esters, thereby establishing the percentages of unsaturated species within individual samples. The efficiency and degree of separation was further ascertained by methanolysis and subsequent analysis of dioleoylphosphatidylcholine and dilinoleniolyphosphatidylcholine (Applied Science, Inc., State College, Penn.) on EGSS-X and OV-17 columns.



### Electron Spin Resonance: Spin Labels

The doxylstearate spin labels (Waggoner et al., 1969) were purchased from SYVA (SYVA, Palo Alto, California). These included 5-doxylstearate (5-NS; 2-(3-Carboxypropyl)-4,4-dimethyl-2-tridecyl-3-oxazolidinyloxyl; Syva #618), 12-doxylstearate (12 NS; 2-(10-carboxydecyl)-2-hexyl-4,4-dimethyl-3-oxazolidinyloxyl; Syva #614), and 16-doxylstearate (16-NS; 2-(14-Carboxytetradecyl-2-ethyle-4,4-dimethyl-3-oxazolidinyloxyl; Syva #616)(Figures 16 and 17). The nomenclature used by Gaffney (1975) to identify the labels as (12,3), (5,10), and (1,14) corresponds to the 5, 12, and 16-doxylstearate spin labels, respectively.\* Purity of the spin labels was determined by TLC according to the methods of Waggoner et al. (1969) using an elution system of ether on silica gel G or by the method described by Gaffney (personal communication) using benzene:ethyl acetate:acetic acid (100:20:2 v/v) with silica gel G as the adsorbant. A single spot migrated in both cases. Spin labels were stored under nitrogen at  $-20^{\circ}\text{C}$ . in the dark. For stock solution preparation, the solutes were weighed on a Cahn microbalance, dissolved at an appropriate concentration in

---

\*In this thesis, the nomenclature used identified the actual position of the nitroxide from the polar carboxyl end group of the fatty acid chain. The positional nomenclature of Gaffney (1975) is thereby defined as (n+2).

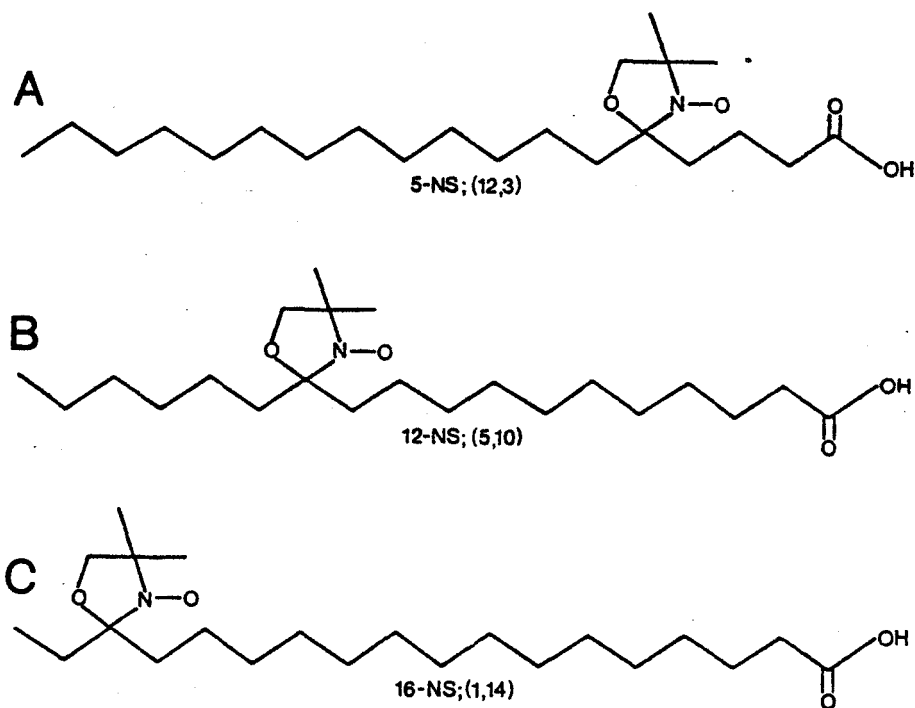


FIG 14: Structure of the nitroxide spin labels. A. 5-NS. B. 12-NS. C. 16-NS. These designations apply to the (12,3), (5,10), and (1,14) nomenclature of Gaffney (1975). The actual position of the nitroxide moiety from the terminal hydroxyl group is (5,12), (12,5), and (16,1) respectively.

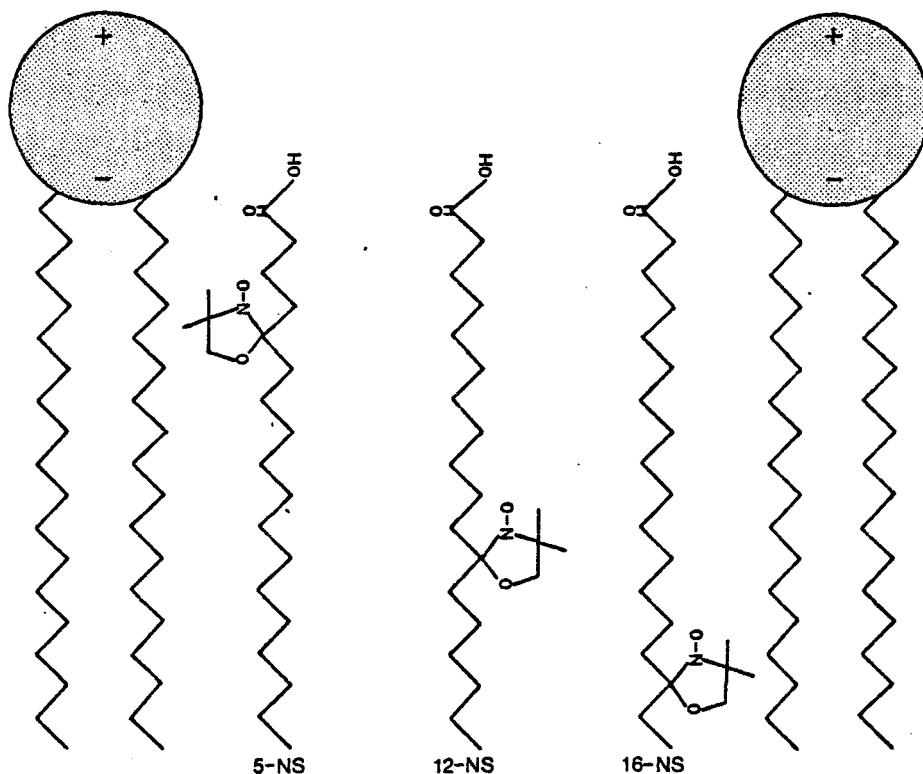


FIG 15 : Orientations of the 5-NS, 12-NS, and 16-NS spin labels intercalated into a lipid bilayer. The 5-NS probe indicates motion nearest the polar phospholipid headgroup region, while the 12-NS label monitors the freedom of motion near the middle of the hydrocarbon chain. The 16-NS monitors motion near the end of the phospholipid acyl side chains in the hydrophobic interior of a bilayer. (Adapted from Knowles *et al.*, 1976.)

absolute ethanol, and stored under identical conditions as the solid spin labels.

### Electron Spin Resonance: Incorporation of Spin Labels into Cells

Cells grown in 25 cm<sup>2</sup> or 75 cm<sup>2</sup> tissue culture dishes, 48 hours after seeding at confluent density were washed three times with prewarmed (37°C.) DMEM. The cell layer was covered with 10 ml of medium without serum containing a specific amount of spin label to provide a probe:lipid ratio of 1:100. NaN<sub>3</sub> was added (0.1% w/v, final concentration) to reduce the rapid reduction of the spin labels. However, considerable reduction did occur despite the NaN<sub>3</sub> with a resulting half-time of approximately twenty minutes. The T-flasks containing cells and spin label were equilibrated with a 10% CO<sub>2</sub>-air mixture and incubated for 5 minutes at 37°C. Excess spin label solution was removed by aspiration, and the cell monolayer washed three times with prewarmed fresh medium (DMEM without serum). Cells were scraped from the plastic surface with the aid of a rubber policeman, dispersed in 5 ml of fresh medium, and centrifuged at 1000 x g x 7 minutes. Lastly, they were taken up into a siliconized 50 µl disposable glass capillary pipet using a minimal amount of fresh media (less than 1 drop) (Corning Glass, Corning, New York). The ends of the pipet were sealed

and immediately used for spectral measurements. Sample pipets were always placed in a quartz tube within the microwave cavity. Approximately  $4 \times 10^6$  to  $1 \times 10^7$  cells were contained in each sample. Cell damage was minimal, as judged by trypan blue dye exclusion, and each sample contained 85-90% viable cells.

### Electron Spin Resonance Measurements

Electron spin resonance measurements were recorded at 9.35 GHz on a Varian E-9 EPR spectrometer located in the Photosynthesis Group, Chemistry Division, Argonne National Laboratory. The center field was held constant at 3240 Gauss. In all measurements, the field sweep was 100 Gauss, the modulation amplitude was 1.0 Gauss, the time constant was set between 0.1 and 0.3 seconds, and the scan time was 0.5 minutes. Microwave power was held constant at 10 mW to avoid signal saturation and sample heating, and Fremy's salt (potassium peroxyamine disulfonate) was used as the field calibration standard (Faber and Frankel, 1967). The spectrometer was coupled to a FabriTech minicomputer on line with the Argonne National Laboratory Sigma V computer (Xerox Data System). All spectra were recorded at least eight times, so that the final spectra were signal averaged spectra (high signal to noise ratios). Individual data points (inner

and outermost hyperfine maxima) were determined from the computer resolved spectra.

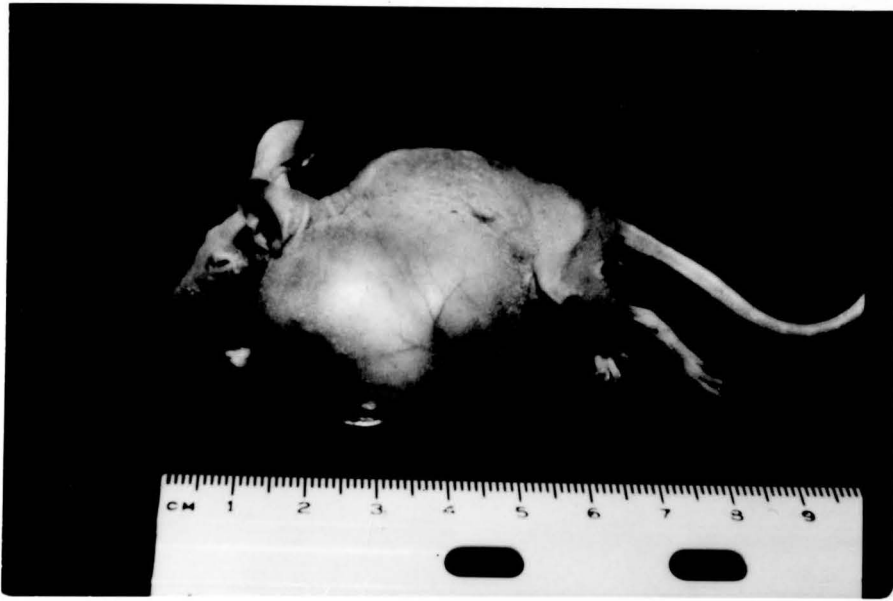
The sample temperature was held constant at 37°C. using a temperature control accessory (Omega Engineering, Stamford, CT.). Nitrogen, at a flow rate of 10 liters per minute, was used to control the heating and cooling of the sample. Temperature was measured by mounting a copper-constantan thermocouple within the quartz tube containing the sample pipet but not within the microwave cavity itself. Samples were equilibrated at least five minutes within the cavity before recording spectra, and the deviation between the cavity and the sample temperature was approximately  $\pm 0.5^{\circ}\text{C}$ .

The concentration of the spin label in the labelling solution and the concentration taken up by the cells was analyzed using double integration (after baseline correction) of the spectra. Appropriate concentrations of spin labels dissolved in absolute ethanol under nitrogen were used as integration standards.

Order parameters were calculated from the inner and outer hyperfine maxima utilizing the equations previously described in the ESR Theory and Order Parameter section.

## RESULTS

Table 1 describes the in vivo and in vitro characteristics of the normal human brain and human brain tumor lines for this dissertation. Two of the cell lines can be considered to be malignant by their tumor production in athymic "nude" mice and soft agar colony-forming efficiency. The SA4 line, initiated from a glioma, produces colonies in 0.33% agar and tumors in nude mice. This line grows to a terminal density of  $3.5 \times 10^5$  cells/cm<sup>2</sup>, approximately an order of magnitude greater than its confluent density. The medulloblastoma, E1202 cell line, possesses the same malignant characteristic; however, it is considered highly malignant due to the rapid rate of tumor development in nude mice (1 x 1 x 1 cm tumor in 14-16 days after subcutaneous injection) (Figure 18). In contrast to their malignant counterparts, the SA101 and TE907 cell lines, derived from a glioma and a medulloblastoma, respectively, have no in vivo or in vitro tumorigenicity characteristics. Although TE907 cells are able to multiply six-fold above their confluent density, they display no tumorigenic activity in "nude" mice or in soft agar assay. These same characteristics, with the exception of actual cell densities, are also observed with the SA101 line.



A



B

FIG 16: Tumor production in athymic "nude" mice. A. typical tumor development upon injection of the SA4 glioma cell line. Tumor is shown 45 days post inoculum. B. Tumor production of the malignant E1202 medulloblastoma cell line. Tumor is depicted at 32 days after subcutaneous inoculation of  $1.0 \times 10^7$  viable cells.



Table 1

Cell Culture Dynamics of Human Brain Tumors in vivo and in vitro

<u>Cell Line</u>	<u>Tumor Type</u>	<u>RPE (%)</u> *	<u>Confluent</u> <sup>f</sup> <u>Density</u>	<u>Terminal</u> <u>Density</u>	<u>Tumorigenicity</u>	
					<u>Nude Mouse</u> <sup>+</sup>	<u>Soft Agar</u> <sup>o</sup>
SA4	Glioma *	88	$5 \times 10^4$ cells/cm <sup>2</sup>	$3.5 \times 10^5$ cells/cm <sup>2</sup>	+ (2/3)	+ (5%)
SA101	Glioma *	80	$4.75 \times 10^4$ cells/cm <sup>2</sup>	$8 \times 10^4$ cells/cm <sup>2</sup>	- (0/3)	- (0%)
E1202	Medullo-+ blastoma	86	$6 \times 10^5$ cells/cm <sup>2</sup>	$22 \times 10^6$ cells/cm <sup>2</sup>	+ (3/3)	+ (10%)
TE907	Medullo-+ blastoma	50	$1 \times 10^5$ cells/cm <sup>2</sup>	$6 \times 10^5$ cells/cm <sup>2</sup>	- (0/3)	- (0%)
251MG3C	Glioma Δ	71.5	$1.3 \times 10^5$ cells/cm <sup>2</sup>	$5.5 \times 10^5$ cells/cm <sup>2</sup>	- (0/3)	+ (7%)
Normal Fetal Brain (NFB)	Normal Fetal ∇ Brain	40	$1.92 \times 10^4$	$4.8 \times 10^4$	-	- (0%)

\* Relative plating efficiency.

<sup>+</sup> Cell lines are scored as + or -; actual tumor production is denoted by tumors produced versus total animals injected.

<sup>o</sup> Cell lines are scored as + or -; actual tumor colony formation is denoted by number of 0.1 mm colonies per 100 or 1000 cells plated.

TABLE 1 (cont.)

## Source of cell lines

- \* R. Manoury, St. Anne's Hospital, Paris, France
- + R. McAllister, Children's Hospital of Los Angeles,  
Los Angeles, California
- Δ A. Lindgren and J. Ponten, Wallenberg Laboratory  
University of Uppsala, Uppsala, Sweden
- ∇ Flow Laboratories, Rockville, Maryland

/Confluent and terminal cell densities are 5%.

Even though the SA101 line was initiated from a malignant glioma, it possesses the characteristics comparable to normal human brain in tissue culture. Normal human fetal brain (NFB), as expected, does not produce tumors in "nude" mice or in the soft agar assay. Under the nutritional conditions used in this study (DMEM with 10% fetal calf serum), the normal fetal brain exhibits a fibroblastic cellular morphology which grows to a confluent density of  $1.9 \times 10^4$  cells/cm<sup>2</sup>. The cell density increases approximately two-fold to a value of  $4.8 \times 10^4$  cells/cm<sup>2</sup> for the terminal cell density. These values are slightly lower than  $5 \times 10^4$  cells/cm<sup>2</sup> and  $8 \times 10^4$  cells/cm<sup>2</sup> for the confluent and terminal cell densities, respectively, which were reported by Ponten (1975). The discrepancy between the literature values and the NFB cell density experimental values may be due to the fact that these cells were near senescence. Interestingly, the SA101 cell line possesses confluent and terminal cell densities comparable to those for normal human brain in tissue culture which were reported by Ponten (1975), but which are slightly above those for the normal fetal brain studied in this dissertation. On the basis of the confluent and terminal cell densities as well as the absence of tumor production in vitro or in vivo, the SA101 line may be considered to

be composed primarily of normal glial cells in culture. Although the 251 MG 3C cell line possesses no in vivo tumorigenic potential (0/0 tumors per total injections in the athymic "nude" mice), the cells form colonies in soft agar. The cell density increases approximately four-fold from confluency to a terminal cell density of  $5.5 \times 10^5$  cells/cm<sup>2</sup>. Under these conditions, the 251 MG 3C line is considered tumorigenic in vitro but non-malignant in vivo. Therefore, this cell line is intermediate in its malignant potential. Comparisons of the relative plating efficiencies for all cell lines reveal that cell derived from tumor tissues, regardless of their tumorigenic activity in vivo and in vitro, possess slightly higher plating efficiencies than normal fetal brain (approximately a two-fold increase), with the exception of the TE907 cell line.

Table 2 shows the overall gross lipid composition of each cell line. All of the cell lines initiated from malignant tissues contain less phospholipid ( $\mu\text{g}/\text{mg}$  protein) than the corresponding normal brain. The levels ranged from 52% to 80% of the level for normal brain phospholipids with the majority of cell lines possessing 60% of the phosphatide level found in NFB cells. In contrast, the total lipid content per cell was greater than

Table 2

## Comparison of Lipid Composition Between Human Cell Lines

<u>Line</u>	<u>Phospholipid</u> ( $\mu\text{gPL/mg Protein}$ )	<u>Cholesterol</u> ( $\mu\text{gCHL/mg Protein}$ )	<u>Total Lipid</u> (g/cell)	<u>CHL/Phospholipid</u> (molar)
SA4 (+,+)	209 $\pm$ 35.2 *	22.42 $\pm$ 6.6	5.66x10 <sup>-11</sup> g	0.21
SA101 (-,-)	128.4 $\pm$ 10.29 *	17.31 $\pm$ 1.45	3.91x10 <sup>-11</sup> g	0.27
E1202 (+,+)	145.6 $\pm$ 4.9 *	20.1 $\pm$ 2.6	2.42x10 <sup>-11</sup> g	0.27
TE907 (-,-)	148.6 $\pm$ 14.9 *	50.65 $\pm$ 7.1	3.55x10 <sup>-11</sup> g	0.69
251MG (-,+)	147.6 $\pm$ 46.2 *	38.8 $\pm$ 13.0	3.99x10 <sup>-11</sup> g	0.49
Normal Fetal Brain	243.5 $\pm$ 27.9	44.47 $\pm$ 11.4	7.29x10 <sup>-11</sup> g	0.37

---

The significance of the difference between the normal fetal brain (NFB) and the tumor derived cell lines is shown by \*P<0.05.

that for the NFB cells in the SA4, SA101, E1202, TE907, and 251 MG 3C cell lines. No striking trend concerning the cholesterol composition of malignant and non-malignant cell pairs can be drawn. Comparison of the cholesterol:phospholipid molar ratios for cultured cells indicates that all cell lines used in this dissertation possess a cholesterol:phospholipid ratio less than 1.0. Values below unity are characteristic of cells cultured in vivo (Wallach, 1975). Cholesterol:phospholipid molar ratios of the malignant cell lines (SA4 and E1202) are lower than those of the non-malignant cell lines (NFB, 251 MG 3C, and TE907) with the exception of SA101 line whose cholesterol:phospholipid ratio is within the range of the tumorigenic cell lines. Although the SA101 cell line possess normal, non-tumorigenic characteristics in vitro and in vivo, the cholesterol:phospholipid molar ratio indicates that there may be a defect in cholesterol biosynthesis for this cell line which is comparable to the other malignant lines but not related to tumorigenicity.

Table 3 lists the individual phospholipid subclass composition and the phosphatide molar ratios for all the cell lines. The levels of phosphatidylethanolamine (PE) do not differ significantly among the tumorigenic, non-tumorigenic, and normal fetal brain cell lines. All of the tumor-derived cell lines (SA4, SA101, E1202, TE907, and 251 MG 3C) contain lower levels of sphingomyelin (SPH) compared to normal fetal brain in vitro. Levels of phosphatidylserine plus phosphatidylinositol (PS + PI) are not significantly lower in the SA4, SA101, and TE907 lines; however, the E1202 and 251 MG 3C lines possess phosphatidylserine plus phosphatidylinositol levels that range from one-half of that for normal fetal brain (as in 251 MG 3C) to approximately one-quarter (as with E1202) of that observed for normal human brain cells. Both malignant and benign cells contain increased concentrations of phosphatidylcholine (PC) as contrasted to normal fetal brain cells. The greatest increases were seen for the SA4, E1202, TE907, and 251 MG 3C lines with some levels nearly double that observed in normal fetal brain cells. A slight increase

Table 3

Comparison of Phospholipid Classes Between Cell Lines (molar %)

<u>Phospholipid Subclass</u>	SA4 (+,+)	SA101 (-,-)	E1202 (+,+)	TE907 (-,-)	251MG (-,+)	NFB (-,-)
Sphingomyelin (Sph)	3.76±0.28†	10.77±5.1†	3.95±0.24†	5.13±1.87†	3.58±2.92†	19.9±0.54
Phosphatidyl Choline (PC)	54.2±1.6†	41.57±3.42†	56.56±1.46†	58.72±2.8†	60.08±0.43†	33.5±0.40
Phosphatidyl Serine + Inositol (PS + PI)	15.1±2.0*	13.13±2.8*	5.86±0.54	12.48±2.95*	10.44±0.52*	19.1±3.2
Phosphatidyl Ethanolamine (PE)	26.9±1.9 <sup>Δ</sup>	34.52±4.34 <sup>Δ</sup>	33.63±0.99 <sup>Δ</sup>	23.66±2.04 <sup>Δ</sup>	25.92±2.17 <sup>Δ</sup>	27.6±4.5
PC/PE	2.0	1.2	1.68	2.48	2.3	1.21
PC/PE + (PS + PI)	1.3	0.87	1.4	1.6	1.65	0.71
PC + Sph/PE + (PS + PI)	1.38†	1.09 <sup>Δ</sup>	1.53†	1.76†	1.75†	1.14 <sup>Δ</sup>

The significance of the difference between normal fetal brain (NFB) and the tumor derived cell lines is shown by: †P<0.005, and \*P<0.05. Δ indicates no difference between the NFB and the other cell lines.



in phosphatidylcholine concentration is seen for the SA101 line, although the level is closer to that observed for NFB cells rather than other non-tumorigenic or tumorigenic cell lines. Examination of the phosphatidylcholine:phosphatidylethanolamine (PC:PE) molar ratios indicates that they are identical for both the SA101 and NFB lines. The malignant cell lines, E1202 and SA4, possess increased PC:PE ratios of 40% and 60% over the NFB level, respectively. For the TE907 and 251 MG 3C cell lines, the ratio is approximately double that of the NFB cell line. Similar trends are observed for the phosphatidylcholine:phosphatidylethanolamine and phosphatidylserine plus phosphatidylinositol molar ratios ( $PC:PE + (PS + PI)$ ) and for the phosphatidylcholine and sphingomyelin:phosphatidylethanolamine and phosphatidylserine plus phosphatidylinositol ( $PC + SPH:PE + (PS + PI)$ ) ratio. For both ratios the SA101 value is nearly identical to that of normal fetal brain while the other values are all greater for the remaining cell lines. With regard to the  $PC:PE + (PS + PI)$  molar ratio, the malignant cell lines E1202 and SA4 possess increased ratios of approximately 40% and 60% above either the SA101 or NFB lines. A doubling of the ratio (100% increase) for the TE907 and 251 MG 3C lines is observed again similar to the increase in the PC:PE molar ratio. Although the  $PC + SPH:PE + (PS + PI)$  ratios for the SA101

and NFB cell lines are identical, the ratio of the other cell lines is not augmented as greatly as for other previously mentioned phosphatide molar ratios. The tumorigenic cell lines, SA4 and E1202, possess increases in the PC + SPH:PE + (PS + PI) ratio; however, the rate of increase (25% and 36%, respectively) is lower compared to the previous cases. Both the TE907 and 251 MG 3C cell lines contain similar increases of about 60% over the levels observed for NFB cells in contrast to the two-fold increase observed for the previous PC:PE and PC:PE + (PS + PI) ratios.

Table 4 (parts 1 and 2) lists the phosphatidylcholine fatty acyl side chain compositions of human brain tumors and normal fetal brain cells in vitro. The percentage of palmitic (hexadecanoic)\* fatty acids (16:0) is increased above NFB levels for only the SA4 and SA101 cell lines. Several fatty acid species: eicosenic acid (20:1), behenic n-docosanoic acid (22:0), eicosatrienoic acid (20:3), and lignoceric (tetracosanoic acid (24:0)) are only observed in tumor-derived cell lines including SA101. On the other hand, docosahexaenoic acid (22:6) levels in the cell lines are approximately 25% of the level

---

\* Common names of the fatty acids and shorthand designations are used whenever possible interchangeably in the dissertation.

Table 4 (1)

Phosphatidyl Choline Fatty Acid Percentage\* Composition of Cell Lines

<u>Fatty Acid</u>	<u>Cell Line</u>					
	<u>E1202</u>	<u>TE907</u>	<u>SA4</u>	<u>SA101</u>	<u>251MG3C</u>	<u>NFB</u>
14:0	0.5 (0.9)	2.6 (0.2)	—	1.0 (0.5)	2.7 (0.3)	0.5
15:0	1.4 (0.2)	1.4 (0.1)	14.2 (3.2)	5.6 (0.8)	1.9 (0.7)	1.6
16:0	14.9 (1.5)	13.7 (0.5) <sup>∇</sup>	7.1 (2.3) <sup>†</sup>	9.4	22.2 (3.1)	17.5 (2.2)
16:1	—	13.6 (2.3) <sup>†</sup>	—	4.8 (0.8) <sup>†</sup>	16.3 (1.2) <sup>†</sup>	0.7
16:2	8.2	—	—	—	—	—
17:0	1.0 (0.5)	—	—	—	0.3	—
18:0	4.2 (0.6) <sup>+</sup>	12.4 (0.2)	4.0 (0.3) <sup>+</sup>	12.2 (1.3)	3.5	13.3 (0.7)
18:1	62.8 (2.0) <sup>+</sup>	35.9 (0.9)	25.5 (2.6) <sup>+</sup>	17.1 (1.1) <sup>+</sup>	37.9 (2.8)	39.9 (2.5)
18:2	1.6 (0.4)	3.8 (0.3)	12.5 <sub>s</sub>	5.2 (1.1)	4.7 (1.2)	2.9 (1.2)
20:0	Trace	Trace	Trace	Trace	Trace	0.1 (0.1)
18:3	1.3 (0.1) <sub>Δ</sub>	2.2 (0.2) <sub>Δ</sub>	8.5 (1.6) <sub>Δ</sub>	2.8 (0.2) <sub>Δ</sub>	0.7 (0.4)	0.3 (0.1)

\* Differences between the sum of the fatty acid percentages in each row and 100% represents the sum of the minor components not given in the table.

Table 4 (2)

<u>Fatty Acid</u>	<u>Cell Line</u>					
	<u>E1202</u>	<u>TE907</u>	<u>SA4</u>	<u>SA101</u>	<u>251MG3C</u>	<u>NFB</u>
20:1	0.3 (0.1)	2.6 (0.4)	6.4 (0.1)	1.9 (0.3)	0.5 (0.2)	—
22:0 + 20:3	0.3 (0.1)	1.3 (0.1)	1.7 (0.2)	2.6 (0.7)	0.7	—
22:1 + 20:4	1.4 (0.1)	4.9 (0.7)†	0.6	2.8 (0.4)¶	0.9 (0.5)	1.8 (0.1)
20:5	0.6	1.0	3.0 (0.5)¶	0.2	Trace	0.6 (0.2)
24:0	0.3	1.0	3.2 (0.1)	3.0	0.8 (0.2)	—
22:4	Trace	0.3 (0.1)Δ	1.4 (0.3)∇	1.4 (0.4)∇	—	2.9
22:5 (n-3)	—	Trace	1.1	3.9 (1.7)	—	—
22:5 (n-6)	0.4 (0.2)¶	0.6 (0.3)¶	1.3 (0.2)¶	—	—	5.8 (0.3)
22:6	1.0 (0.1)¶	0.3 (0.7)¶	3.2 (0.2)¶	23.8 (3.0)†	2.3 (0.8)¶	11.9 (1.1)

\* Differences between the sum of the fatty acid percentages in each row and 100% represents the sum of the minor components not given in the table. Standard deviations are given in parentheses. Differences between the values of the normal fetal brain cells and the other tumor derived cell lines are given by: §P<0.1, ∇P<0.05, ΔP<0.01, ¶P<0.005, and †P<0.001.

Column conditions: 10% EGSS-X on 100/200 Gas Chrom Q, run isothermally at 175°C. Detector and injector temperatures maintained at 250°C.

present in the NFB cell line, with the exception of the SA101 22:6 content which is twice that of the NFB concentration. The same trend is observed for docosate-traenoic (22:4) fatty acids, although the level of the SA101 line is similar to that of the SA4 cell line. Several specific changes are observed when considering the individual phosphatidylcholine acyl chain compositions of malignant and benign cellular pairs, but vary with respect to the levels of the NFB cells. Oleic acid (18:1) levels are greater for the malignant cell lines in the cell tumorigenic:non-tumorigenic cell pairings (i.e., E1202>TE907; SA4>SA101) with the content of normal fetal brain and 251 MG 3C cells being identical. This trend is reversed for stearate acid (n-octadecanoic, 18:0) levels such that the levels of the non-tumorigenic cell lines are increased approximately three-fold, to 12.4% and 12.2% for TE907 and SA101, respectively, compared to 4.2% and 4.0% for the E1202 and SA4 lines, respectively. Normal fetal brain levels of stearic acid are identical to those of non-tumorigenic cell lines in vivo and in vitro (SA101 and TE907); whereas, the 18:0 content of the intermediately malignant line (251 MG 3C0 is closer to that of malignant cells. The linoleic acid (18:2) and pentadecanoic acid (15:0) contents of the medulloblastoma cell lines are similar to that of normal fetal brain cells and 251 MG 3C

cells. In contrast, these levels are increased for both SA series cell lines. For these particular fatty acids, the malignant SA4 line possesses the greatest increases (four-fold and seven-fold for the 18:2 and 15:0 fatty acids, respectively). The SA101 line contains approximately one-half of the 18:2 and 15:0 acyl chain content of the corresponding SA4 line. The overall concentration, however, is increased approximately two-fold and three-fold for the 18:2 and 15:0 species, for both SA4 and SA101 cell lines, respectively, as compared to normal fetal brain levels. Although the malignant cell lines, SA4 and E1202, do not contain detectable levels of palmitoleic acid (hexadecenoic acid, 16:1), the non-tumorigenic cell lines, TE907 and SA101, contain between 13 times (TE907) and five times (SA101) the concentration of 16:1 present in normal fetal brain. It appears that the benign lines, NFB and SA101, contain lower levels of 16:1 than cell lines which possess the intermediate tumorigenicity characteristic of colony formation in soft agar (251 MG 3C) or similar in vitro non-tumorigenic growth characteristics (TE907). Examination of the linolenic acid (18:3) levels reveals that all of the cell lines derived from tumor specimens, regardless of their in vivo or in vitro malignancy characteristics, contain increased concentrations of 18:3 with the largest increase present in the SA4 cell line.

Table 5 (parts 1 and 2) itemizes the fatty acid acyl side chain compositions of the combined phosphatidylserine and phosphatidylinositol subclasses (PS + PI). In contrast to the fatty acid composition of phosphatidylcholine, the phosphatidylserine and phosphatidylinositol subclasses exhibit more distinctive patterns for the tumorigenic and non-tumorigenic cell pairs. Several fatty acids appear to be unique to tumor-derived cell lines. Arachidic acid (n-eicosanoic, 20:0) is present in detectable amounts only within the SA series cell lines (SA4 and SA101); whereas, the behenic (n-docosanoic, 22:0) plus eicosatrienoic acid (20:3) levels are present in low levels in all tumor-derived cells as well as normal fetal brain cells. Unusual monenes, such as palmitoleic acid (hexadecenoic, 16:1) and margaric acid (heptadecanoic, 17:0) also exist in all tumor-derived cell lines with malignant cells having about double the levels of their non-tumorigenic counterparts. Trace amounts are also present in normal fetal brain cells. This is contrasted to the converse situation for the levels of long chain polyunsaturated species. Docosapentaenoic (22:5 (n-6)) concentrations are lower than that of the NFB cellular levels in the glial- and medulloblastomic-originated cell lines. Several cell pairs exhibit correlation of the fatty acid levels with malignancy. For example, docosahexaenoic acid

Table 5 (1)

Phosphatidyl Serine and Phosphatidyl Inositol  
Fatty Acid Percentage\* Composition of Cell Lines

<u>Fatty Acid</u>	<u>Cell Line</u>					
	<u>E1202</u>	<u>TE907</u>	<u>SA4</u>	<u>SA101</u>	<u>251MG3C</u>	<u>NFB</u>
12:0	4.6	—	—	—	—	1.4
14:0	1.6 (0.1)∇	3.3 (0.5)	1.8 (0.5)	3.6 (0.5)∇	2.4 (0.2)	2.6 (0.3)
15:0	2.1	4.4§	4.7 (0.5)§	18.7 (3.8)¶	7.1 (0.3)∇	1.2 (0.2)
16:0	4.0 (0.2)Δ	17.5 (2.1)	1.9 (0.3)Δ	9.9 (2.1)	12.8 (0.8)	13.4 (0.9)
16:1	8.8 (0.3)	0.4	—	3.88	—	—
17:0		1.8	6.9 (0.9)		3.9 (0.5)	Trace
18:0	29.5 (0.9)¶	29.5 (1.7)¶	1.8 (0.5)∇	7.0 (3.2)	3.8 (0.4)∇	9.6 (1.1)
18:1	28.7 (1.2)Φ	30.7 (4.2)Φ	5.7 (1.5)Δ	2.5	15.7 (1.1)	19.1 (1.7)
18:2	2.0 (0.6)Δ	1.7	4.7 (0.5)Δ	5.2	9.4 (0.6)Δ	17.8 (1.6)
20:0	Trace	Trace	0.2	0.4	—	Trace
18:3	Trace	0.8	2.2 (0.3)	5.8 (0.5)∇	8.2 (0.9)∇	2.8 (0.8)

\* Differences between the sum of the fatty acid percentages in each row and 100% represents the sum of the minor components not given in the table.



Table 5 (2)

<u>Fatty Acid</u>	<u>Cell Line</u>					
	<u>E1202</u>	<u>TE907</u>	<u>SA4</u>	<u>SA101</u>	<u>251MG3C</u>	<u>NFB</u>
20:1	1.2 (0.3)	1.5	2.6 (0.2)	3.6	17.3 (2.0)*	0.9 (0.3)
22:0 + 20:3	1.2 (0.5)	0.8 (0.1)	3.5	1.0 (0.1)	—	Trace
22:1 + 20:4	5.5 (0.7)‡	2.7 (0.5)‡	2.6	4.9 (0.3)‡	1.3	1.7
20:5	1.9 (0.7)	1.2 (0.2)	3.5	—	2.9	2.2
24:0	2.3	0.4	1.0 (0.2)	2.4 (0.8)	4.7 (0.2)	2.3
22:4	0.6	Trace	3.1	2.2	0.4	10.0 (1.7)§
22:5 (n-3)	—	—	—	—	0.9	0.5
22:5 (n-6)	—	Trace	5.9 (0.9)¶	3.8	1.9 (0.2)Δ	8.1 (0.2)
22:6	5.9 (0.5)	2.9 (0.8)	47.8 (6.5)*	24.9 (5.3)¶	5.9 (2.0)	6.4 (0.2)

\* Differences between the sum of the fatty acid percentages in each row and 100% represents the sum of the minor components not given in the table. Standard deviations are given in parentheses. Differences between the values of the normal fetal brain cells (NFB) and the other tumor derived cell lines are given by: ‡P<0.25, §P<0.1, ¶P<0.05, §P<0.025, ΔP<0.01, ¶P<0.005, †P<0.001, and \*P<0.0005.

Column conditions: 10% EGSS-X on 100/200 Gas Chrom Q, run isothermally at 175°C. Detector and injector temperatures maintained at 250°C.

acid (22:6) is increased approximately two-fold for malignant lines (E1202 and SA4) over their non-malignant counterparts (TE907 and SA101) and over the NFB levels. Moreover, the SA series glioma levels range from four to eight times the concentration present in normal fetal brain. Short chain saturated fatty acids exhibit a specificity for non-tumorigenic tissues. Myristic acid (14:0) concentrations of the SA101, TE907, and 251 MG 3C are generally comparable to the levels found in normal fetal brain. For the SA101 and the TE907 tissues, pentadecanoic acid (15:0) levels are increased above that of the NFB, SA4, and E1202 lines. The intermediate glioma, 251 MG 3C (-,+), possesses a 15:0 content midway between the malignant SA4 and non-malignant SA101 line content. A similar trend exists for palmitic acid (16:0) where the 251 MG 3C line possesses a concentration between the SA101 and NFB concentrations. Palmitic acid concentrations, however, are greater in the NFB cell line than in the tumor-derived cells as contrasted to the pentadecanoic acid (15:0) levels. As compared to the phosphatidylcholine acyl side chain composition, lipid characteristics of medulloblastoma cell lines cannot be related to the PS + PI fatty acid levels present in NFB cells. Eicosapentaenoic (20:5) levels are decreased for the medulloblastomic E1202 and TE907 lines; however, the glioma-derived cells possess

levels comparable to that of normal fetal brain. The cells of different pathological origins exhibit an inverse relationship between medulloblastoma and glioma derived cells concerning the level of erucic plus arachidonic acid (22:1 + 20:4). These levels in the SA4 glioma are one-half that of the non-tumorigenic counterpart (SA101), and in 251 MG 3C cells, they are comparable to that measured in the NFB cells. On the other hand, the medulloblastomas, which are considerably more malignant, possess a two-fold increase in the 22:1 + 20:4 concentration as measured in the E1202 cell line. Unsaturated fatty acids of stearate origin exhibit fatty acid specific changes correlated with tumorigenicity. Stearic acid (18:0) concentrations are decreased about five-fold in malignant gliomas as compared to the levels present in NFB cells. The degree of malignancy is directly inversely proportional to the concentration of 18:0 for glial type cells, whereby the 251 MG 3C cell line contains 3.8%, SA101 contains 7.0%, and NFB possesses 9.6% of 18:0 PS + PI levels. Both malignant and benign medulloblastomas contain identical levels of 18:0 which are approximately three times that of NFB in contrast to the situation of the glioma-derived lines. Oleic acid (18:1) levels for the E1202 and TE907 cell lines are also similar, and both are greater than the NFB or the glioma levels. Concentrations of 18:1 in the

malignant cell line SA4 are approximately 25% of the NFB level while the intermediate glioma 251 MG 3C has a concentration close to 75% of the normal levels. In the SA101 cell line, the concentration of 18:1 is approximately one-half of the SA4 level as compared to the quantities of 18:0. Linoleic acid (18:2) levels are similarly decreased for the medulloblastoma and the glioma-derived cultures, although the malignant E1202 and non-malignant TE907 cell lines contain equal amounts of 18:2. The gliomas exhibit another partial correlation between 18:2 levels and tumorigenicity. The SA4 line contains approximately one-third the linoleic acid concentration measured in NFB cells; whereas, the 251 MG 3C line has 18:2 levels between SA4 and NFB cells (nearly 50% of the NFB concentration). Lipid analyses show that SA101 cells, however, contain approximately the same concentration of 18:2 fatty acids as the malignant SA4 line. This trend in 18:2 lipid levels is not observed for the linoleic acid (18:3) fatty acid content, whereby the SA4 and NFB lines contain similar concentrations. The 251 MG 3C cells, moreover, have a three-fold increase in their 18:3 levels, compared to a two-fold increase above the 18:3 NFB levels or the SA101 line. Medulloblastoma-derived cells contain substantially lower 18:3 levels, ranging from one-half of the NFB level to trace amounts, in the TE907 and E1202 cell lines,

respectively. Eicosenoic acid (20:1) levels for the TE907 and E1202 lines are identical and comparable to that for the NFB line. The SA4 line contains nearly two times the NFB concentrations of 20:1 while this level is increased three times in the non-malignant SA101 line. As observed with the stearate family, the 251 MG 3C line contains close to a 17-fold increase of 20:1 over the NFB concentrations. Therefore, an inversely proportional concentration gradient is observed for the glioma-derived cell lines which parallels tumorigenicity.

The phosphatidylethanolamine fatty acid acyl side chain composition of tumorigenic and non-tumorigenic cell lines is shown in Table 6 (parts 1 and 2). Several species of fatty acids are selectively decreased in cell lines derived from malignant specimens compared to the same levels in normal human brain cells. Stearic acid (18:0), linoleic acid (18:2), eicosapentaenoic acid (20:5), 4,7,10,13-docosatetraenoic acid (22:4), and 7,10,13,16,19-docosapentaenoic acid (22:5 (n-6)) levels are decreased in the E1202, SA4, SA101, and 251 MG 3C lines compared to the levels present in normal fetal brain. The 18:2 and 22:5 (n-6) lipid concentrations are greater in the tumorigenic cell lines than in their non-malignant counterparts. This effect is not observed with the docosatetraenoic acid (22:4) levels where, of the tumor-derived

Table 6 (1)

Phosphatidyl Ethanolamine Fatty Acid Percentage\* Composition of Cell Lines

Cell Line

<u>Fatty Acid</u>	<u>E1202</u>	<u>TE907</u>	<u>SA4</u>	<u>SA101</u>	<u>251MG3C</u>	<u>NFB</u>
14:0	2.4 (0.1)§	3.9 (0.4)∇	2.6 (0.5)§	6.0 (0.1)∇	5.5 (0.4)∇	0.9 (0.1)
15:0	1.5	2.0	3.1	10.0	3.4	1.9
16:0	9.5 (0.1)	20.0 (0.5)¶	5.4 (0.8)	8.6 (0.2)	28.6 (1.1)¶	9.9 (1.1)
16:1	2.0 (0.1)	4.9 (0.2)¶	4.2 (0.1)¶	6.7 (0.2)¶	Trace(0.1)	0.8 (0.1)
17:0	0.7	Trace			2.8	
18:0	12.9 (0.2)	6.8 (0.4)⊕	4.2 (0.1)⊕	5.3 (0.4)⊕	9.3 (0.3)Δ	16.8 (0.1)
18:1	50.4 (0.5)∇	42.8 (0.1)∇	9.0 (0.1)⊕	10.5 (0.6)⊕	22.6 (0.4)∇	33.6 (0.1)
18:2	3.2 (0.1)∇	2.2 (0.2)∇	5.4 (0.1)	4.8 (0.1)	3.6 (0.3)∇	5.2 (0.1)
20:0	0.3	0.1	Trace	1.2	Trace	0.2 (0.2)
18:3	0.5 (0.2)§	0.8 (0.1)§	3.1 (0.1)⊕	4.2 (0.1)Δ	1.4 (1)	2.0 (0.1)
20:1	0.4	0.1	0.9	Trace	0.9	—

\* Differences between the sum of fatty acid percentages in each row and 100% represents the sum of the minor components not given in the table.

Table 6 (2)

<u>Fatty Acid</u>	<u>Cell Line</u>					
	<u>E1202</u>	<u>TE907</u>	<u>SA4</u>	<u>SA101</u>	<u>251MG3C</u>	<u>NFB</u>
22:0 + 20:3	0.4 (0.1) <sup>Φ</sup>	0.5 (0.1) <sup>Φ</sup>	2.1 (0.2) <sup>§</sup>	—	0.9 (0.2)	1.3 (0.1)
22:1 + 20:4	4.6 (1.0) <sup>∇</sup>	9.6 (0.9) <sup>∇</sup>	2.0 (0.1)	1.6 (0.1) <sup>§</sup>	3.5 (0.5)	2.9 (0.5)
20:5	0.8 (0.1)	0.8 (0.2)	1.8 (0.1)	1.5 (0.3)	1.9 (0.4)	2.5)
24:0	1.9 (0.1)	0.8 (0.1)	2.0 (0.3)	2.4	2.8 (0.4)	2.4 (1.25)
22:4	0.7	0.5	1.4 (0.7) <sup>†</sup>	3.4 (0.1) <sup>∇</sup>	0.7 (0.1) <sup>†</sup>	6.7 (0.9)
22:5 (n-3)	0.6	—	—	—	1.7	Trace
22:5 (n-6)	1.7 (0.1)	0.6 (0.5)	3.6 (0.2) <sup>Δ</sup>	1.5 (0.2)	1.4 (0.1)	2.1 (0.4)
22:6	5.2 (0.4) <sup>∇</sup>	3.3 (0.5) <sup>∇</sup>	42.9 (1.0) <sup>†</sup>	32.3 (0.2) <sup>†</sup>	8.5 (0.3)	10.6 (1.4)

\* Differences between the sum of fatty acid percentages in each row and 100% represents the sum of the minor components not given in the table. Standard deviations are given in parentheses. Differences between the values of the normal fetal brain cells (NFB) and the tumor derived cell lines are given by: §P<0.1, ∇P<0.05, ΦP<0.025, ΔP<0.01, ¶P<0.005, and †P<0.001.

Column conditions: 10% EGSS-X on 100/200 Gas Chrom Q, run isothermally at 175°C. Dectector and injector temperatures maintained at 250°C.

cell lines, the SA101 line possess the highest concentration, approximately one-half of the level present in NFB cells. For both 22:4 and 20:5 fatty acids, the E1202 and TE907 contain similar concentrations, however, both are decreased to one-tenth and one-third of the NFB concentration, respectively. Additionally, both docosapentaenoic acid (22:5 (n-3)) and 9-eicosenoic (20:1) unsaturated fatty acid species are present only in the five tumor-derived cell lines. These lines, furthermore, contain fatty acid levels which are increased over the levels found in normal human fetal brain cells. Myristic acid (14:0) is increased in all five lines (E1202, TE907, SA4, SA101, and 251 MG 3C) with the largest increases being present in the non-malignant TE907 and SA101 cell lines. This same trend is observed only for the SA series and the 251 MG 3C lines containing pentadecanoic acid (15:0) where the non-malignant SA101 line contains five times the concentration present in NFB. A six-fold increase is also observed with respect to the myristic acid (14:0) levels in all tumor-derived lines compared to the NFB cell line. Hexadecanoic acid (palmitic, 16:0) levels are increased as well in all of the tumor-derived cell lines. In particular, the greatest increases occur in the TE907 line (two-fold above the NFB concentration) and in the 251 MG 3C line.



(three-fold above the NFB levels), although the non-malignant SA101 cells contain a 16:0 concentration comparable to that in the NFB line. The 9-hexadecenoic (palmitoleic, 16:1) and heptadecanoic (17:0) concentrations reflect the qualitative trend observed for palmitic acid. The in vivo non-malignant cell lines, TE907, SA101, and 251 MG 3C, exhibit increases ranging from three times (251 MG 3C) to eight times (SA101) the NFB concentration with the TE907 line having six times the NFB 16:1 and 17:0 levels. Interestingly, although the SA4 cells possess approximately four times the NFB level of these two fatty acids, the SA4 levels are only two-thirds of their non-malignant SA101 counterpart.

The medulloblastoma-derived cell lines, E1202 and TE907, contain increased 18:1 fatty acid levels above those observed for the NFB or glioma lines; whereas, this tendency is reversed for docosahexaenoic acid and tetracosanoic (lignoceric, 24:0) acid. For 18:1, 22:6, and 24:0 PE fatty acids, the malignant E1202 line contains approximately 20% (50% for 24:0 levels) more docosahexaenoic acid than its non-malignant counterpart, the TE907 cell line. Glioma-derived SA4 and 251 MG 3C cell lines exhibit systematic increases in both 18:1 and 24:0 fatty acid levels which parallel in vivo tumorigenicity

with the exception of the SA101 line. The SA4 line contains the lowest level of these fatty acid species while the concentrations slightly increase for the SA101 cell line, and are again further increased for the 251 MG 3C cell line. For both 18:1 and 24:0 fatty acids, the SA101 levels are not comparable to those of the NFB line. In contrast, the docosahexaenoic acid level (22:6) presents the converse situation whereby the SA4 line contains four times the NFB level, the SA101 has approximately three times the level of the NFB cells, and the 251 MG 3C cells contain a 22:6 concentration comparable to that of the NFB cells. No correlation between the SA series and the 251 MG 3C lines and malignancy can be made for eicosanoic (arachidic, 20:0), docosanoic acid (behenic, 22:0), eicosatetraenoic (arachidonic, 20:4) fatty acid levels. For the medulloblastomas, the concentration of 22:0 + 20:3 is slightly decreased in E1202 and TE907 cells and increased within the 22:1 + 20:4 subclass. The TE907 line possesses the greatest increase for the medulloblastoma-derived cells of 22:1 + 20:4 lipids. Linoleic acid (18:3) is decreased in the E1202 medulloblastoma compared to NFB, although their non-tumorigenic counterpart possesses a level statistically equivalent to that observed in the malignant cells. The SA series cells on the other hand,

contain increased levels of 18:3 over that of NFB cells. The non-tumorigenic SA101 cells, however, contain approximately a 25% increase in 18:3 concentration above that of the SA4 levels.

Table 7 depicts the fatty acid chain length and saturation of individual phospholipid subclasses as they relate to the in vivo and in vitro cell line tumorigenicity. Of the total phosphatidylcholine fatty acids, the non-malignant cell lines, TE907 and SA101, the glioma SA4, and the intermediate tumorigenic 251 MG 3C line contain approximately 30% saturated fatty acids. No statistically significant correlation can be drawn between the SA4 (+,+) and the SA101 (-,-) cell lines. Considering the medulloblastoma pair, however, the E1201 malignant line contains approximately 22% saturated molecules which is a 10% decrease in the phosphatidylcholine fatty acid saturation level compared to the TE907 line. The trend involving malignancy is more apparent considering the saturation of the phosphatidylserine plus phosphatidylinositol quantities in the TE907 medulloblastoma line. Although the PS + PI levels of the SA101, 251 MG 3C, and NFB cells are statistically identical (nearly 30% in each case of the total fatty acids exist as saturated species). Considering the malignant and non-malignant cell pairs and the fact that the medulloblastoma saturation levels are increased

TABLE 7

Fatty Acid Chain Length and Saturation of Phospholipid Classes

Phospholipid Fraction	<u>Cell Line</u>					
	<u>E1202</u>	<u>TE907</u>	<u>SA4</u>	<u>SA101</u>	<u>251MG3C</u>	<u>NFB</u>
Average Percentage <sup>+</sup> Saturated Fatty Acids						
PC	22.3 (3.7) $\Delta$	31.1 (1.0)	28.5 (5.9) $\Psi$	31.2 (2.6)	31.4 (4.3)	33
PS + PI	44.1 (1.2) $\nabla$	56.9 (4.3) $\nabla$	18.3 (2.9) $\S$	42.0 (10.4) $\Psi$	34.7 (2.4)	29.1 (2.5)
PE	29.2 (0.6)	33.6 (1.6)	11.6 (1.8) $\Pi$	33.5 (0.7)	52.4 (2.2) $\Delta$	32.1 (1.8)
Average Percentage Fatty Acid Chains Less Than C20*						
PC	96 $\Phi$	86 $\Phi$	72	58 $\nabla$	90 $\Phi$	77
PS + PI	81 $\Delta$	90 $\Delta$	30 $\Pi$	57	63	67
PE	83 $\nabla$	83 $\nabla$	37 $\nabla$	56 $\Phi$	77 $\S$	71

<sup>+</sup> 22:0+20:3 Fraction not included in total percentage

\* Excluding C20

TABLE 7 (cont.)

Standard deviations are given in parentheses. Differences between the values of the normal fetal brain cells (NFB) and the other tumor derived cell lines are given by:  $\Psi P < 0.25$ ,  $\S P < 0.1$ ,  $\nabla P < 0.025$ ,  $\Phi P < 0.01$ , and  $\Uparrow P < 0.005$ .

The average percentage of saturated fatty acids represents the mean of three determinations each on the OV-17 (3% OV-17 by weight on 100/200 mesh Gas-Chrom Q at 200°C), and EGSS-X (10% EGSS-X by weight on 100/200 mesh Gas-Chrom Q at 175°C) columns. The average percentage of fatty acid chains less than C20 (excluding C20) is the sum of the means from Tables 4(1), 4(2), 5(1), 5(2), and 6(1), and 6(2).

above that of the NFB cells, the non-tumorigenic TE907 cell line contains 56% saturation as compared to 44% for its malignant E1202 counterpart. The same trend of a non-malignant cell line containing a higher fatty acid saturation level is also observed for the SA4-SA101 cell pair (18% compared to 42%, + 10%, respectively). Moreover, this tendency is observed for the phosphatidylethanolamine saturated fatty acids with the exception of the 251 MG 3C cells. For this phosphatide subclass, the non-tumorigenic SA101 and TE907 cells, as well as the NFB line, contain approximately 30% saturated fatty acids. The difference between the malignant and non-malignant medulloblastomas is not as prominent compared to the previously discussed phospholipid PC or PS + PI subclasses. The non-tumorigenic TE907 cell line contains slightly increased saturation levels compared to its tumorigenic counterpart, E1202 (33% compared to 29%, respectively). Additionally, the SA series cell lines possess statistically significant differences between tumorigenic and non-tumorigenic cell pairs. The malignant SA4 line possesses only 11% of its phosphatidylethanolamine fatty acids as saturated species compared to 33% in the "normal" glial SA101 cells. The 251 MG 3C line is an anomaly, since approximately 50% of the phosphatidylethanolamine fatty acids are saturated.

A common relationship is apparent for the medulloblastoma cell pairs whereby the malignant cell always contains a lower percentage of fatty acid saturation (increased unsaturation) for all the phosphatide subclasses. The SA series cells possess this trend with the exception of the nearly identical phosphatidylcholine fatty acid saturation levels for malignant SA4, non-malignant SA101, and normal fetal brain cells. For the 251 MG 3C cell line, the only major phospholipid fatty acid saturation levels which are not comparable to that of NFB are observed in the phosphatidylethanolamine subclass.

Considering the fatty acid chain length, no striking correlations are observed between tumor-derived in vitro or in vivo non-tumorigenic cells and the NFB line. On the other hand, correlations can be drawn regarding fatty acid total chain lengths of 20 carbons or less and malignancy between benign and malignant cell pairs. In the case of phosphatidylcholine, the malignant cell lines E1202 and SA4 contain 96% and 72%, respectively, of their fatty acids with chain lengths less than 20 methylene groups. This is contrasted to the situation in the non-tumorigenic TE907 and SA101 lines where 86% and 58%, respectively, of the fatty acids are short chain lengths. The malignant cell lines, generally, possess a greater concentration of short chain fatty acids compared

to their non-malignant counterparts. The medulloblastoma levels, moreover, contain increased amounts of short chain fatty acids as compared to the 77% level present in the NFB cells. Concentrations of short chain fatty acids progress from 58% in benign SA101 cells to 72% for the malignant SA4 line to 90% for the 251 MG 3C cells. This trend is reversed for the medulloblastoma and glioma-derived cell lines when considering the phosphatidylserine plus phosphatidylinositol subclasses. For the PS + PI subclass, the medulloblastomas contain increased amounts of short chain fatty acids as compared to the level present in NFB cells. Ninety percent of the fatty acids in the TE907 cell line are short-chained ones as compared to 81% in the malignant E1202 line. A more prominent trend is observed for the SA4-SA101 cell pair where the non-malignant cell line, SA101, contains 57% short chain fatty acids compared to 30% tumorigenic SA4 cells. The glioma-derived cells have lower short chain fatty acid levels compared to those of the NFB cells, although the level for the 251 MG 3C cell line is nearly identical (63%) to that of the normal fetal brain in vitro (67%). Examination of the fatty acid chain lengths less than 20 carbons for the phosphatidylethanolamine subclass reveals no difference between the malignant and benign medulloblastoma cell pairs; however, the levels are approximately 10% greater



than NFB cells (83% and 71%, respectively). As observed with the PS + PI short chain lengths, the non-malignant SA101 cell line contains more short chain fatty acid species than the malignant SA4 line, 37% and 56%, respectively. Furthermore, the SA lines are composed of less short chain fatty acids than a chain length level lower than that of NFB cells; whereas, the intermediate 251 MG 3C cells have approximately the same levels as NFB cells (77%).

Overall, the chain length increase or decrease appears to be specific for tumorigenicity in only medulloblastomas when the phosphatides contain serine, inositol, or choline. The SA-derived cells show increased concentrations of short chain fatty acids with less than 20 methylene groups for the PS + PI and PE subclasses in the non-tumorigenic SA101 line. The 251 MG 3C cells do not appear to fit into a graded membrane tumorigenicity model as this lines' chain length would be expected to, but does not lie between the values obtained for non-malignant and malignant gliomas and paralleled its intermediate tumorigenicity.

The nitroxide spin labels, 5-NS, 12-NS, and 16-NS, intercalated into intact tumor-derived cell lines and normal fetal brain cells are depicted and analysed in the following figures. The 5-doxylostearate probe indicates

few gross differences between malignant, benign, and normal cells as observed in the composite spectra of Figure 19. When these spectra are compared to the normal fetal brain cell line (NFB) and the tumorigenic:non-tumorigenic cell pairs, subtle differences are observed. Figure 20 shows the spectra of the 5-NS spin label intercalated into the medulloblastoma cell pair compared to the spectra of the same label in the NFB cell line. These spectra are indicative of slow rotational motion due to the observable broadening of the outermost hyperfine maxima lineshape. An outermost hyperfine splitting on the highfield portion of the spectra is also observed, although this feature is absent in the spectra of the 12-NS and 16-NS probes. Comparison of the  $T_{\parallel}$  splittings in Table 8 indicates that the splitting (in Gauss) of the TE907 line is comparable to that of the NFB cells, although different from the malignant medulloblastoma E1202 cell line. In this case, the decrease in  $T_{\parallel}$  for the TE907 and E1202 cells from that of the NFB  $T_{\parallel}$  splitting may be perceived as less restrictive motion indicative of an increase in fluidity for the previously mentioned cell lines. Examination of the calculated order parameters in Table 8, moreover, corroborates this finding. Even though the TE907  $T_{\parallel}$  splitting is statistically lower than that of the corresponding malignant medulloblastoma E1202 (i.e.,

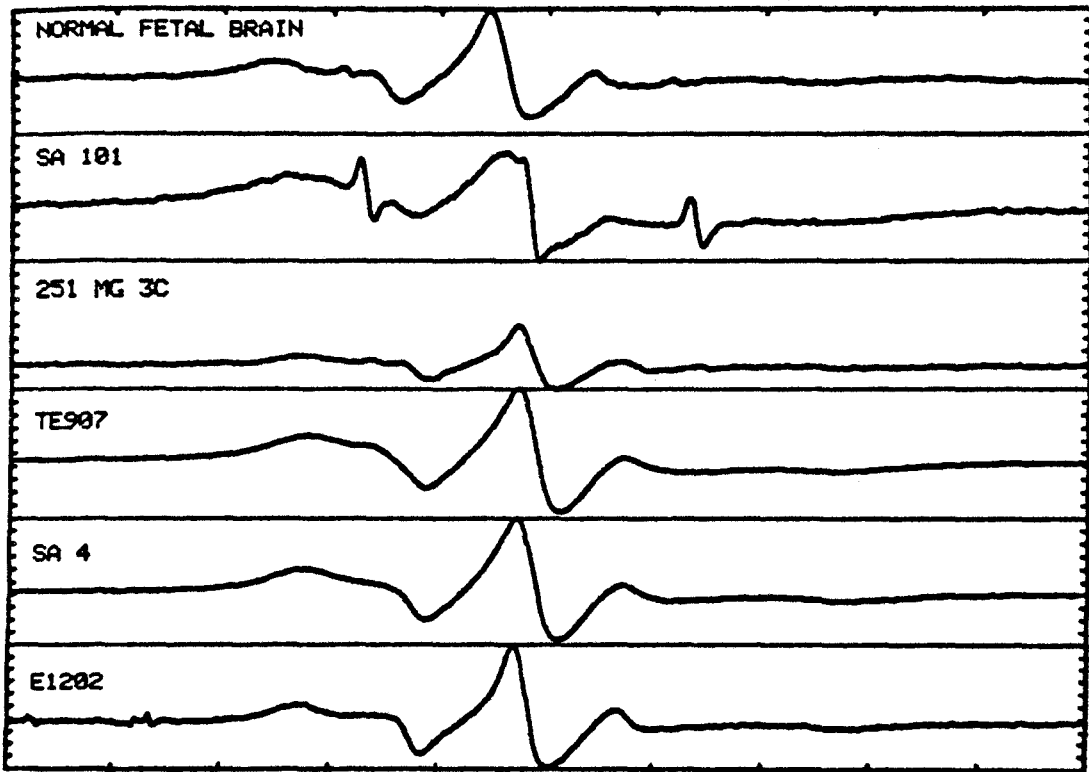


FIG 17: Spectra of the 5-NS spin label (5,12) intercalated into the NFB cell line and the five tumor-derived cell lines. All the following spectra are centered about 3240G and have a 100G scan width.

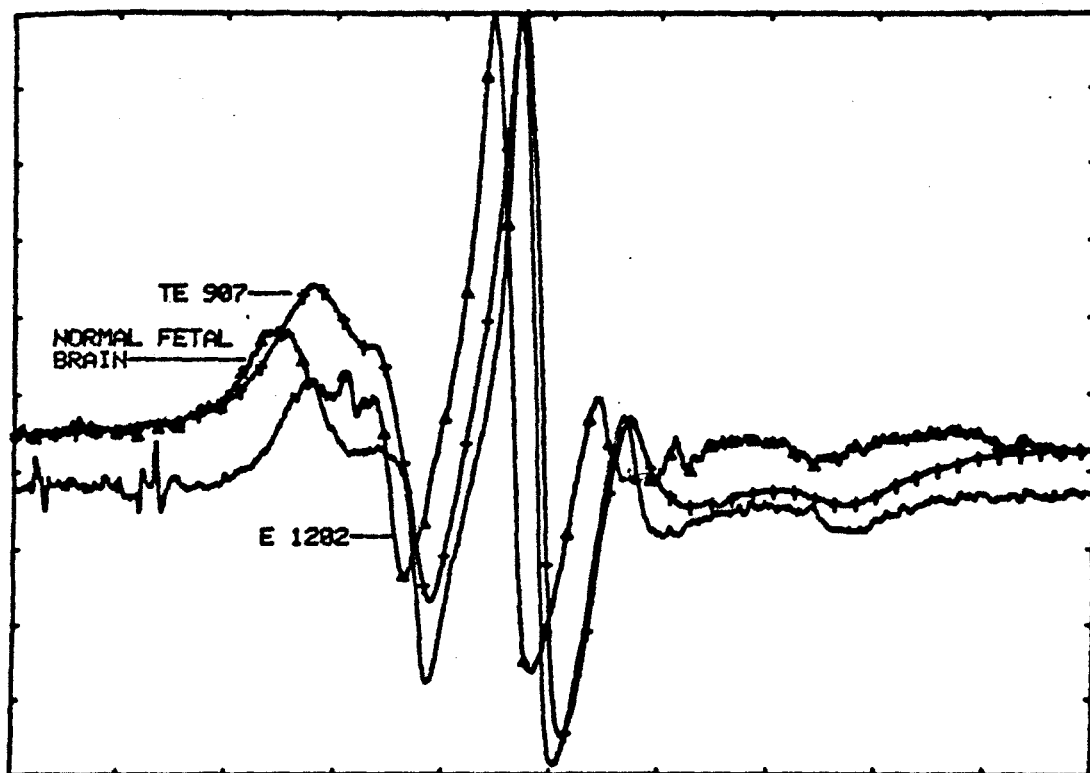


FIG 18: Composite 5-NS (5,12) spectra of the medulloblastoma-derived E1202 and TE907 lines with the NFB cell line.

Table 8

Comparison of ESR Order Parameters for Probe (5,12)  
 Tensor Values  $T_{xx}=T_{yy}=6.1G$   $T_{zz}=32.4G$

Cell Line	$T_{xx}$	$T_{yy}$	$a_n$	$a_n'$	$s'$	$s''$	$s$	$m$
E1202 (+,+)	24.74 $\pm 0.049$	9.06 $\pm 0.10$	14.865	14.29 $\pm 0.07$	0.59 <sup>†</sup> $\pm 0.01$	0.79 <sup>†</sup> $\pm 0.01$	0.62 <sup>†</sup> $\pm 0.01$	0.75 $\pm 0.002$
SA4 (+,+)	24.84 $\pm 0.30$	9.44 $\pm 0.33$	14.865	14.51 $\pm 0.22$	0.58 <sup>†</sup> $\pm 0.01$	0.79 <sup>†</sup> $\pm 0.01$	0.59 <sup>†</sup> $\pm 0.02$	0.73 $\pm 0.01$
TE907 (-,-)	24.43 $\pm 0.18$	9.26 $\pm 0.07$	14.865	14.31 $\pm 0.02$	0.58 <sup>†</sup> $\pm 0.01$	0.78 <sup>†</sup> $\pm 0.01$	0.60 <sup>†</sup> $\pm 0.01$	0.74 $\pm 0.01$
251MG (-,+)	26.65 $\pm 0.09$	8.93 $\pm 0.05$	14.865	14.832	0.67 <sup>†</sup> $\pm 0.01$	0.90 <sup>†</sup> $\pm 0.01$	0.65 $\pm 0.03$	0.75 $\pm 0.01$
SA101 (-,-)	24.53 $\pm 0.35$	8.99 $\pm 0.22$	14.865	14.17 $\pm 0.22$	0.59 <sup>†</sup> $\pm 0.01$	0.78 <sup>†</sup> $\pm 0.02$	0.62 <sup>†</sup> $\pm 0.02$	0.75 $\pm 0.01$
NFB (-,-)	25.45 $\pm 0.15$	8.86 $\pm 0.11$	14.865	14.39 $\pm 0.09$	0.63 $\pm 0.01$	0.84 $\pm 0.01$	0.65 $\pm 0.01$	0.76 $\pm 0.01$

The significance of the difference between the normal fetal brain (NFB) and the tumor derived cell lines is given by  $\dagger P < 0.0005$ .

more fluid), the  $S'$ ,  $S''$ , and  $S$  order parameter values are identical for both cell lines. Table 9 shows the  $S_{\parallel}$  and  $S_{\perp}$  values are also equivalent, although the  $S_{\text{GAF}}$  order parameter indicates that the TE907 line possesses a more fluid membrane than either the E1202 or NFB cells. The isotropic splitting factors (Tables 8 and 9) are identical for the NFB, E1202, and TE907 cells. The value,  $m$ , indicative of probe-probe interactions if less than unity, is approximately 0.75 for all three cell lines, even though probe-lipid ratios of 1:100 or greater were used. In general, the 5-NS spin label order parameters lie within 0.5-0.6\* except for  $S''$  calculations. The calculated  $S''$  5-NS order parameter for E1202, TE907, and NFB is approximately 0.8, indicating extremely restricted motion similar to that of a frozen (powder) spectra. Furthermore, calculations for order parameters done using tensor values of  $T_{xx} = 6.3$  G,  $T_{yy} = 5.8$  G, and  $T_{zz} = 33.6$  G in Tables 10 and 11 present the same qualitative and quantitative picture as the order parameters that calculated with tensor values of  $T_{xx} = T_{yy} = 6.1$  G and  $T_{zz} = 32.4$  G (Tables 8 and 9). Comparisons done among order parameter tensor values indicate that the calculations using the BSA-nitroxide

---

\* It must be noted that a value of 0 is indicative of a "fluid" environment whereas a value of 1.0 indicates restricted motion.

Table 9

Comparison of Corrected ESR Order Parameters for Probe (5,12)  
 Tensor Values  $T_{xx}=T_{yy}=6.1G$   $T_{zz}=32.4G$

Cell Line	$T_{  }$	$T_{\perp}$	$a_n$	$a_n'$	$S_{GAF}$	$S_{  }$	$S_{\perp}$
E1202 (+,+)	24.74 <u>+0.049</u>	9.06 <u>+0.10</u>	14.865	14.29 <u>+0.07</u>	0.54 <sup>T</sup> <u>+0.01</u>	0.56 <sup>+</sup> <u>+0.01</u>	0.59 <u>+0.01</u>
SA4 (+,+)	24.84 <u>+0.30</u>	9.44 <u>+0.33</u>	14.865	14.31 <u>+0.22</u>	0.51 <sup>Δ</sup> <u>+0.02</u>	0.56 <sup>+</sup> <u>+0.01</u>	0.53 <sup>Δ</sup> <u>+0.03</u>
TE907 (-,-)	24.43 <u>+0.18</u>	9.26 <u>+0.07</u>	14.865	14.31 <u>+0.02</u>	0.51 <sup>Δ</sup> <u>+0.01</u>	0.55 <sup>+</sup> <u>+0.01</u>	0.55 <sup>Δ</sup> <u>+0.01</u>
251MG (-,+)	26.65 <u>+0.09</u>	8.93 <u>+0.05</u>	14.865	14.832	0.50 <sup>Δ</sup> <u>+0.01</u>	0.57 <u>+0.03</u>	0.49 <sup>Δ</sup> <u>+0.01</u>
SA101 (-,-)	24.53 <u>+0.35</u>	8.99 <u>+0.22</u>	14.865	14.17 <u>+0.22</u>	0.54 <sup>T</sup> <u>+0.01</u>	0.55 <u>+0.02</u>	0.56 <sup>ψ</sup> <u>+0.05</u>
NFB (-,-)	25.45 <u>+0.15</u>	8.86 <u>+0.11</u>	14.865	14.39 <u>+0.09</u>	0.57 <u>+0.01</u>	0.60 <u>+0.01</u>	0.59 <u>+0.01</u>

The significance of the difference between the normal fetal brain (NFB) and the tumor derived cell lines is given by:  $\psi P < 0.1$ ,  $T P < 0.01$ ,  $\Delta P < 0.005$ , and  $+P < 0.0005$ .

spin label hyperfine tensor values in the latter series of tables result in lower  $S'$ ,  $S''$ , and  $S_{||}$  values.  $S_{GAF}$  and  $S$  values appear equivalent regardless of hyperfine tensor values; whereas, the  $S_{\perp}$  value is smaller when the latter BSA-nitroxide tensor value is used. The  $m$  values, moreover, are slightly increased towards unity, while the isotropic splitting constant,  $a'_n$ , a measure of nitroxide environment hydrophobicity, does not significantly differ with tensor value substitution.

Examination of the 5-NS spin label in the SA4 and SA101 glioma-derived cell lines and the NFB cell lines in Figure 21 depicts the same qualitative features of the previously discussed medulloblastoma-derived cell lines. The SA101 spectra is characterized by large free probe peaks on either side of the centermost splitting. The  $T_{||}$  splittings for all three lines, SA4, SA101, and NFB, appear statistically identical. Calculation of the 5-NS order parameters using crystalline hyperfine tensors from Figure 21 indicates that the SA4 and SA101 values are essentially equivalent but are less than the calculated NFB values of  $S'$ ,  $S''$ ,  $S$  and  $S_{||}$  (Tables 8 and 9). The order parameters of  $S_{\perp}$  are statistically identical for the SA series cell lines and the normal fetal brain cells. No differences, furthermore, are noted for  $a'_n$  values or for the probe-probe interactions value,  $m$ , among the three



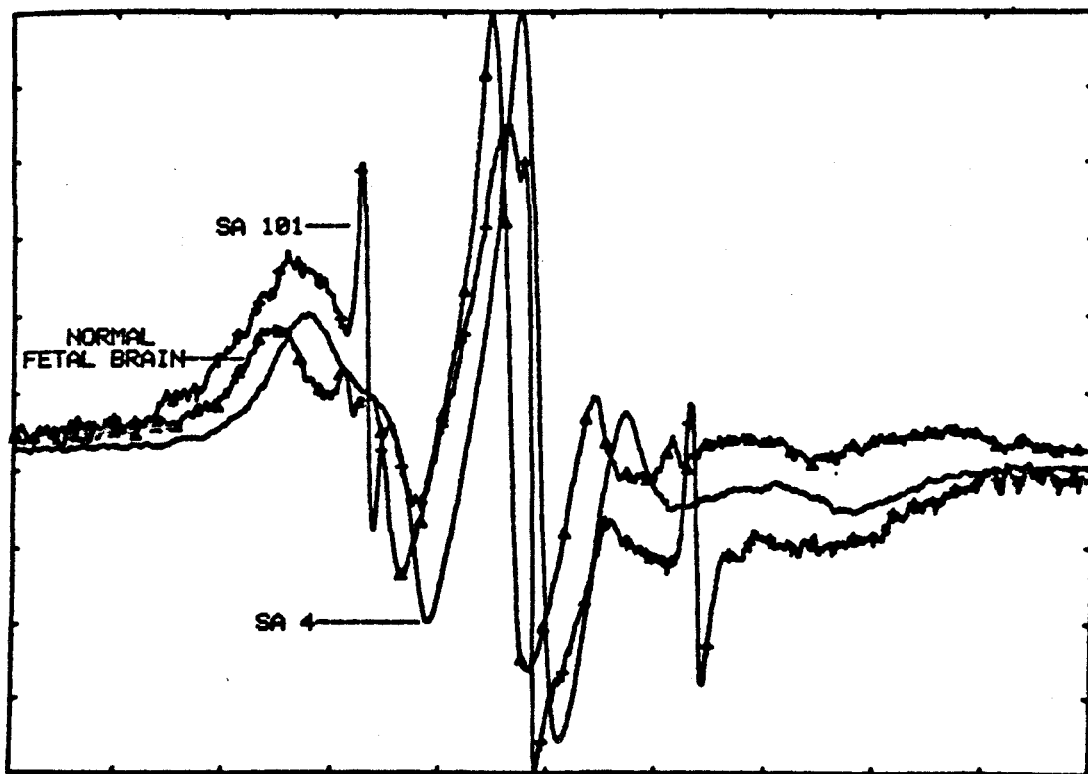


FIG 19: 5-NS (5,12) composite spectra of the SA-series glioma-derived lines SA4 and SA101 with the NFB cell line.

cell lines. The  $S_{\text{GAF}}$  order parameter exhibits a sequential progression of order parameter sensed fluidity. With the  $S_{\text{GAF}}$  parameter, the SA4 cells show greater fluidity than their non-tumorigenic counterpart, the SA101 line. The NFB cells are shown to be less fluid than the SA101 cell line by this same calculation. Therefore, the fluidity progresses in the order SA4>SA101>NFB, which also parallels tumorigenicity in vivo. Considering the VSA-nitroxide hyperfine tensor value order parameter calculations in Tables 10 and 11, the same trends are observed as for the crystalline hyperfine tensor order parameter calculations of Tables 8 and 9.  $S'$ ,  $S''$ ,  $S$ , and  $S$  are again equal for the malignant SA4 cell line and the non-tumorigenic SA101 cells with the order parameter values for both being lower than those of the NFB cells. The  $S'$  's of SA101 and NFB appear equivalent along with the  $a'_n$  and  $m$  calculations, and the  $S_{\text{GAF}}$  order parameter again exhibits a fluidity decrease which progresses sequentially so that the fluidity of SA4>SA101>NFB. As previously shown by comparisons between the NFB and medulloblastoma-derived cell lines using crystalline and BSA-nitroxide tensor values, the same trend is evident for tensor value comparisons of the SA series cells and NFB cell line.  $S$  is increased in the BSA-nitroxide hyperfine tensor value calculations in Tables 10 and 11; whereas, the order

Table 10

Comparison of ESR Order Parameters for Probe (5,12)  
 Tensor Values  $T_{xx}=6.3G$   $T_{yy}=5.8G$   $T_{zz}=33.6G$

Cell Line	$T_{  }$	$T_{\perp}$	$a_n$	$a_n'$	$S'$	$S''$	$S$	$m$
E1202 (+,+)	24.74 <u>+0.049</u>	9.06 <u>+0.10</u>	15.298	14.34 <u>+0.08</u>	0.57† <u>+0.01</u>	0.734† <u>+0.001</u>	0.61† <u>+0.01</u>	0.78 <u>+0.01</u>
SA4 (+,+)	24.84 <u>+0.30</u>	9.44 <u>+0.33</u>	15.298	14.58 <u>+0.32</u>	0.562† <u>+0.002</u>	0.74† <u>+0.02</u>	0.59† <u>+0.01</u>	0.76 <u>+0.02</u>
TE907 (-,-)	24.43 <u>+0.18</u>	9.26 <u>+0.07</u>	15.298	14.31 <u>+0.02</u>	0.56† <u>+0.02</u>	0.74† <u>+0.02</u>	0.59† <u>+0.01</u>	0.76 <u>+0.01</u>
251MG (-,+)	26.65 <u>+0.09</u>	8.93 <u>+0.05</u>	15.298	14.832	0.65† <u>+0.02</u>	0.86† <u>+0.03</u>	0.67 <u>+0.01</u>	0.76 <u>+0.01</u>
SA101 (-,-)	24.53 <u>+0.35</u>	8.99 <u>+0.22</u>	15.298	14.21 <u>+0.26</u>	0.57† <u>+0.02</u>	0.73† <u>+0.03</u>	0.61† <u>+0.02</u>	0.78 <u>+0.01</u>
NFB (-,-)	24.45 <u>+0.15</u>	8.86 <u>+0.11</u>	15.298	14.45 <u>+0.33</u>	0.60 <u>+0.02</u>	0.78 <u>+0.02</u>	0.64 <u>+0.02</u>	0.77 <u>+0.01</u>

The significance of the difference between the normal fetal brain (NFB) and the tumor derived cell lines is given by  $\dagger P < 0.0005$ .

Table 11

Comparison of Corrected ESR Order Parameters for Probe (5,12)  
 Tensor Values  $T_{xx}=6.3G$   $T_{yy}=5.8G$   $T_{zz}=33.6G$

Cell Line	$T_{  }$	$T_{\perp}$	$a_n$	$a_n'$	$S_{GAF}$	$S_{  }$	$S_{\perp}$
E1202 (+,+)	24.74 $\pm 0.049$	9.06 $\pm 0.10$	15.298	14.34 $\pm 0.08$	0.54 <sup>T</sup> $\pm 0.01$	0.506 <sup>†</sup> $\pm 0.003$	0.61 $\pm 0.01$
SA4 (+,+)	24.84 $\pm 0.30$	9.44 $\pm 0.33$	15.298	14.58 $\pm 0.32$	0.52 $\Delta$ $\pm 0.01$	0.51 <sup>†</sup> $\pm 0.02$	0.57 $\Delta$ $\pm 0.04$
TE907 (-,-)	24.43 $\pm 0.18$	9.26 $\pm 0.07$	15.298	14.31 $\pm 0.02$	0.52 $\Delta$ $\pm 0.01$	0.50 <sup>†</sup> $\pm 0.02$	0.593 $\Delta$ $\pm 0.005$
251MG (-,+)	26.65 $\pm 0.09$	8.93 $\pm 0.05$	15.298	14.832	0.51 $\Delta$ $\pm 0.01$	0.54 $\pm 0.03$	0.53 $\Delta$ $\pm 0.01$
SA101 (-,-)	24.53 $\pm 0.35$	8.99 $\pm 0.22$	15.298	14.21 $\pm 0.26$	0.54 <sup>T</sup> $\pm 0.02$	0.50 $\pm 0.03$	0.62 <sup>ψ</sup> $\pm 0.02$
NFB (-,-)	24.45 $\pm 0.15$	8.86 $\pm 0.11$	15.298	14.45 $\pm 0.33$	0.56 $\pm 0.02$	0.55 $\pm 0.02$	0.63 $\pm 0.01$

The significance of the difference between the normal fetal brain (NFB) and the tumor derived cell lines is given by:  $\psi P < 0.1$ ,  $TP < 0.01$ ,  $\Delta P < 0.005$ , and  $\dagger P < 0.0005$ .

parameters of the remaining calculations are slightly lower for the latter BSA tensor values. The  $S_{\text{GAF}}$  order parameter, furthermore, does not exhibit any significant difference with tensor value substitution.

Comparison of the spectra for the 251 MG 3C cell line and the NFB cells in Figure 22 exhibits two large free probe peaks as seen for the 5-NS probe in SA101 cells. The  $T_{\parallel}$  splitting does not significantly differ from that of the NFB line, although the  $S'$  and  $S''$  for the crystalline hyperfine tensor values in Tables 8 and 9 are greater than those of the NFB cells. This is indicative of a more rigid membrane for 251 MG 3C intermediate tumorigenic cell line. The  $S_{\text{GAF}}$  and  $S_{\perp}$  order parameters are decreased for the 251 MG 3C cell line. This is in contrast to the  $S'$  and  $S''$  values, supportive of a more fluid membrane for the intermediate tumorigenic cell line with the largest increase being in the  $S_{\perp}$  calculation. In addition, the  $S$ ,  $S_{\parallel}$ , and  $m$  values are identical for the 251 MG 3C and the NFB cell lines. No conclusion can be drawn regarding the isotropic splitting constant  $a'_n$  for the 251 MG 3C glioma and normal fetal brain cells. Tensor value substitution accounts for some of the partial trends observed among other cell lines. Overall,  $S'$ ,  $S''$ , and  $S$  order parameter values are less for the BSA-nitroxide hyperfine tensor values in contrast to a greater  $S_{\perp}$  value.

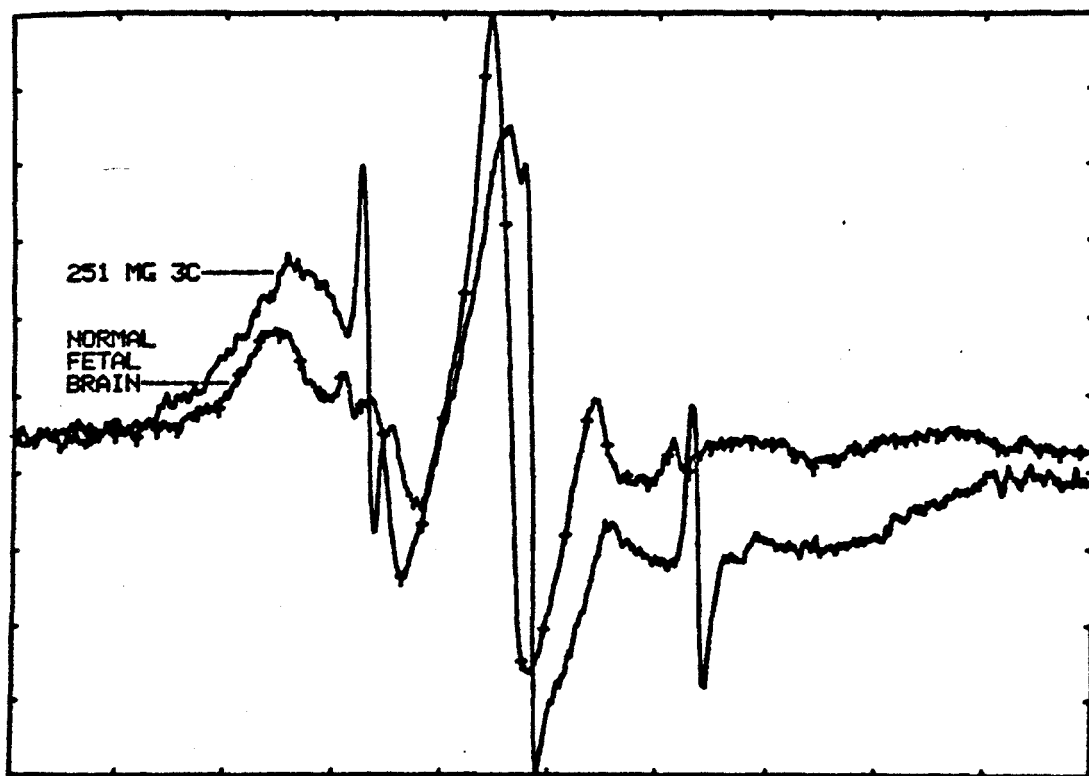


FIG 20: Composite spectra of the 251MG 3C glioma-derived line and NFB cell lines probed with the 5-NS (5,12) spin label.

Although  $S_{\text{GAF}}$  values are equivalent for other cell lines with tensor value substitutions, a comparison of the 251 MG 3C cell line to them indicates that the  $S$ ,  $m$ , and  $a'_n$  values are equivalent as indicated in Tables 8 and 9 and Tables 10 and 11.

The medulloblastoma, SA series, the intermediate tumorigenic 251 MG 3C line, and the NFB cell line intercalated with the 12-NS spin label are depicted in the spectra of Figure 23. The most prominent qualitative feature of Figure 23 is a decrease in the broadening of the hyperfine maxima, indicating an expected overall increase in the motional freedom of the 12-doxylstearate probe. Noticeable free probe peaks are present in the SA101 and the NFB spectra and the 251 MG 3C lineshape possesses a decreased signal-to-noise ratio due to an increased rate of degradation of the 12-NS probe. When the spectra are separated and individually compared to that of the NFB cell line, trends different from those of the 5-NS spectra are observed. For example, comparison of the tumorigenic and non-tumorigenic medulloblastoma cell pair versus normal fetal brain in Figure 24 and Tables 12 and 13 indicates that the  $T_{\parallel}$  splittings increase sequentially in the manner TE907>E1202>NFB. In contrast to the 5-NS order parameters,  $S'$ ,  $S''$ ,  $S$ ,  $S_{\parallel}$ ,  $S_{\text{GAF}}$ , and  $m$  values in Tables 12 and 13 for the crystalline hyperfine tensor

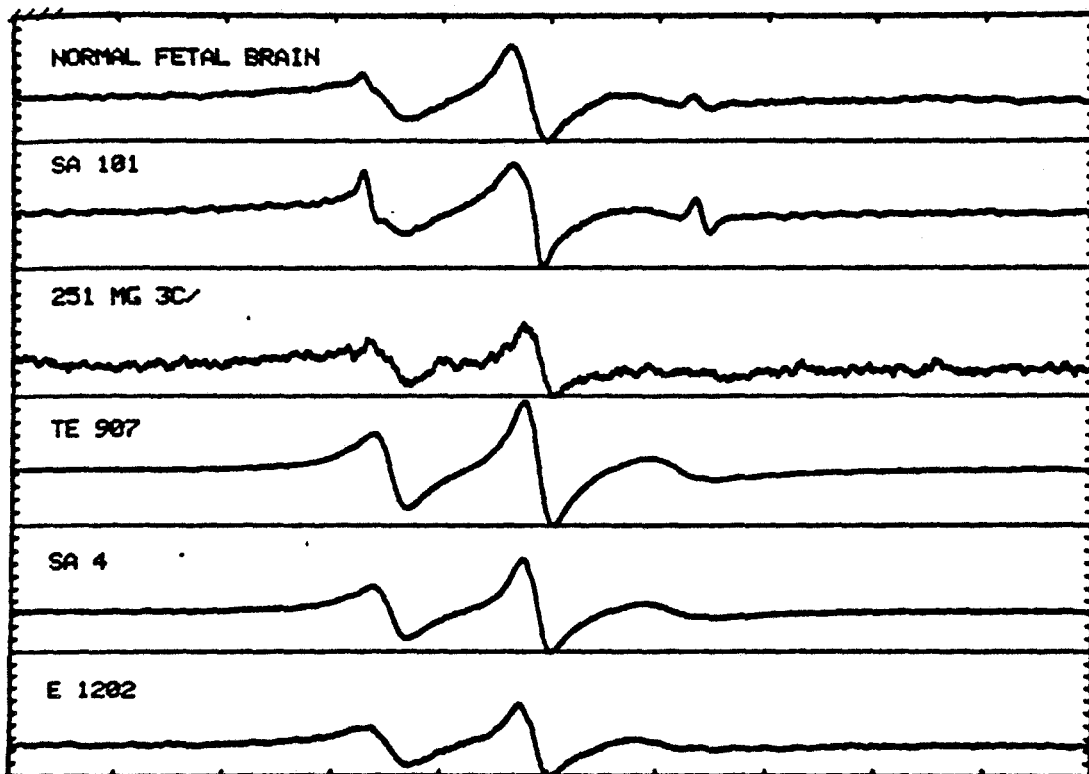


FIG 21: Spectra of the 12-NS spin label intercalated into the normal fetal brain cell line (NFB) and the five corresponding tumor-derived cell lines.



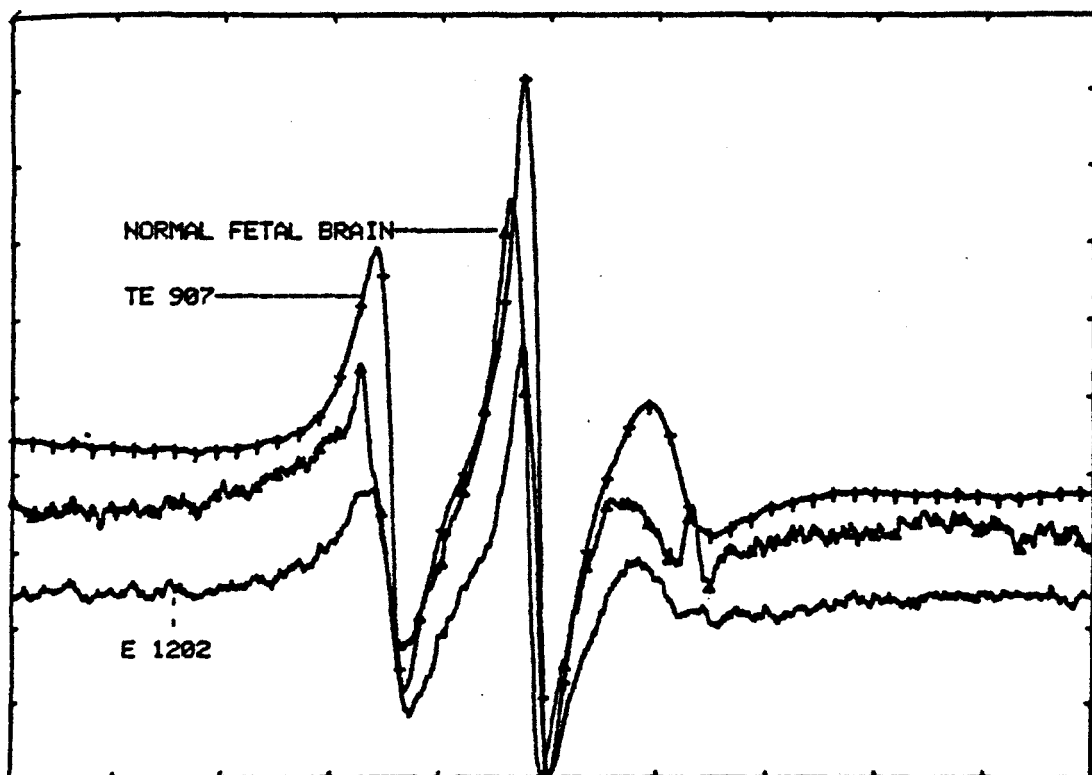


FIG 22: Composite spectra of the 12-NS spin label of the E1202 and TE907 medulloblastoma-derived cells compared to the NFB cell line.

Table 12

Comparison of ESR Order Parameters for Probe (12,5)  
 Tensor Values  $T_{xx}=T_{yy}=6.1G$   $T_{zz}=32.4G$

Cell Line	$T_{  }$	$T_{\perp}$	$a_n$	$a_n'$	$S'$	$S''$	$S$	$m$
E1202 (+,+)	23.98 <sup>†</sup> <u>+0.07</u>	10.26 <sup>†</sup> <u>+0.02</u>	14.865	14.832	0.52 <sup>†</sup> <u>+0.02</u>	0.752 <sup>†</sup> <u>+0.0025</u>	0.523* <u>+0.003</u>	0.694 <sup>†</sup> <u>+0.001</u>
SA4 (+,+)	22.95 <sup>†</sup>	10.78 <sup>†</sup>	14.865	14.832	0.46 <sup>†</sup>	0.69 <sup>†</sup>	0.46 <sup>†</sup>	0.67 <sup>†</sup>
TE907 (-,-)	22.58 <sup>†</sup> <u>+0.15</u>	10.96 <sup>†</sup> <u>+0.08</u>	14.865	14.79 <u>+0.05</u>	0.44 <sup>†</sup> <u>+0.01</u>	0.666 <sup>†</sup> <u>+0.002</u>	0.44 <sup>†</sup> <u>+0.01</u>	0.66 <sup>†</sup> <u>+0.01</u>
251MG (-,+)	24.43 <sup>†</sup>	10.04 <sup>†</sup>	14.865	14.832	0.55 <sup>∇</sup>	0.78 <sup>†</sup>	0.55*	0.70 <sup>∇</sup>
SA101 (-,-)	23.24 <sup>†</sup>	10.63 <sup>†</sup>	14.865	14.832	0.48 <sup>†</sup>	0.71 <sup>†</sup>	0.48 <sup>†</sup>	0.68 <sup>†</sup>
NFB (-,-)	25.08 <u>+0.41</u>	9.70 <u>+0.20</u>	14.865	14.832	0.59 <u>+0.02</u>	0.82 <u>+0.02</u>	0.59 <u>+0.02</u>	0.72 <u>+0.01</u>

The significance of the difference between the normal fetal brain (NFB) and the tumor derived cell lines is given by: \*P<0.05, <sup>∇</sup>P<0.001, and <sup>†</sup>P<0.0005.

Table 13

Comparison of Corrected ESR Order Parameters for Probe (12,5)  
 Tensor Values  $T_{xx}=T_{yy}=6.1G$   $T_{zz}=32.4G$

Cell Line	$T_{  }$	$T_{\perp}$	$a_n$	$a_n'$	$S_{GAF}$	$S_{  }$	$S_{\perp}$
E1202 (+,+)	23.98 <u>+0.07</u>	10.26 <u>+0.02</u>	14.865	14.832	0.34 $\nabla$ <u>+0.01</u>	0.42 $\nabla$ <u>+0.01</u>	0.34 $\nabla$ <u>+0.01</u>
SA4 (+,+)	22.95	10.78	14.865	14.832	0.29 $\nabla$	0.37 $\nabla$	0.28 $\nabla$
TE907 (-,-)	22.58 <u>+0.15</u>	10.96 <u>+0.08</u>	14.865	14.832	0.26 $\nabla$ <u>+0.02</u>	0.35 $\nabla$ <u>+0.01</u>	0.26 $\nabla$ <u>+0.01</u>
251MG (-,+)	24.43	10.04	14.865	14.832	0.38 $\nabla$	0.45*	0.37 $\nabla$
SA101 (-,-)	23.24	10.63	14.865	14.832	0.31 $\nabla$	0.39 $\nabla$	0.30 $\nabla$
NFB (-,-)	25.08 <u>+0.41</u>	9.70 <u>+0.20</u>	14.865	14.832	0.41 <u>+0.02</u>	0.48 <u>+0.02</u>	0.41 <u>+0.02</u>

The significance of the difference between the normal fetal brain (NFB) and the tumor derived cell lines is given by: \*P<0.05 and  $\nabla$ P<0.001.

value substitutions indicate that the fluidity decreases so that TE907>E1202>NFB. The isotropic splitting constant,  $a'_n$ , is equivalent in all three lines, and the BSA-nitroxide hyperfine tensor values used in the order parameter calculations in Tables 14 and 15 exhibit the identical trends as do the crystalline hyperfine tensor value-derived order parameters. Order parameters are identical for BSA or crystalline tensor value substitution for  $S''$ ,  $S$ ,  $S_{GAF}$  and the probe-probe interaction factor,  $m$ . The  $S''$  and  $S$  order parameters are less for the BSA-nitroxide tensor substitutions; whereas, the converse is true for  $S_{\perp}$ . Additionally, the order parameters themselves exhibit a decreasing range of absolute values.  $S''$  values are the largest and nearest to those of the 5-NS spin label. In this case, the order parameters progress from  $S''$  (0.6-0.7) >  $S' = S$  (0.5) >  $S_{GAF} = S_{\parallel} = S_{\perp}$  (0.4-0.5). This feature is also observed with the 5-NS spectral calculations; however, the differences between the latter order parameters ( $S_{GAF}$ ,  $S_{\parallel}$ , and  $S_{\perp}$ ) and those of the former parameters ( $S$ ,  $S'$ , and  $S''$ ) are increased for the 12-NS spin label.

The 12-NS spin label spectra of the SA series cell lines and the NFB cell line are shown in Figure 25. This figure exhibits the opposite effect between tumorigenic potential and fluidity compared to the 12-NS medulloblastoma cells. The  $T_{\parallel}$  splittings (Table 12 and 13) decrease

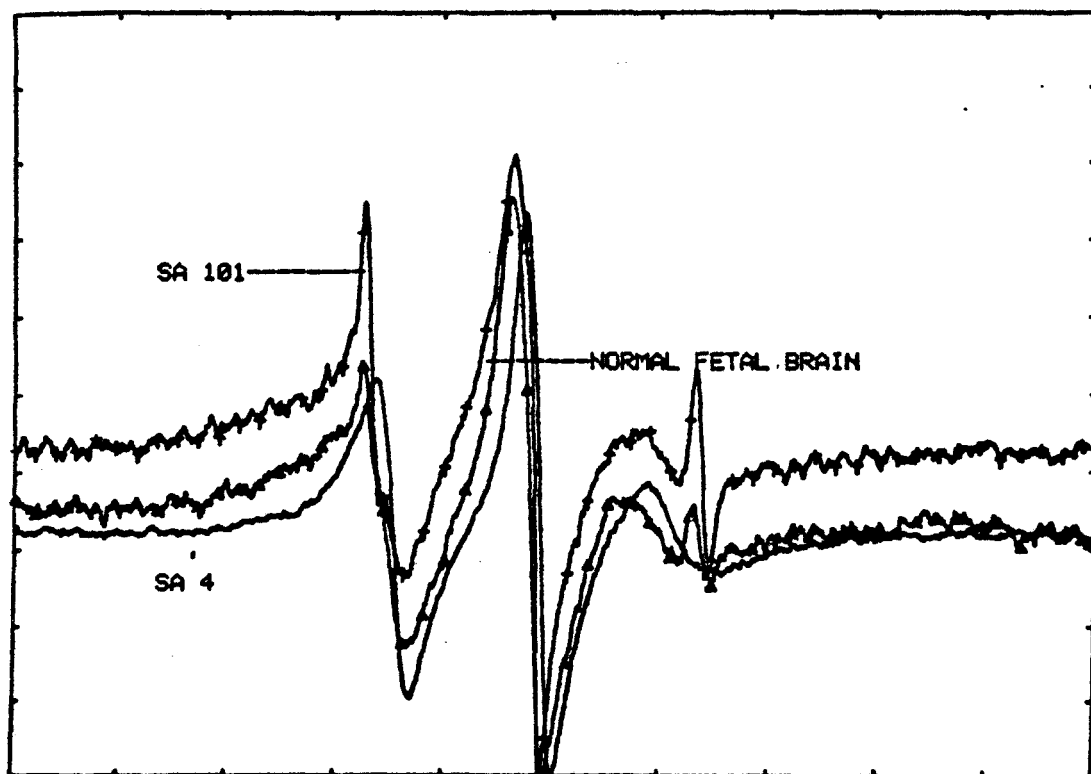


FIG 23: Spectra of the 12-NS spin label within the glioma-derived SA series cell lines, SA and SA101, compared to the NFB cell line.

sequentially in the order NFB>SA101>SA4, whereby the non-tumorigenic normal glial SA101 cells possess fluidity closest to that of normal fetal brain line. Here, the  $T_{||}$  splitting decrease is indicative of greater fluidity for the malignant glioma cells, although this trend is not observed in the order parameter calculations done utilizing the crystalline nitroxide hyperfine tensor values in Tables 12 and 13 or the BSA-nitroxide tensor value splittings in Tables 14 and 15. In either case, all of the order parameters ( $S'$ ,  $S''$ ,  $S$ ,  $S_{GAF}$ ,  $S_{\perp}$ , and  $S_{||}$ ) for the SA4 and SA101 cells are statistically equivalent, but are less than the order parameter values for the NFB line. This indicates that the SA4 and SA101 cells possess a more fluid nitroxide environment than the NFB cells. Using both hyperfine tensor value substitutions, the isotropic splitting constant  $a'_n$  and the probe-probe interaction factor  $m$ , moreover, are equal for all three cell lines. Comparison of the actual values for tensor substitution indicates that the crystalline hyperfine tensor substituted order parameter is greater than that for the BSA-nitroxide substitution in the case of  $S''$ . The reverse is true, however, for the  $S$  order parameter, while the other order parameters,  $S'$ ,  $S''$ ,  $S_{||}$ , and  $S_{GAF}$ , are equivalent for either tensor hyperfine value substitution. A large variation between the order parameters themselves for a particular

Table 14

Comparison of ESR Order Parameters for Probe (12,5)  
 Tensor Values  $T_{xx}=6.3G$   $T_{yy}=5.8G$   $T_{zz}=33.6G$

Cell Line	$T_{  }$	$T_{\perp}$	$a_n$	$a_n'$	$S'$	$S''$	$S$	$m$
E1202 (+,+)	23.98 <sup>†</sup> <u>+0.07</u>	10.26 <sup>†</sup> <u>+0.02</u>	15.298	14.832	0.51 <sup>†</sup> <u>+0.01</u>	0.71 <sup>†</sup> <u>+0.01</u>	0.52* <u>+0.01</u>	0.71 <sup>†</sup> <u>+0.01</u>
SA4 (+,+)	22.95 <sup>†</sup>	10.78 <sup>†</sup>	15.298	14.832	0.45	0.65 <sup>†</sup>	0.46 <sup>†</sup>	0.69 <sup>†</sup>
TE907 (-,-)	22.58 <sup>†</sup> <u>+0.15</u>	10.96 <sup>†</sup> <u>+0.08</u>	15.298	14.832	0.43 <sup>†</sup> <u>+0.01</u>	0.63 <sup>†</sup> <u>+0.01</u>	0.44 <sup>†</sup> <u>+0.01</u>	0.68 <sup>†</sup> <u>+0.01</u>
251MG (-,+)	24.43 <sup>†</sup>	10.04 <sup>†</sup>	15.298	14.832	0.53 <sup>∇</sup>	0.73 <sup>†</sup>	0.54* <u>+0.01</u>	0.73 <sup>∇</sup>
SA101 (-,-)	23.24 <sup>†</sup>	10.63 <sup>†</sup>	15.298	14.832	0.46 <sup>†</sup>	0.66 <sup>†</sup>	0.48 <sup>†</sup>	0.70 <sup>†</sup>
NFB (-,-)	25.08 <u>+0.41</u>	9.70 <u>+0.20</u>	15.298	14.832	0.56 <u>+0.02</u>	0.76 <u>+0.02</u>	0.58 <u>+0.02</u>	0.74 <u>+0.01</u>

The significance of the difference between the normal fetal brain (NFB) and the tumor derived cell lines is given by: \*P<0.05, <sup>∇</sup>P<0.001, and <sup>†</sup>P<0.0005.

Table 15

Comparison of Corrected ESR Order Parameters for Probe (12,5)  
 Tensor Values  $T_{xx}=6.3G$   $T_{yy}=5.8G$   $T_{zz}=33.6G$

Cell Line	$T_{  }$	$T_{\perp}$	$a_n$	$a_n'$	$S_{GAF}$	$S_{  }$	$S_{\perp}$
E1202 (+,+)	23.98 <u>+0.07</u>	10.26 <u>+0.02</u>	15.298	14.832 <u>+0.004</u>	0.348 $\nabla$ <u>+0.004</u>	0.39 $\nabla$ <u>+0.01</u>	0.38 $\nabla$ <u>+0.01</u>
SA4 (+,+)	22.95	10.78	15.298	14.832	0.289 $\nabla$	0.327 $\nabla$	0.332 $\nabla$
TE907 (-,-)	22.58 <u>+0.15</u>	10.96 <u>+0.08</u>	15.298	14.832	0.28 $\nabla$ <u>+0.01</u>	0.31 $\nabla$ <u>+0.01</u>	0.31 $\nabla$ <u>+0.01</u>
251MG (-,+)	24.43	10.04	15.298	14.832	0.375 $\nabla$	0.41*	0.41 $\nabla$
SA101 (-,-)	23.24	10.63	15.298	14.832	0.31 $\nabla$	0.34 $\nabla$	0.35 $\nabla$
NFB (-,-)	25.08 <u>+0.41</u>	9.70 <u>+0.20</u>	15.298	14.832	0.41 <u>+0.02</u>	0.44 <u>+0.02</u>	0.45 <u>+0.02</u>

The significance of the difference between the normal fetal brain (NFB) and the tumor derived cell lines is given by: \*P<0.05 and  $\nabla$ P<0.001.



cell line is observed in the SA cell lines. As observed with the medulloblastoma E1202 and TE907 lines, the  $S''$  values of the SA series cells were the largest being comparable to a highly restricted or rigid membrane environment. The  $S_{\text{GAF}}$ ,  $S'$ , and  $S$  order parameters represent the lowest absolute values and indicate fluid membranes.

When comparing the SA series and the medulloblastoma derived cell lines, the 251 MG 3C cell line also possesses increased nitroxide motion. The 251 MG 3C cells, which are intermediately tumorigenic, possess a 12-NS T splitting value that is lower than that of the NFB line. Comparison of the nitroxide crystalline order parameters in Tables 12 and 13 reveals that for all calculations, the order parameter is less than that for the corresponding NFB line. As previously mentioned, this is indicative of increasing fluidity for cells having a tumorigenic capability. The BSA-nitroxide hyperfine value calculated order parameters in Tables 14 and 15 also indicate increasing fluidity with tumorigenic potential. In contrast to the equivalence found for hyperfine substitution in the SA series, the BSA-nitroxide hyperfine-derived order parameters have lower absolute values than the corresponding  $S'$ ,  $S''$ , and  $S$  crystalline tensor-derived order parameters. This situation is reversed for  $S$

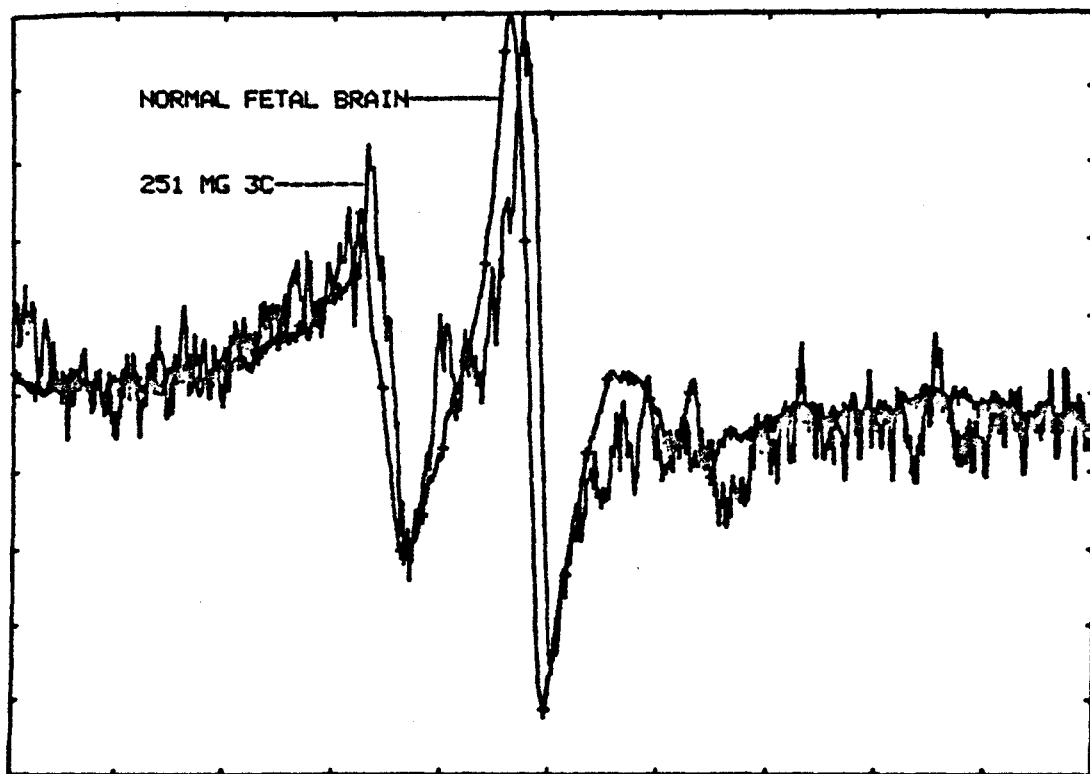


FIG 24: Spectra of the 12-NS spin label intercalated into the glioma-derived 251MG 3C cells compared to the NFB cell line.

although equality is observed for  $S$  and  $S_{\text{GAF}}$ . As seen in previous 12-NS spectra, the  $S_{\parallel}$ ,  $S_{\perp}$ , and  $S_{\text{GAF}}$  251 MG 3C order parameters are consistently lower when compared to their corresponding  $S'$ ,  $S''$ , and  $S$  order parameters. The indicator of probe-probe interactions,  $m$ , is less than unity for the 5-NS and 12-NS probes, although the empirical probe:lipid ratios based on actual cellular lipid compositions were always greater than 1:100.

Intercalation of 16-doxylstearate spin label (16-NS) into intact cells of tumor-derived cell lines and normal fetal brain results in a sharpening of the hyperfine splittings as shown in the spectra of Figure 27. Qualitatively, the spectral lineshapes are indicative of increasing rotational motion or fluidity compared to the motions of the previously discussed 5-NS and 12-NS spin labels. Low signal-to-noise ratios have been observed for the SA101 and 251 MG 3C cell lines.

Several trends seen for the medulloblastoma-derived cell lines probed with 5-NS and 12-NS are also evident when these cells are probed with the 16-NS spin label. Examination of the E1202, TE907, and NFB order parameters (Figure 28) calculated using the crystalline nitroxide hyperfine values may be done by referring to Tables 16 and 17. As a result of these calculations, it may be stated that the fluidity of the non-tumorigenic

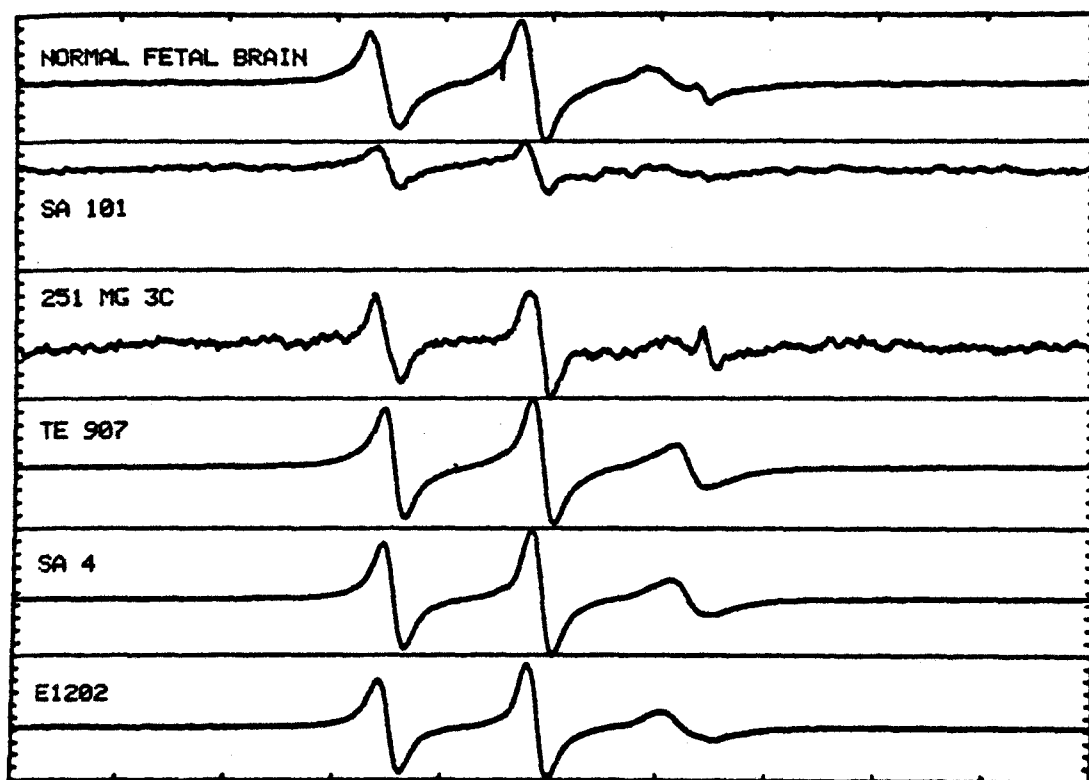


FIG 25: Spectra of the 16-NS spin label intercalated into the NFB cell line and the five corresponding tumor-derived cell lines.

Table 16

Comparison of ESR Order Parameters for Probe (16,1)  
 Tensor Values  $T_{xx}=T_{yy}=6.1G$   $T_{zz}=32.4G$

Cell Line	$T_{  }(G)$	$T_{\perp}(G)$	$a_n$	$a_n'$	$S'$	$S''$	$S$	$m$
E1202 (+,+)	15.42 $\nabla$ <u>+0.08</u>	11.91 $\nabla$ <u>+0.14</u>	14.865	13.07 $\nabla$ <u>+0.11</u>	0.13 $\nabla$ <u>+0.01</u>	0.26 $\Delta$ <u>+0.01</u>	0.15 $\nabla$ <u>+0.01</u>	0.51 $\nabla$ <u>+0.02</u>
SA4 (+,+)	15.18 $\nabla$ <u>+0.06</u>	12.23 $\nabla$ <u>+0.02</u>	14.865	13.21 $\nabla$ <u>+0.01</u>	0.11 $\nabla$ <u>+0.01</u>	0.25 $\Delta$ <u>+0.01</u>	0.126 $\nabla$ <u>+0.003</u>	0.45 $\nabla$ <u>+0.01</u>
TE907 (-,-)	14.95 $\nabla$ <u>+0.13</u>	12.42 $\nabla$ <u>+0.06</u>	14.865	13.26 $\nabla$ <u>+0.02</u>	0.095 $\nabla$ <u>+0.005</u>	0.24 $\Delta$ <u>+0.01</u>	0.11 $\nabla$ <u>+0.01</u>	0.40 $\nabla$ <u>+0.02</u>
251MG (-,+)	15.60 $\Psi$ <u>+0.02</u>	11.94 $\nabla$ <u>+0.27</u>	14.865	13.16 $\nabla$ <u>+0.19</u>	0.14 $\nabla$ <u>+0.01</u>	0.27 <u>+0.01</u>	0.16 $\nabla$ <u>+0.01</u>	0.50 $\nabla$ <u>+0.01</u>
SA101 (-,-)	15.42 $\nabla$	10.97*	14.865	12.456*	0.17	0.26 $\Delta$	0.20	0.64*
NFB (-,-)	15.69 <u>+0.08</u>	11.4 <u>+0.1</u>	14.865	12.84 <u>+0.05</u>	0.16 <u>+0.01</u>	0.28 <u>+0.01</u>	0.19 <u>+0.01</u>	0.58 <u>+0.02</u>

The significance of the difference between the normal fetal brain (NFB) and the tumor derived cell lines is given by:  $\Psi P < 0.1$ ,  $*P < 0.05$ ,  $\Delta P < 0.005$ , and  $\nabla P < 0.001$ .

Table 17

Comparison of Corrected ESR Order Parameters for Probe (16,1)  
 Tensor Values  $T_{xx}=T_{yy}=6.1G$   $T_{zz}=32.4G$

Cell Line	$T_{  }$	$T_{\perp}$	$a_n$	$a_n'$	$S_{GAF}$	$S_{  }$	$S_{\perp}$
E1202 (+,+)	15.42 $\pm 0.08$	11.91 $\pm 0.14$	14.865	13.07 $\pm 0.11$	0.056 $\dagger$ $\pm 0.006$	0.029 $\Delta$ $\pm 0.005$	0.25 $\dagger$ $\pm 0.02$
SA4 (+,+)	15.18 $\pm 0.06$	12.23 $\pm 0.02$	14.865	13.21 $\pm 0.01$	0.034 $\dagger$ $\pm 0.003$	0.020 $\Delta$ $\pm 0.005$	0.20 $\dagger$ $\pm 0.01$
TE907 (-,-)	14.95 $\pm 0.13$	12.42 $\pm 0.06$	14.865	13.26 $\pm 0.02$	0.016 $\dagger$ $\pm 0.007$	0.008 $\Delta$ $\pm 0.002$	0.19 $\dagger$ $\pm 0.01$
251MG (-,+)	15.60 $\pm 0.02$	11.94 $\pm 0.27$	14.865	13.16 $\pm 0.19$	0.06 $\dagger$ $\pm 0.01$	0.042 $\S$ $\pm 0.005$	0.24 $\Delta$ $\pm 0.04$
SA101 (-,-)	15.42	10.97	14.865	12.46	0.10	0.03 $\Delta$	0.35 $\Phi$
NFB (-,-)	15.69 $\pm 0.08$	11.4 $\pm 0.1$	14.865	12.84 $\pm 0.05$	0.09 $\pm 0.01$	0.047 $\pm 0.005$	0.30 $\pm 0.01$

The significance of the difference between the normal fetal brain (NFB) and the tumor derived cell lines is given by:  $\S P < 0.25$ ,  $\Phi P < 0.025$ ,  $\Delta P < 0.005$ , and  $\dagger P < 0.0005$ .

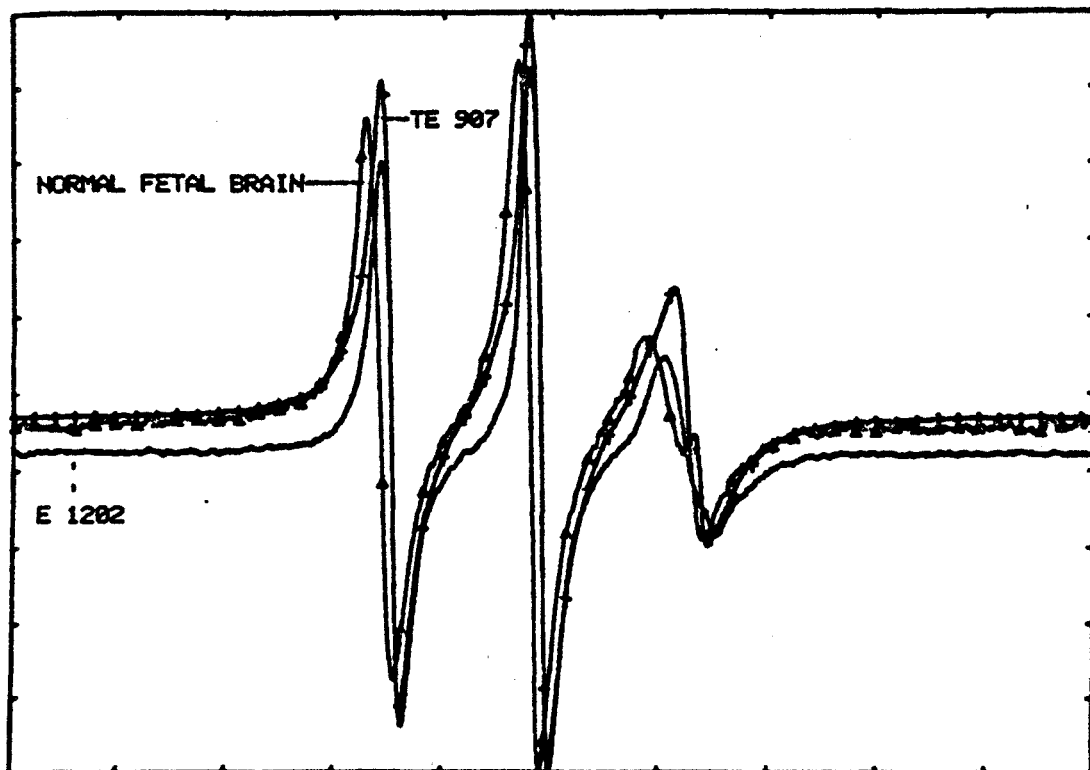


FIG 26: Composite spectra of the 16-NS spin label intercalated into the E1202 and TE907 medulloblastoma-derived cells and the normal fetal brain cell line.

TE907 cells is greater than that of the malignant E1202 line or the NFB cell line. The  $T_{||}$  splitting of the TE907 line is less than that of the E1202, although both are lower than that of normal fetal brain. The trend of increased rigidity (lower fluidity) for the NFB line is observed for all order parameter calculations:  $S'$ ,  $S''$ ,  $S$ ,  $S_{GAF}$ ,  $S_{\perp}$ , and  $S_{||}$ . Although the  $S''$  value is statistically equivalent for the NFB and E1202 cell lines, it is not identical to the non-tumorigenic TE907 cells. The isotropic splitting constant,  $a'_n$ , increases sequentially in the order NFB<E1202<TE907, an order similar to that when considering fluidity. Using the  $a'_n$  value as a measure of the hydrophobicity in the spin label environment, the NFB line indicates there is a more hydrophobic environment at a penetration depth of 16 methylene groups compared to either of the other tumor-derived medulloblastoma lines. Substitution of BSA-nitroxide hyperfine tensor values in the order parameter calculations of Tables 18 and 19 does not change the increased progression of fluidity in the sequence NFB<E1202<TE907. The exception, however, is  $S_{||}$  which cannot be calculated. Hyperfine tensor value substitution preserves the isotropic splitting constant sequence observed for the crystalline nitroxide hyperfine tensor values. The absolute values of the crystalline and BSA-nitroxide order parameters in Tables 16 and 17 and



Tables 18 and 19, respectively, are equivalent except for  $S''$  and  $S_{\perp}$ . BSA-nitroxide values in these two cases generally increase the degree of order sensed by the 16-NS spin label.

The SA-derived cell lines, composed of tumorigenic SA4 and non-tumorigenic SA101 "normal glial" cells, exhibit 16-NS spectra which may be correlated with the degree of tumorigenicity. The sequence appears to be the reverse of the situation observed for the medulloblastoma-derived E1202 and TE907 cell lines, where the fluidity progresses in the order NFB < E1202 < TE907. Examination of the order parameters for the SA4 and SA101 cell lines along with normal fetal brain (NFB) in Figure 29 and in Tables 16 and 17 indicates that the  $T_{\parallel}$  splitting of the NFB and SA101 lines is comparable though larger than that for the corresponding transformed glial SA4 cells. The  $T_{\parallel}$  splitting value may be correlated with the degree of tumorigenicity in the order SA4 < SA101 < NFB. The SA4 cell line appears to possess a highly fluid membrane compared to the rigidity of the SA101 and NFB cells. Overall, this trend is observed for the crystalline hyperfine calculated order parameters in Tables 16 and 17. The values of  $S'$ ,  $S_{\text{GAF}'}$ , and  $S_{\perp}$  for SA101 are statistically equivalent to that of the NFB line; whereas, the  $S''$  value of the SA4 cell line is equivalent to that of the SA101 cells. Malignant SA4

Table 18

Comparison of ESR Order Parameters for Probe (16,1)  
 Tensor Values  $T_{xx}=6.3G$   $T_{yy}=5.8G$   $T_{zz}=33.6G$

Cell Line	$T_{  }$	$T_{\perp}$	$a_n$	$a_n'$	$S'$	$S''$	$S$	$m$
E1202 (+,+)	15.42 $\nabla$ <u>+0.08</u>	11.91 $\nabla$ <u>+0.14</u>	15.298	13.08 $\nabla$ <u>+0.09</u>	0.13 $\nabla$ <u>+0.01</u>	0.23 $\Delta$ <u>+0.01</u>	0.15 $\nabla$ <u>+0.01</u>	0.56 $\nabla$ <u>+0.02</u>
SA4 (+,+)	15.18 $\nabla$ <u>+0.06</u>	12.23 $\nabla$ <u>+0.02</u>	15.298	13.20 $\nabla$ <u>+0.01</u>	0.11 $\nabla$ <u>+0.01</u>	0.23 $\Delta$ <u>+0.01</u>	0.13 $\nabla$ <u>+0.01</u>	0.48 $\nabla$ <u>+0.01</u>
TE907 (-,-)	14.95 $\nabla$ <u>+0.13</u>	12.42 $\nabla$ <u>+0.06</u>	15.298	13.26 $\nabla$ <u>+0.02</u>	0.09 $\nabla$ <u>+0.01</u>	0.20 $\Delta$ <u>+0.01</u>	0.11 $\nabla$ <u>+0.01</u>	0.46 $\nabla$ <u>+0.02</u>
251MG (-,+)	15.60 $\Psi$ <u>+0.02</u>	11.94 $\nabla$ <u>+0.27</u>	15.298	13.16 $\nabla$ <u>+0.19</u>	0.13 $\nabla$ <u>+0.01</u>	0.24 <u>+0.01</u>	0.15 $\nabla$ <u>+0.01</u>	0.56 $\nabla$ <u>+0.04</u>
SA101 (-,-)	15.42 $\nabla$	10.97*	15.298	12.46*	0.16	0.23 $\Delta$	0.20	0.71*
NFB (-,-)	15.69 <u>+0.08</u>	11.4 <u>+0.1</u>	15.298	12.83 <u>+0.06</u>	0.16 <u>+0.01</u>	0.24 <u>+0.01</u>	0.19 <u>+0.01</u>	0.65 <u>+0.02</u>

The significance of the difference between the normal fetal brain (NFB) and the tumor derived cell lines is given by:  $\Psi P < 0.1$ ,  $*P < 0.05$ ,  $\Delta P < 0.005$ , and  $\nabla P < 0.001$ .

Table 19

Comparison of Corrected ESR Order Parameters for Probe (16,1)  
 Tensor Values  $T_{xx}=6.3G$   $T_{yy}=5.8G$   $T_{zz}=33.6G$

Cell Line	$T_{  }$	$T_{\perp}$	$a_n$	$a_n'$	$S_{GAF}$	$S_{  }$	$S_{\perp}$
E1202 (+,+)	15.42 $\pm 0.08$	11.91 $\pm 0.14$	15.298	13.08 $\pm 0.09$	0.058 $\dagger$ $\pm 0.008$	0.003 $\Delta$	0.30 $\dagger$ $\pm 0.02$
SA4 (+,+)	15.18 $\pm 0.06$	12.23 $\pm 0.02$	15.298	13.20 $\pm 0.01$	0.034 $\dagger$ $\pm 0.003$	0.002 $\Delta$	0.25 $\dagger$ $\pm 0.01$
TE907 (-,-)	14.95 $\pm 0.13$	12.42 $\pm 0.06$	15.298	13.26 $\pm 0.02$	0.105 $\dagger$ $\pm 0.007$	— $\Delta$	0.24 $\dagger$ $\pm 0.01$
251MG (-,+)	15.60 $\pm 0.02$	11.94 $\pm 0.27$	15.298	13.16 $\pm 0.19$	0.06 $\dagger$ $\pm 0.01$	0.007 $\S$ $\pm 0.001$	0.30 $\Delta$ $\pm 0.03$
SA101 (-,-)	15.42	10.97	15.298	12.46	0.102	— $\Delta$	0.40 $\Phi$
NFB (-,-)	15.69 $\pm 0.08$	11.4 $\pm 0.1$	15.298	12.83 $\pm 0.06$	0.09 $\pm 0.01$	0.012 $\pm 0.004$	0.36 $\pm 0.01$

The significance of the difference between the normal fetal brain (NFB) and the tumor derived cell lines is given by:  $\S P < 0.025$ ,  $\Phi P < 0.025$ ,  $\Delta P < 0.005$ , and  $\dagger P < 0.0005$ .

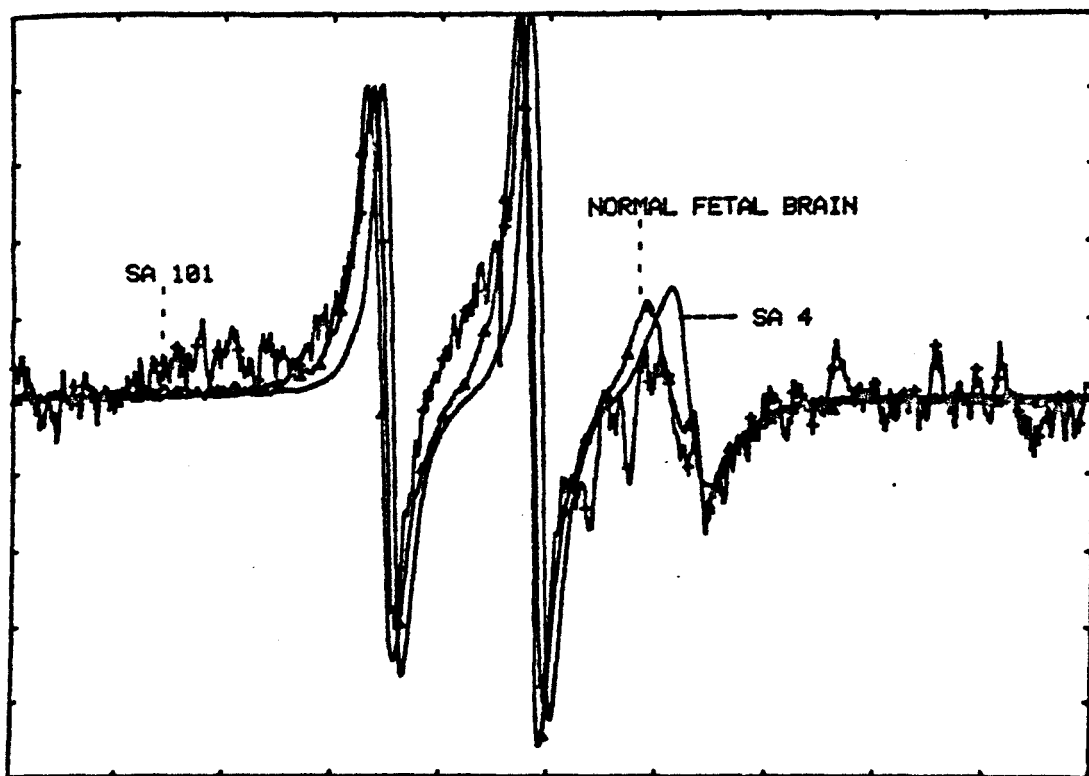


FIG 27: Composite spectra of the 16-NS spin label intercalated into the SA glioma-derived cell lines, SA4 and SA101, compared to the NFB cell line.

cells, moreover, possess a high degree of hydrophobicity in the 16-NS probed membrane environment as is indicated by these cells' greater isotropic splitting constant compared to that of the SA101 or NFB cells. The former cell line, SA101, possesses a more hydrophilic environment at this probe location than that of normal fetal brain cells. Differences are observed, however, with substitution of BSA-nitroxide-derived hyperfine tensors into appropriate order parameter equations in Tables 18 and 19. The sequence of fluidity: SA4>SA101>NFB is preserved for  $S'$ ,  $S$ ,  $S_{\perp}$ , and  $S_{GAF}$ . Tensor substitution, on the other hand, results in the same degree of fluidity for all three cell lines with regard to  $S''$ . The SA101  $S$  value, furthermore, could not be calculated, but the fluidity of the SA4 cells is still greater than normal fetal brain. Hyperfine tensor substitution, moreover, generally did not increase the absolute order parameter. An exception to this trend is  $S''$  in which the crystalline order parameters are greater than the BSA-nitroxide substituted calculations. The situation is reversed for  $S_{\perp}$  calculations. Hyperfine tensor substitution preserves the sequence of hydrophobicity determined by the isotropic splitting constant as well.

Figure 30 shows the 16-NS spectra of the intermediate tumorigenic 251 MG 3C glioma line compared to the 16-NS

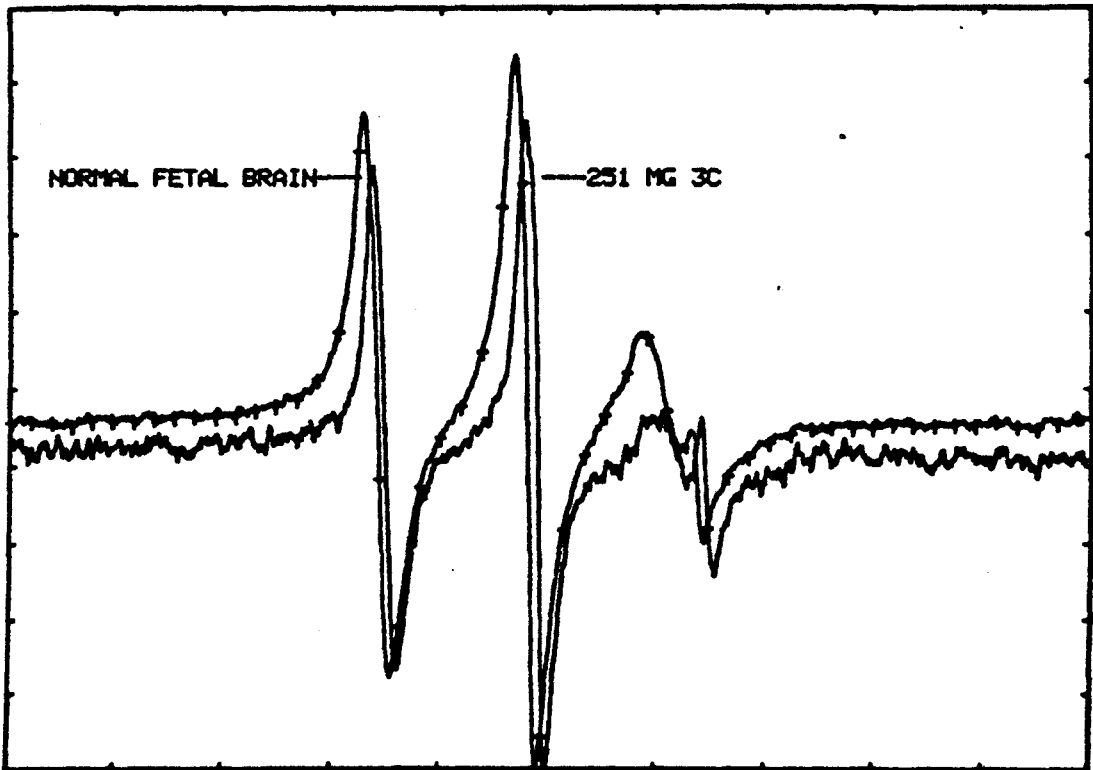


FIG 28: Composite spectra of the 16-NS spin label intercalated into the glioma-derived 251MG 3C cell line compared to the NFB cell line.

spectra of the NFB cell line. The order parameters found in Tables 16 and 17 for this cell line indicate that the  $T_{\parallel}$  splitting as well as  $S'$ ,  $S''$ , and  $S_{\parallel}$  are equal for the NFB and 251 MG 3C lines. For the other order parameters, specifically  $S$  and  $S_{GAF}$ , the fluidity of the 251 MG 3C cell line is greater than that of the normal fetal brain cells, although for  $S_{\perp}$  the fluidity of both lines is statistically equivalent. BSA-nitroxide substitution in Tables 18 and 19 conserves the increase of fluidity for not only  $S$ ,  $S_{GAF}$ , and  $S_{\perp}$  but also for  $S_{\parallel}$  and  $S'$ . Equivalence between the former and latter hyperfine substitutions is also observed for  $S''$  while BSA-nitroxide substitution increases the absolute value of the order parameter in the case of  $S_{\perp}$ . For the remaining calculations, changes in order parameters are nonspecific: the BSA-nitroxide substitution decreases the order parameter values of  $S''$  and  $S_{\parallel}$ , although the 16-NS values of  $S$ ,  $S'$ , and  $S_{GAF}$  for the 251 MG 3C and NFB of Tables 16 and 17 and Table 18 and 19 are equivalent.

Figure 31 illustrates the interdependence of the degree of malignancy with  $T_{\parallel}$  for each individual nitroxide spin label. As previously discussed, the intermediate tumorigenic 251 MG 3C line possesses a  $T_{\parallel}$  value nearest to that of the NFB line except for the 5-NS (5,12) label. Several trends are evident from this graphic representation of Figure 31: (1) the  $T_{\parallel}$  splittings of all the cell lines

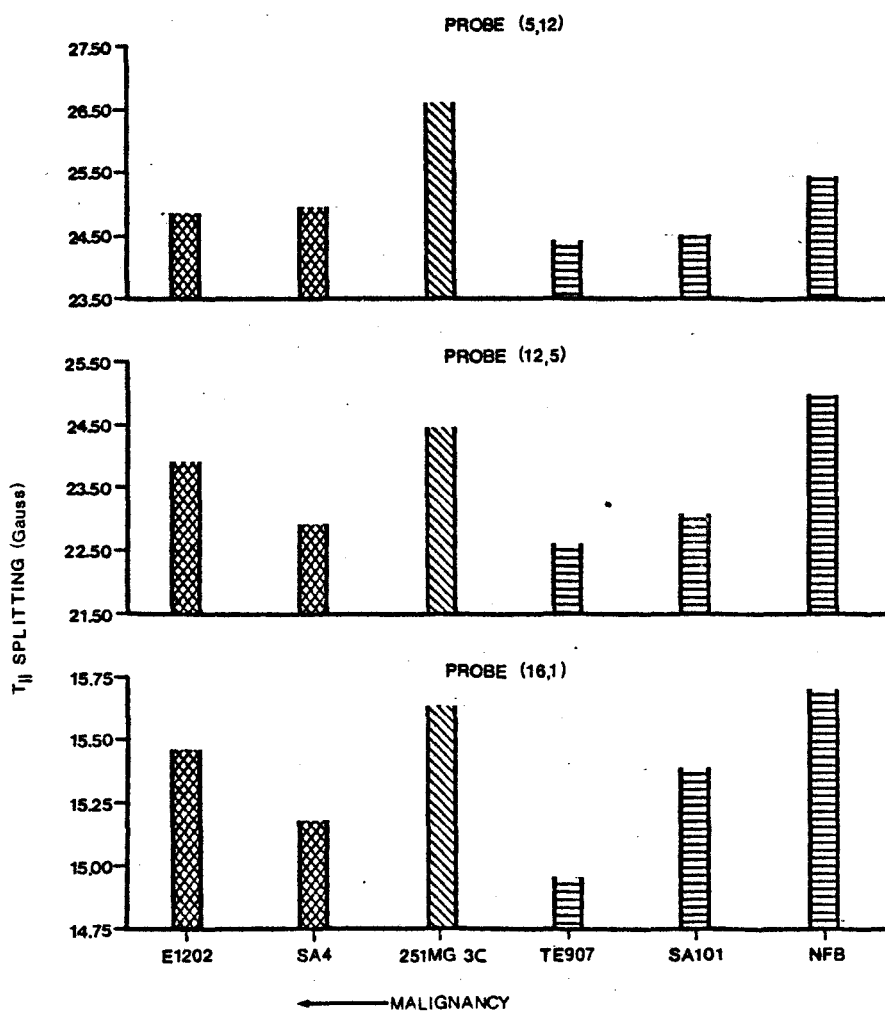


FIG 29: Comparison of the T<sub>||</sub> splittings for the 5-, 12-, and 16-NS spin labels and cell lines.



(with the exception of 251 MG 3C line) are below that for the NFB cells; (2) the least variation in  $T_{\parallel}$  splittings between the medulloblastoma lines and the SA lines occurs approximately at a penetration depth of five methylene groups as sensed by the (5,12) probe; (3) the medulloblastoma cell line follows a sequence in which the fluidity of the non-tumorigenic TE907 line is greater than that of its malignant E1202 counterpart; (4) this sequence is reversed for the SA cell lines so that the fluidity of the malignant SA4 line is always greater than that of the normal SA101 line for each specific probe; and (5) considering both benign cell lines, TE907 and SA101, the  $T_{\parallel}$  splitting of the SA101 cells is more similar to that of NFB cells.

Furthermore, these general trends may also be observed by plotting the order parameter (denoted  $S_{\text{GAF}}$ ) versus malignancy as in Figure 32. The  $S_{\text{GAF}}$  order parameter was used because it does not appear to vary with crystalline-to-BSA-nitroxide hyperfine tensor substitution. It may be concluded that: (1) the least variation occurs for the 5-NS spin label, which suggests similarities in membrane fluidity for all cell lines at this particular probe depth; (2) the order of the NFB cell line is the largest for all probes, thereby indicating the cells possess rigid membranes under these particular experimental conditions; (3) with

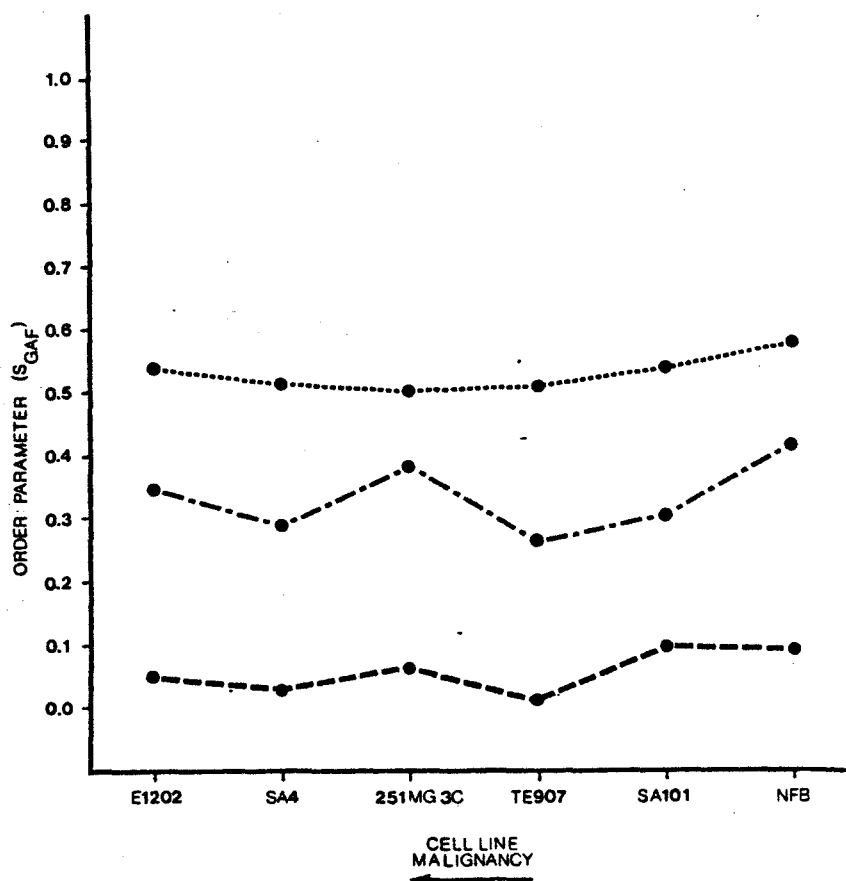


FIG 30: Comparison of the order parameter ( $S_{GAF}$ ) and increasing malignancy for the tumor-derived cell lines and NFB cells.

the exception of the 251 MG 3C cell line probed with the 16-NS spin label, the order parameter increases with decreasing malignancy and is observed as a decrease in fluidity; (4) this aforementioned trend is not observed for the 5-NS and 12-NS probes, whose data are most accurately described by a widened parabolic curve extending from malignant to normal brain cells in vitro; (5) the tendency of a progressive decrease in fluidity from malignant SA4 to non-malignant SA101 to NFB cells is conserved for each individual spin label; (6) a progressive increase is observed in fluidity for the medulloblastoma-derived cell lines; and (7) the 251 MG 3C cells generate characteristic data closest to that of the NFB cells only when probed with 12-NS spin label.

The presence of a flexibility gradient (defined as an increase in fluidity for bilayer regions with increasing hydrocarbon motion) for each of the cell lines is shown in Figures 33 through 38. Examination of the composite spectra for each cell type indicates a narrowing of the spectral lineshape starting with the 5-NS probe localized nearest the polar headgroups and progressing towards the 16-NS situated near the middle of the hydrocarbon bilayer. For each cell line: E1202 (Figure 33), SA4 (Figure 34), 251 MG 3C (Figure 35), TE907 (Figure 36), SA101 (Figure 37), and NFB (Figure 38) probed with 5-NS and 12-NS, the slow

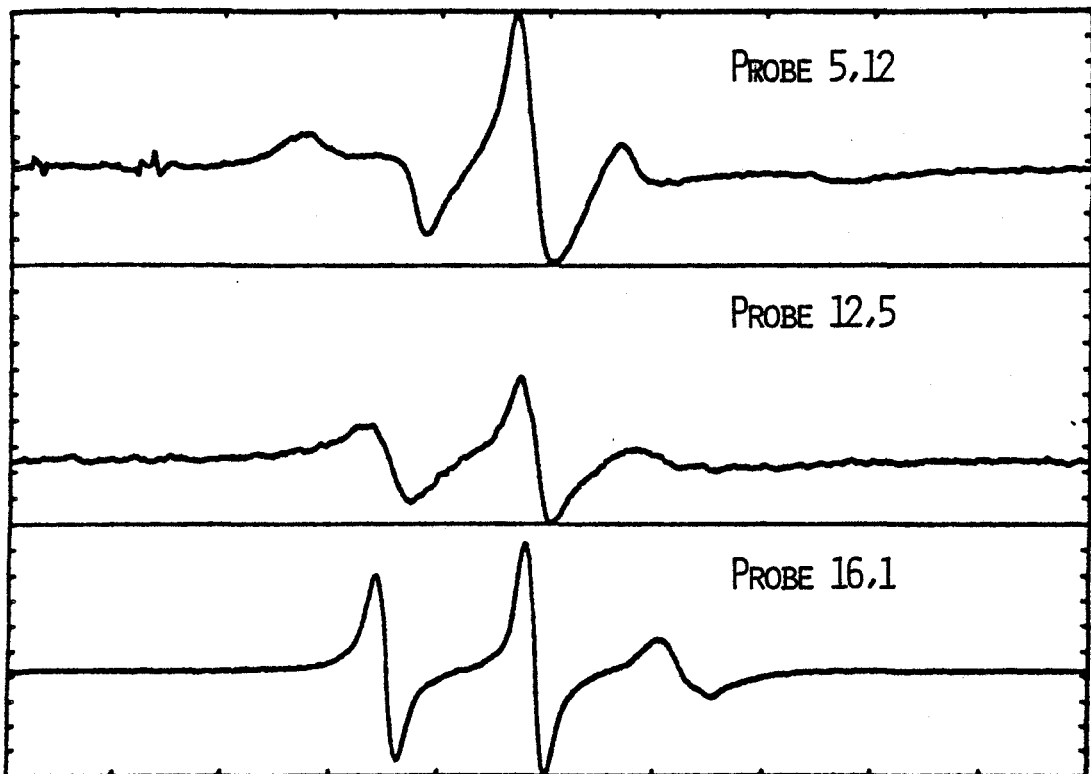


FIG 31: Presence of an ESR spin label flexibility gradient in the malignant E1202 medulloblastoma-derived cell line.

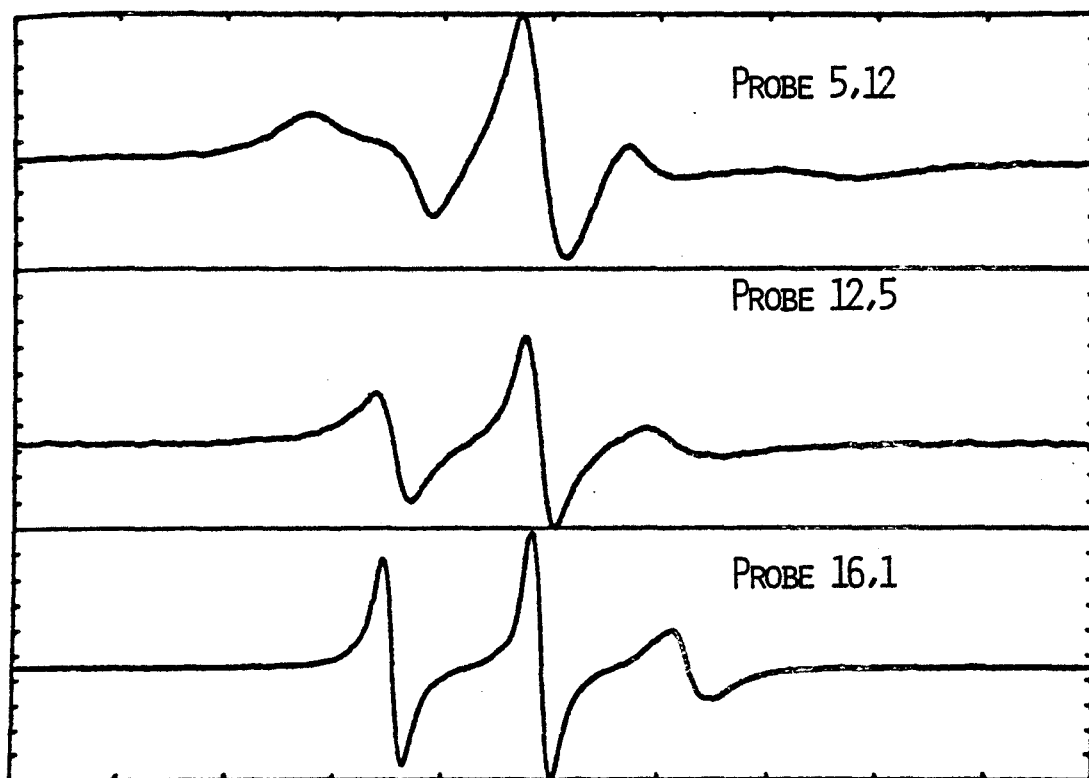


FIG 32: Presence of an ESR spin label flexibility gradient in the malignant SA4 glioma-derived cell line.

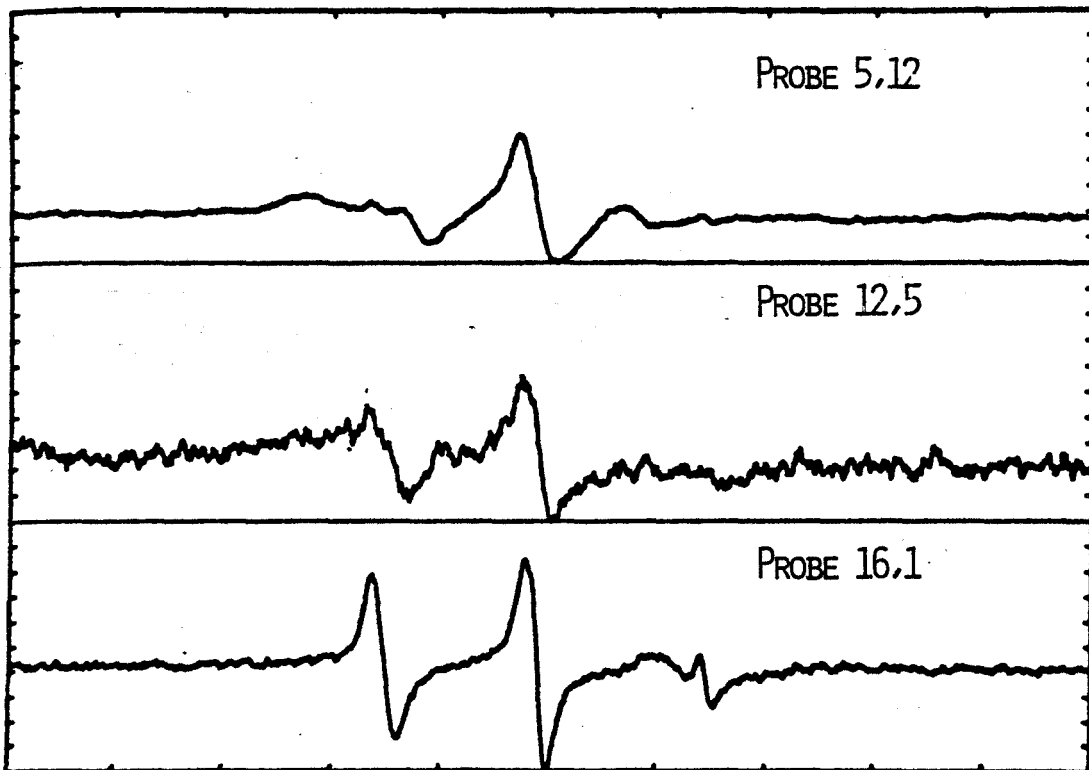


FIG 33: Presence of an ESR flexibility gradient in the 251MG 3C glioma-derived cell line possessing an intermediate degree of tumorigenicity.

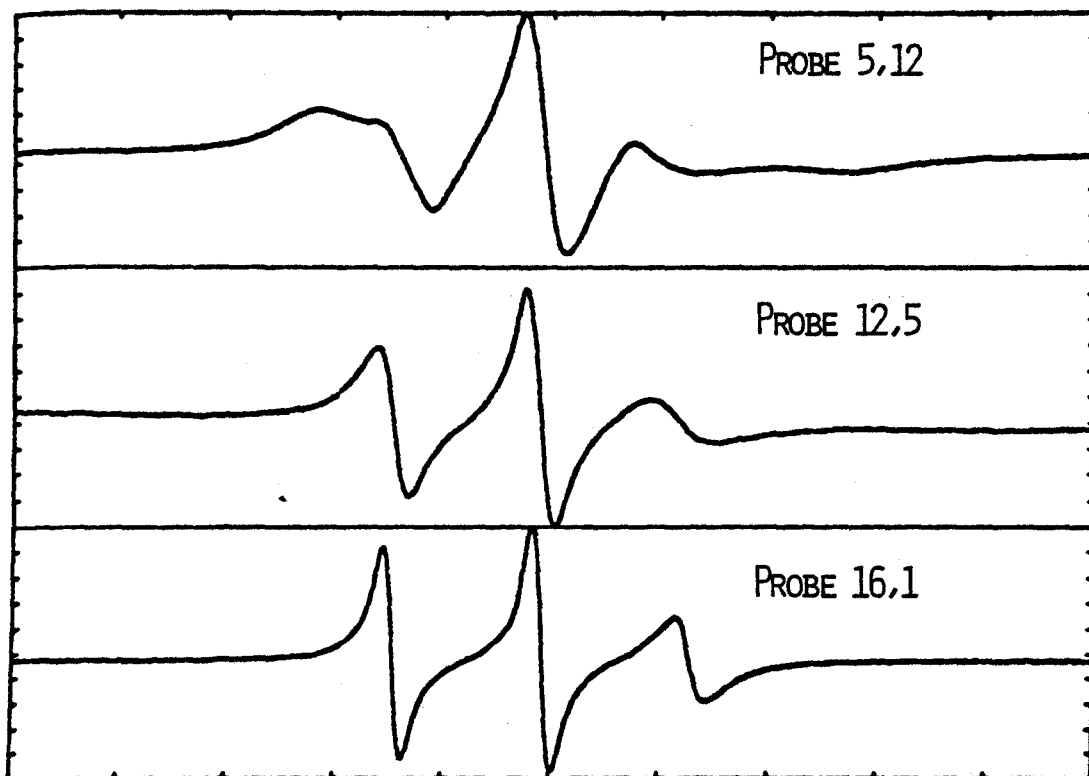


FIG 34: Presence of an ESR spin label flexibility product in the non-tumorigenic TE907 medulloblastoma-derived cell line.

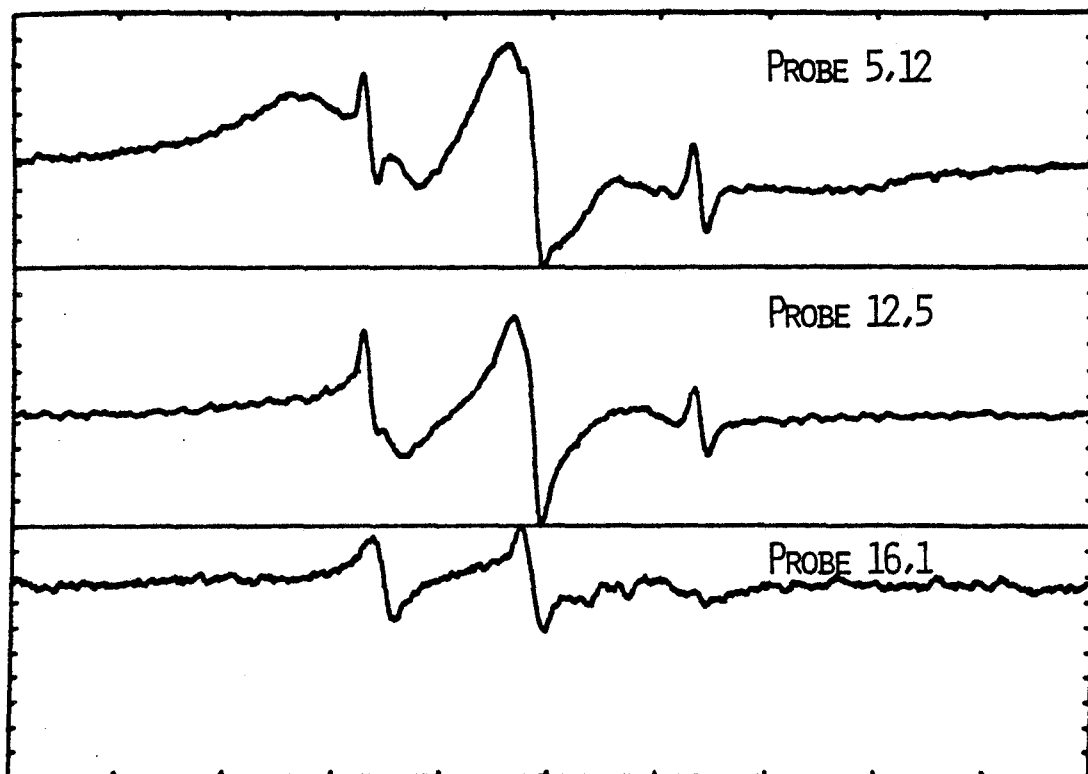


FIG 35 : Presence of an ESR spin label flexibility gradient in the non-malignant SA101 glioma-derived cell line.



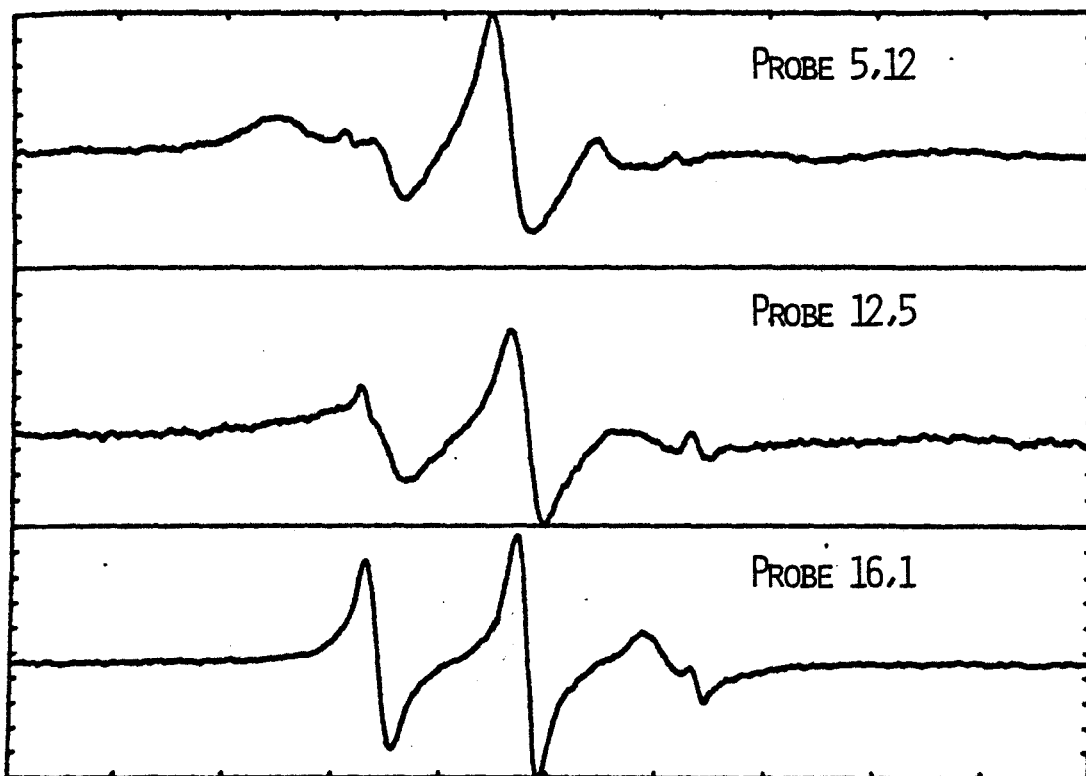


FIG 36.: Presence of an ESR spin label flexibility gradient in the normal NFB cell line.

anisotropic rotation spectra are indicative of highly restrictive environments and may be compared to the motion of the 16-NS spin label which is similar to but not isotropic motion. The flexibility gradient of each cell line versus the  $S_{\text{GAF}}$  order parameter is plotted in Figure 39. Although the non-tumorigenic TE907 and SA101 cell lines have essentially straight flexibility gradients, the shape of the 251 MG 3C gradient is nonlinear and similar to that of the NFB line. Generally, the flexibility gradient is transposed from a nearly straight line to a biphasic curve in the progression from benign to normal for both medulloblastoma and glioma-derived cell lines. Despite the fact that flexibility gradients may not strictly be correlated with a cell's degree of tumorigenicity, a membrane bilayer flexibility gradient remains a general characteristic of a cell regardless of additional factors.

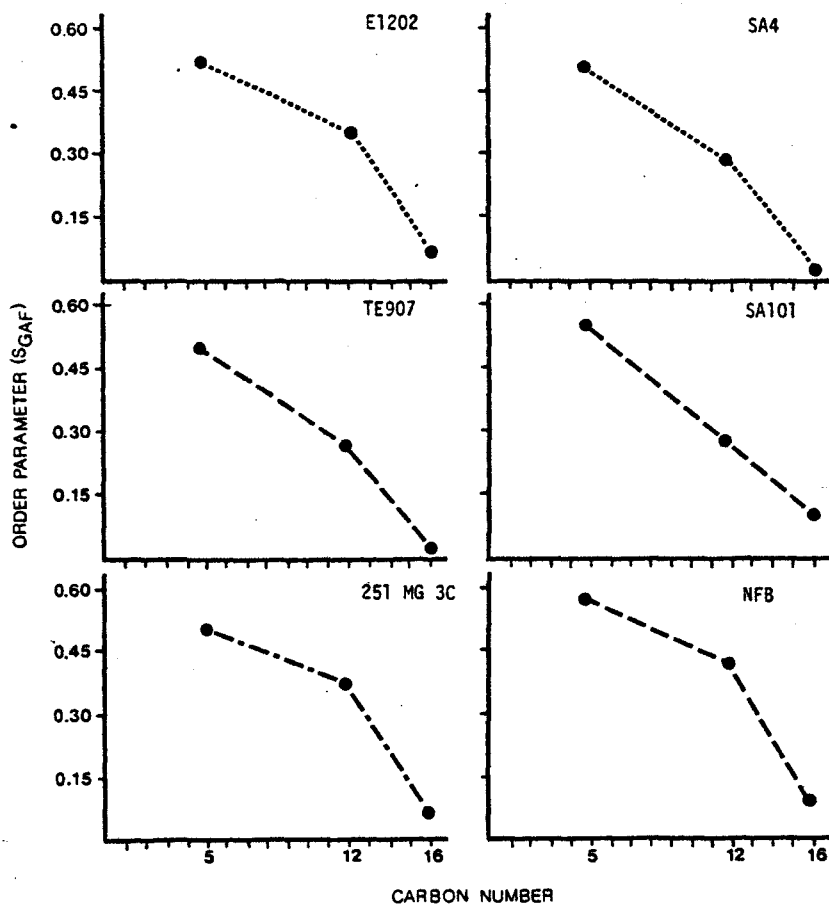


FIG 37 : Comparison of the order parameter ( $S_{GAF}$ ) versus spin label penetration depth for each cell type, indicative of the presence of (ESR spin label) flexibility gradients.

## DISCUSSION

The experiments in this dissertation directly pertain to whether changes in membrane "fluidity" concomitantly occur with the expression of surface membrane lipid alterations in the neoplastic state. Previous experiments (Barnett et al., 1974; Gaffney, 1975) using ESR spin label probes to monitor membrane phospholipid acyl side chain motion and hence a description of the average "fluidity" of the biomembrane have been contradictory. As stated in the preceeding results section, human brain cells in tissue culture which possess malignant characteristics in vivo and in vitro, also possess increases above non-malignant control cells in spin label sensed membrane "fluidity" at positions 5, 14, and 16 carbons away from the phospholipid polar headgroups. This increase in acyl side chain motion for the malignant phenotypes does not correlate with specific alterations in chain length, saturation or desaturation, but rather with increases in phosphatidylcholine headgroup levels. This modulation of phospholipid headgroup composition upon acyl side chain motion and membrane fluidity, even with biophysical probes placed 22 methylene groups from the glycerol backbone has been previously observed

(Glaser et al., 1974, Blank et al., 1975; Schroedet et al., 1976b, Esho et al., 1977; Gilmore et al., 1979b).

Fluorescent polarization studies (Glaser et al., 1974; Gilmore et al., 1979b) have shown that headgroup composition produces the major effect on membrane fluidity. With equal acyl side chain composition, phosphatidyl ethanolamine enriched membranes possess a decrease in fluidity as contrasted to phosphatidyl choline enriched membranes. This headgroup supplementation did not effect the characteristic phase transition temperatures, indicating that acyl side chain composition modulates the phase behavior of biomembranes. Schroeder (1978) coined the term "homeoviscous adaption" to describe in procaryotic and tissue culture cells the modulation of phospholipid headgroup metabolism upon the modification of phospholipid acyl side chain composition.

Given these observations, this dissertation presents the first study to implicate these effects in normal and malignant brain cells in vitro.

Several interesting points are salient upon examination of the phospholipid class compositions in Table 3 (Results section). Considering the PC/PE, PC/PE + (PS + PI), and the PC + SPH/PE + (PI + PS) molar ratios amongst the various cell lines, the ratios of the SA101

line and the NFB line are nearly identical. This provides additional substantiation on a compositional basis, to categorization of SA101 cells as normal glial cells in vitro, although the line was initiated from a malignant tumor. It can be noted, furthermore, that no conclusion can be drawn concerning an increase in the ratios PC/PE and PC/PE + (PS + PI) and malignancy in nude mice nor colony formation in soft agar.

For the PC + SPH/PE + (PS + PI) ratio, malignant cell lines, E1202 and SA4, possess ratios intermediate to those of normal cell lines (SA101 and NFB) and those of intermediately tumorigenic cell lines (TE907 and 251 MG 3C). The TE907 cell line is included in the latter classification because of its lack of an in vivo normal counterpart and not because of its inability to form tumors in vivo and in vitro. By definition, this line is considered to have some degree of tumorigenic potential, although it may not be expressed as fatty acid, phospholipid, or membrane fluidity alterations. Therefore, all cell lines derived from tumor specimens have PC + SPH/PE + (PS + PI) molar ratios greater than normal human brain or "normal" glial SA101 cells and those cell lines with intermediate tumorigenic potentials have the highest molar ratio levels.

Previous studies on phospholipid class and fatty acid alterations in normal and neoplastic neural tissues of animal and human origin support the PC + SPH/PE + (PS + PI) molar ratio increase observed for the cell lines in this dissertation. Analysis of data from Yates et al. (1979) on phospholipid class composition in brain tumors shows that human gray and white matter possesses ratios of 1.2 and 0.92, respectively. Malignant tumor ratios are calculated to be in the range 1.84 to 1.92; whereas, the ratios for neuroectodermal and well-differentiated human brain specimens are between the values for normal and malignant tissues. Culturing the astrocytoma and glioblastoma lines greatly increased these ratios from 1.84 and 1.90 to 3.34 and 2.76, respectively. Sun and Leung (1974) show the same qualitative increase, although the absolute values of the PC + SPH/PE + (PS + PI) ratios are greater (2.98 compared to 1.90). Their data also indicate human gray matter has a PC + SPH/PE + (PS + PI) ratio of 1.48 while the ratio for tissue adjacent to tumors is 2.49, indicating that this tumor tissue cannot be considered "normal" on the basis of this ratio. Application of the PC + SPH/PE + (PS + PI) molar ratio to the data of White (1974) again indicates that normal tissues have ratios that are always lower than those of brain tumors. The

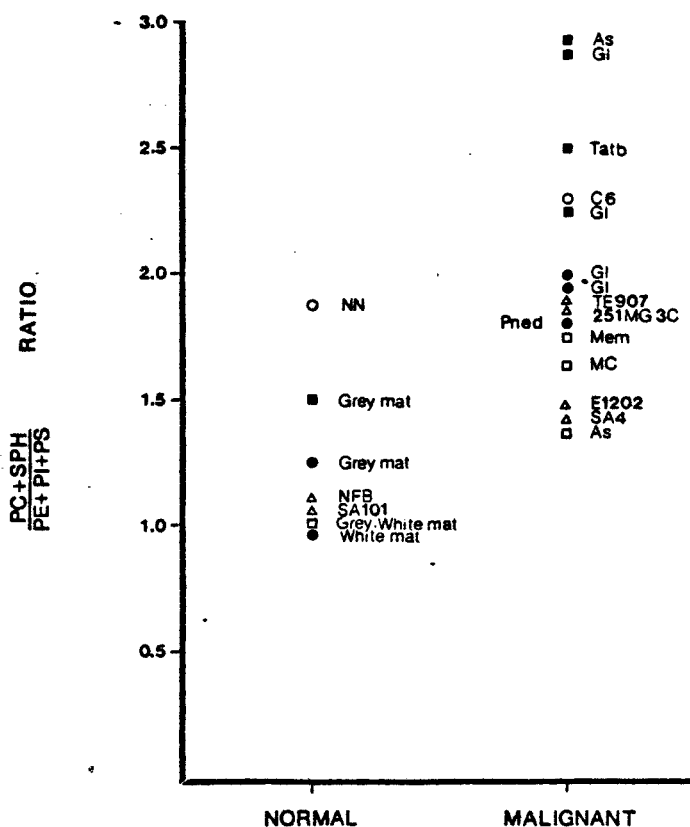


FIG 38.: PC+SPH/PE+PS+PI molar ratio as a function of tumorigenicity of normal and malignant neural cells. Abbreviations: Grey mat=grey matter; white mat=white matter; NH-normal hamster astroblasts; SA101, TE907, NFB, E1202, SA4, and 251 MG 3C cell lines in this study (the SA101 and NFB are non-malignant); AS=astrocytoma; GI=Glioma; MC=metastatic carcinoma; Mem=menigoma, Pned=primary undifferentiated neuroectodermal tissue; C6=rat C6 glioma; and Ta+b=tissue adjacent to brain tumor. Data (●) taken from Yates *et al.*, 1979; (■) of Sun and Leung, 1974; (□) of White, 1974; (o) of Robert *et al.*, 1979; and (△) data presented in this study.  $P < 0.001$  for the difference between the mean of the normal and malignant cell PC+Sph/PE+PS+PI ratios.



ratio values of gray and white matter as well as whole brain from North Americans are approximately 1.0 (0.98, 1.00, and 0.88, respectively). Not only do malignant brain neoplasms have greater PC + SPH/PE + (PS + PI) molar ratios, but the absolute values increase with increasing malignant potential. Meningiomas, which are non-invasive in vivo, have the greatest molar ratio values. Metastatic carcinomas possess slightly lower values along with gliomas although the PC + SPH/PE + (PS + PI) molar ratios of low-grade astrocytomas, interestingly, are closer to that of normal brain values rather than that of metastatic or malignant gliomas. No conclusion, however, can be made relating phospholipid fatty acid acyl side chain unsaturation, the PC + SPH/PE + (PS + PI) ratio, and malignancy.

Similar trends are also seen for the non-human neural cells in vitro. Examination of the data of Robert et al. (1979) and application of the phospholipid subclass composition to the PC + SPH/PE + (PS + PI) ratio equation reveals that the C6 glioma line has a greater molar ratio than the normal astrocytic NN line as was previously found for comparable human tissues.

Considering the data of previous investigations and the data from the normal and tumor-derived human lines studied in this dissertation, it appears that neoplastic

tissues always have PC + SPH/PE + (PS + PI) molar ratios and that malignant cell ratios always fall between those of the normal and intermediate tumorigenic lines. It might be expected that the effects of this ratio would be reflected by spin label membrane fluidity, particularly in the fluidity sensed by 5-NS spin labels which are located nearest to the phosphatide headgroup region.  $^{31}\text{P}$  and  $^2\text{H}$ -NMR studies stronger intramolecular interactions which enables these molecules to compact more tightly than phosphatidylcholine headgroups (Seelig and Gally, 1977; Michaelson et al., 1974; Yeagle, 1978). These studies have also found that the distances between headgroups increase with greater fatty acid unsaturation, which enables the phosphatide headgroups to possess a greater degree of fluid motion. Because phosphatidylethanolamine headgroups as compared to phosphatidylcholine headgroups would possess less freedom for acyl side chain motion, membrane bilayers with high concentrations of phosphatidylethanolamine would therefore, be rigid. Interestingly, this concept is compatible with the PC + SPH/PE + (PS + PI) ratio value, and generally these cell lines with a decreased ratio have more rigid membranes (an increase in order parameters) than their malignant counterparts. This conclusion cannot be exclusively inferred from the 5-NS data since this probe

does not monitor rotations as close to the phospholipid polar headgroups as a 2-NS probe (labelled at the second position of the hydrocarbon chain and penetrating two methylene groups into the acyl side chain region of the membrane bilayer.

Notwithstanding, there are a number of reasons which support the results presented in this study and may possibly explain the previous inconclusive findings using ESR techniques to assess membrane fluidity of normal and transformed cells. First, and of prime importance, is the selection of the cell lines and the specific normal-transformed cell model. As has been pointed out in the introduction, there are subtle but unique differences between malignant cell lines derived from spontaneous tumors and those induced by chemical or viral oncogens. There is no evidence at this date to equate spontaneous or induced tumors with respect to alterations in membrane structure and function. Therefore, the 3T3 SV40 transformed 3T3 fibroblast may be an inappropriate model system because viral transformation may not necessarily affect membrane fluidity. Alterations in membrane fluidity may possibly be noted only in cells derived by spontaneous tumors. Electron spin label techniques, prior to this study, have not been used to examine similarities or differences in membrane fluidity of spontaneous human neoplasms.

Secondly, apparently "normal" cell lines in tissue culture (with regards to morphology, growth kinetics, etc.) may produce tumors when either cultured under appropriate conditions or inoculated in suitable hosts. 3T3 fibroblasts are non-tumorigenic when injected at high concentrations ( $10^8$  cells) in mice (Aaronson and Todaro, 1968). "Normal" 3T3 cells attached to small glass beads and implanted into BALB/C mice, however, form hemangiocndotheliomas (Boone, 1975). Tissue culture especially permanent cell lines such as 3T3 or SV40 transformed 3T3 fibroblasts, may also result in selection of a small proportion of cells so that in time, a heterogenous cell population is produced. Many of the phenotypes characteristic of cells in vitro, furthermore, vary with passage level (time in culture). This feature is well illustrated with the C-6 rat glioma line (Vernadakis et al., 1980). Morphologically the cells change from oligodendrogloma cells to astrocytoma-like cells with increasing age in culture. Biochemical changes also accompany this phenomenon. The cells in early passage possess high levels of 2', 3'- cyclic nucleotide 3'-phosphohydrolyase (CNP) which is specific for oligendrocytes. Glutamine synthetase (GS), which is specific for astrocytes, on the other hand, increases in late passage cells with a concomittant

decrease in the level of CNP. To alleviate this problem in this study, all repetitive measurements were performed on cell lines only if the samples did not differ by more than two passage levels.

The problem of adequate controls of normal and transformed cell lines maintained in culture can be illustrated by comparison of spin label sensed fluidity and in vivo and in vitro malignancy of the glioma and medulloblastoma derived cell lines. The glioma derived lines possess an increased spin label fluidity which also parallels the production of tumors in athymic nude mice and in soft agar colony formation assay. This feature, however, is reversed for the medulloblastoma derived TE907 and E1202 cell lines. The latter line is malignant by its production of tumors in the above mentioned in vivo and in vitro assay systems; whereas the former cell line possess no tumorigenic properties, however, originally initiated from a malignant tumor. In contrast to the glial cell lines, the non-tumorigenic TE907 cell line possess an increase in membrane fluidity as compared to its malignant counterpart, E1202. This illustrates the point that the previous discrepancies between studies examining membrane fluidity of normal and transformed

cells may be the result of comparing non-compatible cell types. It is, therefore, possible that any reproducible alterations of membrane fluidity in the neoplastic state may be cell-type or species specific and not applicable to normal-transformed model systems in general.

Thirdly, tissue culture conditions can play an important role in affecting cell growth and resulting lipid metabolism and structure. This subject of lipid modification by exogenous lipid supplementation through serum or specific fatty acids is extremely important when comparing lipid and membrane fluidity between different cell lines and different investigators. The similarities or differences between previous studies may be attributed to changes in nutritional supplements, particularly serum. Cell density and the length of time when the cells are analyzed after tryptic dispersion, furthermore, can easily influence phospholipid composition through phospholipid turnover. Because these variables are often neglected and play an important role in membrane structure and the resulting estimation of membrane fluidity, these factors will be discussed in detail. It must be pointed out the experiments in this study were designed with these problems in mind. All experiments utilized identical lots of media, serum and trypsin, and moreover, were probed at identical timespans after passaging.

There are a variety of advantages and disadvantages for cells in culture with regard to the manipulation of lipid compositions in vitro. Compared to the applications of transplanted tumors propagated by in situ injection, transformed cells in culture usually represent a heterogeneous population of cells for biochemical and physiological experimentation. Cells in culture may be studied without the array of complex physiological, hormonal, and circadian influences that may affect the metabolic processes in host animals. Moreover, cell cultures allow the inhibition or stimulation of de novo lipid biosynthesis through the manipulation of exogenous lipids and addition of enzyme inhibitors in the culture media. Although these manipulative effects may also be manifested by altering the lipid composition (for example, experimental essential fatty acid deficiencies in rodents), the effect of exogenous lipids upon the physical state of cellular membrane structures is most direct and easily accomplished with cells in vitro.

Variations can also be introduced into the experimental study by changes in cell density and cell cycle (Griffiths, 1972). These variations are further multiplied by the mode of culture (cells in monolayers possess different nutritional requirements compared to

cells maintained as spheroids or aggregates) and the composition of the tissue culture medium itself. (For example, the effects of using basal essential medium (BME) which is limiting in essential nutrients in contrast to Dulbecco's modified Eagle's medium (DMEM) which contains copious amounts of all nutrients.)

With regard to these variables, the cells used in this study were maintained and propagated in a medium rich in essential nutrients (DMEM supplemented with 10% fetal calf serum). The tissue culture media, furthermore, were replaced every 48 hours to prevent the introduction of variations in fluidity and lipid metabolism by ensuring that cell nutrients were not rate limiting.

Mammalian cells grown in vitro obtain the majority of their cellular and membrane lipids from serum usually supplemented in the growth media (Rothblat and Kritchevsky, 1967; Rothblat, 1972; Spector, 1972; Bailey and Dunbar, 1973; Howard and Howard, 1974). The exceptions to this are cell lines capable of growth in chemically defined serum-free media (usually supplemented with insulin, cortisone, and exogenous sources of fatty acid precursors). The growth stimulation property of sera is not to be confused with its use as a source of lipid: the growth promoting property is primarily protein in nature Temin et al., 1972).



Animal sera, in particular fetal calf and bovine sera, contains large amounts of lipids usually found in association with serum proteins. Triglycerids, phospholipids and cholesterol are associated with serum lipoproteins while free fatty acids are bound to albumin. Typically, the fetal bovine serum used in this dissertation contained approximately 25% sphingomyelin, 50% phosphatidylcholine, 20% lyso-phosphatidylcholine, and 0.12  $\mu\text{M}/\text{ml}$  unesterified fatty acids. Only human serum contains a greater amount of lipid and, in some cases, is toxic to cells when they are supplemented with 10% quantities (the same quantity as newborn and fetal bovine supplementation) (Fox and Sanford, 1976).

There are two methods to modify the lipid composition of cells in vitro. First, with the serum supplementation used in this dissertation, the cellular pathways for de novo synthesis of several lipid components are inhibited, and the cells utilize exogenously supplied serum lipids. Bailey et al. (1964) observed that as little as 0.5% serum in the tissue culture medium can inhibit as much as 50% of the de novo synthesis of phospholipids and neutral lipids. Under these conditions, the fatty acid composition of the serum, to some degree, is reflected in the composition of the intracellular membranes and plasma

(Geyer et al., 1961; Boyle and Ludwig, 1962; Rothblat, 1972). Geyer (1967) postulated that the lipid metabolism in murine L-cells (a fibroblastic line) can be divided into several stages. Exogenous lipids such as long chain fatty acids (C18 or greater) are able to enter the metabolic pool through nonenzymatic processes such as diffusion or free exchange (Howard and Howard, 1974). These lipids, once absorbed, are metabolically converted to triglycerides, phospholipids and CO<sub>2</sub>. After a period of time (24 hours) the lipids are no longer exchangeable with the media and can be thought of as progressing from a transient stage to one of cellular permanence where the induced lipid changes are maintained during subsequent cell proliferation over several passages.

Another process leading to the modification of fatty acid levels (and therefore membrane composition) may be accomplished using two generalized procedures that involve the growth of cells in the presence of delipidized serum. In the presence of delipidized serum, cells are able to absorb the required quantities of lipids if they are supplemented in the defatted serum. Compared to cells grown in serum, the addition of exogenous lipids to delipidized serum proteins results in cells with greatly altered fatty acid compositions. This approach has been used to modify the structure of plasma membranes and study

the effects of defined lipid alterations on dynamic membrane properties. Exogenous lipids in the form of sonicated dispersions can be added directly to tissue culture media that has been supplemented with delipidized serum. This method is direct and rapid and allows for the incorporation of molecules normally foreign to plasma membranes. A problematic disadvantage of incubating cells with lipid supplements in lipid-free media is that the exogenous lipids may not be homogeneously interdispersed among the bulk lipids or protein-lipid complexes (Horwitz, 1977). Fluorescent probe or ESR spin-labelled studies of lipid-manipulated plasma membranes may indicate specific alterations pertinent only to distinct micro-environments and not the general membrane.

The second technique of altering membrane fatty acid levels involves the inhibition of catabolic and anabolic processes by the removal of biotin from the culture media. Biotin is one of the vitamins required for de novo fatty acid biosynthesis, and although cells are able to proliferate in tissue culture media supplemented with delipidized serum, the removal of biotin and supplementation of specific lipids forces the cells to inhibit endogenous biosynthetic lipid pathways and utilize the exogenously supplied lipids that are either free, sonicated dispersions or bound to albumin. Using this technique, unnatural fatty

acid analogues may be incorporated into intact membranes. For example, supplementation of L-cells with nondecanoate (19:0) in delipidized medium results in approximately 40% of the phospholipid fatty acid acyl side chains to be occupied by this analogue (Horwitz et al., 1974, 1976; Williams et al., 1974). Supplementation with elaidate (18:1 trans) results in over 50% of the phosphatide acyl side chains being replaced by this unnatural fatty acid. These selective alterations are substantial compared to exogenous lipid supplementation. When cells are grown in serum-supplemented media, approximately 30%-40% of the acyl side chains are occupied by oleoate (the major fatty acid present in bovine serum); whereas, cells grown in lipid-depleted media supplemented with oleate have cellular fatty acid levels approaching 60%.

The ability to grow in lipid-depleted media and the ease of lipid substitution plasma and intracellular membranes is cell and lipid specific. For example, many cell lines exhibit no dependence upon the linoleic and linolenic essential fatty acids for growth (Bailey and Dunbar, 1973). Removal of choline from the growth medium, however, inhibits phosphatidylcholine biosynthesis and cell proliferation. Normally, there are sufficient levels of choline available in the tissue culture medium or incorporated into the serum phosphatidylcholine. In animal cells it is not possible

to completely substitute naturally occurring fatty acids with unnatural ones. This is not the case among lower prokaryotes, (notably E. coli), where essentially all of the membrane lipids may be replaced by abnormal fatty acid analogues. In animal cells in vitro, some type of regulatory mechanism maintains the overall membrane composition which limits total lipid substitution.

The conversion of choline to ethanolamine in phospholipid headgroup substitution and interconversion has been postulated by Horwitz (1977) to occur minimally in the metabolism of cells supplemented with sera or delipidized serum and exogenous lipid sources. From this statement, two conclusions can be drawn: 1) there are insignificant rates of phospholipid turnover, and 2) there is little, if any, interconversion among the phospholipid subclasses. According to the latter statement, since fetal bovine serum contains no phosphatidylethanolamine, cells cultured in this type of serum supplement should have decreasing amounts of phosphatidylethanolamine which become smaller as the cellular pools become diluted. Cells in culture, however, display considerable phospholipid turnover as well as phosphatide headgroup interconversion even in the presence of serum that inhibits de novo lipid biosynthesis. Ward and Falch (1973) examined the effect of

media lipids on cellular phospholipids in cultured hepatoma cells. Certain phospholipid classes common to hepatoma and normal liver cells produced similar changes as serum supplied lipids were modulated. The same trend is more pronounced for the cellular phosphatide fatty acid acyl side chain composition. The phospholipids of cells grown in high serum levels not only exhibited changes in the phosphatidylcholine class (which accounts for approximately 50% of the serum phosphatides) but also in the phosphatidylethanolamine, phosphatidylserine, and phosphatidylinositol classes normally absent in fetal bovine sera. Increasing the fetal bovine serum concentration from 2.5% to 5.0% increased the cellular phosphatidylcholine levels by approximately 4%; however, the phosphatidylethanolamine concentration remained the same. The phosphatidylserine and phosphatidylinositol levels only increased 0.4%. With respect to the phospholipid headgroup composition, serum lipids can only affect phosphatidylcholine levels. Therefore, interconversion and turnover of phospholipid headgroups must occur at an appreciable rate to maintain the cellular membrane lipids at genetically predetermined levels. The fatty acid composition of the hepatoma cells in vitro are sensitive to alterations in serum and media lipids. Increasing the serum concentration from 2.5% to 5.0% increased the levels

of 16:0 and 18:0 phosphatidylcholine species while decreasing the 18:1 phosphatidylcholine concentration which is normally the highest among serum phosphatidylcholine fatty acids. Doubling the serum levels increased the 16:0, 16:1, and 18:0 phosphatidylethanolamine fatty acid levels accompanied by an overall decrease in long chain unsaturated species as well as the 18:1 and 18:2 fatty acid levels. All phospholipid classes exhibited decreases in the poly-unsaturated fatty acids and increases in the 18:0 levels as serum levels were decreased (which resulted in diminished supplies of exogenously available serum lipids). Thus, even in the presence of serum-derived lipids, cells possess the ability to partially saturate and desaturate specific lipids for the maintenance of genetically predetermined levels. Snyder and Falch (1973) postulated that decreased fatty acid biosynthesis in the presence of tissue culture media supplemented with serum (Rothblat, 1969; Bailey et al., 1972) may be the result of increased levels of linoleate within the serum. These authors make a substantial point when considering fatty acid alterations in vitro: "These data indicate that care must be exercised when comparing phospholipid data, even from the same cell line, with that obtained in other laboratories, especially when the growth conditions are not known".

A unique problem specific to cells in vitro is the alteration (inhibition or acceleration) of phospholipid turnover as they are stimulated into division. This is usually a consequence of the addition or replenishment of serum or tryptic action on a resting confluent layer of cells. Studying 3T3 and polyoma transformed 3T3 cells (Py3T3), Cunningham (1972) observed that the rates of phospholipid incorporation (specifically  $^{32}\text{P}$ -orthophosphate incorporation) were identical for nonconfluent 3T3, confluent 3T3, nonconfluent Py3T3, and confluent Py3T3 cells three days after the initiation of division by passaging. Addition of serum to confluent monolayers of normal and transformed cells produced increased turnover rates only for contact-inhibited 3T3 cells. The rates of phosphatidylcholine turnover increases two-fold although the phosphatidylethanolamine synthesis decreases when cells are grown to confluent density. If cells are supplemented with serum and the contact inhibition is removed, 3T3 and chick skin fibroblasts have high rates of turnover, especially in the phosphatidylinositol subclass (Cunningham and Pardee, 1969; Pasternak, 1972).

The net consequence of phospholipid turnover and its significance to lipid changes observed for malignant and non-malignant cell lines is that potentially malignant cells which have been virally transformed possess higher



rates of phospholipid turnover than their normal counterparts (Pasternak, 1973). In Cunningham's (1972) analysis of his results which measure the incorporation of  $^{32}\text{P}$ -orthophosphate into normal and transformed cells, he assumes that incorporation of the label in the absence of net synthesis (allowing for differences in radiolabel uptake (Cunningham and Pardee, 1969) is equivalent to turnover. For the case where the addition of serum relieves contact inhibition, there is an increase in turnover. Tumorigenic cells, however, have lost their contact inhibition and Cunningham (1972) infers that the phospholipid turnover (of which phosphatidylserine is the fastest) is dependent on the density inhibition of division which can be relieved by serum factors. Treating Py3T3 cells with serum to relieve density inhibition should not have any effect since transformed cells already lack density growth inhibition (i.e. decreased contact inhibition). In glioma cells in vitro (Lindgren, 1976), serum factors may be responsible for the cell density when growth inhibition occurs, but growth inhibition itself may be due to cellular interactions. Moreover, the increased rate of phosphatidylcholine turnover is also observed in SV40-3T3 transformed cells when compared to their normal 3T3 counterparts (Pasternak, 1973). Phospholipid turnover,

however, may be able to explain the previously published discrepancies between fatty acid composition and fluorescence or spin-labelled membrane fluidities for normal and transformed cells. In this dissertation, the phospholipid turnover rates of malignant and non-malignant cells should be similar since all cells were passaged by tryptic digestion and grown in fresh media containing serum. These normal and malignant cells, as they are being analyzed for lipid changes and measured with ESR for fluidity, are actively proliferating, and therefore, are not contact-inhibited. This, in all probability, may not be the case in previous studies where the metabolic states of the cells are not known. For example, a typical experimental method involves growing cells from a nonconfluent state to a confluent one. The time required for cells to make this transition is directly proportional to the cell density of the initial inoculation. A long period of time may elapse before the cells become confluent and are usable for experiments. Undoubtedly, the cell media will have to be replenished during this time period whereupon fresh serum will remove the contact inhibition and increase the phospholipid turnover above that of transformed cells. Since serum lipids are used preferentially over de novo lipid synthesis, the membrane fluidities and fatty acid compositions of the normal and transformed phenotypes would be

similar. These similarities reflect changes in the unstable lipid pool undergoing a higher rate of turnover rather than phospholipid changes resulting from neoplastic induced anabolic and catabolic enzymes. Therefore, any similarities in membrane fluidity between the normal and transformed state of previous studies may be entirely due to an exchange of cellular lipids and those extracellular as well as the membrane bilayer.

A. Relevance of Lipid Alterations to Normal and Transformed Cells in vitro

To reiterate from the results section, it can be stated that all tumor derived lines contain less total lipid ( $\mu\text{g}/\text{cell}$ ) than normal brain cells. These same lines, moreover, contain lower amounts of phospholipid ( $\mu\text{g}/\text{mg}$  protein) as well. The only exception to this is the SV40 line which has a phospholipid content statistically equivalent to that of the NFB line. Cholesterol contents are smaller in tumor derived cell lines except for the TE907 and 251 MG 3C lines. No correlations may be drawn between cell line malignancy and total lipid, cholesterol, or phospholipid. However, analysis of the phospholipid compositions of these cell lines indicates that sphingomyelin decreases in tumor derived cells and phosphatidylcholine increases which is similar to the changes induced in 3T3 cells by transformation. The

phosphatidylserine plus phosphatidylinositol (PS + PI) levels of tumor derived cells are lower although no significant differences are observed for the phosphatidylethanolamine concentrations of these cells. These results are dissimilar to the phosphatidylserine (PS), phosphatidylinositol (PI), and phosphatidylethanolamine (PE) levels assayed in the 3T3 transformation system. Again it may be stated that no direct correlation between a specific phospholipid subclass and malignancy can be made although the phosphatidylcholine and sphingomyelin levels of the tumor derived glial SA101 cell line is closest in absolute values to that of the NFB line. With respect to specific fatty acid alterations and increasing malignancy in the phosphatidylcholine subclass, no distinct changes are observed for the normal and tumor derived cell lines (SA series and 251 MG 3C). In contrast, the SA4 cell line exhibits selective decreases in the 14:0, 16:0, 18:0, 18:1, and 18:2 PI+PS lipids compared to the NFB cell line. Part of this is similar to the selective changes in the 18:0 and 18:1 PI levels noted for SV40 transformed 3T3 fibroblasts. Many of the lipid concentrations of the non-malignant SA101 cell line and the intermediate tumorigenic 251 MG 3C line are closer to those levels in the NFB cells than in other tumor derived lines. Lastly, the same qualitative differences in the phosphatidylethanolamine

fatty acid profiles of the tumor-derived and the NFB lines also exist in the 3T3 transformation system. There are no distinct trends in fatty acid contents among cell with increasing malignancy, although in some instances, the non-malignant tumor derived SA101 line has fatty acid levels closer to those of the NFB line.

A unique feature of the five tumor derived cell lines and the NFB cell line is a lower cholesterol:phospholipid molar ratio which is below unity (in the range of 0.2-0.3). This lowered ratio appears to be characteristic to normal and neoplastic cells grown in vitro on solid substrates (Wallach, 1975; Adam et al., 1975). Cholesterol:phospholipid molar ratios of unity are characteristic of most solid tumors. In the 3T3 transformation system, the cholesterol:phospholipid (CHL:PL) molar ratios are centered around 0.3 for normal and transformed (Py3T3 and SV101-3T3) variants assayed by whole cell analysis (Adam et al., 1975). CHL:PL values of 0.76 to 0.84 have been observed for intact plasma membrane preparations of 3T3 and Sv40 transformed 3T3 cells, respectively (Perkins and Scott, 1978). WI-38 and WI-38VA13A cells possess CHL:PL molar ratio values of about 0.46 (Howard et al., 1973). Wallach (1975) postulated that these lower CHL:PL ratios in vitro are indicative of cholesterol depletion as a result of the culturing conditions since neoplastic growth in vivo does not demonstrate this trend.

These ratios, moreover, do not reflect a correlation with the degree of malignancy for the glioma and medulloblastoma derived lines and the NFB line. This observation has been previously noted in other studies (MacKenzie et al., 1964; Kawanani et al., 1966; Weinstein et al., 1969; Klenk and Choppin, 1969, 1970) where the CHL:PL ratios lie between 0.11 and 0.49 for normal and tumor cell lines.

B. Lipid Alterations in Relation to Normal and Malignant Neural Tissues in vivo and in vitro

As discussed, many of the lipid alterations noted for normal human cells and human brain tumors in culture are indicative of general trends in neoplasia rather than specific phospholipid or phosphatide acyl side chain alterations. Since the cell lines in this dissertation were derived from human brain specimens in situ, one would expect that many of the lipid trends would be similar to those observed for human normal brain and brain tumors in vivo. This does not appear to be the case as fatty acid profiles only re-emphasize the individuality of cells in culture. Remembering how the manipulation of exogenously supplied lipids can influence the lipid composition of cells in vitro, the conclusion that lipid changes in neoplasia are only general trends is not surprising.

Generally, human neural tumors in vitro contain similar amounts of total lipid and phospholipid as their

parental tissues in vivo. The exceptions are cholesterol and ganglioside quantities (Yates et al., 1979) for cells grown in monolayer cultures. Variability in lipid composition can be influenced by the mode of culture. For example, cells grown in aggregating cultures possess extremely low levels of phospholipids, cholesterol, total lipids, and glycolipids (Bourre et al., 1979; Matthieu et al., 1979).

With respect to the lipid alterations of the cell lines used in this dissertation, the tumor lines contain lower amounts of total lipids compared to normal tissues (Cumings, 1943; White, 1974; Yates et al., 1979). Variability in both phospholipid and cholesterol concentrations is seen for cells with different malignant potentials, although normal and malignant cell lines contain similar total quantities of phospholipid and cholesterol. Specifically, the tumor-derived cell lines contain less sphingomyelin and PS + PE (phosphatidylserine plus phosphatidylinositol) but more phosphatidylcholine. Phosphatidylethanolamine levels are not statistically different for the tumor and normal cell lines. These data in general contradict the trends observed in phospholipid compositions of human brain neoplasms with the exception of the greater phosphatidylcholine levels (see Section C. Brain Tumors, page 133). Examination of White's

data (1974) indicate a large variability in the phospholipid subclass composition of human brain tumors with the phosphatidylcholine levels being the only common trend tying together the cell lines used in this dissertation. Overall, the data presented here in Table 3 (page 218) closely correlate to the decrease in total lipids and sphingomyelin and the large increase in the phosphatidylcholine concentrations seen by Yates et al. (1979) for a graded series of human neural tumors in vivo.

The phospholipid fatty acid acyl side chain compositions of the lines studied in this dissertation also display a great deal of variation compared to the profiles for human brain tumors in vivo. Many of the trends noted for human neural tumors of in situ specimens do not carry over to the fatty acid compositions of the cell lines presented in this study. For example, neoplastic brain tissue has been postulated to have lost the specificity for 18:2 uptake, with its concentration usually being extremely low in tumor tissue but not in fetal or human adult brain. The 18:2 composition of PC (phosphatidylcholine) (Table 4), PS + PI (phosphatidylserine plus phosphatidylinositol) (Table 5), and PE (phosphatidylethanolamine) (Table 6) indicates that this fatty acid concentration increases for the tumor-derived



cell lines when considering phosphatidylcholine, phosphatidylserine, and phosphatidylinositol but is only present in the non-malignant tumor-derived cell lines bound to phosphatidylethanolamine molecules. Even for PE, variability is observed where the malignant SA4 line contains nearly identical levels of PE to those of the normal glial cell line. Sun and Leung (1974) proposed that the overall 20:4 (n-6) levels are indicative of rapid cell growth while increases in 22:6 (n-6) fatty acids are a measure of neuronal maturity. These proposals were disputed by White (1974) who observed that 20:4 (n-6) levels are proportional to cellular growth potential. Examination of the 20:4 (n-6) levels among phosphatidylcholine, phosphatidylethanolamine, phosphatidylserine, and phosphatidylinositol (Tables 4, 5, and 6) molecules discloses that this conclusion can only be applied to a select few of the cell lines used in this dissertation. The 20:4 levels are greater for malignant, rapidly growing cell lines with regard to the phosphatidylserine plus phosphatidylinositol totals; whereas, among phosphatidylcholine and phosphatidylethanolamine molecules, the slow-growing non-tumorigenic TE907 and normal glial SA101 cells have the greatest 20:4 content, signifying poor cellular growth and differentiation in vitro. The specific fatty acid alterations obtained for human neural tissues from

in vivo solid specimens, therefore, are not repeated in human brain tumor tissue cultures.

A notable aspect of the tumor-derived cell lines used in this dissertation is that their phospholipid distributions are close to that of normal human fetal brain reported by Svennerholm (1968) where the phosphatidylcholine class accounts for about 50%, phosphatidylethanolamine for 30%, and the remaining phospholipids (phosphatidylserine, phosphatidylinositol, and sphingomyelin) constitute nearly 20% of the total phospholipid composition.

The profiles published by White (1974) and Sun and Leung (1974) contain appreciable variability when highlighting the fatty acid composition of the ethanolamine- and choline-containing phosphoglycerides. The ethanolamine phosphoglycerides (White, 1974) have been assayed as containing: (a) decreased concentrations of 18:1 and 20:1 fatty acids, (b) increased concentrations of 18:2 and 20:4 fatty acids, and (c) decreased amounts of the  $C_{22}$  fatty acid family. Sun and Leung (1974), however, saw increased amounts of 18:1, 18:2 and 20:4 fatty acids of the phosphatidylethanolamine class with lower proportions of the  $C_{22}$  fatty acids (22:4 and 22:6, in agreement with White (1974)). One would expect that the malignant lines E1202 and SA4 as well as the 251 MG 3C and the TE907 cell lines would reflect these changes. These changes are not

similar to those listed in Table 6 with regard to tumor-derived cell lines. In some instances, only the medulloblastoma-derived lines have increased 18:1 levels, and these are accompanied by a similar increase in the 20:4 phosphatidylethanolamine fatty acids. The converse of this is represented by the SA series which should contain lower concentrations of the C<sub>22</sub> fatty acids, but instead, contain three to four times the NFB or 251 MG 3C levels. The phosphatidylcholine fatty acid chain profiles, similar to those of the phosphatidylethanolamine fatty acids (White, 1974), outline increases in 16:0, 18:0 and 18:1 with fewer long chain polyunsaturated species (Sun and Leung, 1974). These profiles, moreover, are not mimicked among the phosphoglyceride components of the tumor-derived cell lines in this dissertation. As a result, these trends must be considered non-specific, non-correlatable to human neural tumors in vitro or their degree of malignant potential. The correlations linking specific fatty acids (18:2, 22:4, 22:5, and 22:6) in both phosphatidylethanolamine and phosphatidylethanolamine subclasses (White, 1974) to neural tumors are not obvious among any of the phospholipid fatty acid class compositions for tumor-derived cell lines used in this dissertation. Diminished levels of 18:2 fatty acids in cultured human brain and neural tumors are not a surprise since 18:2 is

primarily associated with serum and red cell membranes which are abundant in most biopsy specimens, although absent from cells in culture.

Examination of the unsaturation levels (presented as saturated fatty acids, Table 7) indicates that there are no gross differences in the phosphatidylcholine subclass between the tumor-derived and normal glial cell lines. This is in opposition to the data of White (1974) and Sun and Leung (1974) who observed that malignant cells in vivo have greater unsaturated phosphatidylcholine fatty acid levels. The phosphatidylethanolamine subclass, on the other hand, displays more variability with respect to the fatty acid unsaturation levels. Comparable to Sun and Leung's (1974) data, the medulloblastoma cell lines E1202 and TE907 have an approximately 70% unsaturated phosphatidylethanolamine titer. Among the glioma-derived lines the SA101 line has an identical unsaturation level to that of the NFB line, while the SA4 glioma is considerably more unsaturated. An even greater degree of variability exists for the phosphatidylinositol and phosphatidylserine acyl side chain unsaturation so much so that no correlation can be drawn to previously reported literature data (Sun and Leung, 1974; White, 1974) on the differences between normal and tumor-derived cells or the degree of tumorigenicity within medulloblastoma and glioma-derived cell lines.

An example of the large degree of variability in phospholipid composition and phosphatide fatty acid acyl side chain profiles can be observed by examining the data of Robert et al. (1976), Robert et al. (1979), and Eichberg et al. (1976) who studied the lipid compositions of hamster astroblasts (NN line) and rat gliomas (C6). These studies provide a good model for the comparison of lipid alterations in human neural tumors (gliomas and medulloblastomas) and in normal human glial cells (NFB and SA101 lines) in vitro. Robert et al. (1976) found that the total lipid and phospholipid content of the C6 line is smaller than the content of the NN line. In a later study (Robert et al., 1979) using the same cell lines, however, the C6 cells were assayed as having the greater phospholipid content. The phosphatidylethanolamine composition of the NN and C6 lines are nearly identical (slight increase in the C6 cells), although the phosphatidylcholine levels are always greater for the C6 tumor line in both previously discussed studies. Sphingomyelin levels are similar for the C6 and NN lines, but the C6 cells contain less phosphatidylserine and phosphatidylinositol. Eichberg et al. (1976) have found that phosphatidylcholine levels of C6 glioma cells are greater than the PC levels of cultured astrocytes (through one to 52 passages) and newborn hamster brain dispersions. The

sphingomyelin concentrations, however, increase in the C6 line and are accompanied by a simultaneous decrease in the phosphatidylethanolamine and phosphatidylserine plus phosphatidylinositol concentrations. These observations contrast to the phospholipid alterations observed by Robert et al. (1976) and Robert et al. (1979) whose phospholipid profiles of the C6 glioma generally reflect those alterations seen for the cell lines used in this dissertation with the exception of a sphingomyelin decrease observed in cultured human neural tumors. Considering the phosphatidylcholine acyl side chain compositions of C6 and normal NN astroblasts (Robert et al., 1976), the 15:0, 16:0, 16:1, 17:0, 18:1, 18:2, 20:0, 20:1, 20:2, and 20:3 concentrations are elevated in C6 glioma cells while the 18:0, 18:3, 20:4, 22:5, and 22:6 concentrations are depressed. No differences are observed in the concentrations of 14:0, 17:1, and 22:1 species. These fluctuations are also qualitatively present for the tumor-derived cell lines in this dissertation. Specifically, 16:1, 17:0, 18:1 (for the medulloblastoma cells only), 18:2 (for the glioma lines only), 20:1, and 20:3 phosphatidylcholine fatty acid levels are increased; whereas, the 18:0 and 22:5 (n-6) levels are decreased for all the neural tumors in culture. No differences were noted for the 18:3 and 20:4 concentrations among the

glioma, medulloblastoma, and NFB cell lines. The 22:6 levels are diminished in all of the tumor-derived cell lines with the exception of the SA101 line. Robert et al. (1976), furthermore, have found that 80% of the choline phosphoglyceride acyl side chains are shorter than 20 carbon atoms in length and approximately 20% of these fatty acids are polyunsaturates. For the phosphatidylcholine subclass, these data do not correspond to any specific fluctuation seen for non-malignant and malignant cell lines or glial cell lines. For the phosphatidylethanolamine fatty acid acyl side chain composition, Robert et al. (1976) reported that the 15:0, 16:0, 16:1, 18:2, 20:5, 22:5, and 22:6 species are less abundant in the C6 glioma cells. Increased levels in these same cells are observed for the 17:0, 18:0, 20:0, 20:1, 20:2, 20:3, and 22:0 fatty acid species. Essentially similar quantities of 14:0, 17:1, 18:3, 20:4, and 22:1 were assayed for the C6 and NN cell lines. The profiles observed by Robert et al. (1976) with regard to the 18:2, 20:5, 22:5, 20:1 and 17:0 phosphatidylethanolamine fatty acids are similar to the trends observed for the cell lines used in this dissertation. Reflecting the trends of unsaturation in the C6 and NN cell line (Robert et al., 1976), the values for human neural tumors listed in Table 7 are similar with the exception of the SA4 and 251 MG 3C lines. For the

glioma-derived cell lines, there is a decrease in the percentage of phosphatidylethanolamine fatty acids with chain lengths less than 20 carbons long compared to that in the NFB cell line. This is analogous to the data of Robert et al. (1976) who observed a decrease in chain length for C6 glioma cells. The greatest disparity between the C6 and NN lines is found when considering the PS + PI (phosphatidylserine plus phosphatidylinositol) acyl group composition. The 16:0, 17:0, 18:0, 18:1, and 19:0 fatty acid species are increased; whereas, 16:1, 18:2, 20:0, 20:1, 20:2, and 20:4 species are greatly decreased in the tumorigenic cell type. Only changes for the 17:0 and 18:2 fatty acids are like the trends found for the cell lines presented in this dissertation. The increase in short chain fatty acids indicated by the phosphatidylserine plus phosphatidylinositol subclass (Robert et al., 1976) for the C6 glioma line is seen only among the medulloblastoma-derived cell lines used in this dissertation.

Comparing the lipid alterations of the cell lines in this dissertation with those studies of human neural tumor specimens, normal animal and human brain lines, it may generally be stated that the phospholipid class compositions are nearly identical. However, no conclusions may be drawn from the comparisons of phospholipid fatty acid acyl side chain compositions of specific phospholipid



classes. It must be pointed out that this disparity most likely exists since (a) many of the previous studies on lipid alterations in human brain tumors examined solid in vivo specimens, and (b) cells in culture are easily manipulated with regard to lipid composition and metabolism. Each system that examines lipid alterations in normal brain and neural tumors must be considered on its own merits (i.e., direct analysis of the tissue or culture of this specimen and subsequent analysis after many passages in tissue culture) with careful evaluation of culturing conditions before being thought as exemplifying the general lipid alterations of neural tumors. Each normal brain-tumorigenic brain system, therefore, is unique with many of the phospholipid fatty acid alterations being specific for that particular tumor rather than brain tumor in general.

### C. Fidelity of Spin Label Studies

A firm conclusion cannot be made concerning the physical state of normal and transformed membrane bilayers estimated using differing biophysical probes. Each method examines non-related aspects of membrane structure and function. Fluorescent, spin label, and deuterium NMR studies of neoplastic alterations illustrate this incompatibility between techniques. Electron spin

resonance and nuclear magnetic resonance, using spin labels or specifically deuterated phospholipids, monitor rotations and isomeric conformations of cholesterol, phospholipids, and phosphatide fatty acid acyl side chains in membrane bilayers. In contrast, fluorescent probes sense probe-induced motions rather than the conformations of individual membrane components. Mely-Goubert and Freedan (1980) postulate that the fluorescent polarization studies do not indicate overall membrane fluidity, but rather the interactions of these probes with proteins positioned in inner membrane bilayer. The similarities indicated by fluorescent polarization between normal and transformed cells may therefore be attributed to the monitoring of identical hydrophobic pockets of membrane proteins (Mely-Goubert et al., 1979) rather than indicating any real differences of lipid bilayer fluidity. The membrane intrinsic fluidity, moreover, is not to be confused with the degree of mobility of membrane proteins. This mobility is believed to be a dynamic feature which determines normal and malignant cell growth (Inbar, 1979). Eldridge et al. (1980), for example, observed that the lateral mobility of either a fluorescent-labelled ganglioside or concanavalin A molecule in normal and SV40 transformed 3T3 cells is not mediated through increased

membrane fluidity, but is associated with distinct alteration of cell surface receptors. The overall membrane fluidity defines a complex situation applicable to different properties of different regions of the membrane bilayer rather than hydrocarbon conformations sensed by magnetic resonance probes.

The ESR studies in this dissertation indicate that differences between normal and malignant human neural cells exist with respect to "spin-label-sensed membrane fluidity". Using the 5-, 12-, and 16-doxylstearate probes, the tumorigenic cells possess decreased  $T_1$ , splitting and consequently possess increased membrane fluidity. Order parameters relating membrane fluidity to an arbitrary range between 0 and 1 (0 being a fluid state and 1 indicating a rigid environment) further correlate an increase in fluidity (decrease in order) for the malignant cell types. The spin label data in this dissertation are presented as order parameters which possess no absolute units, rather than rotational correlation times which indicate an actual timescale of motion. Thieret (1979, and personal communication) and Schreier *et al.* (1979) point out that rotational correlation times cannot describe slow anisotropic motion characteristic of membrane immobilized spin labels. The timescale of these motions

is greater than allowed by ESR theory and may be only described by NMR or saturation-transfer EPR techniques. The spin label spectra presented in this dissertation exhibit slow anisotropic motion, even in the case of the mobile 16-doxylstearate probe when compared to the isotropic motion of Fremys salt (Figure 12, Page 172).

It is also observed that nitroxide crystalline-BSA tensor value substitution effects the absolute value of the order parameters. Only the  $S_{\text{GAF}}$  order parameter equation is independent of tensor value substitution. Unless the specific order parameter equation is known, therefore, correlations cannot be made between absolute order parameter values among differing studies and investigators.

The spin label results of this dissertation can be validated by several points. The probe:lipid ratio is critical and can significantly alter membrane fluidity. Minimal perturbation of the membrane bilayer occurs when probe:lipid ratios are 1:100 or greater in biological systems and 1:600 in liposome studies. In previous studies, based on whole cell-lipid analysis, the probe:lipid ratios were in the range of 30-10-5:1. These studies show no differences between the fluidity of normal and transformed cells because of spin-spin interactions due to saturation of the membrane signal by the spin labels. The probe:

lipid ratios of the spin-labelled cells in this dissertation reflect a ratio adjusted to one probe molecule per 100 molecules of total cellular lipid. If one considers that a specific proportion of the cellular lipid lies in the cell membrane bilayer, this probe:lipid ratio may be realistically increased. The ratio used in this dissertation, however, is several orders of magnitude lower than the ratios of other spin label studies. The value of  $m$ , as a measure of probe-probe interactions, is below unity for the 5-, 12-, and 16-doxylstearate probes in both normal and malignant cell lines. This conclusion indicates that the actual probe:lipid ratio is increased. The relative probe:lipid ratio does not accurately take into account the proportion of lipid present in the plasma membrane. The labelling procedure used in this study initially labels cell-media surface membrane, not the entire plasma membrane. The spin label partitions into a reduced area rather than over the entire membrane surface. With this procedure there would be a greater density of spin label per given surface area which should decrease the value of  $m$ . With disruption of cell-cell contacts, an increase in the value of  $m$  as spin labels distribute laterally with a corresponding decreasing in spin-spin interactions.

This conclusion, however, cannot be substantiated due to the rapid destruction of the spin labels in both

normal and neural tumor cells (Figure 43). The semiquinone free radical of ubiquinone of the mitochondrial respiratory chain (Quintanilha and Paker, 1977) or free sulfhydryl groups (Dr. R. Huageland, personal communication) is reported to be involved with nitroxide group reduction. Since the cell lines in this study were labelled and analyzed within a short period of time (10 to 45 minutes), the amount of spin label that diffused into the cytoplasm or intracellular membranes should be minimized. The fast reduction of spin label supports the view that the transformed cells possess an increase in concentration of sulfhydryl groups in plasma membrane bound proteins. For all spin label combinations with cell lines, the half-life of the spectral signal was 25 to 30 minutes. This rapid reduction of nitroxide signal also has been observed in liposome systems and is dependent upon temperature, buffer, pH, and the lipid:water ratio (Hare et al., 1979). Spin label partitioning studies measuring the vertical heights of the spectral intensities conclude that there are no differences between the membranes of normal and transformed cells. This may be due to the inaccuracy of measuring rapidly decreasing signals. The horizontal shape of  $T_{\parallel}$  and  $T_{\perp}$  splittings is not affected by this rapid nitroxide reduction. Furthermore, in this

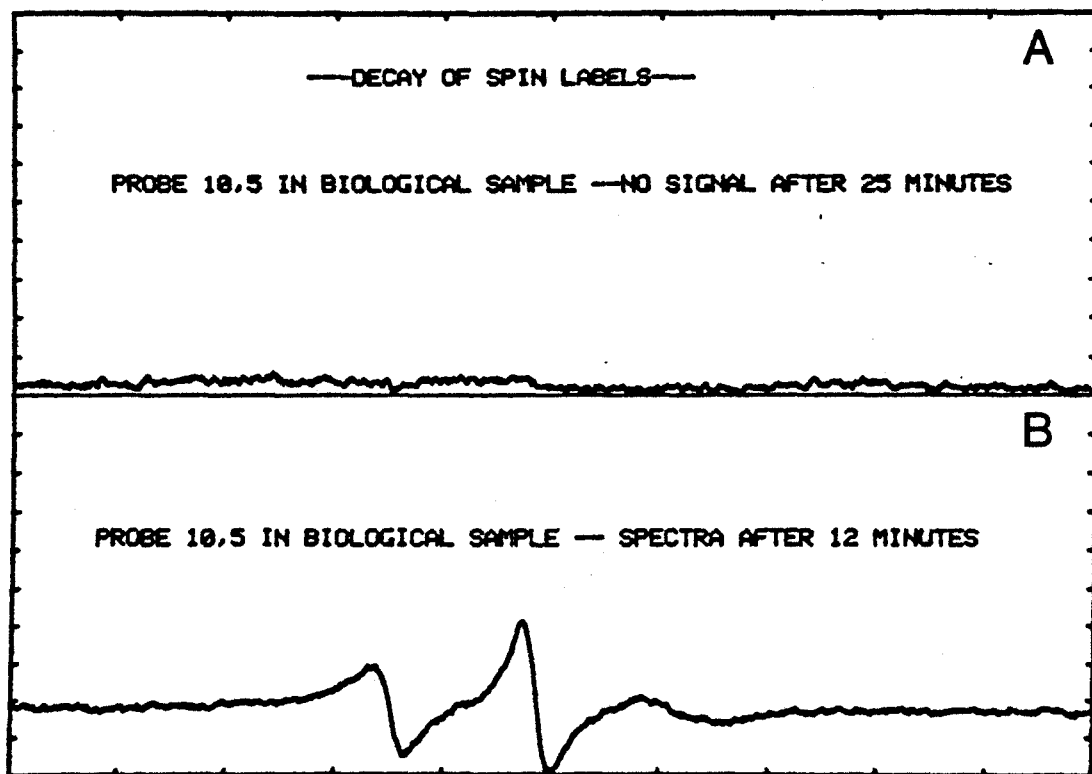


FIG 39.: Rapid reduction of spin labels when incorporated in viable intact neural tumor cells. A. Signal after 25 minutes. B. Signal after 12 minutes.

dissertation protein carriers (bovine serum albumin, for example) are not used to incorporate the spin label into the cells and consequently monitor membrane fluidity changes rather than reflecting motion of the probe bound to hydrophobic protein pockets.

The spin label studies of the human normal and malignant neural cell lines presented in this dissertation indicate that the malignant cells possess greater degrees of lipid rotation, indicative of increased "membrane fluidity". Although there are statistically significant differences between the normal and tumorigenic order parameters, these reflect small changes in the number of gauche-transphospholipid fatty acyl side chain isomerizations (Appendix II) on the order of 2 to 10%. All cell lines display a flexibility gradient with regard to increasing degree of fluidity as the spin label probe moves from the rigid, restricted phospholipid headgroup region toward the hydrophobic mobile fatty acid side chains in the membrane interior.

#### D. Summary and Conclusion

A normal-transformed in vitro cell model derived from normal human brain and spontaneously induced human brain tumors is presented. The system is composed of normal glial cells (NFB line) and five tumor-derived cell lines, one of which, the SA101 line, presents cell



culture characteristics and lipid alterations similar to cultured normal glial cells. Among the remaining lines, two were initiated from medulloblastomas (E1202 and TE907 cell lines), and the other two were initiated from gliomas (SA4 and 251 MG 3C). Using growth in athymic nude mice and colony forming efficiency in soft agar tumorigenicity assay methods, the SA4 and E1202 lines are malignant (+,+), the SA101, TE907 and NFB lines are non-tumorigenic (-,-) and the 251 MG 3C glioma-derived cell line is intermediately malignant (-,+).

The tumor-derived cell lines contain increased levels (on a mole percentage basis) of phosphatidylcholine, decreased levels of sphingomyelin and phosphatidylserine plus phosphatidylinositol, and similar levels of phosphatidylethanolamine when compared to the phospholipid levels of the normal glial cell line (NFB). This increase in phosphatidylcholine concentration agrees with increases observed in human normal brain and in vivo neural tumor specimens as well as non-neural fibroblast transformation systems (i.e., 3T3 fibroblasts, etc.). No overall correlation is observed relating the phospholipid acyl side chain composition to that of other transformed cell systems, to that of human brain tumors in vivo, or to malignant potential, although there are specific instances where

particular fatty acids are increased or decreased in the neoplastic state. Considering the percentage of saturated fatty acids in phospholipid subclasses, no correlation is observed between that of the five tumor-derived cell lines and that of the NFB line. Correlations, however, may be made for individual normal-transformed cell pairs. In the case of the non-tumorigenic TE907 and SA101 lines, in all phospholipid subclasses they contain decreased levels of unsaturated fatty acids. The malignant SA4 cell line does not show this feature in the phosphatidylcholine class; however, decreased levels of unsaturated fatty acids is observed in the phosphatidylethanolamine and phosphatidylserine plus phosphatidylinositol subclasses. The medulloblastoma derived cell lines do not exhibit this effect. Cholesterol:phospholipid molar ratios are below unity for all cells, a common feature of cell lines maintained in tissue culture.

Membrane fluidity was investigated by the spin label technique using the 5, 12, and 16-doxylstearate probes to estimate hydrocarbon rotations at 5, 12, and 16 methylene groups in the bilayer. Comparison of the  $T_{\parallel}$  splitting and order parameter calculations for  $S$ ,  $S'$ ,  $S''$ ,  $S_{\parallel}$ ,  $S_{\perp}$ , and  $S_{\text{GAF}}$  as well as the isotropic splitting

constant  $a'_n$  indicates a correlation between tumorigenicity and spin label membrane fluidity. For all three probes, cell lines which produce tumors or form colonies in the in vivo and in vitro tumorigenicity assays, respectively, possess an increase in fluidity above the NFB level, with the largest absolute increases being seen as the spin label position moved toward the bilayer interior. The  $S_{GAF}$  order parameter possesses little change with nitroxide tensor value substitution, while this substitution affects other order parameter calculations,  $S'$ ,  $S''$ ,  $S_1$ ,  $S_{11}$ , and  $S$ . A flexibility gradient can be generated for each cell line, indicating that this is a common denominator of membranes in general and is not just restricted to malignant human neural cells or normal cells in vitro. The increase in spin label membrane fluidity for the malignant cell line is correlated with a small increase in unsaturated fatty acid molecules.

Evidence is presented which indicates malignant cell lines possess increased PC + SPH/PE + (PS + PI) molar ratios. This also correlates with literature values of the PC + SPH/PE + (PS + PI) ratios presented in the literature of normal human brain and human brain tumors. The data supports the concept of previous investigators that membrane fluidity can be primarily modulated by

phospholipid headgroup composition, interactions, and metabolism rather than by the degree of unsaturation and chain length of phospholipid acyl side chains.

## REFERENCES

- Aaronson, S.P. and Todaro, G.J. (1968) Basis for the Acquisition of Malignant Potential by Mouse Cells Cultivated In Vitro. *Science* 162: 1024-6.
- Abrahamsson, S., Dahlen, B., Lofgren, H., Pascher, I., and Sundell, S. (1976) Molecular Arrangement and Conformation of Lipids of Relevance to Membrane Structure. In *Structure of Biological Membranes*, ed. S. Abrahamsson and I. Pascher, Plenum Press, New York, pp. 1-23.
- Adam, G. and Adam, G. (1975) Cell Surface Charge and Regulation of Cell Division of 3T3 Cells and Transformed Derivatives. *Exp. Cell Res.* 93: 71-8.
- Adam, G., Alpes, H., Blaser, K., and Heubert, B. (1975) Cholesterol and Phospholipid Content of 3T3 Cells and Transformed Derivatives. *Z. Naturforsch* 30: 638-42.
- Ahmad, P. and Mellors, A. (1978) Nuclear Magnetic Resonance Studies of Liposomes: Effects of Steroids on Lecithin Fatty Acyl Chain Mobility. *J. Membrane Biol.* 41: 235-47.
- Allt, G. (1979) Electron Microscopy of Cerebral Tumors. *Trends Neurosciences* 2: 94.
- Aloni, B., Shinitzky, M., and Liune, A. (1974) Dynamics of Erythrocyte Lipids in Intact Cells, in Ghost Membranes and in Liposomes. *Biochim. Biophys. Acta* 348: 438-41.
- Anderson, H.C. (1978) Probes of Membrane Structure. *Ann. Rev. Biochem.* 47: 359-83.
- Ansell, G.B. and Dohmen, H. (1957) The Metabolism of Individual Phospholipids in Rat Brain During Hypoglycaemia, Anaesthesia and Convulsions. *J. Neurochem.* 2: 1-10.
- Axel, F.S. (1976) Biophysics with Nitroxyl Radicals. *Biophys. Struct. Mech.* 2: 181-218.
- Azzi, A. (1975) The Application of Fluorescent Probes in Membrane Studies. *Quart. Rev. Biophys.* 8: 237-316.
- Bailey, J.M. and Dunbar, L.M. Essential Fatty Acid Requirement of Cells in Tissue Culture: A Review. *Exp. Mol. Pathol.* 18: 142-61.

Bailey, J.M., Gey, G.O., and Gey M.K. (1964) Lipid Metabolism in Cultured Cells. V. Comparative Lipid Nutrition in Serum and in Lipid-free Chemically Defined Medium. Proc. Soc. Exp. Biol. Med. 115: 747-52.

Bailey, J.M., Horward, B.U., and Tillman, S.F. (1972) Lipid Metabolism in Cultured Cells. XI. Utilization of Serum Triglycerides. J. Biol. Chem. 248: 1240-7.

Balakrishnan, S., Goodwin, H., and Cumings, J.N. (1961) The Distribution of Phosphorus-containing Lipid Compounds in the Human Brain. J. Neurochem. 8: 276-84.

Baldassare, J.J., Brenckle, G.M., Hoffman, M., and Silbert, D.F. (1977) Modification of Membrane Lipid. Functional Properties of Membrane in Relation to Fatty Acid Structure. J. Biol. Chem. 252: 8797-803.

Bales, B.L. and Leon, V. (1978) Magnetic Resonance Studies of Eukaryotic Cells. III. Spin-labeled Fatty Acids in the Plasma Membrane. Biochim. Biophys. Acta 509: 90-9.

Bales, B., Lesin, E.S., and Oppenheimer, S.B. (1977) On Cell Membrane Lipid Fluidity and Plant Lectin Agglutinability. A Spin Label Study of Mouse Ascites Tumor Cells. Biochim. Biophys. Acta 465: 400-7.

Bar, K.S., Deamer, D.W., and Cornwell, D.G. (1966) Surface Area of Human Erythrocyte Lipids. Reinvestigation of Experiments on Plasma Membrane. Science 153: 1010-2.

Barnes, R.G. (1974) Deuteron Quadrupole Tensors in Solids. In Advances in Nuclear Quadrupole Resonance, vol. I, ed. J.A.S. Smith, Heyden, London, England, pp. 335-55.

Barnett, R.E., Fucht, L.T., and Scott, R.E. (1974) Differences in Membrane Fluidity and Structure in Contact-inhibited and Transformed Cells. Proc. Natl. Acad. Sci. USA 71: 1992-5.

Barnett, R.E. and Grisham, C.M. (1972) Spin Exchange of Spin Labeled Probes in a Natural Membrane. Biochem. Biophys. Res. Comm. 48: 1362-70.

Bartlett, G.R. (1959) Phosphorus Assay in Column Chromatography. J. Biol. Chem. 234: 466-8.

Belle, J. and Bothorel, P. (1974) Theoretical Study of Spin Labelled Aliphatic Chains in Bilayers. Biochem. Biophys. Res. Comm. 58: 433-6.

- Belle, J., Bothorel, P., and Lemaire, B. (1974) Melting Entropy and Structure of Aliphatic Chains in Mono and Bilayers. FEBS Lett. 39: 115-7.
- Ben-Bassat, H., Polliak, A., Rosenbaum, S.M., Naparstek, E., Shouval, D., and Inbar, M. (1977) Fluidity of Membrane Lipids and Lateral Mobility of Concanavalin A Receptors in the Cell Surface of Normal Lymphocytes and Lymphocytes From Patients With Malignant Lymphomas and Leukemias. Cancer Res. 37: 1309-12.
- Benson, A.A. (1966) On the Orientation of Lipids in Chloroplast and Cell Membranes. J. Am. Oil Chemists Soc. 43: 265-70.
- Bergelson, L.D. (1970) Tumor Lipids. Prog. Chem. Fat Other Lipids 13: 1-59.
- Bergelson, L.D. and Barsukov, L.I. (1977) Topological Asymmetry of Phospholipids in Membranes. Science 197: 224-30.
- Bergelson, L.D. and Dyatlovitskaya, E.V. (1973) Molecular Structures of Tumor Lecithins and Their Relevance to Some Properties of Tumor Cell Membranes. In Tumor Lipids: Biochemistry and Metabolism, ed. R. Wood, American Oil Chemist's Society Press, Champaign, Ill., pp. 111-25.
- Bergelson, L.D., Dyatlovitskaya, E.V., Torkhovskaya, T.I., Sorokina, I.B., and Gorkova, N.P. (1970) Phospholipid Composition of Membranes in the Tumor Cell. Biochim. Biophys. Acta 210: 287-98.
- Bergerson, J.J.M., Warmsley, A.M.H., and Pasternak, C.A. (1970) Phospholipid Synthesis and Degradation During the Life-cycle of P815Y Mast Cells Synchronized With Excess of Thymidine. Biochem. J. 119: 489-92.
- Bernard, L. (1958) Associations Moleculaires Entre les Lipides. II. Lecithine et Cholesterol. Bull. Soc. Chim. Biol. 40: 161-70.
- Binns, R.M., Symons, D.A., and White, D.J. (1972) Demonstration of the Movement of Histocompatibility Antigen and Immunoglobulin on the Pig Lymphocyte Membrane by Immunofluorescence. J. Physiol. 226: 33P.
- Birrell, G.B., Griffith, O.H., and French, D. (1973b) Observation of Z-axis Anisotropic Motion of a Nitroxide Spin Label. J. Am. Chem. Soc. 95: 8171-2.

- Birrell, G.B., Van, S.P., and Griffith, O.H. (1973a) Electron Spin Resonance of Spin Labels in Organic Inclusion Crystals. Models for Anisotropic Motion in Biological Membranes. *J. Am. Chem. Soc.* 95: 2451-8.
- Black, P.H. (1966) Transformation of Mouse Cell Line 3T3 by SV40: Dose Response Relationship and Correlation With SV40 Tumor Antigen Production. *Virology* 28: 760-3.
- Blaise, J.K., Dewey, M.M., Blaurock, A.E., and Worthington, C.R. (1965) Electron Microscope and Low Angle X-ray Diffraction Studies on Outer Segment Membranes From the Retina of the Frog. *J. Mol. Biol.* 14: 143-52.
- Blaise, J.K. and Worthington, C.R. (1969) Planar Liquid-like Arrangement of Photopigment Molecules in Frog Retinal Disk Membrane. *J. Mol. Biol.* 39: 417-39.
- Blaise, J.K., Worthington, C.R., and Dewey, M.M. (1969) Molecular Localization of Frog Retinal Receptor Photopigment by Electron Microscopy and Low Angle X-ray Diffraction. *J. Mol. Biol.* 39: 407-17.
- Blank, M.L., Piantadosi, C., Ishaq, K.S., and Synder, F. (1975) Modification of Glycerolipid Metabolism in L-M Fibroblasts by an Unnatural Amino-alcohol, N-isopropyl-ethanolamine. *Biochem. Biophys. Res. Comm.* 62: 983-88.
- Blaurock, A.E. (1971) Structure of the Nerve Myelin Membrane: Proof of Low Resolution Profile. *J. Mol. Biol.* 56: 35-52.
- Blaurock, A.E. (1973a) X-ray Diffraction Pattern From a Bilayer With Protein Outside. *Biophys. J.* 13: 281-9.
- Blaurock, A.E. (1973b) The Structure of a Lipid-cytochrome c Membrane. *Biophys. J.* 13: 290-8.
- Blaurock, A.E. and Stoeckenius, W. (1971) Structure of the Purple Membrane. *Nature (New Biology)* 233: 152-5.
- Blaurock, A.E. and Wilkins, M.H.F. (1969) Structure of Frog Photoreceptor Membranes. *Nature* 223: 906-9.
- Blazyk, J.F. and Steim, J.M. (1972) Phase Transitions in Mammalian Membranes. *Biochim. Biophys. Acta* 266: 737-41.
- Blough, H.A. and Tiffany, J.M. (1973) Lipids in Viruses. *Adv. Lipid Res.* 11: 267-339.



- Blumenfeld, T.A., Stark, R.I., James, L.S., George, J.D., Dyrenfurth, I., Freda, V.I., and Shinitzky, M. Determination of Fetal Lung Maturity by Fluorescence Polarization of Amniotic Fluid. *Am. J. Obstet. Gyn.* 130: 782-7.
- Bodansky, O. (1975) *Biochemistry of Human Cancer*. Academic Press, New York.
- Boone, C.W. (1975) Malignant Hemangioendotheliomas Produced by Subcutaneous Inoculation of Balb/3T3 Cells Attached to Glass Beads. *Science* 188: 68-70.
- Borochoy, A., Halevy, A.H., and Shinitzky, M. (1976) Increase in Microviscosity With Aging in Protoplast Plasmalemma of Rose Petals. *Nature* 263: 158-9.
- Borochoy, H., Zahler, P., Wilbrandt, W., and Shinitzky, M. (1977) The Effect of Phosphatidylcholine to Sphingomyelin Mole Ratio on the Dynamic Properties of Sheep Erythrocyte Membrane. *Biochim. Biophys. Acta* 470: 382-8.
- Bossmann, H.B. and Winton, R.A. (1970) Synthesis of Glycoprotein, Glycolipid, Protein and Lipid in Synchronized L5178Y Cells. *J. Cell Biol.* 45: 23-33.
- Boure, J.M., Honegger, P., Daudu, O., and Matthieu, J.M. (1979) The Lipid Composition of Rat Brain Aggregating Cell Cultures During Development. *Neuroscience Lett.* 11: 275-8.
- Boyle, J.J. and Ludwig, E.H. (1962) Analysis of Fatty Acids of Continuously Cultured Mammalian Cells by Gas-liquid Chromatography. *Nature* 196: 893-4.
- Brante, G. (1949) *Studies on Lipids in the Nervous System With Special Reference to Quantitative Chemical Determination and Topical Distribution*. *Acta Physiol. Scand.* 18(Suppl.): 63.
- Bretscher, M.S. (1972) Phosphatidylethanolamine: Differential Labeling in Intact Cells and Cell Ghosts of Human Erythrocytes by a Membrane-impermeable Reagent. *J. Mol. Biol.* 71: 523-8.
- Bretscher, M.S. (1972) Asymmetrical Lipid Bilayer Structure for Biological Membranes. *Nature (New Biology)* 236: 11-2.
- Bretscher, M.S. (1973) *Membrane Structure: Some General Principles*. *Science* 181: 622-9.

- Brown, A.D. (1965) Hydrogen Ion Titrations of Intact and Dissolved Lipoprotein Membranes. *J. Mol. Biol.* 12: 491-508.
- Brown, J.C. (1973) Effect of Concanvalin A on the Sensitivity of Mouse L Cell Surface Glycoproteins to Proteolysis. *Biochem. Biophys. Res. Comm.* 51: 686-92.
- Brown, P.K. (1972) Rhodopsin Rotates in the Visual Receptor Membrane. *Nature (New Biology)* 236: 35-9.
- Burger, M.M. and Goldberg, A.R. (1967) Identification of a Tumor Specific Determinant on Neoplastic Cell Surfaces. *Proc. Natl. Acad. Sci. USA* 57: 359-66.
- Burleson, R., Kulpa, C.F., Edwards, H.E., and Thomas, J.K. (1978) Fluorescent Probe Studies of Normal, Persistently Infected, Rous Sarcoma Virus-transformed and Trypsinized Rat Cells. *Exp. Cell Res.* 116: 291-300.
- Burnett, L.J. and Muller, B.H. (1971) Deuteron Quadrupole Coupling Constants in Three Solid Deuterated Paraffin Hydrocarbons:  $C_2D_6$ ,  $C_4D_{10}$ ,  $C_6D_{14}$ . *J. Chem. Phys.* 55: 5829-31.
- Calpaldi, R.A. and Green, D.E. (1972) Membrane Proteins and Membrane Structure. *FEBS Lett.* 25: 205-9.
- Carlsson, J. and Brunk, U. (1977) The Fine Structure of Three-dimensional Colonies of Human Glioma Cells in Agarose Culture. *Acta Path. Microbiol. Scand.* 85(A): 183-92.
- Caspar, D.L.D. and Kirschner, D.A. (1971) Myelin Membrane Structure at 10 Å Resolution. *Nature (New Biology)* 231: 46-52.
- Chan, S.J., Feigenson, G.W., and Seiter, C.H.A. (1971) Nuclear Relaxation Studies of Lecithin Bilayers. *Nature* 231: 110-1.
- Chan, S.I., Seiter, C.H., and Feigenson, G.W. (1972) Anisotropic and Restricted Motion in Lecithin Bilayers. *Biochem. Biophys. Res. Comm.* 46: 1488-92.
- Chao, F.C., Eng, L.F., and Griffin, A. (1972) Compositional Differences of Lipid in Transformed Hamster Fibroblasts. *Biochim. Biophys. Acta* 260: 197-202.
- Chap, H.J., Zwaal, R.F.A., and van Deenen, L.L.M. (1977) Action of Highly Purified Phospholipases on Blood Platelets. Evidence for an Asymmetric Distribution of Phospholipids in the Surface Membrane. *Biochim. Biophys. Acta* 467: 146-64.

- Chapman, D. (1975) Phase Transitions and Fluidity Characteristics of Lipids and Cell Membranes. *Quart. Rev. Biophys.* 8: 185-235.
- Chapman, D. and Wallach, D.F.H. (1968) Physical Studies of Phospholipids and Natural Membranes. In *Biological Membranes*, ed. D. Chapman, Academic Press, London, England.
- Chapman, D., Williams, R.M., and Ladbroke, B.D. (1967) Physical Studies of Phospholipids. VI. Thermotropic and Lyotropic Mesomorphism of Some 1,2-diacyl-phosphatidylcholine (Lecithins). *Chem. Phys. Lipids* 1: 445-75.
- Chapman, D. and Urbina, J. (1971) Phase Transitions and Bilayer Structure of Mycoplasma laidlawii B. *FEBS Lett.* 12: 169-72.
- Chapman, D., Urbina, J., and Keough, K.M. (1974) Biomembrane Phase Transitions. Studies of Lipid-water Systems Using Differential Scanning Calorimetry. *J. Biol. Chem.* 249: 2512-21.
- Charalampous, F.C. (1977) Differences in Plasma Membrane Organization of Neuroblastoma Cells Grown in the Differentiated and Undifferentiated States. *Arch. Biochem. Biophys.* 181: 103-16.
- Charalampous, F.C. (1979) Levels and Distributions of Phospholipids and Cholesterol in the Plasma Membrane of Neuroblastoma Cells. *Biochim. Biophys. Acta* 556: 38-51.
- Charvolin, J., Manneville, P., and Deloche, B. (1973) Magnetic Resonance of Perdeuterated Potassium Laurate in Oriented Soap-water Multilayers. *Chem. Phys. Lett.* 23: 345-8.
- Chen, Y.S. and Hubbell, W.L. (1973) Temperature- and Light-dependent Structural Changes in Rhodopsin-lipid Membranes. *Exp. Eye Res.* 17: 517-32.
- Cheng, S. and Levy, D. (1979) The Effects of Cell Proliferation on the Lipid Composition and Fluidity of Hepatocyte Plasma Membranes. *Arch. Biochem. Biophys.* 196: 424-9.
- Cheng, S., Thomas, J.K., and Kulpa, C.F. (1974) Dynamics of Pyrene Fluorescence in Escherichia coli Membrane Vesicles. *Biochemistry* 13: 1135-9.
- Cherry, R. (1975) In *Biological Membranes*, vol. III, ed. D. Chapman and Wallach, D.F.H., Academic Press, London, England.

Christensen-Lou, H.O.C. and Clausen, J. (1968) Polar Lipids of Oligodendrogliomas. *J. Neurochem.* 15: 263-4.

Christensen-Lou, H.O., Clausen, J., and Bierring, F. (1965) Phospholipids and Glycolipids of Tumours in the Central Nervous System. *J. Neurochem.* 12: 619-27.

Cogen, U., Shinitzky, M., Weber, G., and Nishida, T. (1973) Microviscosity and Order in the Hydrocarbon Region of Phospholipid-cholesterol Dispersions Determined With Fluorescent Probes. *Biochemistry* 12: 521-8.

Cohen, M.D. (1955) Quantitation of Phosphorus Compounds in the Normal and Pathologic Human Brain. *J. Neuropath. Exp. Neurol.* 14: 70-83.

Colburn, N.H., Bruegge, W.F.V., Bates, J.R., Gray, R.H., Rossen, J.D., Kelsey, W.H., and Shimada, T. (1978) Correlation of Anchorage-independent Growth With Tumorigenicity of Chemically Transformed Mouse Epidermal Cells. *Cancer Res.* 38: 624-34.

Collard, J.G. and Temmink, J.H.M. (1975) Differences in Density of Concanavalin A- Binding Sites Due to Differences in Surface Morphology of Suspended Normal and Transformed 3T3 Fibroblasts. *J. Cell Science* 19: 21-32.

Collins, F.D. and Shortlander, V.L. (1961) Studies on Phospholipids. 8. Phospholipids in Rat-liver Mitochondria and Microsomes. *Biochem. J.* 79: 321-4.

Comoglio, P.M. and Filogamo, G. (1973) Plasma Membrane Fluidity and Surface Mobility of Mouse C1300 Neuroblastoma Cells. *J. Cell Science* 13: 415-20.

Cone, R.A. (1972) Rotational Diffusion of Rhodopsin in the Visual Receptor Membrane. *Nature (New Biology)* 236: 39-43.

Cooper, R.A. (1977) Abnormalities of Cell-membrane Fluidity in the Pathogenesis of Disease. *N. Engl. J. Med.* 297: 371-7.

Cooper, R.A. (1978) Influence of Increased Membrane Cholesterol on Membrane Fluidity and Cell Function in Human Red Blood Cells. *J. Supramolecular Struct.* 8: 413-30.

Cooper, R.A., Durocher, I.R., and Leslie, M.H. (1977) Decreased Fluidity of Red Cell Membrane Lipids in Abetalipoproteinemia. *J. Clin. Invest.* 60: 115-21.

- Cooper, R.A., Leslie, M.H., Fischkoff, S., Shinitzky, M., and Shattil, S.J. (1978) Factors Influencing the Lipid Composition and Fluidity of Red Cell Membranes In Vitro: Production of Red Cells Possessing More Than Two Cholesterols Per Phospholipid. *Biochemistry* 17: 327-31.
- Cotterill, F.M.J. (1976) Computer Simulation of Model Lipid Membrane Dynamics. *Biochim. Biophys. Acta* 433: 264-70.
- Courbe, J.P. (1834) Du Cerveau, Considere Sous le Point de Vue Chimique et Physiologique. *Ann. Chim. Phys. (Paris)* 1: 160-93.
- Cullis, P.R., Dekruyff, B., and Richards, R.E. (1976) Factors Affecting the Motion of the Polar Headgroup in Phospholipid Bilayers. A  $^{31}\text{P}$  NMR Study of Unsonicated Phosphatidylcholine Liposomes. *Biochim. Biophys. Acta*. 426: 433-46.
- Cumings, J.N. (1943) The Chemistry of Cerebral Tumors and of Cerebral Cyst Fluids. *Brain* 66: 316.
- Cumings, J.N., Goodwin, H., Woodward, F.M., and Curzon, G. (1958) Lipids in the Brains of Infants and Children. *J. Neurochem.* 2: 289-94.
- Cunningham, D.D (1972) Changes in Phospholipid Turnover Following Growth of 3T3 Mouse Cells to Confluency. *J. Biol. Chem.* 247: 2464-70.
- Cunningham, D.D. and Pardee, A.B. (1969) Transport Changes Rapidly Initiated by Serum Addition to Contact Inhibited 3T3 Cells. *Proc. Natl. Acad. Sci. USA* 64: 1049-56.
- Dallner, G., Siekevitz, P., and Palade, G.E. (1966) Biogenesis of Endoplasmic Reticulum Membranes. I. Structural and Chemical Differentiation in Developing Rat Hepatocyte. *J. Cell Biol.* 30: 73-96.
- Danielli, J.F. and Davson, H. (1935) A Contribution to the Theory of Permeability of Thin Films. *J. Cell Comp. Physiol.* 5: 495-508.
- Darke, A., Finer, E.G., Flook, A.G., and Phillips, M.C. (1972) Nuclear Magnetic Resonance Study of Lecithin-cholesterol Interactions. *J. Mol. Biol.* 63: 265-79.
- Das, M.L. and Crane, F.L. (1964) Proteolipids. I. Formation of Phospholipid-cytochrome c Complexes. *Biochemistry* 3: 696-700.

- Davidson, R.L. and Bick, M. (1973) Bromodeoxyuridine Dependence--A New Mutation in Mammalian Cells. Proc. Natl. Acad. Sci. USA 70: 138-42.
- Davis, J.H. (1979) Deuterium Magnetic Resonance Study of the Gel and Liquid Crystalline Phases of Dipalmitoyl Phosphatidylcholine. Biophys. J. 27: 339-58.
- Davis, W.C. (1972) H-2 Antigen on Cell Membranes: An Explanation for the Alteration of Distribution by Indirect Labeling Techniques. Science 175: 1006-7.
- Dekruyff, B., Demel, R.A., and van Deenen, L.L.M. (1972) The Effect of Cholesterol and Epicholesterol Incorporation on the Permeability and on the Phase Transition of Intact Acholeplasma laidlawii Cell Membranes and Derived Liposomes. Biochim. Biophys. Acta 255: 331-47.
- DeLaat, S.W., van der Saag, P.T., and Shinitzky, M. (1977) Microviscosity Modulation During the Cell Cycle of Neuroblastoma Cells. Proc. Natl. Acad. Sci. USA 74: 4468-61.
- DeLaat, S.W., van der Saag, P.T., and Shinitzky, M. (1978) Microviscosity Changes During Differentiation of Neuroblastoma Cells. Biochim. Biophys. Acta 509: 188-93.
- Demel, R.A., Bruckdorfer, K.R., and van Deenen, L.L. (1972) Structural Requirements of Sterols for the Interaction With Lecithin at the Air Water Interface. Biochim. Biophys. Acta 255: 311-20.
- Demel, R.A. and Dekruyff, B. (1976) The Function of Sterols in Membranes. Biochim. Biophys. Acta 457: 109-32.
- Demel, R.A., van Deene, L.L.M., and Pethica, B.A. (1967) Monolayer Interactions of Phospholipids and Cholesterol. Biochim. Biophys. Acta 135: 11-9.
- DePetris, S. and Raff, M.C. (1973) Normal Distribution, Patching and Capping of Lymphocyte Surface Immunoglobulin Studied by Electron Microscopy. Nature 241: 257-9.
- DePierre, J.W. and Dallner, G. (1975) Structural Aspects of the Membrane of the Endoplasmic Reticulum. Biochim. Biophys. Acta 415: 411-72.
- DeSalle, L., Munakata, N., Pauli, R.M., and Strauss, B.S. (1972) Receptor Sites for Concanavalin A on Human Peripheral Lymphocytes and on Lymphoblasts Grown in Long Term Culture. Cancer Res. 32: 2463-8.

Devaux, P. and McConnell, H.M. (1972) Lateral Diffusion in Spin-labeled Phosphatidylcholine Multilayers. *J. Am. Chem. Soc.* 94: 4475-81.

Dijck, P.W.N., van Zoelen, E.J.J., Seldenrijk, R., van Deenen, L.L.M., and de Gier, J. (1976) Calorimetric Behavior of Individual Phospholipid Classes From Human and Bovine Erythrocyte Membranes. *Chem. Phys. Lipids* 17: 336-43.

Doi, O., Doi, F. Alberts, A.W., and Vagelos, P.R. (1978) Manipulation of Fatty Acid Composition of Membrane Phospholipid and Its Effect on Cell Growth in Mouse LM Cells. *Biochim. Biophys. Acta* 509: 239-50.

Dryer, W.J., Papermaster, D.S., and Kuhn, H. (1972) On the Abundance of Ubiquitous Structural Protein Subunits in Biological Membranes. *Ann. N.Y. Acad. Sci.* 195: 61-74.

Dulbecco, R. (1970) Topo Inhibition and Serum Requirement of Transformed and Untransformed Cells. *Nature* 227: 802-6.

Dunham, P.B. and Hoffman, J.F. (1970) Partial Purification of the Oubain-binding Component and of Na,k-ATPase From Human Red Cell Membranes. *Proc. Natl. Acad. Sci. USA* 66: 936-43.

DuPont, Y., Harrison, S.C., and Hasselbach, W. (1973) Molecular Organization in the Sarcophomic Reticulum Membrane Studied by X-ray Diffraction. *Nature* 244: 555-8.

Dyatlovitskaya, E.V., Torkhovskaya, T.I., and Bergelson, L.D. (1969) Phospholipids of Cellular Membranes of Rat Liver and Hepatoma. *Dokl. Akad. Nauk. USSR* 186: 948.

Dyatlovitskaya, E.V., Yanchevskaya, G.V., and Bergelson, L.D. (1974) Molecular Species and Membrane Forming Properties of Lecithins in Normal Liver and Hepatoma. *Chem. Phys. Lipids* 12: 132-49.

Dyer. (1978) The Metabolism of Linolenic Acid in Developing Rat Brain. Ph.D. Dissertation, Loyola University of Chicago.

Edidin, M. (1972) In Transplantation Antigens, ed. R. Kahan and B. Reisfeld, pp. 125-40.

Edwards, H.E., Thomas, J.K., Burleson, G.R., and Kulpa, C.F. (1976) The Study of Rous Sarcoma Virus-transformed Baby Hamster Kidney Cells Using Fluorescent Probes. *Biochim. Biophys. Acta* 448: 451-9.

- Eibl, H. and Blume, A. (1979) The Influence of Charge on Phosphatide Acid Bilayer Membranes. *Biochim. Biophys. Acta* 553: 476-88.
- Eichberg, J., Shein, H.M., and Hauser, G. (1976) Lipid Composition and Metabolism of Cultured Hamster Brain Astrocytes. *J. Neurochem.* 27: 679-85.
- Eldridge, C.A., Elson, E.L., and Webb, W.W. (1980) Fluorescence Photobleaching Recovery Measurements of Surface Lateral Mobilities on Normal and SV-40-transformed Mouse Fibroblasts. *Biochemistry* 19: 2075-9.
- Emmelot, P. and van Hoeven, R.P. (1975) Phospholipid Unsaturation and Plasma Membrane Organization. *Chem. Phys. Lipids* 14: 236-46.
- Engelman, D.M. (1969) Surface Area Per Lipid Molecule in the Intact Membrane of the Human Red Cell. *Nature* 223: 1279-80.
- Engelman, D.M. (1970) X-ray Diffraction Studies of Phase Transitions in the Membrane of Mycoplasma laidlawii. *J. Mol. Biol.* 47: 115-7.
- Engelman, D.M. (1971) Membrane Bilayer Structure in the Membrane of Mycoplasma laidlawii. *J. Mol. Biol.* 58: 153-6.
- Engelman, D.M. and Rothman, J.E. (1972) The Planar Originization of Lecithin-cholesterol Bilayers. *J. Biol. Chem.* 247: 3694-7.
- Esfahani, M., Barnes, E.M., Jr., and Wakil, S.J. (1969) Control of Fatty Acid Composition in Phospholipids of Escherichia coli: Response to Fatty Acid Supplements in a Fatty Acid Auxotroph. *Proc. Natl. Acad. Sci. USA* 64: 1057-64.
- Esko, J.D., Gilmore, J.R., and Glaser, M. (1947) Use of a Fluorescent Probe to Determine the Viscosity of LM Cell Membranes With Altered Phospholipid Compositions. *Biochemistry* 16: 1881-90.
- Esser, A.F. and Lanyi, J.K. (1973) Structure of the Lipid Phase in Cell Envelope Vesicles From Halobacterium cutirubrum. *Biochemistry* 12: 1933-9.
- Faber, R.J. and Fraenkel, G.K. (1967) Dynamic Frequency Shifts and the Effects of Molecular Motions in the Electron Spin Resonance Spectra of Dinitrobenzene Anion Radicals. *J. Chem. Phys.* 47: 2462-76.



- Feinstein, M.G., Fernandex, S.M., and Sha'afi, R.I. (1975) Fluidity of Natural Membranes and Phosphatidylserine and Ganglioside Dispersions. Effects of Anesthetics, Cholesterol and Protein. *Biochim. Biophys. Acta* 413: 354-70.
- Feo, F., Bonelli, G., and Matli, A. (1970) Effect of Trypsin on Morphological Integrity and Some Functional Activities of Mitochondria From Normal Liver and AH-130 Yoshida Ascites Hepatoma. *Life Science* 9: 1235-41.
- Ferguson, J.L. and Brown, G.H. (1968) Liquid Crystals and Living Systems. *J. Am. Oil Chem. Soc.* 45: 120-7.
- Ferguson, K.A., Glaser, M., Bayer, W.H., and Vagelos, P.R. (1975) Alteration of Fatty Acid Composition of LM Cells by Lipid Supplementation and Temperature. *Biochemistry* 14: 146-51.
- Fernandez-Moran, H. (1962) Ultrastructure and Metabolism of the Nervous System. In *The Interpretation of Ultrastructure*, ed. R.J.C. Harris, Academic Press, New York, p. 411.
- Fieser, L.F. and Fieser, M. (1935) The Reduction Potentials of Various Naphthoquinones. *J. Am. Chem. Soc.* 57: 491-4.
- Figard, P.H. and Greenberg, D.M. (1962) The Phosphatides of Some Mouse Ascites Tumors and Rat Hepatomas. *Cancer Res.* 22: 361-7.
- Finean, J.B., Bramley, T.A., and Coleman, R. (1971) Lipid Bilayer in Cell Membranes. *Nature* 229: 114.
- Finer, E.G. and Philips, M.C. (1973) Factors Affecting Molecular Packing in Mixed Lipid Monolayers and Bilayers. *Chem. Phys. Lipids* 10: 237-52.
- Fisher, K.A. (1976) Analysis of Membrane Halves: Cholesterol. *Proc. Natl. Acad. Sci. USA* 73: 173-7.
- Fogh, J., Fogh, J.M., and Orfeo, T. (1977) One Hundred and Twenty Seven Cultured Human Tumor Cell Lines Producing Tumors in Nude Mice. *J. Natl. Cancer Inst.* 59: 221-6.
- Fogh, J. and Hajdu, S.I. (1975) The Nude Mouse as a Diagnostic Tool in Human Tumor Research. *J. Cell Biol.* 67: 117.

- Folch, J. (1955) In Biochemistry of the Developing Nervous System, ed. H. Waelsch, Academic Press, New York, p. 121.
- Folch, J., Lees, M., and Sloane-Stanley, G.H. (1957) A Simple Method for the Isolation and Purification of Total Lipids From Animal Tissues. J. Biol. Chem. 226: 497-509.
- Foley, G.E., Handler, A.H., Adams, R.A., and Craig, J.M. (1962) Assessment of Potential Malignancy of Cultured Cells: Further Observations on the Differentiation of "Normal" and "Neoplastic" Cells Maintained In Vitro by Heterotransplantation in Syrian Hamsters. Natl. Cancer Inst. Mono. 7: 173-204.
- Fontaine, R.N. and Schroeder, F. (1979) Plasma Membrane Aminophospholipid Distribution in Transformed Murine Fibroblasts. Biochim. Biophys. Acta 558: 1-12.
- Fox, C.H. and Sanford, K.K. (1976) Chemical Analyses of Mammalian Sera Commonly Used as Supplements for Tissue Culture Media. Tissue Culture Assoc. Manual, pp. 233-7.
- Freeman, A.E. and Huebner, R.J. (1973) Problems in Interpretation of Experimental Evidence of Cell Transformation. J. Natl. Cancer Inst. 50: 303-6.
- Frye, L.D.F. and Edidin, M.J.E. (1970) The Rapid Inter-mixing of Cell Surface Antigens After Formation of Mouse-human Heterokaryons. J. Cell Science 7: 319-33.
- Fuchs, P., Parola, A., Robbins, P.W., and Blout, E.R. (1975) Fluorescence Polarization and Viscosities of Membrane Lipids of 3T3 Cells. Proc. Natl. Acad. Sci. USA 72: 3351-4.
- Furcht, T. and Scott, R.E. (1974) Influence of Cell Cycle and Cell Movement on the Distribution of Intramembraneous Particles in Contact-inhibited and Transformed Cells. Exp. Cell Res. 88: 311-8.
- Gaffney, B.J. (1975) Fatty Acid Chain Flexibility in Membranes of Normal and Transformed Fibroblasts. Proc. Natl. Acad. Sci. USA 72: 664-8.
- Gaffney, B.J. (1976) Practical Considerations for the Calculation of Order Parameters for Fatty Acid or Phospholipid Spin Labels in Membranes. In Spin Labeling Theory and Applications, ed. L.J. Berliner, Academic Press, New York, pp. 567-71.

- Gaffney, B.J. and McConnell, H.M. (1974) The Paramagnetic Resonance Spectra of Spin Labels in Phospholipid Membranes. *J. Magnetic Resonance* 16: 1-28.
- Gaffney, B.J. and Mich, R.J. (1976) A New Measurement of Surface Charge in Model and Biological Lipid Membranes. *J. Am. Chem. Soc.* 98: 3044-5.
- Galla, H.J. and Sackmann, E. (1974) Lateral Diffusion in the Hydrophobic Region of Membranes: Use of Pyrene Examers as Optical Probes. *Biochim. Biophys. Acta* 339: 103-15.
- Galla, H.J. and Sackmann, E. (1975) Chemically Induced Phase Separation in Mixed Vesicles Containing Phosphatidic Acid. An Optical Study. *J. Am. Chem. Soc.* 97: 4114-20.
- Gallagher, W.R., Weinstein, D.B., and Blough, H.A. (1973) Rapid Turnover of Principal Phospholipids in BHK-21 Cells. *Biochem. Biophys. Res. Comm.* 52: 1252-6.
- Gally, H.U., Pluschke, G., Overath, P., and Seelig, J. (1979) Structure of Escherichia coli Membranes. Phospholipid Conformation in Model Membranes and Cells as Studied by Deuterium Magnetic Resonance. *Biochemistry* 18: 5605-10.
- Gally, H.U., Pluschke, G., Overath, P., and Seelig, J. (1980) Structure of Escherichia coli Membranes. Fatty Acyl Chain Order Parameters of Inner and Outer Membranes and Derived Liposomes. *Biochemistry* 19: 1638-43.
- Garrido, J. (1975) Ultrastructural Labeling of Cell Surface Lectin Receptors During the Cell Cycle. *Exp. Cell Res.* 94: 159-75.
- Gazitt, Y., Loyter, A., Reichler, Y., and Ohad, I. (1976) Correlation Between Changes in Membrane Organization and Susceptibility to Phospholipase C Attack Induced by ATP Depletion of Rat Erythrocytes. *Biochim. Biophys. Acta* 419: 479-92.
- Getz, G.S., Bartley, W., Stirpe, F., Nottom, B.M., and Renshaw, A. (1962) The Lipid Composition of Rat-liver Mitochondria, Fluffy-layer and Microsomes. *Biochem. J.* 83: 181-91.
- Getz, G.S., Bartley, W., Lurie, D., and Nottom, B.M. (1968) The Phospholipids of Various Sheep Organs, Rat Liver, and of Their Subcellular Fractions. *Biochim. Biophys. Acta* 152: 325-9.

- Geyer, R.P., Bennett, A., and Rohr, A. (1962) Fatty Acids of the Triglycerides and Phospholipids of HeLa Cells and Strain L Fibroblasts. *J. Lipid Res.* 3: 80-3.
- Giard, D.J., et al. (1973) In Vitro Cultivation of Human Tumors: Establishment of Cell Lines Derived From a Series of Solid Tumors. *J. Natl. Cancer Inst.* 51: 1417-21.
- Gilmore, R., Cohn, N., and Glaser, M. (1979a) Fluidity of LM Cell Membranes With Modified Lipid Compositions as Determined With 1,6-diphenyl-1,3,5-hexatriene. *Biochemistry* 18: 1042-9.
- Gilmore, R., Cohn, N., and Glaser, M. (1979b) Rotational Relation Times of 1,6-diphenyl-1,3,5-hexatriene in Phospholipids Isolated From LM Cell Membranes. Effects of Phospholipid Polar Head-group and Fatty Acid Composition. *Biochemistry* 18: 1050-6.
- Girardi, A.J., Jensen, F.C., and Koprowski, H. (1965) SV-40 Induced Transformation of Human Diploid Cells: Crisis and Recovery. *J. Cell Comp. Physiol.* 65: 69-83.
- Gitler, C. (1972) Plasticity of Biological Membranes. *Ann. Rev. Biophys. Bioeng.* 1: 51-92.
- Gitler, C. and Montal, M. (1972) Thin-proteolipid Films: A New Approach to the Reconstitution of Biological Membranes. *Biochem. Biophys. Res. Comm.* 47: 1486-91.
- Glaser, M., Ferguson, K.A., and Vagelos, P.R. (1974) Manipulation of the Phospholipid Composition of Tissue Culture Cells. *Proc. Natl. Acad. Sci. USA* 71: 4072-6.
- Glaser, M., Simpkins, H., Singer, S.J., Sheetz, M., and Chan, S.I. (1970) On the Interaction of Lipids and Proteins in the Red Blood Cell Membrane. *Proc. Natl. Acad. Sci. USA* 65: 721-8.
- Gluck, L., Kulovick, M., Eidelman, A.I., Coldero, L., and Khazin, A.F. (1972) Biochemical Development of Surface Activity in Mammalian Lung. IV. Pulmonary Lecithin Synthesis in the Human Fetus and Newborn and Etiology of the Respiratory Distress Syndrome. *Pediatr. Res.* 6: 81-99.
- Gopal, K., Grossi, E., Paoletti, P., and Usardi, M. (1963) Lipid Composition of Human Intracranial Tumors: A Biochemical Study. *Acta Neurochirurgica* 11: 335-47.

- Gordesky, S.E. and Marinetti, G.V. (1973) The Asymmetric Arrangement of Phospholipids in the Human Erythrocyte Membrane. *Biochem. Biophys. Res. Comm.* 50: 1027-31.
- Gordon, L.M., Sauerheber, R.D., and Esgate, J.A. (1978) Spin Label Studies on Rat Liver and Heart Plasma Membranes: Effects of Temperature, Calcium, and Lanthanum on Membrane Fluidity. *J. Supramolecular Struct.* 9: 299-326.
- Gorter, E. and Grendel, F. (1925) Bimolecular Layers of Lipids on Chromocytes of the Blood. *J. Exp. Med.* 41: 439-43.
- Graham, J.M. and Wallach, D.F.H. (1971) Protein Conformational Transitions in the Erythrocyte Membrane. *Biochim. Biophys. Acta* 241: 180-94.
- Grant, C.W.M., Wu, S.H.W., and McConnell, H.M. (1974) Lateral Phase Separations in Binary Lipid Mixtures: Correlation Between Spin Label and Freeze-fracture Electron Microscopic Studies. *Biochim. Biophys. Acta* 363: 151-8.
- Gras, W.J. and Worthington, C.R. (1969) X-ray Analysis of Retinal Photoreceptors. *Proc. Natl. Acad. Sci. USA* 63: 233-8.
- Green, D.E., Allman, D.W., Bachmann, E., Baum, H., Kopaczyk, K., Korman, E.F., Lipton, S., MacLennan, D.H., McConnell, D.G., Perdue, J.F., Rieske, J.S., and Tzagoloff, A. (1967) Formation of Membranes by Repeating Units. *Arch. Biochem. Biophys.* 119: 312-35.
- Griffith, O.H. (1964) ESR and Molecular Motion of the  $\text{RCH}_2\text{CHOOR}'$  Radicals in X-irradiated Ester-urea Inclusion Compounds. *J. Chem. Phys.* 41: 1093-1105.
- Griffith, O.H. and Jost, P.C. (1977) Lipid Spin Labels in Biological Membranes. *In Spin Labeling Theory and Applications*, ed. L.J. Berliner, Academic Press, New York, pp. 453-523.
- Griffiths, J.B. (1972) The Effect of Cell Population Density on Nutrient Uptake and Cell Metabolism: A Comparative Study of Human Diploid and Heteroploid Cell Lines. *J. Cell Science* 10: 515-24.
- Gruen, D.W.R. (1980) A Statistical Mechanical Model of the Lipid Bilayer Above Its Phase Transition. *Biochim. Biophys. Acta* 595: 161-83.

Gulik-Krzywicki, T. (1975) Structural Studies of the Associations Between Biological Membrane Components. *Biochim. Biophys. Acta* 415: 1-28.

Haest, C.W.M., Verkleij, A.J., DeGier, J., Scheek, R., Ververgaert, P.H.J., and van Deenen, L.L.M. (1974) The Effect of Lipid Phase Transitions on the Architecture of Bacterial Membranes. *Biochim. Biophys. Acta* 356: 17-26.

Hagins, W.A. and Jennings, W.H. (1959) Radiationless Migration of Electronic Excitation in Retinal Rods. *Dis. Faraday Soc.* 27: 180-90.

Hale, A.H., Yeu, T.M., and Weber, M.J. (1976) Membrane Lipid Acyl Group Alterations in Cells Infected With a Temperature-conditional Mutant of Rous Sarcoma Virus. *Biochim. Biophys. Acta* 443: 618-22.

Hare, F., Amiell, J., and Lussan, C. (1979) Is an Average Viscosity Tenable in Lipid Bilayers and Membranes? A Comparison of Semi-empirical Equivalent Viscosities Given by Unbound Probes: A Nitroxide and a Fluorophore. *Biochim. Biophys. Acta* 555: 388-408.

Harlos, K. and Eibl, H. (1980) Influence of Calcium on Phosphatidylglycerol. Two Separate Lamellar Structures. *Biochemistry* 19: 895-9.

Harlos, K., Stuempel, J., and Eibl, H. (1979) Influence of pH on Phosphatidic Acid Multilayers. A Rippled Structure at High pH Values. *Biochim. Biophys. Acta* 555: 409-16.

Hatten, M.E. (1975) The Influence of Membrane Lipids on the Lectin-induced Agglutination of Transformed and Untransformed Cell Lines. Ph.D. Thesis, Princeton University.

Hatten, M.E. and Burger, M.M. (1979) Effect of Polyene Antibiotics on the Lectin-induced Agglutination of Transformed and Untransformed Cell Lines. *Biochemistry* 18: 739-45.

Hatten, M.E., Scandella, C.J., Horwitz, A.F., and Burger, M.M. (1978) Similarities in Membrane Fluidity of 3T3 and SV101-3T3 Cells and Its Regulation to Concanavalin -A and Wheat Germ Agglutinin-induced Agglutination. *J. Biol. Chem.* 253: 1972-7.

- Hauser, G., Eichberg, J., and Shein, H.M. (1976) Lipid Composition of Experimental Astrocytomas Originating From Transformed Rat and Hamster Astrocyte Cultures. *Brain Res.* 109: 636-42.
- Hauser, H. and Guyer, W. (1979) Clustering of Fatty Acids in Phospholipid Bilayers. *Biochim. Biophys. Acta* 553: 359-63.
- Hayflick, L. (1973) Screening Tissue Cultures for Mycoplasma Infections. In *Tissue Culture: Methods and Applications*, ed. P.F. Kruse and M.K. Patterson, Jr., Academic Press, New York, pp. 722-8.
- Helgerson, S.L., Cramer, W.A., Harris, J.M., and Lytle, F.E. (1974) Evidence for a Microviscosity Increase in the Escherichia coli Cell Envelope Caused by Calicin E1. *Biochemistry* 13: 3057-61.
- Hemminga, M.A. (1975a) An ESR Study of the Mobility of the Cholestane Spin Label in Oriented Lecithin-cholesterol Multibilayers. *Chem. Phys. Lipids* 14: 141-50.
- Hemminga, M.A. (1975b) An ESR Spin Label Study of Structural and Dynamic Properties of Oriented Lecithin-cholesterol Multibilayers. *Chem. Phys. Lipids* 14: 151-73.
- Hendler, R.W. (1974) Protein Disposition in Biological Membranes. In *Biomembranes*, vol. 5, ed. L.A. Mason, Plenum Press, New York, pp. 251-73.
- Higgins, J.A. and Dawson, R.M.C. (1977) Asymmetry of the Phospholipid Bilayer of Rat Liver Endoplasmic Reticulum. *Biochim. Biophys. Acta* 470: 342-56.
- Hinz, H-J. and Sturtevant, J.M. (1972) Calorimetric Investigation of the Influence of Cholesterol on the Transition Properties of Bilayers Formed From Synthetic L- $\alpha$ -lecithins in Aqueous Suspension. *J. Biol. Chem.* 247: 3697-701.
- Hirano, N.H., Parkhouse, B., Nicolson, G., Lennox, E.S., and Singer, J.S. (1972) Distribution of Saccharide Residues on Membrane Fragments From a Myeloma-cell Homogenate: Its Implications for Membrane Biogenesis. *Proc. Natl. Acad. Sci. USA* 69: 2945-9.

Hitchcock, P.B., Mason, R., Thomas, K.M., and Shipley, G.G. (1974) Structural Chemistry of 1,2-dilauroyl-DL-phosphatidylethanolamine Molecular Conformation and Intermolecular Packing of Phospholipids. Proc. Natl. Acad. Sci. USA 71: 3036-40.

Holley, R.W. and Kierman, J.A. (1971) In Growth Control in Cell Cultures, eds. G.E.W. Wolsteinholme and J. Knight, Churchill Livingstone, London, England.

Horwitz, A.F. (1977) The Structural and Functional Roles of Lipids in the Surface of Animal Cells Grown In Vitro. In Growth, Nutrition and Metabolism of Cells in Culture, vol. III, eds. C.H. Rothblat and V.J. Cristofalo, Academic Press, New York.

Horwitz, A.F., Hatten, M.E., and Burger, M.M. (1974) Membrane Fatty Acid Replacement and Their Effect on Growth and Lectin-induced Agglutinability. Proc. Natl. Acad. Sci. USA 71: 3115-9.

Howard, B.V., Butler, J.D., and Bailery, J.M. (1973) In Tumor Lipids: Biochemistry and Metabolism, ed. R. Wood, American Oil Chemist's Society Press, Champaign, Ill, pp. 200-14.

Howard, B.V. and Howard, W.J. (1974) Lipid Metabolism in Cultured Cells. Adv. Lipid Res. 12: 51-96.

Hsia, J.C. and Boggs, J.M. (1972) Influenza of pH and Cholesterol on the Structure of Phosphatidylethanolamine Multibilayers. Biochim. Biophys. Acta 266: 18-25.

Hsia, J.C., Long, R.A., Hruska, F.E., and Gesser, H.D. (1972) Steroid-phosphatidylcholine Interactions in Oriented Multibilayers--A Spin Label Study. Biochim. Biophys. Acta 290: 22-31.

Hsia, J.C., Schneider, H., and Smith, I.C. (1970) A Spin Label Study of the Effects of Cholesterol in Liposomes. Chem. Phys. Lipids 4:238-42.

Hsia, J.C., Schneider, H., Smith, I.C. (1970) Spin Label Studies of Oriented Phospholipids: Egg Lecithin. Biochim. Biophys. Acta 202: 399-402.

Hsia, J.C., Schneider, H., and Smith, I.C.P. (1971) A Spin Label Study of the Influence of Cholesterol on Phospholipid Multibilayer Structures. Can. J. Biochem. 49: 614-22.



Hubbell, W.L. and McConnell, H.M. (1968) Spin Label Studies of the Excitable Membranes of Nerve and Muscle. Proc. Natl. Acad. Sci. USA 61: 12-6.

Hubbell, W.L. and McConnell, H.M. (1969) Motion of Steroid Spin Labels in Membranes. Proc. Natl. Acad. Sci. USA 63: 16-22.

Hubbell, W.L. and McConnell, H.M. (1969) Orientation and Motion of Amphiphilic Spin Labels in Membranes. Proc. Natl. Acad. Sci. USA 64: 20-7.

Hubbell, W.L. and McConnell, H.M. (1971) Molecular Motion in Spin-labeled Phospholipids and Membranes. J. Am. Chem. Soc. 93: 314-26.

Hui, S-W. and Parsons, D.F. (1976) Phase Transition of Plasma Membranes of Rat Hepatocyte and Hepatoma Cells by Electron Diffraction. Cancer Res. 36: 1918-22.

Hunt, R.C., Bullis, C.M., and Brown, J.C. (1975) Isolation of Concanavalin A Receptor From Mouse L-cells. Biochemistry 14: 109-15.

Inbar, M. (1976) Fluidity of Membrane Lipids: A Single Cell Analysis of Mouse Normal Lymphocytes and Malignant Lymphoma Cells. FEBS Lett. 67: 180-5.

Inbar, M. (1979) Membrane Fluidity and Cell Transformation. Abstracts of the 5th Meeting of the European Association for Cancer Research. Vienna, Austria, p. 35.

Inbar, M. and Ben-Bassat, H. (1976) Fluidity Differences in the Surface Membrane Core of Human Lymphoblastoid and Lymphoma Cell Lines. Int. J. Cancer 18: 293-7.

Inbar, M., Ben-Bassat, H., Huet, C., Oseroff, A.R., and Sacks, L. (1973) Inhibition of Lectin Agglutinability by Fixation of the Cell Surface Membrane. Biochim. Biophys. Acta. 311: 594-9.

Inbar, M. and Shinitzky, M. (1974) Increase of Cholesterol Level in the Surface Membrane of Lymphoma Cells and Its Inhibitory Effect on Ascites Tumor Development. Proc. Natl. Acad. Sci. USA 71: 2128-30.

Inbar, M., Yuli, I., and Raz, A. (1979) Contact-mediated Changes in the Fluidity of Membrane Lipids in Normal and Malignant Transformed Mammalian Fibroblasts. Exp. Cell Res. 105: 325-35.

- Israelachvilli, J., Sjosten, J., Erickson, G., Ehrstrom, L.E., Graslund, A., and Ehrenberg, A. (1974) Theoretical Analysis of the Molecular Motion of Spin Labels in Membranes. ESR Spectra of Labeled *Bacillus subtilis* Membranes. *Biochim. Biophys. Acta* 339: 164-72.
- Israelachvilli, J., Sjosten, J., Eriksson, G., Ehrstrom, M., Graslund, A., and Ehrenberg, A. (1975) ESR Spectral Analysis of the Molecular Motion of Spin Labels in Lipid Bilayers and Membranes Based on a Model in Terms of Two Angular Motional Parameters and Rotational Correlation Times. *Biochim. Biophys. Acta* 381: 125-41.
- Ito, T. and Ohnishi, S. (1974) Calcium (2+)-induced Lateral Phase Separation in Phosphatidic Acid-phosphatidylcholine Membranes. *Biochim. Biophys. Acta* 352: 29-37.
- Jackson, M.B. (1976) A  $\beta$ -coupled Gauche Kink Description of the Lipid Bilayer Phase Transition. *Biochemistry* 15: 2555-61.
- Jackson, M.B. and Cronan, J.E. (1978) An Estimate of the Minimum Amount of Fluid Lipid Required for the Growth of *Escherichia coli*. *Biochim. Biophys. Acta* 512: 472-9.
- Jackson, M.B. and Sturtevant, J.M. (1977) Studies of the Lipid Phase Transitions of *Escherichia coli* by High Sensitivity Differential Scanning Calorimetry. *J. Biol. Chem.* 252: 4749-51.
- Jacobs, R.E., Hudson, B., and Anderson, H.C. (1975) A Theory of the Chain Melting Phase Transition of Aqueous Phospholipid Dispersions. *Proc. Natl. Acad. Sci. USA* 72: 3993-7.
- Jacobsen, K. and Papahadjopoulos, D. (1975) Phase Transitions and Phase Separations in Phospholipid Membranes Induced by Changes in Temperature, pH, and Concentration of Bivalent Cations. *Biochemistry* 14: 152-61.
- Jain, M.K. (1973) Introduction to the Complexities of Membrane Structure. *J. Chem. Education* 50: 596-8.
- Jain, M.K. and Wagner, R.C. (1980) Introduction to Biological Membranes, John Wiley and Sons, New York.
- Johnson, A.C., McNabb, A.R., and Rossiter, R.J. (1948a) Lipids of Normal Brain. *Biochem. J.* 43: 573-7.

Johnson, A.C., McNabb, A.R., and Rossiter, R.J. (1948b) Lipids of Peripheral Nerve. *Biochem. J.* 43: 578-80.

Johnson, A.C., McNabb, A.R., and Rossiter, R.J. (1948c) Chemical Studies of Peripheral Nerve During Wallerian Degeneration. I. Lipids. *Biochem. J.* 45: 500-8.

Johnson, S.M. (1973) The Effect of Charge and Cholesterol on the Size and Thickness of Sonicated Phospholipid Vesicles. *Biochim. Biophys. Acta* 307: 27-41.

Johnson, S.M. and Robinson, R. (1979) The Composition and Fluidity of Normal and Leukaemic or Lymphomatous Lymphocyte Plasma Membranes in Mouse and Man. *Biochim. Biophys. Acta* 558: 282-95.

Jonas, A. (1977) Microviscosity of Lipid Domains in Human Serum Lipoproteins. *Biochim. Biophys. Acta* 486: 10-22.

Jonas, A., Krajnovich, N.J., and Paterson, B.W. (1977) Physical Properties of Isolated Complexes of Human and Bovine A-I Apolipoproteins with L- $\alpha$ -dimyristoyl Phosphatidylcholine. *J. Biol. Chem.* 252: 2200-5.

Jost, P.C., Griffith, O.H., Capaldi, R.A., and Vanderkooi, G. (1973) Evidence for Boundary Lipid in Membranes. *Proc. Natl. Acad. Sci. USA* 70: 480-4.

Jost, P., Libertini, L.J., Hebert, V.C., and Griffith, O.H. (1971) Lipid Spin Labels in Lecithin Multilayers. Motion Along Fatty Acid Chains. *J. Mol. Biol.* 59: 77-98.

Junge, W. (1972) Brownian Rotation of the Cytochrome Oxidase in the Mitochondrial Inner Membrane. *FEBS Lett.* 25: 109-12.

Junge, W. and Eckhoff, A. (1973) On the Orientation of Chlorophyll  $a_1$  in the Functional Membrane of Photosynthesis. *FEBS Lett.* 36: 207-12.

Kahlenberg, A., Walker, C., and Rohplick, R. (1974) Evidence for an Asymmetric Distribution of Phospholipids in the Human Erythrocyte Membrane. *Can. J. Biochim.* 52: 803-6.

Kaneko, I., Satoh, H., and Ukita, T. (1973) Effect of Metabolic Inhibitors on the Agglutination of Tumor Cells by Concanavalin A and Ricinus communis Agglutinin. *Biochem. Biophys. Res. Comm.* 50: 1087-94.

- Kanunaga, T. (1978) Neoplastic Transformation of Human Diploid Fibroblast Cells by Chemical Carcinogens. Proc. Natl. Acad. Sci. USA 75: 1334-8.
- Kaplan, J., Canonico, P.G., and Caspary, W.J. (1973) Electron Spin Resonance Studies of Spin-labeled Mammalian Cells by Defection of Surface-membrane Signals. Proc. Natl. Acad. Sci. USA 70: 66-70.
- Karnovsky, M.J. and Unanue, E.R. (1973) Mapping and Migration of Lymphocyte Surface Macromolecules. Fed. Proc. 32: 55-9.
- Karnovsky, M.J., Uranue, E.R., and Leventhal, M. (1972) Ligand-induced Movement of Lymphocyte Membrane Macromolecules. II. Mapping of Surface Moieties. J. Exp. Med. 136: 907-30.
- Kawanami, J., Tsuji, T., and Otsuka, H. (1966) Lipids of Cancer Tissues. I. Lipid Composition of Shionogi Carcinoma 115 and Nakahara-Fukuoka Sarcoma. Biochemistry (Japan) 59: 151-9.
- Keana, J.F.W., Lee, T.D., and Bernard, E.M. (1976) Side Chain Substituted 2,2,5,5-tetramethylpyrrolidine-N-oxyl (Proxyl) Nitroxides. A New Series of Lipid Spin Labels Showing Improved Properties for the Study of Biological Membranes. J. Am. Chem. Soc. 98: 3052-3.
- Kehry, M., Yguerabide, J., and Singer, S.J. (1977) Fluidity in the Membranes of Adult and Neonatal Human Erythrocytes. Science 195: 486-7.
- Keith, A.D., Sharnoff, M., and Cohn, G.E. (1973) A Summary and Evaluation of Spin Labels Used as Probes for Biological Membrane Structure. Biochim. Biophys. Acta 300: 379-419.
- Keith, A.D., Waggoner, A.S., and Griffith, O.H. (1968) Spin-labeled Mitochondrial Lipids in Neurospora crassa. Proc. Natl. Acad. Sci. USA 61: 819-26.
- Keough, K.M., Oldfield, E., and Chapman, D. (1973) Carbon-13 and Proton Nuclear Magnetic Resonance of Unsociated Model and Mitochondrial Membranes. Chem. Phys. Lipids 10: 37-50.
- Kerr, S.E., Kfoury, G.A., and Hoddad, F.S. (1964) A Comparison of the Polyphosphoinositide in Human and Ox Brain. Biochim. Biophys. Acta 84: 461.

- Kiessling, R., Petranyi, G., Klein, G., and Wigzell, V.H. (1976) Non T-cell Resistance Against a Mouse Moloney Lymphoma. *Inst. J. Cancer* 17: 275-81.
- Kimelberg, H.K. and Lee, C. (1969) Binding and Electron Transfer to Cytochrome c in Artificial Phospholipid Membranes. *Biochem. Biophys. Res. Comm.* 34: 784-90.
- Kimelberg, H.K. and Papahadjopoulos, D. (1974) Effects of Phospholipid Acyl Chain Fluidity, Phase Transitions and Cholesterol on  $(Na^+ + K^+)$  Stimulated Adenosine Triphosphatase. *J. Biol. Chem.* 249: 1071-80.
- King, M.E. and Spector, A.A. (1978) Effects of Specific Fatty Acid Enrichment on Membrane Physical Properties Detected With a Spin Label Probe. *J. Biol. Chem.* 253: 6493-501.
- King, M.E., Stavens, B.W., and Spector, A.A. (1977) Diet-induced Changes in Plasma Membrane Fatty Acid Composition Affect Physical Properties Detected With a Spin-label Probe. *Biochemistry* 16: 5280-5.
- Kleeman, W., Grant, C.W.M., and McConnell, H.M. (1974) Lipid Phase Separations and Protein Distribution in Membranes. *J. Supramol. Struct.* 2: 609-16.
- Kleeman, W. and McConnell, H.M. (1974) Lateral Phase Separations in E. coli Membranes. *Biochim. Biophys. Acta* 345: 220-30.
- Kleeman, W. and McConnell, H.M. (1976) Interactions of Proteins and Cholesterol With Lipids in Bilayer Membranes. *Biochim. Biophys. Acta* 219: 206-22.
- Klenk, H.D. and Choppin, P.W. (1969) Plasma Membrane Lipids and Parainfluenza Virus Assembly. *Virology* 40: 939-47.
- Klenk, H.D. and Choppin, P.W. (1970) Lipids of Plasma Membranes of Monkey and Hamster Kidney Cells and of Parainfluenza Virions Grown in These Cells. *Virology* 38: 255-68.
- Knowles, P.F., Marsh, D., and Rattle, H.W.E. (1976) Magnetic Resonance of Biomolecules. An Introduction to the Theory and Practice of NMR and ESR in Biological Systems. John Wiley and Sons, New York.

- Koizumi, K., Tamiya-Koizumi, K., Fujii, T., and Kojima, K. (1977) Phospholipids of Plasma Membranes Isolated From Rat Ascites Hepatomas and From Normal Rat Liver. *Cell Struct. Function* 2: 145-53.
- Koizumi, K., Tamiya-Koizumi, K., Fujii, T., Okuda, J., and Kojima, K. (1980) Comparative Study of the Phospholipid Composition of Plasma Membranes Isolated From Rat Primary Hepatomas Induced by 3'-methyl-4-dimethylaminobenzene and From Normal Growing Rat Livers. *Cancer Res.* 40: 909-13.
- Kornberg, R.D. and McConnell, H.M. (1971a) Lateral Diffusion of Phospholipids in a Vesicle Membrane. *Proc. Natl. Acad. Sci. USA* 68: 2564-8.
- Kornberg, R.D. and McConnell, H.M. (1971b) Inside-outside Transitions of Phospholipids in a Vesicle Membrane. *Biochemistry* 10: 1111-20.
- Kroon, P.A., Kainosho, M., and Chan, S.I. (1975) State of Molecular Motion of Cholesterol in Lecithin Bilayers. *Nature* 256: 582-4.
- Kourilsky, F.M., Silvestre, D., Neauport-Sautes, C., Loosfelt, Y., and Dausset, J. (1972) Antibody Induced Redistribution of HL-A Antigens at the Cell Surface. *Eur. J. Immunol.* 12: 249.
- Kruse, P.F. and Patterson, M.K. (1973) *Tissue Culture: Methods and Applications.* Academic Press, New York.
- Kutachi, H., Barenholz, Y., Ross, T.F., and Wermer, D.E. (1976) Developmental Changes in Plasma Membrane Fluidity in Chick Embryo Heart. *Biochim. Biophys. Acta* 436: 101-12.
- Ladbroke, B.D. and Chapman, D. (1969) Thermal Analysis of Lipids, Proteins, and Biological Membranes. Review and Summary of Some Recent Studies. *Chem. Phys. Lipids* 3: 304-56.
- Ladbroke, B.D., Williams, R.M., and Chapman, D. (1968) Studies on Lecithin-cholesterol-water Interactions by Differential Scanning Calorimetry and X-ray Diffraction. *Biochim. Biophys. Acta* 150: 333-40.
- Lagaly, G., Weiss, A., and Stuke, E. (1977) Effects of Double Bonds on Bimolecular Films in Membrane Models. *Biochim. Biophys. Acta* 470: 331-41.
- Lantos, P.L. (1979) *In Brain Tumors: Scientific Basis, Clinical Investigation and Current Therapy*, ed. D.G.I. Thomas and D. Graham, Butterworths, London, England.

Lantos, P.L. and Pilkington, G.J. (1979) The Development of Experimental Brain Tumors: A Sequential Light and Electron Microscope Study of the Subependymal Plate. I. Early Lesions (Abnormal Cell Clusters). *Acta Neuropath.* 45: 167-75.

Lanyi, J.K., Plachy, W.Z., and Kates, M. (1974) Lipid Interactions in Membranes of Extremely Halophilic Bacteria. II. Modification of Bilayer Structure by Squalene. *Biochemistry* 13: 4914-20.

Lee, A.G., Birdsall, N.J.M., Levine, Y.K., and Metcalfe, J.C. (1972) High Resolution Proton Relation Studies of Lecithins. *Biochim. Biophys. Acta* 255: 43-56.

Lee, A.G., Birdsall, N.J.M., and Metcalfe, J.C. (1974) Nuclear Magnetic Relaxation and the Biological Membrane. *In Methods in Membrane Biology*, vol. 2, ed. E.D. Korn, Plenum Press, New York, pp. 1-156.

LeGrimellec, C. and LeBlanc, G. (1978) Effect of Membrane Cholesterol on Potassium Transport in *Mycoplasma mycoides* vav. capri (P63). *Biochim. Biophys. Acta* 514: 152-63.

Lanaz, G., Curatola, G., and Masotti, L. (1975) Perturbation of Membrane Fluidity. *J. Bioenergetics* 7: 223-99.

Lenaz, G., Pasquali, P., Bertoli, E., Sechi, A.M., Parenti-Castelli, G., and Masotti, L. (1972) Effect of Protein Binding on Phospholipase C Hydrolysis of Aqueous Phospholipid Dispersions. *Biochem. Biophys. Res. Comm.* 49: 278-82.

Lenaz, G., Sechi, A.M., Masotti, L., and Castelli, G.P. (1969) Nonionic Interaction Between Proteins and Lipids in the Mitochondrial Membranes. *Biochem. Biophys. Res. Comm.* 34: 392-7.

Lesslauer, W., Cain, J.E., and Blasie, J.K. (1972) X-ray Diffraction Studies of Lecithin Bimolecular Leaflets With Incorporated Fluorescent Probes. *Proc. Natl. Acad. Sci. USA* 69: 1499-503.

Levanon, A., Kohn, A., and Inbar, M. (1977) Increase in Membrane Fluidity of Cellular Membranes Induced by Adsorption of RNA and DNA Virions. *J. Virol.* 22: 353-60.

Levine, Y.K. and Wilkins, M.H.F. (1971) Structure of Oriented Lipid Bilayers. *Nature (New Biology)* 230: 69-72.

- Linden, C.D., Blasie, J.K., and Fox, C.F. (1977) A Confirmation of the Phase Behavior of Escherichia coli Cytoplasmic Membrane Lipids by X-ray Diffraction. *Biochemistry* 16: 1621-5.
- Linden, C.D. and Fox, C.F. (1975) Membrane Physical State and Function. *Accounts Chem. Res.* 8: 321-7.
- Linden, C.D., Wright, K.L., McConnell, H.M., and Fox, C.F. (1973) Lateral Phase Separations in Membrane Lipids and the Mechanism of Sugar Transport in Escherichia coli. *Proc. Natl. Acad. Sci. USA* 70: 2271-5.
- Lindgren, A. (1976) Growth Characteristics and Gl Kinetics in Growth Control of Normal and Neoplastic Glia Cells in Culture. Ph.D. dissertation, *Acta Universitatis Upsaliensis*: 254.
- Lindgren, A., Westermarck, B., and Ponten, J. (1975) Serum Stimulation of Stationary Human Glia and Glioma Cells in Culture. *Exp. Cell Res.* 95: 311-9.
- Lippert, J.L. and Peticolas, W.L. (1972) Raman Active Vibrations in Long Chain Fatty Acids and Phospholipid Sonicates. *Biochim. Biophys. Acta* 282: 8-17.
- Loor, F. (1973) Lectin-induced Lymphocyte Agglutination: An Active Cellular Process. *Exp. Cell Res.* 82: 415-25.
- Lowry, O.H., Rosebrough, N.J., Farr, A.L., and Randall, R.L. (1951) Protein Measurement With the Folin-phenol Reagent. *J. Biol. Chem.* 193: 265-75.
- Lundberg, B. (1974) An X-ray and Vapour Pressure Study on Lecithin-cholesterol-water Interactions. *Acta Chem. Scand. B* 28: 673-6.
- Luzzati, V. (1968) X-ray Diffraction Studies of Lipid Water Systems. *In* *Biological Membranes*, vol. I, ed. D. Chapman, Academic Press, New York, pp. 71-121.
- MacFarlane, M.G., Gray, G.M., and Wheeldon, L.W. (1960) Fatty Acid Composition of Phospholipids From Subcellular Particles of Rat Liver. *Biochem. J.* 77: 626-31.
- MacKenzie, C.G., MacKenzie, J.B., and Reiss, O.K. (1964) Regulation of Cell Lipid Metabolism and Accumulation. III. The Lipid Content of Mammalian Cells and the Response to the Lipogenic Activity of Rabbit Serum. *Exp. Cell Res.* 36: 533-47.



MacPherson, I. (1965) Reversion in Hamster Cells Transformed by Rous Sarcoma Virus. *Science* 148: 1731-3.

MacPherson, I. (1966) Mycoplasmas in Tissue Culture. *J. Cell Science* 1: 145-68.

MacPherson, I. and Montagnier, I. (1964) Agar Suspension Culture for the Selective Assay of Cells Transformed by Polyoma Virus. *Virology* 23: 291-4.

Maldonado, R.L. and Blough, H.A. (1980) A Comparative Study of the Lipids of Plasma Membranes of Normal Cells and Those Infected and Transformed by Rous Sarcoma Virus. *Virology* 102: 62-70.

Marcelja, S. (1974) Chain Ordering in Liquid Crystals. II. Structure of Bilayer Membranes. *Biochim. Biophys. Acta* 367: 165-76.

Marsh, D. (1975) Spectroscopic Studies of Membrane Structure. *Essays Biochem.* 11: 139-80.

Marsh, D. (1980) Molecular Motion in Phospholipid Bilayers in the Gel Phase: Long Axis Rotation. *Biochemistry* 19: 1632-7.

Marsh, D. and Smith, I.C.P. (1973) An Interacting Spin Label Study of the Fluidizing and Condensing Effects of Cholesterol on Lecithin Bilayers. *Biochim. Biophys. Acta* 298: 133-44.

Martin, C.E. and Thompson, G.A., Jr. (1978a) Use of Fluorescence Polarization to Monitor Intracellular Membrane Changes During Temperature Acclimation. Correlation With Lipid Composition and Ultrastructural Changes. *Biochemistry* 17: 3581-6.

Mason, R.P. and Freed, J.H. (1974) Estimating Microsecond Rotational Correlation Times From Lifetime Broadening of Nitroxide Electron Spin Resonance Spectra Near the Rigid Limit. *J. Phys. Chem.* 78: 1321-3.

Mason, R.P. and Polnaszek, C.F. (1978) Spin-label and Deuterium Order Parameter Discrepancies in Bilayers: One Possible Explanation. *Biochemistry* 17: 1758-60.

Mason, R.P., Polnaszek, C.F., and Freed, J.H. (1974) Comments on the Interpretation of Electron Spin Resonance Spectra of Spin Labels Undergoing Very Anisotropic Rotational Reorientation. *J. Phys. Chem.* 78: 1324-9.

- Matthieu, J.M., Honegger, P., Favrod, P., Gautier, E., and Dolivo, M. (1979) Biochemical Characterization of a Myelin Fraction Isolated From Rat Brain Aggregating Cell Cultures. *J. Neurochem.* 32: 869-81.
- Maunoury, R. (1979) Establishment and Characterization of 5 Human Cell Lines Derived From a Series of 50 Primary Intracranial Tumors. *Acta Neuropath.* 39: 33-41.
- Maunoury, R., Delpech, A., Delpech, B., Vidard, M.N., and Vedrenna, C. (1976) Presence of Neurospecific Antigen NSAI in Fetal Human Astrocytes in Long Term Culture. *Brain Res.* 112: 383-7.
- Maziere, C., Maziere, J.C., and Polonovski, J. (1980) Fatty Acid Composition and Metabolism in Normal and SV40 Transformed Hamster Fibroblasts. *Biochimie* 62: 283-5.
- McAlister, J. Yathindra, N., and Sundaralingam, M. (1973) Potential Energy Calculations on Phospholipids. Preferred Conformations With Intramolecular Stacking and Mutually Tilted Hydrocarbon Chains. *Biochemistry* 12: 1189-95.
- McAllister, R.M., Issacs, H., and Rongey, R. (1977) Establishment of a Human Medulloblastoma Cell Line. *Int. J. Cancer* 20: 206-12.
- McAllister, R.M. and MacPherson, I. (1969) Transformation of Rat Embryo Cells by Adenovirus Type 1. *J. Gen. Virol.* 4: 29-36.
- McAllister, R.M. and Reed, G. (1968) Growth Control in Agar of Cells Derived From Neoplastic and Non-neoplastic Tissues of Children. *Pediatr. Res.* 2: 356-60.
- McCabe, P.J. and Green, C. (1977) The Dispersion of Cholesterol With Phospholipids and Glycolipids. *Chem. Phys. Lipids* 20: 319-30.
- McConnell, H.M. and McFarland, B.G. (1970) Physics and Chemistry of Spin Labels. *Quart. Rev. Biophys.* 3: 91-136.
- McConnell, H.M. and McFarland, B.G. (1972) The Flexibility Gradient in Biological Membranes. *Ann. N.Y. Acad. Sci.* 195: 207-17.
- McConnell, H.M., Wright, K.L., and McFarland, B.G. (1972) The Fraction of Lipid in a Biological Membrane That is in the Fluid State: A Spin Label Assay. *Biochem. Biophys. Res. Comm.* 47: 273-81.

- McElhaney, R.N. (1974) The Effect of Alterations in the Physical State of the Membrane Lipids on the Ability of Acholeplasma laidlawii B to Grow at Various Temperatures. J. Mol. Biol. 84: 145-57.
- McElhaney, R.N., de Gier, J., and van der Neut-kok, E.C.M. (1973) The Effect of Alterations in Fatty Acid Composition and Cholesterol Content on the Nonelectrolyte Permeability of Acholeplasma laidlawii B Cells and Derived Liposomes. Biochim. Biophys. Acta 298: 500-12.
- McFarland, B.G. (1972) The Molecular Basis of Fluidity in Membranes. Chem. Phys. Lipids 8: 303-13.
- McFarland, B.G. and McConnell, H.M. (1971) Bent Fatty Acid Chains in Lecithin Bilayers. Proc. Natl. Acad. Sci. USA 68: 1274-8.
- McReynolds, W.O. (1970) Characterization of Some Liquid Phases. J. Chromatographic Science 8: 685-91.
- Melichor, D.L., Morowitz, N.J., Sturtevant, J.M., and Tsong, T.Y. (1970) Characterization of the Plasma Membrane of Mycoplasma laidlawii. VII. Phase Transitions of Membrane Lipids. Biochim. Biophys. Acta 219: 114-22.
- Mely-Goubert, B., Calvo, F., and Rosenfeld, C. (1979) Does Fluorescence Polarization Reveal Fluidity or Membrane Protein Changes? Abstracts of the 5th Meeting of the European Association for Cancer Research, Vienna, Austria, p. 35.
- Mely-Goubert, B. and Freedman, M.H. (1980) Lipid Fluidity and Membrane Protein Monitoring Using 1,6-diphenyl-1,3,5-hexatriene. Biochim. Biophys. Acta 601: 315-27.
- Metcalfe, J.C., Birdsall, N.J.M., and Lee, A.G. (1972) <sup>13</sup>C NMR Spectra of Acholeplasma Membranes Containing <sup>13</sup>C Labelled Phospholipids. FEBS Lett. 21: 335-40.
- Michaelson, D.M., Horwitz, A.F., and Klein, M.P. (1973) Transbilayer Asymmetry and Surface Homogeneity of Mixed Phospholipids in Cosonicated Vesicles. Biochemistry 12: 2637-45.
- Michaelson, D.M., Horwitz, A.F., and Klein, M.P. (1974) Head Group Modulation of Membrane Fluidity in Sonicated Phospholipid Dispersions. Biochemistry 13: 2605-12.

- Micklem, K.J., Abra, R.M., Knutton, S., Graham, J.M., and Pasternak, C.A. (1976) The Fluidity of Normal and Virus-transformed Cell Plasma Membrane. *Biochem. J.* 154: 561-6.
- Mitchell, R.F. (1969) The Lipid Content of Mitochondria From Transplantable Animal Tumors. *Biochim. Biophys. Acta* 176: 764-73.
- Montagnier, I. (1970) Alterations de la Surface Cellulaire Induites par des Virus Oncogenes et Leur Role Dans le Transformation Maligne. *Bull. Cancer* 57: 13-22.
- Montagnier, L. (1971) Factors Controlling the Multiplication of Untransformed and Transformed BHK21 Cells Under Various Environmental Conditions. *In Growth Control in Cell Cultures*, Ciba Symposium, ed. G.E.W. Wölstenholme and J. Knight, Churchill-Livingston, London, England, pp. 33-41.
- Montagnier, L., MacPherson, I., and Jarrett, O. (1966) An Epithelial Variant of the BHK21 Hamster Fibroblast Line and Its Transformation by Polyoma Virus. *J. Natl. Cancer Inst.* 36: 503-12.
- Montesano, R., Drevon, C., Kuroki, T., Saint Vincent, L., Handleman, S., Sanford, K.K., DeFreo, D., and Weinstein, I.B. (1977) Test for Malignant Transformation of Rat Liver Cells in Culture: Cytology, Growth in Soft Agar, and Production of Plasminogen Activator. *J. Natl. Cancer Inst.* 59: 1651-7.
- Morrison, W.R. and Smith, L.M. (1964) Preparation of Fatty Acid Methyl Esters and Dimethylacetals From Lipids With Boron Trifluoride-methanol. *J. Lipid Res.* 5: 600-8.
- Nagle, J.F. (1973) Lipid Bilayer Phase Transition: Density Measurements and Theory. *Proc. Natl. Acad. Sci. USA* 70: 3443-4.
- Nayyar, N. (1963) A Study of Phosphate, Desoxyribonucleic Acid and Phospholipid Fractions in Neural Tumors. *Neurology* 13: 287-91.
- Neal, M.J., Bulter, K.W., Polnaszek, C.F., and Smith, I.C.P. (1976) The Influence of Anesthetics and Cholesterol on the Degree of Molecular Organization and Mobility of Ox Brain White Matter. *Mol. Pharmacol.* 12: 144-55.
- Nelson, G.J. (1975) Isolation and Purification of Lipids From Animal Tissues. *In Analysis of Lipids and Lipoproteins*, ed. E.G. Perkins, American Oil Chemist's Society, Champaign, Ill., pp. 1-22.

Newman, G.C. and Huang, C. (1975) Structural Studies on Phosphatidylcholine-cholesterol Mixed Vesicles. *Biochemistry* 14: 3363-70.

Nicolau, C., Dietrich, C., Steiner, M.R., Steiner, S., and Melnick, J.L. (1975)  $^1\text{H}$  and  $^{13}\text{C}$  Nuclear Magnetic Resonance Spectra of the Lipids in Normal and SV40 Virus Transformed Hamster Embryo Fibroblast Membranes. *Biochim. Biophys. Acta* 382: 311-21.

Nicolau, C., Hildenbrand, K., Reimann, A., Johnson, S., Vaheri, A., and Friis, R.R. (1978) Membrane Lipid Dynamics and Density Dependent Growth Control in Normal and Transformed Avian Cells. *Exp. Cell Res.* 113: 63-73.

Nicolson, G.L. (1971) Difference in the Topology of Normal and Tumor Cell Membranes as Shown by Different Distributions of Ferritin-conjugated Concanavalin A on Their Surfaces. *Nature (New Biology)* 233: 244-6.

Nicolson, G.L. (1977) In *Dynamic Aspect of Cell Surface Organization*, ed. G. Poste and G.L. Nicolson, North Holland Publishing Co., New York.

Nicolson, G.L. and Singer, S.J. (1971) Ferritin-conjugated Plant Agglutinins as Specific Saccharide Stains for Electron Microscopy: Application to Saccharides Bound to Cell Membranes. *Proc. Natl. Acad. Sci. USA* 68: 942-5.

Nicolson, G.L. and Singer, S.J. (1974) The Distribution and Asymmetry of Mammalian Cell Surface Saccharides Utilizing Ferritin Conjugated Plant Agglutinins as Specific Saccharide Stains. *J. Cell Biol.* 60: 236-48.

Nicolson, G.L. and Yanagimachi, R. (1974) Mobility and Restriction of Plasma Membrane Lectin-Binding Components. *Science* 184: 1294-6.

Niederberger, W. and Seelig, J. (1974) Deuterium-magnetische Resonanz-spektroskopie an Spezifisch Deuterierten Flüssigen Kristallen. *Ber. Bunsenges. Physik. Chem.* 78: 947-9.

Niederberger, W. and Seelig, J. (1976) Phosphorus-31 Chemical Shift Anisotropy in Unsonicated Phospholipid Bilayers. *J. Am. Chem. Soc.* 98: 3704-6.

Nieva-Gomez, D. and Gennis, R.B. (1977) Affinity of Intact Escherichia coli for Hydrophobic Membrane Probes is a Function of the Physiological State of the Cells. *Proc. Natl. Acad. Sci. USA* 74: 1811-5.

- Nikolesev, V., Resch, E.A., and Meszaros, J. (1974) Phospholipids and Their Fatty Acid Content in Normal Human Embryonic Brain Tissue. *Steroids Lipids Res.* 5: 123-32.
- Nilsson, O. and Dallner, G. (1975) Distribution of Constitutive Enzymes and Phospholipids in Microsomal Membranes of Rat Liver. *FEBS Lett.* 58: 190-3.
- Nilsson, O.S. and Dallner, G. (1977) Transverse Asymmetry of Phospholipids in Subcellular Membranes of Rat Liver. *Biochim. Biophys. Acta* 464: 453-8.
- Nilsson, O.S. and Dallner, G. (1977) Enzyme and Phospholipid Asymmetry in Liver Microsomal Membranes. *J. Cell Biol.* 72: 568-83.
- Noonan, K.D. and Burger, M.M. (1973) Binding of [<sup>3</sup>H] Concanavalin A to Normal and Transformed Cells. *J. Biol. Chem.* 248: 4286-92.
- Noonan, K.D. and Burger, M.M. (1974) Role of the Cell Surface in Contact Inhibition of Cell Division. *Prog. Surf. Membrane Sci.* 8: 245-84.
- O'Brien, J.S. and Sampson, E.L. (1965) Lipid Composition of the Normal Human Brain: Gray Matter, White Matter, and Myelin. *J. Lipid Res.* 6: 537-44.
- O'Brien, J.S. and Sampson, E.L. (1965) Fatty Acid and Fatty Aldehyde Composition of the Major Brain Lipids in Normal Human Gray Matter, White Matter, and Myelin. *J. Lipid Res.* 6: 545-611.
- Ohnishi, S. and Ito, T. (1973) Clustering of Lecithin Molecules in Phosphatidylserine Membranes Induced by Calcium Binding to Phosphatidylserine. *Biochem. Biophys. Res. Comm.* 51: 132-8.
- Ohnishi, S. and Ito, T. (1974) Calcium-induced Phase Separations in Phosphatidylserine-phosphatidylcholine Membranes. *Biochemistry* 13: 881-7.
- Oldfield, E., Chapman, D., and Derbyshire, W. (1971) Deuteron Resonance: A Novel Approach to the Study of Hydrocarbon Chain Mobility in Membrane Systems. *FEBS Lett.* 16: 102-4.
- Oldfield, E., Chapman, D., and Derbyshire, W. (1972) Lipid Mobility in Acholeplasma Membranes Using Deuteron Magnetic Resonance. *Chem. Phys. Lipids* 9: 69-81.

Onsager, L. (1970) In Physical Principles in Biological Membranes, ed. F. Snell, J. Wolken, G. Inverson, and J. Lam, Gordon and Breach, New York, p. 137.

Op der Kamp, J.A.F. (1979) Lipid Asymmetry in Membranes. Ann. Rev. Biochem. 48: 47-71.

Oppenheimer, S.B., Bales, B.L., Brenneman, G., Knapp, L., Lesin, E.S., Neri, A., and Pollock, E.G. (1977) Modulation of Agglutinability by Alteration of the Surface Topography in Mouse Ascites Tumor Cells. Exp. Cell Res. 105: 291-300.

Oseroff, A.R., Robbins, P.W., and Burger, M.M. (1973) The Cell Surface Membrane: Biochemical Aspects and Biophysical Probes. Ann. Rev. Biochem. 42: 647-82.

Overath, P., Brenner, M., and Gulick-Krzywicki, T. (1975) Lipid Phase Transitions in Cytoplasmic and Outer Membranes of Escherichia coli. Biochim. Biophys. Acta 389: 358-69.

Overath, P. and Trouble, H. (1973) Phase Transitions in Cells, Membranes, and Lipids of Escherichia coli. Detection by Fluorescent Probes, Light Scattering and Dilatometry. Biochemistry 12: 2625-34.

Ozanne, B. and Sambrook, J. (1971) Binding of Radioactively Labeled Concanavalin A and Wheat Germ Agglutinin to Normal and Virus-transformed Cells. Nature (New Biology) 232: 156-60.

Papahadjopoulos, D. (1968) Surface Properties of Acidic Phospholipids: Interaction of Monolayers and Hydrated Liquid Crystals With Uni- and Bivalent Metal Ions. Biochim. Biophys. Acta 163: 240-54.

Papahadjopoulos, D., Hui, S., Vail, W.J., and Poste, G. (1976) Studies on Membrane Fusion. I. Interactions of Pure Phospholipid Membranes and the Effect of Fatty Acids (Myristic Acid), Lysolecithin, Proteins, and Dimethylsulfoxide. Biochim. Biophys. Acta 448; 245-64.

Papahadjopoulos, D. and Miller, N. (1967) Phospholipid Model Membranes. I. Structural Characteristics of Hydrated Liquid Crystals. Biochim. Biophys. Acta 135: 624-38.

Papahadjopoulos, D. and Kimelberg, H.K. (1973) Phospholipid Vesicles (Liposomes) as Models for Biological Membranes: Their Properties and Interactions With Cholesterol and Protein. In Progress in Surface Science, ed. S.G. Davison, vol. 3, Pergamon Press, Oxford, England, pp. 141-232.

- Papahadjopoulos, D. and Poste, G. (1975) Calcium-induced Phase Separation and Fusion in Phospholipid Membranes. *Biophys. J.* 15: 945-8.
- Papahadjopoulos, D., Poste, G., and Schaeffer, B.E. (1973) Fusion of Mammalian Cells by Unilamellar Lipid Vesicles. Influence of Lipid Surface Charge, Fluidity, and Cholesterol. *Biochim. Biophys. Acta* 232: 23-8.
- Papahadjopoulos, D., Vail, W., Pangborn, W.A., and Poste, G. (1976) Studies of Membrane Fusion. II. Induction of Fusion in Pure Phospholipid Membranes by Calcium Ions and Other Divalent Metals. *Biochim. Biophys. Acta* 448: 265-83.
- Parola, A., Robbins, P.W., and Blout, E.R. (1976) Nanosecond Fluorescence Lifetime and Anisotropy Studies of Membrane Lipids of 3T3 Cells. *Israel J. Med. Sci.* 12: 1362.
- Pasternak, C.A. (1972) Relief From Contact Inhibition. Early Increase in Phospholipid Turnover. *J. Cell Biol.* 53: 231-4.
- Pasternak, C.A. (1973) Phospholipid Turnover in Normal and Cancer Cells. *In Tumor Lipids: Biochemistry and Metabolism*, ed. R. Wood, American Oil Chemist's Society Press, Champaign, Ill., pp. 66-74.
- Pasternak, C.A. and Bergeron, J.J.M. (1970) Turnover of Mammalian Phospholipids. Stable and Unstable Components in Neoplastic Mast Cells. *Biochem. J.* 119: 473-80.
- Pasternak, C.A. and Friedrichs, B. (1970) Turnover of Mammalian Phospholipids. Rates of Turnover and Metabolic Heterogeneity in Cultures Human Lymphocytes and in Tissues of Healthy, Starved, and Vitamin A-deficient Rats. *Biochem. J.* 119: 481-8.
- Paul, D., Henahan, M., and Walter, S. (1974) Changes in Growth Control and Growth Requirements Associated With Neoplastic Transformation In Vitro. *J. Natl. Cancer Inst.* 53: 1499-503.
- Pauling, L. (1942) *The Nature of the Chemical Bond*. Cornell University Press, Ithaca, N.Y.
- Perdue, J.F., Kletzien, R., and Miller, K. (1971) The Isolation and Characterization of Plasma Membranes From Cultured Cells. I. The Chemical Composition of Membrane Isolated From Uninfected and Oncogenic RNA Virus-converted Chick Embryo Fibroblasts. *Biochim. Biophys. Acta* 249: 419.



- Perdue, J.F., Kletzien, R., and Wray, V.L. (1972) The Isolation and Characterization of Plasma Membrane From Cultured Cells. IV. The Carbohydrate Composition of Membranes Isolated From Oncogenic RNA Virus-converted Chick Embryo Fibroblasts. *Biochim. Biophys. Acta* 266: 505-10.
- Perdue, J.F., Warner, D., and Miller, K. (1973) The Isolation and Characterization of Plasma Membranes From Cultured Cells. V. The Chemical Composition of Plasma Membranes Isolated From Chicken Tumors Initiated With Virus-transformed Cells. *Biochim. Biophys. Acta* 298: 817-26.
- Perkins, R.G. and Scott, R.E. (1978) Differences in the Phospholipid, Cholesterol, and Fatty Acyl Composition of 3T3 and SV3T3 Plasma Membranes. *Lipids* 13: 653-7.
- Pessin, J.E., Salter, D.W., and Glaser, M. (1978) Use of a Fluorescent Probe to Compare the Plasma Membrane Properties in Normal and Transformed Cells. Evaluation of the Interference by Triacylglycerols and Alkyldiacylglycerols. *Biochemistry* 17: 1997-2004.
- Peterson, N.O. and Chan, S.I. (1977) More on the Motional State of Lipid Bilayer Membranes. Interpretation of Order Parameters Obtained From Nuclear Magnetic Resonance Experiments. *Biochemistry* 16: 2657-67.
- Petricciani, J.C., Wallace, R.E., and McCoy, D.W. (1974) A Comparison of Three In Vivo Assays for Cell Tumorigenicity. *Cancer Res.* 34: 105-8.
- Philips, B. and Gazet, J.C. (1968) Effect of Antilymphocyte Serum on the Growth of HEp-2 and HeLa Cells in Mice. *Nature* 220: 1140-1.
- Phillips, M.C. (1972) Physical State of Phospholipids and Cholesterol in Monolayers, Bilayers, and Membranes. *Progr. Surf. Membrane Sci.* 5: 139-221.
- Phillips, M.C. and Chapman, D. (1968) Monolayer Characteristics of 1,2 Diacylphosphatidylcholines (Lecithins) and Phosphatidylethanolamines at Air-water Interface. *Biochim. Biophys. Acta* 163: 301-13.
- Phillips, M.C., Ladbroke, B.D., and Chapman, D. (1970) Molecular Interactions in Mixed Lecithin Systems. *Biochim. Biophys. Acta* 196: 35-44.

- Phillips, M.C., Williams, R.M., and Chapman, D. (1969) On the Nature of Hydrocarbon Chain Motions in Lipid Liquid Crystals. *Chem. Phys. Lipids* 3: 234-44.
- Pilkington, G.J. and Lantos, P.L. (1979) The Development of Experimental Brain Tumors. A Sequential Light and Electron Microscope Study of the Subependymal Plate. II. Microtumors. *Acta Neuropathol.* 45: 177-85.
- Pink, D.A. and Zuckermann, M.J. (1980) Lipid Chain Order in Acholeplasma laidlawii Membranes. What Does  $^2\text{H}$  NMR Tell US? *FEBS Lett.* 109: 5-8.
- Pinto da Silva, P. and Branton, D. (1972) Membrane Intercalated Particles: The Plasma Membrane as a Planar Fluid Domain. *Chem. Phys. Lipids* 8: 265-78.
- Pluschke, G., Hirota, Y., and Overath, P. (1978) Function of Phospholipids in Escherichia coli. Characterization of a Mutant Deficient in Cardiolipin Synthesis. *J. Biol. Chem.* 253: 5048-55.
- Pollack, R., Risser, R., Conlon, S., Freedman, V., Shin, S., and Rifkin, D.B. (1975) Production of Plasminogen Activator and Colonial Growth in Semisolid Medium Are In Vitro Correlates of Tumorigenicity in the Immune-deficient Nude Mouse. In *Proteases and Biological Control*, ed. E. Reich, D. Rifkin, and E. Shaw, Cold Spring Harbor Conferences on Cell Proliferation, vol. 2, Cold Spring Harbor Laboratory, pp. 885-99.
- Polnaszek, C.F. and Freed, J.H. (1975) Electron Spin Resonance Studies of Anisotropic Ordering, Spin Relaxation, and Slow Tumbling in Liquid Crystalline Solvents. *J. Phys. Chem.* 79: 2283-306.
- Ponten, J. (1975) Neoplastic Human Glia Cells in Culture. In Human Tumor Cells In Vitro, ed. J. Fogh, Plenum Press, New York, pp. 175-206.
- Poo, M.M. and Cone, R.A. (1974) Lateral Diffusion of Rhodopsin in the Photoreceptor Membrane. *Nature* 247: 438.
- Porter, K.R., Toderò, G.J., and Fonte, V. (1973) A Scanning Electron Microscope Study of Surface Features of Viral and Spontaneous Transformants of Mouse Balb/3T3 Cells. *J. Cell Biol.* 59: 633-42.

- Pritchard, O.J., Clayton, R.M., and de Pomerat, D.I. (1978) Transdifferentiation of Chicken Neural Retina into Lens and Pigment Epithelium in Culture: Controlling Influences. *J. Embryol. Exp. Morphol.* 48: 1-21.
- Prives, J. and Shinitzky, M. (1977) Increased Membrane Fluidity Precedes Fusion of Muscle Cells. *Nature* 268: 761-3.
- Quintanilha, A.T. and Packer, L. (1977) Surface Localization of Sites of Reduction of Nitroxide Spin-labeled Molecules in Mitochondria. *Proc. Natl. Acad. Sci. USA* 74: 570-4.
- Raff, M.C. and DePetris, S. (1973) Movement of Lymphocyte Surface Antigen and Receptors: The Fluid Nature of the Lymphocyte Plasma Membrane and Its Immunological Significance. *Fed. Proc.* 32: 48-54.
- Raison, J.K., Lyons, J.M., Mehlhorn, R.J., and Keith, A.D. (1971) Temperature-induced Phase Changes in Mitochondrial Membranes Detected by Spin-labeling. *J. Biol. Chem.* 246: 4036-40.
- Rand, R.P. and Luzzati, V. (1968) X-ray Diffraction Study in Water of Lipids Extracted From Human Erythrocytes: The Position of Cholesterol in the Lipid Lamellae. *Biophys. J.* 8: 125-37.
- Randall, L.O. (1940) Lipid Composition of Intracranial Tumors. *Am. J. Cancer* 38: 92-4.
- Rao, K.V.S., Polnaszek, C.F., and Freed, J.H. (1977) Electron Spin Resonance Studies of Anisotropic Ordering, Spin Relaxation and Slow Tumbling in Liquid Crystalline Solvents 2. *J. Phys. Chem.* 81: 449-56.
- Razi-Naqui, K., Gonzales-Rodriguez, J., Cherry, R.J., and Chapman, D. (1973) Spectroscopic Technique for Studying Protein Rotation in Membranes. *Nature (New Biology)* 245: 249-51.
- Razin, S. (1975) The Mycoplasma Membrane. *Progr. Surf. Membrane Sci.* 9: 257-312.
- Reiber, H. (1978) Cholesterol-lipid Interactions in Membranes. The Saturation Concentration of Cholesterol in Bilayers of Various Lipids. *Biochim. Biophys. Acta* 512: 72-83.

- Reid, R.V. and Vaida, M.L. (1972) Quadrupole Moment of the Deuteron. *Phys. Rev. Lett.* 29: 494-6.
- Reinert, J.C. and Steim, J.M. (1970) Calorimetric Detection of a Membrane-lipid Phase Transition in Living Cells. *Science* 168: 1580-2.
- Renooij, W., Van Golde, M.G., Zwaal, R.F.A., and van Deenen, L.L.M. (1976) Topological Asymmetry of Phospholipid Metabolism in Rat Erythrocyte Membranes. Evidence for Flip-flop of Lecithin. *Eur. J. Biochem.* 61: 53-8.
- Rey, P. and McConnell, H.M. (1977) Clusterin of Nitroxide Spin Labels in Lipid Bilayer Membranes. *J. Am. Chem. Soc.* 99: 1637-42.
- Rigaud, J.L., Gary-Bobo, C.M., and Lange, Y. (1972) Diffusion Processes in Lipid-water Lamellar Phases. *Biochim. Biophys. Acta* 266: 72-84.
- Rittenhouse, H.G., Williams, R.E., Wisnieski, B.J., and Fox, C.F. (1974) Alterations of Characteristic Temperatures for Lecithin Interactions in LM Cells With Altered Lipid Composition. *Biochem. Biophys. Res. Comm.* 58: 222-8.
- Robbins, J.C. and Nicolson, G.L. (1975) Surfaces of Normal and Transformed Cells. *In Cancer: A Comprehensive Treatise. Biology of Tumors: Surfaces, Immunology, and Comparative Pathology*, vol. 4, ed. H. Becker, Plenum Press, New York, pp. 3-54.
- Robert, J., Mandel, P., and Rebel, G. (1976) Neutral Lipids and Phospholipids From Cultured Astroblasts. *J. Neurochem.* 26: 771-7.
- Robert, J., Mandel, P., and Rebel, G. (1979) Membrane Lipids in Bromodeoxyuridine-differentiated Astroglial Cells in Culture. *Lipids* 14: 852-9.
- Robertson, J.D. (1959) The Ultrastructure of Cell Membranes and Their Derivatives. *Biochem. Soc. Symp. (Cambridge)* 16: 1-43.
- Roelofsen, B., Zwaal, R.F.A., Comfuricus, P., Woodward, C. B., and van Deenen, L.L.M. (1971) Action of Pure Phospholipase A<sub>2</sub> and Phospholipase C on Human Erythrocytes and Ghosts. *Biochim. Biophys. Acta* 241: 925-9.
- Rohrschneider, G. (1975) *In Gas Chromatographic Applications in Microbiology and Medicine*, ed. B.M. Mitruka, John Wiley and Sons, New York, pp. 42-4.

- Rosenfeld, C., Jasmin, C., Mathe, G., and Inbar, M. (1979) Dynamic and Composition of Cellular Membranes and Serum Lipids in Malignant Disorders. *Recent Results Cancer Res.* 678: 62-77.
- Rosenthal, S.L., Parola, A.H., Blout, E.R., and Davidson, R.L. (1978) Membrane Alterations Associated With "Transformation" by BUdR in BUdR-dependent Cells. *Exp. Cell Res.* 112: 419-29.
- Rothblat, G.H. (1969) Lipid Metabolism in Tissue Culture Cells. *Adv. Lipid Res.* 7: 135-63.
- Rothblat, G.H. (1972) Cellular Sterol Metabolism. In *Growth, Nutrition and Metabolism in Cells in Culture*, vol. 1, ed. G. Rothblat and V. Cristafalo, Academic Press, New York, pp. 297-325.
- Rothblat, G.H. and Kritchevsky, D. (eds.) (1967) *Lipid Metabolism in Tissue Culture Cells*, The Wistar Institute Press, Philadelphia.
- Rothman, J.E. and Lenard, J. (1977) Membrane Asymmetry. *Science* 195: 743-53.
- Rottem, S. (1980) Membrane Lipids of Mycoplasma. *Biochim. Biophys. Acta* 604: 65-90.
- Rottem, S., Carillo, V.P., DeKruyff, B., Shinitzky, Y., and Razin, S. (1973) Cholesterol in Mycoplasma Membranes. Correlation of Enzymatic and Transport Activities With Physical State of Lipids in Membranes of Mycoplasma mycoides var. capri Adapted to Grow With Low Cholesterol Concentrations. *Biochim. Biophys. Acta* 323: 509-19.
- Rottem, S. and Greenberg, A.S. (1975) Changes in Composition, Biosynthesis and Physical State of Membrane Lipids Occurring Upon Aging of Mycoplasma hominis Cultures. *J. Bacteriol.* 121: 631-9.
- Rottem, S., Hasin, M., and Razin, S. (1973) Differences in Susceptibility to Phospholipase C of Free and Membrane-bound Phospholipids of Mycoplasma hominis. *Biochim. Biophys. Acta* 323: 520-31.
- Rottem, S. and Leive, L. (1977) Effect of Variations in Lipopolysaccharide on the Fluidity of the Outer Membrane of Escherichia coli. *J. Biol. Chem.* 252: 2077-81.

Rottem, S. and Samuni, A. (1973) Effects of Proteins on the Motion of Spin-labeled Fatty Acids in Mycoplasma Membranes. *Biochim. Biophys. Acta* 298: 32-8.

Rottem, S., Yashouv, J., Ne'eman, Z., and Razin, S. (1973) Cholesterol in Mycoplasma Membranes. Composition, Ultrastructure and Biological Properties of Membranes From Mycoplasma mycoides var. capri Cells Adapted to Grow With Low Cholesterol Concentrations. *Biochim. Biophys. Acta* 323: 495-508.

Rouser, G., Bauman, A.J., Kritehevsky, G., Heller, D., and O'Brien, J.S. (1961) Quantitative Chromatographic Fractionation of Complex Lipid Mixtures: Brain Lipids. *J. Am. Oil Chem. Soc.* 38: 544-55.

Rouser, G., Kritchevsky, G., and Yamamoto, A. (1967) Column Chromatographic and Associated Procedures for Separation and Determination of Phosphatides and Glycolipids. In *Lipid Chromatographic Analysis*, vol. 1, ed. G.V. Marinetti.

Rubin, H. (1966) A Substance in Conditioned Medium Which Enhances the Growth of Small Numbers of Chick Embryo Cells. *Exp. Cell Res.* 41: 138-48.

Rubinstein, L.J. (1972) Cytogenesis and Differentiation of Primitive Central Neuroepithelial Tumors. *J. Neuropath. Exp. Neurol.* 31: 7-26.

Rubsamen, H., Barald, P., and Podleski, T. (1976) A Specific Decrease of the Fluorescence Depolarization of Perylene in Muscle Membranes From Mice With Muscular Dystrophy. *Biochim. Biophys. Acta* 455: 767-79.

Rudell, L.L. and Morris, M.D. (1973) Determination of Cholesterol Using O-phthalaldehyde. *J. Lipid Res.* 14: 364-6.

Rudy, B. and Gilter, C. (1972) Microviscosity of the Cell Membrane. *Biochim. Biophys. Acta* 288: 231-6.

Ruggieri, S. and Fallani, A. (1968) Lipid Composition of Cytoplasmic Fractions From Rat Liver and From Yoshida Ascites Hepatoma. *Lo Sperimentale* 118: 313-35.

Rule, G.S., Kruuv, J., and Lepock, J.R. (1979) Membrane Lipid Fluidity as Rate Limiting on the Concanavalin A-mediated Agglutination of pyBHK Cells. *Biochim. Biophys. Acta* 556: 399-407.

- Rygaard, J. and Poulsen, C.O. (1969) Heterotransplantation of a Human Malignant Tumor to "Nude" Mice. *Acta Pathol. Microbiol. Scand.* 77: 758-60.
- Saito, Y. and McElhaney, R.N. (1977) Membrane Lipid Biosynthesis in Acholeplasma laidlawii B: Incorporation of Exogenous Fatty Acids into Membrane Glyco- and Phospholipids by Growing Cells. *J. Bacteriol.* 132: 485-96.
- Sandra, A. and Pagano, R.E. (1978) Phospholipid Asymmetry in LM Cell Plasma Membrane Derivatives: Polar Head Group and Acyl Chain Distributions. *Biochemistry* 17: 332-8.
- Sauerheber, R.D. Gordon, L.M., Crosland, R.D., and Kuwahara, M.D. (1977) Spin Label Studies on Rat Liver and Heart Plasma Membranes: Do Probe-probe Interactions Interfere With the Measurement of Membrane Properties. *J. Membrane Biol.* 31: 131-69.
- Sauerheber, R.D., Zimmermann, T.S., Esgate, J.A., Vanderlaan, W.P., and Gordon, L.M. (1980) Effects of Calcium, Lanthanum, and Temperature on the Fluidity of Spin-labeled Human Platelets. *J. Membrane Biol.* 52: 201-19.
- Scandella, C.J., Devaux, P., and McConnell, H.M. (1972) Rapid Lateral Diffusion of Phospholipids in Rabbit Sarco-plasmic Reticulum. *Proc. Natl. Acad. Sci. USA* 69: 2056-60.
- Scandella, C.J., Hayward, J.A., and Lee, N. (1979) Cholesterol Levels and Plasma Membrane Fluidity in 3T3 and SV101-3T3 Cells. *J. Supramol. Struct.* 11: 477-83.
- Schechter, E., Gulik-Krzywicki, T., and Habat, H.R. (1972) Correlations Between Fluorescence, X-ray Diffraction, and Physiological Properties in Cytoplasmic Membrane Vesicles Isolated From Escherichia coli. *Biochim. Biophys. Acta* 274: 466-77.
- Schick, P.K., Kurica, K.B., and Chacko, G.K. (1976) Location of Phosphatidylethanolamine and Phosphatidylserine in the Human Platelet Plasma Membrane. *J. Clin. Invest.* 57: 1221-6.
- Schindler, H. and Seelig, J. (1973) EPR Spectra of Spin Labels in Lipid Bilayers. *J. Chem. Phys.* 59: 1841-50.
- Schindler, H. and Seelig, J. (1974) EPR Spectra of Spin Labels in Lipid Bilayers. II. Rotation of Steroid Spin Probes. *J. Chem. Phys.* 61: 2946-9.

Schindler, H. and Seelig, J. (1975) Deuterium Order Parameters in Relation to Thermodynamic Properties of a Phospholipid Bilayer. A Statistical Mechanical Interpretation. *Biochemistry* 14: 2283-7.

Schreier, S., Polnaszek, C.F., and Smith, I.C.P. (1978) Spin Labels in Membranes. Problems in Practice. *Biochim. Biophys. Acta* 515: 375-436.

Schroeder, F. (1978) Isothermal Regulation of Membrane Fluidity in Murine Fibroblasts With Altered Phospholipid Polar Head Groups. *Biochim. Biophys. Acta* 511: 356-76.

Schroeder, F. (1978) Differences in Fluidity Between Bilayer Halves of Tumour Cell Plasma Membranes. *Nature* 276: 528-30.

Schroeder, F., Holland, J.F., and Vagelos, P.R. (1976) Use of  $\beta$ -parinaric Acid, a Novel Fluorimetric Probe, to Determine Characteristic Temperatures of Membranes and Membrane Lipids From Cultured Animal Cells. *J. Biol. Chem.* 251: 6739-46.

Schroeder, F., Holland, J.F., and Vagelos, P.R. (1976) Physical Properties of Membranes Isolated From Tissue Culture Cells With Altered Phospholipid Composition. *J. Biol. Chem.* 251: 6747-56.

Scott, H.L., Jr. (1974) A Model for Phase Transitions in Lipid Bilayers and Biological Membranes. *J. Theoret. Biol.* 46: 241-53.

Scott, H.L. (1977) Monte Carlo Studies of the Hydrocarbon Region of Lipid Bilayers. *Biochim. Biophys. Acta* 469: 264-71.

Seelig, J. (1970) Spin Label Studies of Oriented Liquid Crystals (a Model System for Bilayer Membranes). *J. Am. Chem. Soc.* 92: 3881-7.

Seelig, J. (1977) Deuterium Magnetic Resonance: Theory and Application to Lipid Membranes. *Quart. Rev. Biophys.* 10: 353-418.

Seelig, J. and Browing, J.L. (1978) General Features of Phospholipid Conformation in Membranes. *FEBS Lett.* 92: 41-4.



- Seelig, J. and Gally, H.U. (1976) Investigation of Phosphatidylethanolamine Bilayers by Deuterium and Phosphorus-31 Nuclear Magnetic Resonance. *Biochemistry* 15: 5199-204.
- Seelig, J. and Hasselbach, W. (1971) A Spin Label Study of Sarcoplasmic Vesicles. *Eur. J. Biochem.* 21: 17-21.
- Seelig, J. and Niederberger, W. (1974a) Deuterium Labeled Lipids as Structural Probes in Liquid Crystalline Bilayers. *J. Am. Chem. Soc.* 96: 2069-72.
- Seelig, J. and Niederberger, W. (1974b) Two Pictures of a Lipid Bilayer. A Comparison Between Deuterium Label and Spin Label Experiments. *Biochemistry* 13: 1585-8.
- Seelig, J. and Seelig, A. (1974a) Deuterium Magnetic Resonance Studies of Phospholipid Bilayers. *Biochem. Biophys. Res. Comm.* 57: 406-11.
- Seelig, A. and J. Seelig, (1974b) The Dynamic Structure of Fatty Acyl Chains in a Phospholipid Bilayer Measured by Deuterium Magnetic Resonance. *Biochemistry* 13: 4839-45.
- Seelig, A. and Seelig, J. (1975) Bilayers of Dipalmitoyl-3-sn-phosphatidylcholine. Conformational Differences Between the Fatty Acyl Chains. *Biochim. Biophys. Acta* 406: 1-5.
- Seelig, A. and Seelig, J. (1977) Effect of a Single Cis-Double Bond on the Structure of a Phospholipid Bilayer. *Biochemistry* 16: 45-50.
- Seelig, J. and Waespe-Sarcevic, N. (1978) Molecular Order in Cis and Trans Unsaturated Phospholipid Bilayers. *Biochemistry* 17: 3310-5.
- Selkirk, J., Elwood, J.C., and Morris, H.P. (1971) Study on the Proposed Role of Phospholipid in Tumor Cell Membranes. *Cancer Res.* 31: 27-31.
- Silverstone, B. and Moulton, M.J. (1957) The Phosphorus Metabolism of Gliomas: A Study With Radioactive Isotopes. *Brain* 80: 362.
- Shah, D.O. and Schulman, J.H. (1967) Enzymatic Hydrolysis of Various Monolayers Employing Surface Pressure and Potential Technique. *J. Colloid Interface Sci.* 25: 107-19.
- Sheetz, M.P. and Chan, S.I. (1972) Effect of Sonication on the Structure of Lecithin Bilayers. *Biochemistry* 11: 4573-81.

- Sherbet, G.V. and Lakshmi, M.S. (1974) The Surface Properties of Some Human Intracranial Tumor Cell Lines in Relation to Their Malignancy. *Oncology* 29: 335-47.
- Shimshik, E.J., Kleemann, W., Hubbell, W.L., and McConnell, H.M. (1973) Lateral Phase Separations in Membranes. *J. Supramol. Struct.* 1: 283-94.
- Shimshik, E.J. and McConnell, H.M. (1973) Lateral Phase Separations in Binary Mixtures of Cholesterol and Phospholipids. *Biochem. Biophys. Res. Comm.* 53: 446-51.
- Shimshik, E.J. and McConnell, H.M. (1972) Lateral Phase Separation in Phospholipid Membranes. *Biochemistry* 12: 2351-60.
- Shin, S., Freedman, V.H., Risser, P., and Pollack, R. (1975) Tumorigenicity of Virus-transformed Cells in Nude Mice is Correlated Specifically With Anchorage Independent Growth In Vitro. *Proc. Natl. Acad. Sci. USA* 72: 4435-9.
- Shinitzky, M. and Barenholz, Y. (1978) Fluidity Parameters of Lipid Regions Determined by Fluorescence Polarization. *Biochim. Biophys. Acta* 515: 367-94.
- Shinitzky, M., Goldfisher, A., Bruck, A., Goldman, A., Stern, E., Barkai, G., Mashiach, S., and Serr, D.M. (1976) A New Method for Assessment of Fetal Lung Matrix. *Brit. J. Obstet. Gynecol.* 83: 838-44.
- Shinitzky, M. and Inbar, M. (1974) Differences in Microviscosity Induced by Different Cholesterol Levels in the Surface Membrane Lipid Layer of Normal Lymphocytes and Malignant Lymphoma Cells. *J. Mol. Biol.* 85: 603-15.
- Shinitzky, M. and Inbar, M. (1976) Microviscosity Parameters and Protein Mobility in Biological Membranes. *Biochim. Biophys. Acta* 433: 133-49.
- Shiple, G.G., Atkinson, D., and Scanu, A.M. (1972) Small Angle X-ray Scattering of Human Serum High Density Lipoproteins. *J. Supramol. Struct.* 1: 98-104.
- Siegel, G.J., Albers, R.W., Katzman, R., and Agranoff, B.W. (1976) *Basic Neurochemistry*. Little, Brown and Co., Boston.
- Simon, I., (1979) Differences in Membrane Unsaturated Fatty Acids and Electron Spin Resonance in Different Types of Myeloid Leukemia Cells. *Biochim. Biophys. Acta* 556: 408-22.

Singer, S.I. (1971) The Molecular Organization of Biological Membranes. In Structure and Function of Biological Membranes, ed. L.I. Rothfield, Academic Press, New York, pp. 145-222.

Singer, J.S. and Nicolson, G. (1972) The Fluid Mosaic Model of the Structure of Cell Membranes. Science 175: 720-31.

Sjostrand, F.S. (1963) A New Repeat Structural Element of Mitochondrial and Certain Cytoplasmic Membranes. Nature 199: 1262-4.

Skipski, V.P., Peterson, R.F., and Barclay, M. (1964) Quantitative Analysis of Phospholipids by Thin-layer Chromatography. Biochem. J. 90: 374-8.

Sklar, L.A., Hudson, B.S., and Simoni, R.D. (1975) Conjugated Polyene Fatty Acids as Membrane Probes: Preliminary Characterization. Proc. Natl. Acad. Sci. USA 72: 1649-53.

Slagel, D.E., Dittmer, J.S., and Wilson, C.B. (1967) The Lipid Composition of Human Glial Tumor and Adjacent Brain. J. Neurochem. 14: 789-98.

Small, D.M. (1968) A Classification of Biologic Lipids Based Upon Their Interaction in Aqueous Systems. J. Am. Oil. Chem. Soc. 45: 108-19.

Smith, H.S., Scher, C.D., and Todaro, G.J. (1971) Induction of Cell Division in Medium Lacking Serum Growth Factor by SV40. Virology 44: 359-70.

Smith, I.C.P., Bennet, L.G., Blackwell, B., Bloom, M., Btter, K.W., Dauris, J.H., Jennings, H.J., Johnson, K.G., and Martin, A. (1978) Organization and Mobility in Biological Membranes as Seen by Deuterium and Carbon 13 Nuclear Magnetic Resonance. In Biomolecular Structure and Function (Symposium), ed. P.F. Agris, Academic Press, New York, pp. 3-24.

Smith, I.C.P., Bulter, K.W., Tulloch, A.P., Davis, J.H., and Bloom, M. (1979) The Properties of Gel State Lipid in Membranes of *Acholeplasma laidlawii* as Observed by  $^2\text{H}$  NMR. FEBS Lett. 100: 57-61.

Solomonson, L.P., Liepkalns, V.A., and Spector, A.A. (1976) Changes in  $(\text{Na}^+ + \text{K}^+)\text{-ATPase}$  Activity of Ehrlich Ascites Tumor Cells Produced by Alterations of Membrane Fatty Acid Composition. Biochemistry 15: 892-7.

Spector, A.A. (1972) Fatty Acid, Glyceride, and Phospholipid Metabolism. In Growth, Nutrition, and Metabolism of Cells in Culture, vol. 1, ed. G. Rothblat and V. Cristafalo, Academic Press, New York, pp. 257-96.

Spector, A.A., Kiser, R.E., Denning, G.M., Koh, S-W.M., and DeBault, L.E. (1979) Modification of the Fatty Acid Composition of Cultured Human Fibroblasts. *J. Lipid Res.* 20: 536-47.

Spiro, M.J. and McKibbin, J.M. (1956) The Lipids of Rat Liver Cell Fractions. *J. Biol. Chem.* 219: 643-51.

Stanbridge, E.J. and Perkins, F.T. (1969) Tumor Nodule Formation as an In Vivo Measure of the Suppression of Cellular Immune Response by Antilymphocyte Serum. *Nature* 221: 80-1.

Steim, J.M., Tourtellotte, M.E., Reinert, J.C., McElhaney, R.N., and Rader, R.L. (1969) Calorimetric Evidence for the Liquid-crystalline State of Lipids in a Biomembrane. *Proc. Natl. Acad. Sci. USA* 63: 104-9.

Stier, A. and Sackmann, E. (1973) Spin Labels as Enzyme Substrates. Heterogenous Lipid Distribution in Liver Microsomal Membranes. *Biochim. Biophys. Acta* 311: 400-8.

Stocken, G.W., Johnson, K.G., Bulter, K.W., Polnaszek, C. F., Cry, R., and Smith, I.C.P. (1975) Molecular Motion in Acholeplasma laidlawii Membranes as Determined by Deuterium Magnetic Resonance of Biosynthetically Incorporated Specifically Labeled Lipids. *Biochim. Biophys. Acta* 401: 535-9.

Stocken, G.W., Johnson, K.G., Bulter, K.W., Tulloch, A.P., Boulanger, Y., Smith, I.C.P., Davis, J.H., and Bloom, M. (1977) Deuterium NMR Study of Lipid Organization in Acholesplasma laidlawii Membranes. *Nature* 269: 267-8.

Stocken, G.W., Polnaszek, C.F., Leitch, L.C. Tulloch, A.P., and Smith, I.C.P. (1974) A Study of Mobility and Order in Model Membranes Using  $^2\text{H}$  NMR Relaxation Rates and Quadrupole Splittings of Specifically Deuterated Lipids. *Biochem. Biophys. Res. Comm.* 60: 844-50.

Stocken, G.W., Polnaszek, C.F., Tulloch, A.P., Hasan, F., and Smith, I.C.P. (1976) Molecular Motion and Order in Single-bilayer Vesicles and Multilamellar Dispersions of Egg Lecithin and Lecithin Cholesterol Mixtures. A Deuterium Nuclear Magnetic Resonance Study of Specifically Labeled Lipids. *Biochemistry* 15: 954-66.

Stoffel, W., Tunggal, B.D., Zierenberg, O., Schreiber, E., and Binczek, E. (1974)  $^{13}\text{C}$  Nuclear Magnetic Resonance Studies of Lipid Interactions in Single and Multi Component Lipid Vesicles. Hoppe-Seyler's Z. Physiol. Chem. 355: 1367-80.

Stoker, M. (1967) Contact and Short-range Interactions Affecting Growth of Animal Cells in Culture. In Current Topics in Developmental Biology, vol. 2, ed. A.A. Moscono and A. Monroy, Academic Press, New York, pp. 108-27.

Stoker, M. and MacPherson, I. (1961) Studies on Transformation of Hamster Cells by Polyoma Virus In Vitro. Virology 14: 359-70.

Strickland, E.H. and Benson, A.A. (1960) Neutron Activation Paper Chromatographic Analysis of Phosphatides in Mammalian Cell Fractions. Arch. Biochem. Biophys. 88: 344-8.

Stubbs, G.W., Litman, B.J., and Barenholz, Y. (1976) Microviscosity of the Hydrocarbon Region of the Bovine Retinal Segment Disk Membrane Determined by Fluorescent Probe Measurements. Biochemistry 15: 2766-72.

Stubbs, G.W., Litman, B.J., and Barenholz, Y. (1976) Membrane Microviscosity and Human Platelet Function. Biochemistry 15: 4832-7.

Sun, G.Y. and Leung, B.S. (1974) Phospholipids and Acyl Groups of Subcellular Membrane Fractions From Human Intracranial Tumors. J. Lipid Res. 15: 423-31.

Sundler, R., Sarcione, S.L., Alberts, A.W., and Vagelos, P.R. (1977) Evidence Against Asymmetry in Intracellular Membranes From Rat Liver. Proc. Natl. Acad. Sci. USA 74: 3350-4.

Svennerholm, L. (1963) In Brain Lipids and Lipoproteins and the Leukodystrophies, ed. J. Folch-Pi and H. Bauer, Elsevier North-Holland, New York, pp. 104-19.

Svennerholm, L. (1964) The Distribution of Lipids in the Human Nervous System. I. Analytical Procedure. Lipids of Foetal and Newborn Brain. J. Neurochem. 11:839-53.

Svennerholm, L. (1968) Distribution and Fatty Acid Composition of Phosphoglycerides in Normal Human Brain. J. Lipid Res. 9: 570-9.

- Tanaka, K-I. and Ohnishi, S-I. (1976) Heterogeneity in the Fluidity of Intact Erythrocyte Membrane and Its Homogenization Upon Hemolysis. *Biochim. Biophys. Acta* 426: 218-31.
- Tanford, C. (1972) *The Hydrophobic Effect*, John Wiley and Sons, New York.
- Tanford, C. (1972) Hydrophobic Free Energy, Micelle Formation and Micelle Formation and the Association of Proteins With Amphiphiles. *J. Mol. Biol.* 67: 59-74.
- Tasaki, I., Watanabe, A., and Hallet, M. (1973) Fluorescence of Squid Axon Membrane Labeled With Hydrophobic Probes. *J. Membr. Biol.* 8: 109-32.
- Taylor, R.B., Duffus, W.P.H., Raff, M.D., and DePetris, S. (1971) Redistribution and Pinocytosis of Lymphocyte Surface Immunoglobulin Molecules Induced by Anti-immunoglobulin Antibody. *Proc. Natl. Acad. Sci. USA* 233: 225-9.
- Temin, H.M., Pierson, R.W., Jr., and Dulak, N.C. (1972) The Role of Serum in the Control of Multiplication of Quian and Mammalian Cells in Culture. *In Growth, Nutrition and Metabolism of Cells in Culture*, ed. G.H. Rothblat and V.J. Cristafalo, Academic Press, New York, pp. 50-81.
- Tenny, J.R., Cowan, D.L., Berney, R.L., Vorbeck, M.L., and Martin, A.P. (1978) Stochastic ESR Analysis of Rat Liver and Hepatoma Mitochondrial Lipids. *Biophys. Struct. Mech.* 4: 111-4.
- Thieret, T.E. (1979) Investigation of the Motion of Stable Free Radicals in Isotropic and Anisotropic Media Using Electron Spin Resonance Spectroscopy. Ph.D. thesis, Duke University.
- Thompson, T.E., Lentz, B.R., and Bareholz, Y. (1977) A Colorimetric and Fluorescent Probe Study of Phase Transitions in Phosphatidylcholine Liposomes. *FEBS Symp.* 42: 47-71.
- Thulborn, K.R., Tilley, L.M., Sasyer, W.H., and Treloar, F.E. (1979) The Use of n-(9-anthroloxy) Fatty Acids to Determine Fluidity and Polarity Gradients in Phospholipid Bilayers. *Biochim. Biophys. Acta* 558: 166-78.
- Tiddy, G.J.T. (1972) NMR Relaxation Times of the Lamellar Phases of the System Sodium Caprylate/decanol/water. *J. Chem. Soc., Faraday Trans.* 68:369-80.

- Tilley, L., Thulborn, K.R., and Sawyer, W.H. (1979) An Assessment of the Fluidity Gradient of the Lipid Bilayer as Determined by a Set of n-(9-anthroxyloxy Fatty Acids) (n = 2,6,9,12,16). *J. Biol. Chem.* 254: 2592-4.
- Todaro, G.J. and Green, H. (1963) Quantitative Studies on the Growth of Mouse Embryo Cells in Culture and Their Development into Established Lines. *J. Cell Biol.* 17: 299-313.
- Tourtellote, M.E., Branton, D., and Keith, A. (1970) Membrane Structure: Spin Labeling and Freeze Etching of Mycoplasma laidlawii. *Proc. Natl. Acad. Sci. USA* 66: 909-16.
- Trapp, B.D. (1977) Lipid and Ultrastructural Changes in Brain After Induction of Essential Fatty Acid Deficiency During Development. Ph.D. dissertation, Loyola University of Chicago.
- Trauble, H. and Eibl, H. (1974) Electrostatic Effects on Lipid Phase Transitions: Membrane Structure and Ionic Environment. *Proc. Natl. Acad. Sci. USA* 71: 214-9.
- Trauble, H. and Eibl, H. (1975) Cooperative Structural Changes in Lipid Bilayers. In Functional Linkage in Biomolecular Systems, ed. F.O. Schmitt, D.M. Schneider, and D.M. Crothers, Raven Press, New York, pp. 59-90.
- Trauble, H. and Haynes, D.H. (1971) The Volume Change in Lipid Bilayer Lamellae at the Crystalline-liquid Crystalline Phase Transition. *Chem. Phys. Lipids* 7: 324-35.
- Trauble, H. and Overath, P. (1973) The Structure of Escherichia coli Membranes Studied by Fluorescence Measurements of Lipid Phase Transitions. *Biochim. Biophys. Acta* 307: 491-512.
- Trauble, H. and Sackmann, E. (1972) Studies of the Crystalline-liquid Crystalline Phase Transition of Lipid Model Membranes. III. Structure of a Steroid-lecithin System Below and Above the Phase Transition. *J. Am. Chem. Soc.* 94: 4499-510.
- Valic, M.I., Gorrissen, H., Cushley, R.J., and Bloom, M. (1979) Deuterium Magnetic Resonance Study of Cholesteroyl Estrus in Membranes. *Biochemistry* 18: 854-9.

- Van, S.P., Birell, G.B., and Griffith, O.H. (1974) Rapid Anisotropic Motion of Spin Labels. Models for Motion Averaging of the ESR Parameters. *J. Magnetic Resonance* 15: 444-59.
- Vanderkooi, J. and Callis, B.J. (1974) Pyrene. A Probe of Lateral Diffusion in the Hydrophobic Region of Membranes. *Biochemistry* 13: 4000-6.
- Vanderkooi, J., Fischhoff, S., Chance, B., and Cooper, R.A. (1974) Fluorescent Probe Analysis of the Lipid Architecture of Natural and Experimental Cholesterol-rich Membranes. *Biochemistry* 13: 1589-95.
- Vanderkooi, G. and Green, D.E. (1970) On the Relationship of Phospholipids to Proteins in Biological Membranes. *Biophys. Soc. Abstracts* 10: 190a.
- Vanderkooi, G. and Green, D.E. (1970) Biological Membrane Structure. I. The Protein Crystal Model for Membranes. *Proc. Natl. Acad. Sci. USA* 66: 615-21.
- Vanderkooi, G., Senior, A.E., Capaldi, R.A., and Hayashi, H. (1972) Biological Membrane Structure. II. The Lattice Structure of Membranous Cytochrome Oxidase. *Biochim. Biophys. Acta* 274: 38-48.
- Vanderkooi, G. and Sundaralingam, M. (1970) Biological Membrane Structure. II. A Detailed Model for the Retinal Rod Outer Segment Membrane. *Proc. Natl. Acad. Sci. USA* 67: 233-8.
- Van Dijck, P.W.M., DeKruyff, B., van Deenen, L.L.M., de Gier, J., and Demel, R.A. (1976) The Preference of Cholesterol for Phosphatidylcholine in Mixed Phosphatidylcholine-phosphatidylethanolamine Bilayers. *Biochim. Biophys. Acta* 455: 576-87.
- Van Dijck, P.W.M., DeKruyff, B., Verkleij, A.J., van Deenen, L.L.M., and de Gier, J. (1978) Comparative Studies on the Effects of pH and  $Ca^{2+}$  on Bilayers of Various Negatively Charged Phospholipids and Their Mixtures With Phosphatidylcholine. *Biochim. Biophys. Acta* 512: 84-96.
- Van Dijck, P., Ververgaert, P., Verkleij, A., van Deenen, L., and de Gier, J. (1975) Influence of Calcium and Magnesium Ions on the Thermotropic Behavior and Permeability Properties of Liposomes Prepared From Dimyristoyl Phosphatidylglycerol and Mixtures of Dimyristoyl Phosphatidylglycerol and Dimyristoyl Phosphatidylcholine. *Biochim. Biophys. Acta* 406: 465-8.



Van Hoeven, R.P. and Emmelot, P. (1972) Plasma Membranes. XVIII. Lipid Class Composition of Plasma Membranes Isolated From Rat and Mouse Liver and Hepatomas. *J. Membr. Biol.* 9: 105-26.

Van Hoeven, R.P. and Emmelot, P. (1973) Plasma Membrane Lipids of Normal and Neoplastic Tissues. In *Tumor Lipids: Biochemistry and Metabolism*, ed. R. Wood, American Oil Chemist's Society Press, Champaign, Ill., pp. 126-38.

Van Hoeven, R.P., Emmelot, P., Krol, J.H., and Oomen-Meulemaris, E.P.M. (1975) Studies on Plasma Membranes. XXII. Fatty Acid Profiles of Lipid Classes in Plasma Membranes of Rat and Mouse Livers and Hepatomas. *Biochim. Biophys. Acta* 380: 1-11.

Van Hoeven, R.P., von Blitterswijk, W.J., and Emmelot, P. (1979) Fluorescence Polarization Measurements on Normal and Tumor Cells and Their Corresponding Plasma Membranes. *Biochim. Biophys. Acta* 551: 44-54.

Vauquelin, L.N. (1811) *Analyse de la Matiere Cerebrale de Homme et de Quelques Animaux*. Thesis, University of Paris, Faculty of Medicine, Paris, No. 96, Vol. 85, p. 26.

Veerkamp, J.H., Mulder, I., and van Deenen, L.L.M. (1961) Comparative Studies on the Phosphatides of Normal Rat Liver and Primary Hepatoma. *Z. Krebsforsch.* 64: 137-48.

Veerkamp, J.H., Mulder, I., and van Deenen, L.L.M. (1962) Comparison of the Fatty Acid Composition of Lipids From Different Animal Tissues Including Some Tumours. *Biochim. Biophys. Acta* 57: 299-309.

Verkleij, A.J., DeKruyff, B., Ververgaert, P.H.J.Th., Tozanne, J.F., and van Deenen, L.L.M. (1974) The Influence of pH,  $Ca^{2+}$ , and Protein on the Thermotropic Behavior of the Negatively Charged Phospholipid, Phosphatidylglycerol. *Biochim. Biophys. Acta* 339: 432-7.

Verkleij, A.J., Ververgaert, P.H.J., DeKruyff, B., and van Deenen, L.L.M. (1974) The Distribution of Cholesterol in Bilayers of Phosphatidylcholine as Visualized by Freeze-fracturing. *Biochim. Biophys. Acta* 373: 495-501.

- Verkleij, A.J., Ververgaert, P.H.J., van Deenen, L.L.M., and Elbers, P.F. (1972) Phase Transitions of Phospholipid Bilayers and Membranes of Acholeplasma laidlawii B Visualized by Freeze-fracture Electron Microscopy. *Biochim. Biophys. Acta* 288: 326-32.
- Verkleij, A.J., Zwaal, R.F.A., Roelofsen, B., Comfurius, P., Kastelijn, D., and van Deenen, L.L.M. (1973) The Asymmetric Distribution of Phospholipids in the Human Red Cell Membrane. A Combined Study Using Phospholipases and Freeze-etch Electron Microscopy. *Biochim. Biophys. Acta* 323: 178-93.
- Verna, S.P. and Wallach, D.F.H. (1975) Evidence for Constrained Lipid Mobility in the Erythrocyte Ghost. A Spin Label Study. *Biochim. Biophys. Acta* 382: 73-82.
- Vernadakis, A., Parker, K., and Norenberg, M. (1980) Changes in Biochemical Properties of Glial Cells in Culture: In Vitro Differentiation. In Tissue Culture in Neurobiology, ed. E. Giacobini, Raven Press, New York, pp. 411-26.
- Ververgaert, P.H.J., Elbers, P.F., Luitingh, A.J., and van Den Berg, H.J. (1972) Surface Patterns of Freeze-fractured Liposomes. *Cytobiologie* 6: 86-96.
- Ververgaert, P.H.J., Verkleij, J.J., Verhoeven, J.J., and Elbers, P.F. (1973) Spray-freezing of Liposomes. *Biochim. Biophys. Acta* 311: 651-4.
- Waggoner, A.S., Kingzett, T.J., Griffith, O.H., and Keith, A.D. (1969) A Spin-labeled Lipid Probing Biological Membranes. *Chem. Phys. Lipids* 3: 245-53.
- Waggoner, A.S. and Stryer, L. (1970) Fluorescent Probes of Biological Membranes. *Proc. Natl. Acad. Sci. USA* 67: 579-89.
- Wallace, R., Vasington, P.J., and Petricciani, J.C. (1971) Heteroplasmtation of Cultured Cell Lines in Newborn Hamsters Treated With Antilymphocyte Serum. *Nature* 230: 454-5.
- Wallach, D.F.H. (1972) *The Plasma Membrane: Dynamic Perspectives, Genetics and Pathology*. Springer, New York.
- Wallach, D.F.H. (1975) *Membrane Molecular Biology of Neoplastic Cells*. Elsevier Scientific, New York.

- Wallach, D.F.H. and Gordon, A.S. (1968) Lipid Protein Interactions in Cellular Membranes. Fed. Proc. 27: 1263-8.
- Wallach, D.F.H., Krantz, B., Ferber, E., and Fischer, H. (1972) Affinity Density Perturbation: A New Fractionation Principle and Its Illustration in a Membrane Separation. FEBS Lett. 21: 29-33.
- Wallach, D.F.H. and Winzler, R.J. (1974) Evolving Strategies and Tactics in Membrane Research. Springer, New York.
- Wallach, D.F.H. and Zahler, P.H. (1968) Infrared Spectra of Plasma Membrane and Endoplasmic Reticulum of Ehrlich Ascites Carcinoma. Biochim. Biophys. Acta 150: 186-93.
- Weber, G. (1977) Enzymology of Cancer Cells. New Engl. J. Med. 296: 486-93.
- Weber, G. and Cantero, A. (1957) Phospholipid Content in Novikoff Hepatoma, Regenerating Liver and in Liver of Fed and Fasted Normal Rats. Exp. Cell Res. 13: 125-31.
- Weber, G., Prajda, N., and Williams, J.C. (1975) Biochemical Strategy of the Cancer Cell: Malignant Transformation-linked Enzymatic Imbalance. Adv. Enzyme Regulation 13: 3-25.
- Weinstein, D.B., Marsh, J.B., Glick, M.C., and Warren, L. (1969) Membranes of Animal Cells. IV. Lipids of the L Cell and Its Surface Membrane. J. Biol. Chem. 244: 4103-11.
- Westermarck, B. (1973) Growth Control of Normal and Neoplastic Human Glia-like Cells in Culture. Ph.D. dissertation, Acta Universtatis Upsaliensis, 164.
- Westermarck, B. (1973) The Deficient Density-dependent Growth Control of Human Malignant Glioma Cells and Virus-transformed Glia-like Cells in Culture. Int. J. Cancer 12: 438-51.
- Westermarck, B., Ponten, J., and Hugosson, R. (1973) Determinants for the Establishment of Permanent Tissue Culture Lines From Human Gliomas. Acta Pathol. Microbiol. Scand. A 81: 791-805.
- White, H.B., Galli, C., and Paoletti, R. (1971) Ethanolamine Phosphoglyceride Fatty Acids in Aging Brain. J. Neurochem. 18: 1337-9.

White, H.B. and Smith R.R. (1968) Cholesteryl Esters of the Glioblastoma. *J. Neurochem.* 15: 293-8.

White, S.H. (1970) A Study of Lipid Bilayer Membrane Stability Using Precise Measurements of Specific Capacitance. *Biophys. J.* 10: 1127-48.

Wieslander, A., Christiansson, A., Rilfors, L., and Lindblom, G. (1980) Lipid Bilayer Stability in Membranes. Regulation of Lipid Composition in Acholeplasma laidlawii as Governed by Molecular Shape. *Biochemistry* 19: 3650-5.

Wilkins, M.H.F., Blaurock, A.E., and Engleman, D.E. (1971) Bilayer Structure in Membranes. *Nature (New Biology)* 230: 72-6.

Williams, J. (1968) Unpublished data cited in *Soft Agar Techniques*, I. MacPherson. In Tissue Culture: Methods and Applications, ed. P.F. Kruse and M.K. Patterson, Jr., Academic Press, New York, p. 276.

Williams, J.H., Kuchmak, M., and Witter, R.F. (1966) Phospholipids of Human Serum. *Lipids* 1: 89-97.

Williams, R.E., Wisnieski, B.J., Rittenhouse, H.G., and Fox, C.F. (1974) Utilization of Fatty Acid Supplements by Cultured Animal Cells. *Biochemistry* 13: 1969-77.

Williams, R.M. and Chapman, D. (1968) Phospholipids, Liquid Crystals and Cell Membranes. *Progr. Chem. Fats Other Lipids* 11: 3-74.

Wingvist, L., Eriksson, L.C., and Dallner, G. (1974) Binding of Concanavalin A-sepharose to Glycoproteins of Rat Liver Microsomal Membranes. *FEBS Lett.* 42: 27-31.

Wisnieski, B.J., Williams, R.E., and Fox, C.F. (1973) Manipulation of Fatty Acid Composition in Animal Cells Grown in Culture. *Proc. Natl. Acad. Sci. USA* 70: 3669-73.

Wisnieski, B.J., Parkes, J.G., Huang, Y.O., and Fox, C.F. (1974a) Physical and Physiological Evidence for Two Phase Transitions in Cytoplasmic Membranes of Animal Cells. *Proc. Natl. Acad. Sci. USA* 71: 4381-5.

Wisnieski, B.J., Huang, Y.O., and Fox, C.F. (1974b) Physical Properties of the Lipid Phase of Membranes From Cultured Animal Cells. *J. Supramol. Struct.* 2: 593-608.

- Wisnieski, B.J. and Iwata, K.K. (1977) Electron Spin Resonance Evidence for Vertical Asymmetry in Animal Cell Membranes. *Biochemistry* 16: 1321-6.
- Wollemann, M. (1972) Biochemistry of Brain Tumors. In Handbook of Neurochemistry, vol. VII. Pathological Chemistry of the Nervous System, ed. A. Lajtha, Plenum Press, New York, pp. 503-42.
- Wood, R. (1973) Embryonic vs. Tumor Lipids. II. Changes in the Phospholipids of Developing Chick Brain, Heart and Liver. *Lipids* 9: 429-39.
- Wood, R. and Falch, J. (1973) Lipids of Culture Hepatoma Cells. II. Effect of Media Lipids on Cellular Phospholipids. *Lipids* 8: 702-10.
- Wunderlich, F., Ronai, A., Speth, V., Seelig, J., and Blume, A. (1975) Thermotropic Lipid Clustering in Tetrahymena Membranes. *Biochemistry* 14: 3730-5.
- Yates, A.J., Thompson, D.K., Boesel, C.P., Albrightson, C., and Hart, R.W. (1979) Lipid Composition of Human Neural Tumors. *J. Lipid Res.* 20: 428-36.
- Yau, T.M., Buckman, T., Hale, A.H., and Weber, M.J. (1976) Alterations in Lipid Acyl Group Composition and Membrane Structure in Cells Transformed by Rous Sarcoma Virus. *Biochemistry* 15: 3212-9.
- Yeagle, P.L. (1978) Phospholipid Headgroup Behavior in Biological Assemblies. *Acc. Chem. Res.* 11: 321-7.
- Zampighi, G. and Robertson, J.D. (1973) Fine Structure of the Synaptic Disc Separated From the Goldfish Medulla Oblongata. *J. Cell Biol.* 56: 92-105.
- Zwaal, R.F.A., Roelofsen, B., Comfurius, P., and van Deenen, F.F.M. (1977) Complete Purification and Some Properties of Phospholipase C from Bacillus cereus. *Biochim. Biophys. Acta* 233: 474-9.

## APPENDIX I

### Deuterium NMR Order Parameters

Deuterium NMR spectra of phospholipids labelled in specific positions consist of a doublet where the distance between the two splittings (absorption peaks) is defined as the quadrupole coupling or quadrupole splitting  $\Delta\nu$  (Kz). The lines of deuterated phospholipids are broad suggesting that the splitting is a composite of two signals with slightly different quadrupole couplings (i.e., non-equivalence of the sn-1 and sn-2 chains of phospholipids).

From the quadrupole splitting,  $\Delta\nu$ , the deuterium order parameter ( $S_{CD}$ ) of the C-D bond on a deuterated phospholipid can be calculated:

$$\Delta\nu = (3/4) (e^2 q Q / h) S_{CD} \quad (1)$$

where  $e$  denotes the charge on an electron ( $1.60 \times 10^{-19}$  C),  $h$  is Planck's constant ( $6.63 \times 10^{-34}$  J·s),  $Q$  is the scalar quadrupole moment ( $Q$  deuteron =  $2.875 \times 10^{-27}$  cm<sup>2</sup>) (Reid and Vaida, 1972),  $eq$  is the largest field gradient and  $e^2 q Q / h$  is referred to as the static quadrupolar coupling constant. For paraffin chains the deuteron quadrupole splitting constant is 170 kHz (Burnett and Muller, 1971) and has been determined for a variety of other C-D bonds (Barnes, 1974; Seelig, 1977). The relationship between the splitting constant and deuterium order parameter can be expanded in a similar fashion as the ESR order parameter:

$$S_{CD} = (1/2) (3 \langle \cos^2 \alpha \rangle - 1) \quad (2)$$

(Schindler and Seelig, 1975).

$\alpha$  is defined as the angle between the deuterium bond vector and the bilayer normal. For dipalmitoyl-3-phosphatidylcholine in a statistical model proposed by Marcelja (1974) and expanded by Schindler and Seelig (1975), the corresponding deuterium bond vectors are  $\alpha = 90^\circ$ ,  $35.3^\circ$  and  $90^\circ$ , and  $35.3^\circ$ , and they represent the three types of probable segmental motion. Therefore, the probability,  $p$ , of the respective orientations is important and contributes to the overall deuterium order parameter.

The relationship between the segmental order parameter ( $S_{\text{mol}}$ ) and the  $^2\text{H}$  order parameter ( $S_{\text{CD}}$ ) can be defined as

$$S_{\text{mol}} = -2S_{\text{CD}} \quad (3)$$

(Seelig and Niderberger, 1974a). This equation is valid only if the segmental motion can be characterized by axially symmetric  $\text{CD}_2$  segment. When this relationship holds true, the average orientation of the C-D bond is perpendicular to the bilayer and the hydrocarbon chain is frozen in an all-trans conformation.

The segmental order parameter can similarly be expanded like that of the  $S_{\text{CD}}$  value:

$$S_{\text{mol}} = (1/2) (3\langle \cos^2 \beta \rangle - 1) \quad (4)$$

(Schindler and Seeling, 1975).

The rate of motion producing gauche-trans isomerizations are delineated by measurements of the nuclear relaxation times. (For a recent review of relaxation times more applicable to liquids and solids than biomembranes, see Poole and Farach, 1979).  $T_1$ , the spin lattice relaxation time, and  $T_2$ , the spin-spin relaxation time are the most commonly used terms. The spin lattice relaxation time is indicative of motion on the order of  $10^2$ - $360$  MHz; whereas,  $T_2$  measures slower motions (near 0.1 Hz). Thus,  $T_1 \approx T_2$  for low viscosity liquids and  $T_1 \gg T_2$  for crystalline phases.  $T_1$  is the time constant required for a spin system to attain thermal equilibrium, and  $T_2$  is the time constant for the spin system to establish thermal equilibrium with itself. For the case when  $I = \frac{1}{2}$  (nuclear spins),  $T_1$  and  $T_2$  can be defined by:

$$\frac{1}{T_1} = \frac{3}{10} \left( \frac{g^4 \mu_n^2}{h^2 r^6} \right) \left( \frac{\tau_c}{1 + \omega^2 \tau_c^2} + \frac{4\tau_c}{1 + 4\omega_0^2 \tau_c^2} \right) \quad (5)$$

$$\frac{1}{T_2} = \frac{3}{20} \left( \frac{g^4 \mu_n^2}{h^2 r^6} \right) \left( 3\tau_c + \frac{5\tau_c}{1 + 4\omega_0^2 \tau_c^2} + \frac{2\tau_c}{1 + \omega_0^2 \tau_c^2} \right) \quad (6)$$

where the rotational correlation time is  $\tau_c = 4\pi r^3 / 3kT$  (for water  $\tau_c = 3.5 \times 10^{-12}$  sec), the quantity  $g_N I$  defines the magnetic moment, and  $r$  is the distance between nuclear spins. More simply, for dipole-dipole interactions between  $^{13}\text{C}$  and  $^1\text{H}$  or deuterium quadrupole interactions within asymmetric environments:

$$\frac{1}{T_1} = A \cdot f(\tau_i) \quad (7)$$

$A$  describes the interaction energy and where  $f$  defines the function of correlation times for various motions.

Qualitatively, the expression may be reduced to

$$NT_1 \propto \text{Mobility} \quad (8)$$

for  $^{13}\text{C}$  magnetic resonance where  $N$  is the number of directly attached hydrogen atoms. For deuterium:

$$T_1 \propto \text{Mobility} \quad (9)$$



## APPENDIX II

Calculation of Trans-Gauche Hydrocarbon  
Conformation as a Function of  
Order Parameter and n Values

The number of trans-gauche hydrocarbon isomerizations can be statistically estimated as a function of the spacing between the nitroxide ring and the carboxyl end of spin-labelled fatty acids ( $n$ , value) and their order parameters. This calculation is based upon the assumption that all carbon-carbon bonds in the fatty acid chain are equivalent and that the probability of adjacent gauche<sup>+</sup>-gauche<sup>-</sup> conformations are negligible (Hubbell and McConnell, 1971).

The probability of a single carbon-carbon bond in an all trans position is defined as  $P_t$  while  $P_g$  denotes the probability that any two hydrocarbon bonds are in the gauche (either gauche<sup>+</sup> or gauche<sup>-</sup>) conformations. The total probabilities are equal to one:

$$P_t + P_g = 1.0 \quad (1)$$

The order parameter can be approximated by the following polynomial function:

$$S_n = P_t^n \eta_0 + n P_t^{n-1} P_g \eta_1 + \frac{n(n-1)}{2!} P_t^{n-2} P_g^2 \eta_2 + \dots \quad (2)$$

$n$  denotes the distance between the nitroxide ring and carboxyl end of fatty acid chain. The quantity  $P_t^n$  is defined as the probability of an all trans hydrocarbon conformation and  $n P_t^{n-1} P_g$  corresponds to the probability that the hydrocarbon chain possesses a single gauche conformation. The term  $\eta_0$  represents the quantity  $1/2(3\gamma^2 - 1)^*$  and is a value of 1 when the hydrocarbon chain has an all trans conformation.  $\eta_1$  has a value of  $-1/8$  when the chain has one gauche<sup>+</sup> (and one gauche<sup>-</sup>) conformation;  $\eta_2$  equals  $1/16$  and represents the average value of

---

\* The order parameter can be defined as  $S = 1/2(3\gamma^2 - 1)$ .

$1/2(3\gamma^2 - 1)$  for two gauche transitions. Equal weight is given to  $g^+g^+$ ,  $g^+g^-$ ,  $g^-g^+$ , and  $g^-g^-$  isomeric states and gauche conformations separated by unequal numbers of methylene groups. The values of  $\eta$  decrease as the number of methylene groups between the nitroxide ring and the carboxyl end of the fatty acid chain increases ( $\eta_0=1$ ,  $\eta_1=-1/8$ ,  $\eta_2=1/16$ ,  $\eta_3=-1/32$  . . .).

Equation 1 can be rewritten as:

$$P_g = 1 - P_t \quad (3)$$

such that equation 2 can be calculated in terms of  $P_t$ . Arbitrary values of  $P_t$  (for example, 0.01 to 0.99 in  $0.01$  steps) are inserted until this equation yields the probability of gauche and trans conformations that equals the experimentally derived order parameter.

Equation 2 can be rewritten as an exponential function and used to estimate the number of gauche-trans conformers. Therefore,

$$\log S_n - C = n \log P_t \quad (4)$$

where

$$C = \log(\eta_0 \quad n(P_g/P_t) \eta_1 + \frac{n(n-1)}{2!} (P_g/P_t)^2 + \dots) \quad (5)$$

Computer iteration of equations 4 and 5 easily calculates the value of  $P_t$  and  $P_g$ . Neglecting  $C$ , the initial  $P_t$  value, defined as  $P_t'$ , is calculated by the insertion of the  $n$  and order parameter values into equation 4. Then,  $P_t'$  value is inserted into equation 5 to obtain a  $C'$  term which is inserted in place of original  $C$  term in equation 4 to yield  $P_t''$ . This looping calculation is carried out until there is rapid convergence of  $P_t$ .

The polynomial and exponential equations yield the same results. Calculation of the number of gauche-trans conformations as a function of order parameters for the 5-, 12-, 16-doxylstearate spin labels (corresponding to a nitroxide-carboxyl methylene separation values of 5, 12, and 16 groups, respectively) is listed in Tables 20, 21, and 22 (Appendix II). In these tables,  $P_g$  refers to the probability of gauche conformers and  $P_t$  defines the corresponding probability of trans hydrocarbon conformations.

```

EXPERIMENTAL S= ~/
METHYLENE GROUP SEPARATION= ^5/
DEF=0.1 FIRST INCREMENT= ~/
DEF=0.01 INITIAL VALUE OF % TRANS= ~/
S= .6708857E-02PT= .9999998E-02
S= .1042709E-02PT= .1100000E+00
S= .2521290E-03PT= .2099999E+00
S= .2147167E-02PT= .3099999E+00
S= .8694217E-02PT= .4099998E+00
S= .2620354E-01PT= .5099998E+00
S= .6642175E-01PT= .6099996E+00
S= .1497108E+00PT= .7099997E+00
S= .3062245E+00PT= .8099997E+00
S= .5090682E+00PT= .9099997E+00
DEF=0.01 SECOND INCREMENT= ^
DEF=0.99 UPPER LIMIT OF % TRANS= ~/
S= .2877772E+00PT= .8000000E+00PG= .2000000E+00
S= .3082250E+00PT= .8099999E+00PG= .1900001E+00
S= .3298814E+00PT= .8199999E+00PG= .1800001E+00
S= .3526825E+00PT= .8299999E+00PG= .1700001E+00
S= .3770466E+00PT= .8399999E+00PG= .1600001E+00
S= .4026740E+00PT= .8499999E+00PG= .1500001E+00
S= .4297462E+00PT= .8599999E+00PG= .1400001E+00
S= .4583274E+00PT= .8699999E+00PG= .1300001E+00
S= .4884833E+00PT= .8799999E+00PG= .1200001E+00
S= .5202818E+00PT= .8899999E+00PG= .1100001E+00
S= .5537931E+00PT= .8999999E+00PG= .1000001E+00
S= .5890889E+00PT= .9099998E+00PG= .9000015E-01
S= .6262433E+00PT= .9199998E+00PG= .8000016E-01
S= .6653325E+00PT= .9299998E+00PG= .7000017E-01
S= .7064350E+00PT= .9399998E+00PG= .6000018E-01
S= .7496314E+00PT= .9499998E+00PG= .5000019E-01
S= .7950043E+00PT= .9599998E+00PG= .4000020E-01
S= .8426390E+00PT= .9699998E+00PG= .3000021E-01
S= .8926228E+00PT= .9799998E+00PG= .2000022E-01
S= .9450452E+00PT= .9899998E+00PG= .1000023E-01

```

TABLE 20: 5-doxyl stearate probe trans-gauche fatty acid conformations.

```

EXPERIMENTAL S= ~/
METHYLENE GROUP SEPARATION= ^12/
DEF=0.1 FIRST INCREMENT= ~/
DEF=0.01 INITIAL VALUE OF % TRANS= ~/
S= .4234877E-04PT= .9999998E-02
S= .4994399E-06PT= .1100000E+00
S= .6037226E-08PT= .2099999E+00
S= .5969435E-06PT= .3099999E+00
S= .1692408E-04PT= .4099998E+00
S= .2322493E-03PT= .5099998E+00
S= .1997269E-02PT= .6099998E+00
S= .1257172E-01PT= .7099997E+00
S= .6428707E-01PT= .8099997E+00
S= .2857215E+00PT= .9099997E+00
DEF=0.01 SECOND INCREMENT= ~/
S= .5499982E-01PT= .8000000E+00PG= .2000000E+00
S= .6428730E-01PT= .8099999E+00PG= .1900001E+00
S= .7504028E-01PT= .8199999E+00PG= .1800001E+00
S= .8747530E-01PT= .8299999E+00PG= .1700001E+00
S= .1018405E+00PT= .8399999E+00PG= .1600001E+00
S= .1184179E+00PT= .8499999E+00PG= .1500001E+00
S= .1375283E+00PT= .8599999E+00PG= .1400001E+00
S= .1595367E+00PT= .8699999E+00PG= .1300001E+00
S= .1848577E+00PT= .8799999E+00PG= .1200001E+00
S= .2139616E+00PT= .8899999E+00PG= .1100001E+00
S= .2473817E+00PT= .8999999E+00PG= .1000001E+00
S= .2857222E+00PT= .9099998E+00PG= .9000015E-01
S= .3296664E+00PT= .9199998E+00PG= .8000016E-01
S= .3799874E+00PT= .9299998E+00PG= .7000017E-01
S= .4375577E+00PT= .9399998E+00PG= .6000018E-01
S= .5033621E+00PT= .9499998E+00PG= .5000019E-01
S= .5785103E+00PT= .9599998E+00PG= .4000020E-01
S= .6642529E+00PT= .9699998E+00PG= .3000021E-01
S= .7619954E+00PT= .9799998E+00PG= .2000022E-01
S= .8733185E+00PT= .9899998E+00PG= .1000023E-01

```

TABLE 21: 12-doxyl stearate probe trans-gauche fatty acid conformations.

```

EXPERIMENTAL S= ^/
METHYLENE GROUP SEPARATION= ^16/
DEF=0.1 FIRST INCREMENT= ^/
DEF=0.01 INITIAL VALUE OF % TRANS= ^/
S= .2343190E-05PT= .9999998E-02
S= .6288474E-08PT= .1100000E+00
S= .3223022E-10PT= .2099999E+00
S= .5448907E-08PT= .3099999E+00
S= .4783357E-06PT= .4099998E+00
S= .1571064E-04PT= .5099998E+00
S= .2758270E-03PT= .6099998E+00
S= .3154407E-02PT= .7099997E+00
S= .2691881E-01PT= .8099997E+00
S= .1904098E+00PT= .9099997E+00
DEF=0.01 SECOND INCREMENT= ^
S= .2509990E-02PT= .7000000E+00PG= .3000000E+00
S= .3154434E-02PT= .7100000E+00PG= .2900000E+00
S= .3952820E-02PT= .7200000E+00PG= .2800000E+00
S= .4939485E-02PT= .7300000E+00PG= .2700000E+00
S= .6155979E-02PT= .7399999E+00PG= .2600001E+00
S= .7652439E-02PT= .7499999E+00PG= .2500001E+00
S= .9489387E-02PT= .7599999E+00PG= .2400001E+00
S= .1173973E-01PT= .7699999E+00PG= .2300001E+00
S= .1449126E-01PT= .7799999E+00PG= .2200001E+00
S= .1784954E-01PT= .7899999E+00PG= .2100001E+00
S= .2194137E-01PT= .7999999E+00PG= .2000001E+00
S= .2691890E-01PT= .8099999E+00PG= .1900001E+00
S= .3296465E-01PT= .8199999E+00PG= .1800001E+00
S= .4029734E-01PT= .8299999E+00PG= .1700001E+00
S= .4917878E-01PT= .8399999E+00PG= .1600001E+00
S= .5992221E-01PT= .8499998E+00PG= .1500002E+00
S= .7290202E-01PT= .8599998E+00PG= .1400002E+00
S= .8856606E-01PT= .8699998E+00PG= .1300002E+00
S= .1074483E+00PT= .8799998E+00PG= .1200002E+00
S= .1301858E+00PT= .8899998E+00PG= .1100002E+00
S= .1575382E+00PT= .8999998E+00PG= .1000002E+00
S= .1904103E+00PT= .9099998E+00PG= .9000021E-01
S= .2298781E+00PT= .9199998E+00PG= .8000022E-01
S= .2772221E+00PT= .9299998E+00PG= .7000023E-01
S= .3339632E+00PT= .9399998E+00PG= .6000024E-01
S= .4019065E+00PT= .9499997E+00PG= .5000025E-01
S= .4831929E+00PT= .9599997E+00PG= .4000026E-01
S= .5803592E+00PT= .9699997E+00PG= .3000027E-01
S= .6964079E+00PT= .9799997E+00PG= .2000028E-01
S= .8348882E+00PT= .9899997E+00PG= .1000029E-01

```

TABLE 22: 16-doxy1 stearate probe trans-gauche fatty acid conformations.



APPENDIX III, FIGURE 40: Fatty acid methyl ester chart from the varian 2100 Gas Chromatograph (EGSS-X as liquid phase).

## APPROVAL SHEET

The dissertation submitted by Robert Wersto has been read and approved by the following committee:

Joseph Bernsohn, Ph.D.  
Professor of Biochemistry  
Loyola University Stritch School of Medicine

Mary Ellen Druyan, Ph.D.  
Assistant Professor of Biochemistry  
Loyola University Stritch School of Medicine

Mary Druse Manteuffel, Ph.D.  
Assistant Professor of Biochemistry  
Loyola University Stritch School of Medicine

Richard M. Schultz, Ph.D.  
Professor of Biochemistry  
Loyola University Stritch School of Medicine

James R. Norris, Ph.D.  
Photosynthesis Group Leader  
Chemistry Division  
Argonne National Laboratory

O. Howard Reichman, M.D.  
Professor and Chairman  
Division of Neurological Surgery  
Loyola University Stritch School of Medicine

The final copies have been examined by the director of the dissertation and the signature which appears below verifies the fact that any necessary changes have been incorporated and that the dissertation is now given final approval by the Committee with reference to content and form.

The dissertation is therefore accepted in partial fulfillment of the requirements for the degree of Doctor of Philosophy.

October 27, 1981  
Date

Abraham Rosenbery  
Director's Signature